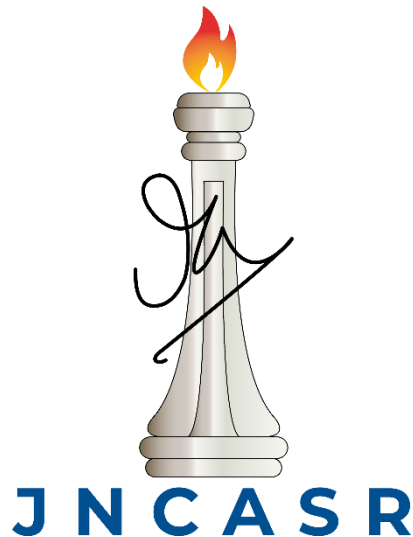


**Altered proteostasis in a mouse model of
Huntington's disease: Insights into pathogenic
dysfunction and therapeutic modulation**



**Thesis submitted for the degree of
Doctor of Philosophy**

by

Vijay Kumar M J

Clement, and Autophagy Lab

Neuroscience Unit

Molecular biology and Genetics unit

Jawaharlal Nehru Centre for Advanced Scientific Research

Jakkur, Bengaluru, Karnataka – 560064, India

May 2021

Table of contents

Declaration.....	1
Certificate	2
Acknowledgements	4
Abbreviations.....	7
Thesis Synopsis	9
List of publications	17
Chapter- 1 Introduction.....	18
1.1 Protein homeostasis.....	19
1.2 Protein aggregation in neurodegenerative diseases.....	21
1.3 Autophagy	23
1.4 Aggrephagy: The selective degradation of aggregates	25
1.5 Neuronal autophagy	26
1.6 Autophagy in neurodegenerative diseases	28
1.6.1 Alzheimer’s disease	28
1.6.2 Parkinson’s disease	31
1.6.3 Amyotrophic Lateral Sclerosis (ALS)	32
1.6.4 Huntington’s disease (HD).....	34
1.7 Pathophysiology of Huntington’s disease	36
1.7.1 Functions of HUNTINGTIN (HTT) protein.....	40
1.8 Mouse models to study Huntington’s disease	42
1.9 Detailed insights into HD mouse model – R6/2.....	43
1.10 Autophagy as a therapeutic strategy for HD	47
1.10.1 mTOR dependent modulators	48
1.10.2 mTOR independent modulators	49
1.11 Nilotinib (Tasigna™)	50
1.12 Aim and scope of the study	52
Chapter- 2 Material and Methods	53
2.1 Mouse studies.....	54
2.2 Genotyping.....	54
2.3 Injection regimen.....	56
2.4 Bodyweight measurement and survival	56
2.5 Behavioural Studies.....	56

2.5.1	Open Field Test.....	57
2.5.2	Rotarod test	58
2.5.3	Hind-limb clasping.....	59
2.6	Immunoblot Analysis	60
2.6.1	Lysate preparation.....	60
2.6.2	Protein estimation	61
2.6.3	SDS-PAGE and immunoblotting	62
2.7	Histology	63
2.7.1	Perfusion	63
2.7.2	Slide coating.....	65
2.7.3	Cryosectioning	65
2.8	Immunohistochemistry.....	65
2.9	Cell culture experiments.....	66
2.9.1	Autophagy Assay	67
2.10	Statistics.....	67
Chapter- 3	68
Characterisation of mutant HUNTINGTIN aggregate formation in R6/2 mice	68
3.1	Introduction	69
3.2	Methods.....	70
3.3	Results	71
3.3.1	Mutant HUNTINGTIN aggregates were detected as early as 2 weeks in R6/2 mice ...	71
3.3.2	Ubiquitination is increased in the striatum at the end stage of disease progression in R6/2 mice	74
3.4	Discussion	76
Chapter- 4	78
Spatio-temporal analysis of autophagy and its efficiency in clearing polyglutamine aggregates in R6/2 mice	78
4.1	Introduction	79
4.2	Methods.....	79
4.3	Results	80
4.3.1	Basal autophagy is unaltered and spatiotemporally maintained in R6/2 mice.....	80
4.3.2	mHTT aggregates form intranuclear inclusions and co-localise with p62/SQSTM1 in R6/2 mice	81
4.4	Discussion	86
Chapter- 5	88

5.1	Introduction	89
5.2	Methods.....	90
5.3	Results	90
5.3.1	Nilotinib (Tasigna™) induces autophagy in HeLa cells	90
5.3.2	Nilotinib (Tasigna™) is ineffective in inducing autophagy in Wild-type and R6/2 mice 91	
5.3.3	Nilotinib (Tasigna™) is unable to clear mHTT aggregates in R6/2 mice	99
5.4	Discussion	110
Chapter- 6		112
Nilotinib (Tasigna™) is not neuroprotective and is unable to rescue motor functions in R6/2 mice.....		112
6.1	Introduction	113
6.2	Methods.....	114
6.2.1	Behavioural studies.....	114
6.3	Results	114
6.3.1	Nilotinib (Tasigna™) is ineffective in improving the body weight and survival rate in R6/2 mice	114
6.3.2	Nilotinib (Tasigna™) is unable to ameliorate motor functions in R6/2 mice	115
6.4	Discussion	117
Chapter- 7		118
Discussion and future directions		118
References		127

Table of Figures

Figure 1-1 Diagram illustrating the intraneuronal proteostasis network	21
Figure 1-2 Overview of the autophagy pathway.....	24
Figure 1-3 Impaired autophagy mechanism in neurodegenerative diseases.....	29
Figure 1-4 Autophagy dysfunction in Huntington’s disease	35
Figure 1-5 Genetics of Huntington’s disease (HD)	37
Figure 1-6 Pathway illustrating disruption in basal ganglia circuitry in Huntington’s disease	40
Figure 2-1 Representative image for <i>Htt</i> (R6/2) PCR	55
Figure 2-2 Injection regime in R6/2 mice.....	56
Figure 2-3 Representative images showing Open-field arena and trajectory	57
Figure 2-4 Image representing Rotarod apparatus.....	59
Figure 2-5 Image representing typical hind-limb clasp phenotype in R6/2 mice.....	60
Figure 2-6 Graph depicting Bradford assay to measure protein concentration	62
Figure 3-1 Detection of mHTT aggregates at different regions of the brain in R6/2 mice from 12 weeks of age.....	72
Figure 3-2 Dynamics of mHTT aggregate formation across different stages of disease progression in R6/2 mice	74
Figure 3-3 Ubiquitination is increased in the striatum at the end-stage of disease progression in R6/2 mice	75
Figure 4-1 Basal autophagy is not altered in Cortex across different stages of disease progression in R6/2 mice	82
Figure 4-2 Basal autophagy is unaltered in R6/2 mice across different stages of disease progression in the region hippocampus	83
Figure 4-3 Spatio-temporal regulation of ATG proteins in striatum across different stages of disease progression in R6/2 mice.....	84
Figure 4-4 ATG protein expression is unaltered in cerebellum across different stages of disease progression in R6/2 mice	85
Figure 4-5 mHTT aggregates form intranuclear inclusions and get co-localised with p62/SQSTM1 in R6/2 mice in the striatum at 12 weeks	86
Figure 5-1 Nilotinib (Tasigna™) induces autophagy in HeLa cells in a dosage-dependent manner.....	91

Figure 5-2 Tasigna is ineffective in inducing autophagy in Cortex across different age groups in wild-type mice	92
Figure 5-3 Tasigna is unable to induce autophagy in Hippocampus in wild-type mice.....	93
Figure 5-4 Tasigna is ineffective in inducing autophagy in the striatum in wild-type across different age groups	94
Figure 5-5 Tasigna is ineffective in inducing autophagy in the cerebellum across different age groups in wild-type mice	95
Figure 5-6 Tasigna is ineffective in inducing autophagy in the cortex across different stages of disease progression in R6/2 mice.....	96
Figure 5-7 Tasigna is ineffective in inducing autophagy in Hippocampus across different stages of disease progression in R6/2 mice	97
Figure 5-8 Tasigna is ineffective in inducing autophagy in striatum across different stages of disease progression in R6/2 mice.....	98
Figure 5-9 Tasigna is ineffective in inducing autophagy in Cerebellum across different stages of disease progression in R6/2 mice	99
Figure 5-10 Tasigna is ineffective in clearing mHTT aggregates in Cortex across different stages of disease progression in R6/2 mice.....	101
Figure 5-11 Tasigna is ineffective in clearing mHTT aggregates in the hippocampus across different stages of disease progression in R6/2 mice.....	102
Figure 5-12 Tasigna is ineffective in clearing mHTT aggregates in striatum across different stages of disease progression in R6/2 mice.....	103
Figure 5-13 Tasigna is ineffective in clearing mHTT aggregates in the cerebellum across different stages of disease progression in R6/2 mice.....	104
Figure 5-14 UBIQUITIN profile of the cell is unchanged in cortex and hippocampus across different age groups in wild-type mice	105
Figure 5-15 UBIQUITIN profile of the cell is unchanged in striatum and cerebellum across different age groups in wild-type mice	106
Figure 5-16 UBIQUITIN profile of the cell is unchanged despite the presence of mHTT aggregates in cortex and hippocampus across different stages of disease progression in R6/2 mice.....	107
Figure 5-17 UBIQUITIN profile of the cell is unchanged despite the presence of mHTT aggregates in striatum and cerebellum across different stages of disease progression in R6/2 mice.....	108

Figure 5-18 Nilotinib (Tasigna™) does not affect the expression of ATG proteins and clearance of mHTT aggregates at 12 weeks in Striatum in R6/2 mice.....	110
Figure 6-1 Nilotinib is unable to improve the body weight and survival rate in R6/2 mice .	115
Figure 6-2 Nilotinib (Tasigna™) is ineffective in rescuing the motor functions in R6/2 mice	116

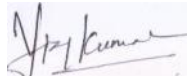
List of tables

Table 1-1 Overview of different stages of Huntington’s disease and its varied symptoms	39
Table 1-2 Mouse models of Huntington’s disease.....	45
Table 2-1 PCR protocol for Htt (R6/2) genotyping	55
Table 2-2 Protocol followed during training in rotarod on different days.....	58
Table 2-3 Protocol showing the method to score based on Racine scale	59
Table 2-4 Functions of components of RIPA buffer.	61
Table 2-5 Details of primary and secondary antibodies used in the study to check the expression of ATG proteins, Ub, and mHTT aggregates	64
Table 2-6 Functions of the solutions used for perfusion and IHC	64
Table 2-7 Details of the list of primary and secondary antibodies used for immunostaining .	66

Declaration

I, Vijay Kumar M J, hereby declare that the thesis entitled “**Altered proteostasis in a mouse model of Huntington’s disease: Insights into pathogenic dysfunction and therapeutic modulation**” is a research work carried out by myself under the supervision of Dr James P. Clement Chelliah, Neuroscience Unit and in collaboration with Dr Ravi Manjithaya, Molecular Biology and Genetics Unit, Jawaharlal Nehru Centre for Advanced Scientific Research (JNCASR), Bengaluru, India.

This part of the research work has not been submitted elsewhere for the award of any academic degree. Keeping in consideration to report scientific observations, due acknowledgements, and references have been cited wherever the work has been described based on the findings of other investigators. Any omission owing to oversight or misjudgement is regretted.



Vijay Kumar M J

Bengaluru, India

Date: 14 Sep 2021

Certificate

This is to certify that the research work described in this thesis entitled “**Altered proteostasis in a mouse model of Huntington’s disease: Insights into pathogenic dysfunction and therapeutic modulation**” is the result of investigations carried out by Mr Vijay Kumar M J under the supervision of Dr James P Chelliah Clement, Neuroscience Unit, in collaboration with Dr Ravi Manjithaya, Molecular Biology and Genetics Unit, Jawaharlal Nehru Centre for Advanced Scientific Research, Bengaluru, India, under my guidance and the results presented here have previously not formed the basis for the reward of any other diploma, degree, or fellowship.



James P Clement Chelliah
(Principal Investigator)

Date: 14 Sep 2021

Place: Bengaluru

Dedicated to Kausalya...

Acknowledgements

I wish to express my sincere appreciation to many generous people who have contributed to this thesis and supported me in one way or the other during this amazing journey.

First of all, I am extremely grateful and fortunate to have Prof James P Clement Chelliah and Prof Ravi Manjithaya as my research supervisors for their invaluable advice, continuous support, and for always encouraging me throughout my PhD.

I appreciate James (this is how he likes to address him) for constantly providing me with all the facilities and support and helping me to remain focused on achieving my targets for my experiments. His critical observations and comments have helped me to establish the overall direction of the research work and to move forward with the investigation in depth. James insightful feedback has pushed me to sharpen and broaden my thinking and brought my work to a higher level. His constant reviewing of my work has helped me to be productive without generating junk data in my PhD work. He has always set very higher standards in terms of work ethics, discipline, and time management and as far as I have come across, he never compromised on anything when it comes to the quality of work. This has helped me a lot in growing as a scientist as well as an individual and developing patience in dealing with things in life. Sometimes, it would be very difficult and challenging to reach his expectations, but in the end, when I looked back after completing the task, everything made sense. He always pushed me to improve on my abilities and skills and that helped me grow as an independent researcher. I am grateful to James for helping me in developing my soft skills in presentation, data storage, time management and adapting to new technologies. I thank him for providing me with an opportunity to work in his lab and supporting me in every aspect of my PhD work.

Next, I would like to extend my appreciation to Ravi sir for always motivating and inspiring me during my PhD study. His constant source of support and expertise helped me formulating the research questions and methodology and aided me in realising the power of critical reasoning in all my experiments. I thank him for his guidance and all the useful discussions and brainstorming sessions in designing and analysing the mice data with James in every meeting. I still remember the day when he gave me 20 questions to address regarding my project and that had helped me in understanding the concepts and findings of the study. His deep insights helped me at various stages of my research.

I would like to thank Professor Nihar Ranjan Jana (IIT Kharagpur) for providing the R6/2 mice for my PhD work. I also acknowledge him for giving his valuable suggestions on this project during his visit to JNCASR.

My sincere thanks to all my comprehensive examination committee members: Dr Ravi Muddashetty, Prof. Anuranjan Anand, and Dr Sarit S Agasti for giving me all the invaluable suggestions and comments on my PhD work.

My special thanks and appreciation to Shruthi, Vidya, Devanshi, Mridhula, and Niraj for all the help and assistance for this project. I especially thank Shruthi and Vidya for helping me in my initial days in establishing and maintaining the R6/2 mice colony. I am also grateful to

Devanshi and Mridhula for providing me with all the help in designing and performing the experiments (especially behaviour), analysing the data, and aiding me in all the presentations on Friday meetings with James and Dr Ravi.

I would also like to thank Dr SN Suresh and Dr Vidyadhara for all the valuable suggestions in designing my experiments for this project.

I thank the NSU chairperson Prof. Anuranjan Anand, and MBGU chairs Prof. Maneesha S Inamdar, and Prof. Ranga Udaykumar for creating a vibrant scientific environment and providing all facilities in the department.

I would like to thank Dr Sheeba Vasu for her constant guidance and support for my work. Her suggestions in answering the reviewer's comments in my manuscript have helped me a lot.

I would also like to extend my gratitude to all the faculty members of both units: Prof. M.R.S. Rao, Prof. Namita Surolia, Prof. Hemalatha Balaram, Prof. Ranga Udaykumar, Prof. Tapas K Kundu, Prof. Kaustuv Sanyal, Dr Sheeba Vasu, and Dr Kushagra Bansal for all their insightful and critical comments during annual work presentations and course works.

I would like to express my sincere thanks to Prof. Ranga Udaykumar and his lab members for allowing me to use the I-bright Chemidoc system for my western blot experiments. I thank Prof Ranga for his critical comments and suggestions on my project in all my work presentations and NSU journal clubs.

I especially thank and offer my appreciation to all the present and past members of Clement lab for their constant support and fun times during my PhD work. A special mention to Vijay Bhaiya for assisting with all the help needed in the lab and supporting me during the tough times.

I would also like to thank Saurabh Yadav (IISc) for all the support and help for my manuscript in answering the reviewer's questions.

I am also grateful to all the present and past members of the Autophagy laboratory for their assistance and support for my work. I especially thank Veena, Mridhula, Anushka, and Akshaya for giving me the antibodies and other reagents whenever needed for my work.

I thank all the labs of the unit: Molecular mycology lab, HIV-AIDS lab, Transcription and disease lab, Molecular parasitology lab, Chromatin biology lab, Human molecular genetics lab, Molecular parasitology and protein engineering lab, Bansal lab, and Chronobiology and behavioural neurogenetics lab for their support whenever needed.

I would like to thank Dr Prakash and the staff for providing all the facilities in the smooth functioning of the animal facility.

I thank Suma mam and other staff members in the confocal facility for helping me with all the microscopy and imaging work for my project.

I thank FACS facility, Narendra Nala, and Leena for giving all their help whenever needed.

I thank NSU-MBGU office staff: Vidhya, Raju, and Nandini for their assistance in all the paperwork related to the academics and the project.

I would like to express my gratitude to the hostel office, library, Dhanvantari, academic staff, administrative staff, purchase department, housekeeping, garden staff, security, technical and support staff of JNCASR for their indispensable role in providing all the facilities for the students, and keeping the campus safe, vibrant, and beautiful all the time.

I would like to thank CSIR-UGC and JNCASR for all the financial and academic support for my PhD tenure in JNCASR.

I am grateful to all my batch mates: Arijit, Chitrang, Rajarshi, Priya, Jindal, Sreshtha, Shubham, Ankit, Kuladeep, Saheli, Irine, Rashi, and Chhavi for all their constant support, motivation and all the fun times on the campus.

I thank all my friends in JNCASR: Akash, Sourav, Arijit, Chitrang, Preeti, Priya, Sreshtha, Shubham, Ankit, Sambhavi, Arun, Srilaxmi, Mridhula, Devanshi, Veena, Krishnendu, Bhupesh for all their kind and generous help, support and listening to me patiently during tough times.

I thank all my CDFD and NII friends for supporting me and providing me with all the guidance needed during the early days of my research career. I would like to especially extend my gratitude to Debasish and Rajendra who trusted me and guided me in pursuing research as my career. Apart from being good friends, they are always a source of inspiration.

I sincerely apologise to the friends and people if I miss any of the names in my acknowledgements.

I would like to make a special say on Shubham and Ankit, who consider me as their brother. They were very helpful and kind enough to me. They supported me in all the tough times and always present whenever there is a crisis. We had a very good time and shared some beautiful memories.

I am extremely grateful and lucky to share a special bond with Chhavi and Rashi. They played a significant role and have been a strong pillar to me for my entire PhD. They both were the main reasons for me to stay back in JNC and pursue my PhD and I will be always grateful for that. I enjoy cooking a lot with them and shared many beautiful memories with both of them and I would always cherish them for a lifetime. We also had some tough and bad times, but we always find a way to get back together as one family. I will always be indebted for the love and care shown to me. I am lucky to find a sister in Rashi and I thank her for making me her Bhratashri. I thank them for all the love and being a part of my family and without their presence, this journey would not have been possible.

I am extremely lucky and fortunate to have such supporting parents, my brothers Ajay and Sanjay, all my cousins, my Mama and Rasagna, without them I wouldn't have come so far and this journey would have been merely impossible. They were very patient and immensely supportive in every aspect of this journey, and I am deeply indebted for the encouragement and showing belief in me.

Abbreviations

NDDs	Neurodegenerative diseases
PD	Parkinson's disease
AD	Alzheimer's disease
ALS	Amyotrophic lateral sclerosis
HD	Huntington's disease
UPS	Ubiquitin proteasome system
CMA	Chaperone mediated autophagy
ATG	Autophagy-related
MVBs	Multivesicular bodies
NBR1	Neighbour of BRCA1
ALFY	Autophagy-linked FYVE protein
OPTN	Optineurin
MAPLC3	Microtubule Associated Protein Light Chain 3
mTOR	Mammalian target of rapamycin
GFP-LC3	Green fluorescent protein-tagged Light Chain 3
NSCs	Neural stem cells
SGZ	Sub granular zone
SVZ	Sub ventricular zone
HTT	HUNTINGTIN
APP	Amyloid precursor protein
PS-1	Presenilin-1
A β	β -amyloid
PICALM	Phosphatidylinositol-binding clathrin assembly protein
SNAREs	Soluble NSF attachment protein receptors
AP2	Assembly polypeptide 2
FTD	Frontotemporal dementia
PSP	Supranuclear palsy
CBD	Cortico-basal degeneration
LAMP1	Lysosomal-associated membrane protein-1

α -SYN	α -SYNUCLEIN
SNpc	Substantia nigra pars compacta
VPS35	Vacuolar protein sorting-associated protein 35
PINK1	Parkin and phosphatase and tensin homolog-induced putative kinase 1
KO	Knockout
SYT11	SYNAPTOTAGMIN 11
LAMP-2A	Lysosomal-associated membrane protein 2A
PolyQ	Polyglutamine
mHTT	Mutant HUNTINGTIN
PGC-1 α	Proliferator-activated receptor gamma coactivator 1- α
Gpi	Globus pallidus internal
Gpe	Globus pallidus external
MSN	Medium spiny neurons
D1, D2	Dopaminergic receptors 1 and 2
STN	Subthalamic nucleus
SNr	Substantia nigra pars reticulata
VA/VL	Ventral anterior/ventral lateral nucleus of the thalamus
NES	Nuclear export signal
NLS	Nuclear localisation signal
HEAT	HUNTINGTIN, elongation factor 3, protein phosphatase 2A and TOR1
PSD-95	Postsynaptic density-95
BDNF	Brain-derived neurotrophic factor
FDA	Food and drug administration
MPTP	1-methyl-4-phenyl- 1,2,3,6-tetrahydropyridine
MSA	Multiple system atrophy
DDR	Discoidin Domain Receptors
CSF	Cerebrospinal fluid
PVDF	Polyvinylidene fluoride
PFA	Paraformaldehyde
PND	Post-natal day

Thesis Synopsis

**Altered proteostasis in a mouse model of Huntington's disease:
Insights into pathogenic dysfunction and therapeutic modulation**

Submitted by

Vijay Kumar M J

Clement, and Autophagy laboratory

Neuroscience Unit

Molecular Biology and Genetics Unit

Jawaharlal Nehru Centre for Advanced Scientific Research

Jakkur, Bangalore – 560064, India.

Thesis advisor: Dr James PC Chelliah

Co-PI: Dr Ravi Manjithaya

Introduction

Protein homeostasis (proteostasis) is regulated by maintaining the balance between the synthesis and degradation of proteins. Proteostasis is essential to maintain normal cellular metabolic functions and is crucial for the cell to respond to the dynamic changes for a given stimulus. An extensive complex network of signalling pathways safeguard cells and the overall organism against various proteotoxic stress^{1,2}. The proteostasis network comprises pathways that regulate biogenesis, folding, subcellular localisation, trafficking, and degradation of proteins^{1,2}. Any cellular stress, such as mutations, may damage proteins leading to their misfolding and eventually forming aggregates. To combat the toxic gain of function of these aggregates, cells rely on pathways such as the ubiquitin-proteasome system (UPS) and autophagy to degrade them. Any imbalance in proteostasis state due to the impairment of these degradation pathways leads to the accumulation of misfolded protein aggregates. These toxic aggregates cause cell death, especially in post-mitotic cells like neurons, and it has been shown that progressive temporal loss of proteostasis balance results in neurodegenerative diseases (NDDs)³⁻⁵. Accumulation of toxic protein aggregates due to impairment of protein degradation pathways is the common root cause for many NDDs. Well known examples of such aggregates causing NDDs include β -amyloid plaques in Alzheimer's disease (AD), α -SYNUCLEIN in Parkinson's disease (PD), Superoxide dismutase (SOD) in Amyotrophic Lateral Sclerosis (ALS) and HUNTINGTIN in Huntington's disease (HD)^{4,6}. The work carried out in this thesis is focused on understanding the pathophysiology of HD, mainly focusing on autophagy dysfunction.

Autophagy is an evolutionarily conserved catabolic process that involves the capture and lysosomal degradation of superfluous and damaged intracellular components^{7,8}. It involves *de novo* formation of double-membrane vesicles known as autophagosomes that engulf cytoplasmic cargo such as proteins and organelles. These autophagosomes eventually fuse with lysosomes to form autolysosomes wherein the captured cargo is degraded and building blocks, thus generated, are recycled back to the cytoplasm. Biogenesis of autophagosomes, their maturation, and finally fusion with lysosomes involves a discrete set of protein complexes that regulate every step of autophagy flux. Studies have shown that in most NDDs, autophagy is impaired at multiple steps. For example, in HD, autophagy is impaired at its initial phagophore formation, maturation of autophagosomes, and at the fusion step with lysosomes^{6,9,10}. HD is an autosomal dominant trinucleotide repeat disorder caused by an expansion of CAG repeats which codes for the amino acid glutamine (Q). The expanded polyQ are the characteristic

feature of the mutant HTT (mHTT) protein¹¹⁻¹³. The mHTT protein forms toxic aggregates and gets accumulated at specific regions of the brain such as the striatum, the region responsible for the control and coordination of motor functions. The presence of toxic mHTT aggregates in neurons is responsible for the failure of several fundamental cellular processes characterised by severe motor dysfunction, dementia, and cognitive impairment¹³⁻¹⁵. Due to the large size and dynamic nature of the mHTT aggregates, UPS has been shown to be inefficient in detecting and clearing them. Rather, these aggregates act as substrates for autophagy, wherein autophagy machinery has the potential to efficiently recognise aggregates and enhance their clearance^{16,17}. The autophagy pathway that involves selective degradation of protein aggregates such as mHTT is called aggrephagy, and studies have shown that aggrephagy however is impaired in HD^{9,18,19}.

Extensive research has been carried out to understand the pathophysiology of such neurological disorders, including HD with respect to autophagy dysfunction, and has helped in designing disease-modifying strategies to ameliorate the severity of the phenotype. One of the effective strategies is to target pathways involved in regulating autophagy, which has been implicated as a promising therapeutic approach to identify scalable drug targets for many NDDs^{3,6,7,20-22}. Detection and development of specific active modulators of autophagy are ongoing and the ones with high therapeutic value have been employed for clinical interventions towards the treatment of many severe forms of NDDs. In the context of HD, the need of the hour is to identify small molecules that upregulate autophagy and effectively clear aggregate-prone intracytoplasmic mHTT protein complexes, thereby ameliorating disease pathology and conferring neuroprotective roles in various cellular and animal models of HD²³.

Aims and scope of the study

In this study, a robust HD mouse model, R6/2, that manifest pathophysiological symptom such as motor impairment was used to understand the proteostasis defects, including autophagy dysfunction²⁴⁻²⁶. Despite being a widely used model to study HD, basal autophagy in R6/2 or any other related mouse models have not been characterised. In this study, some of the fundamental questions were addressed, such as how proteostasis can be restored in NDDs? Can toxic intracellular aggregates be cleared by inducing autophagy, thereby preventing the neurons from dying? At what stage of disease progression autophagy has to be induced? Since many NDDs are age-related, it is very important to identify the stage at which autophagy has to be induced. Intervention at the right stage should not only help in clearing the aggregates inside

the neuronal cells but also aid in delaying the onset of symptoms, thereby improving the quality and lifespan of an individual.

Despite the detailed investigation of aggregate formation and mechanisms related to autophagy dysfunction in HD, the comprehensive study establishing the Spatio-temporal expression of mHTT aggregate formation across the disease progression has not yet been characterised in any of the available HD mouse models. The study contributes to understanding the pathophysiology of NDDs with respect to autophagy dysfunction since age-related diseases such as AD, PD, and HD, show distinct phenotypic differences and are caused due to the accumulation of specific protein aggregates leading to severe brain atrophy.

The study carried out in the thesis investigates the expression of mHTT aggregates and autophagy proteins at different stages of disease progression in R6/2 across various brain regions, i.e., cortex, hippocampus, striatum, and cerebellum. Nilotinib (TasignaTM), an anti-cancer drug commonly used to treat chronic myeloid leukaemia ^{27,28}, is currently in clinical trials for PD and HD, but its potency has not been evaluated in any of the rodent models of HD. In this thesis, the efficacy of Tasigna was tested in ameliorating physiological and behavioural deficits in an HD mouse model, R6/2.

Chapter 1 is the review of the literature and the overall background to the concept of the study. This chapter explains protein homeostasis and how altered proteostasis leads to neurodegenerative diseases. In these diseases, in addition to the accumulation of toxic intracellular aggregates, autophagy dysfunction plays a vital role in the disease progression. A detailed description of the autophagy pathway and its dysfunction in various NDDs including HD is discussed. In this study, the pathophysiology of HD is studied in detail with respect to autophagy dysfunction and in this regard, HD mouse model R6/2 is used as a model system. Pathophysiology of HD, various functions of HTT protein, and different mouse models used to study HD are discussed. Importantly, upregulation of autophagy by pharmacological intervention to combat the toxicity of protein aggregates in HD is highlighted in this section. Nilotinib (TasignaTM) which is currently in clinical trials for PD and HD is used in this study to test its efficacy in ameliorating the disease pathology in the HD mouse model, R6/2. The properties and importance of Tasigna are discussed in the section. In the end, this chapter concludes by providing the rationale, hypothesis and overall aims and scope of this study.

Chapter 2 explains the detailed methodology by providing all the necessary information on the material and methods used in the study. A complete description of the protocols used for

the mouse study, such as genotyping, injection regime, bodyweight measurement, behavioural experiments to study the motor function test (Open-field test, rotarod test, hind-limb clasping test) are mentioned in detail. We used immunoblotting and immunohistochemistry to investigate the expression of mHTT aggregate formation and state of basal autophagy in R6/2 mice. Besides the protocols, the tables with all the necessary components of buffers, salts, and antibodies are mentioned. All the statistical analysis done in this study are discussed.

Chapter 3 discusses the results obtained in understanding the mHTT aggregate formation in R6/2 mice. Four different age groups (2, 4, 8, and 12 weeks) corresponding to different stages of disease progression were used to check the accumulation of toxic mHTT aggregates. Apart from investigating the temporal expression, various regions of the brain such as the cortex, hippocampus, striatum, and cerebellum were also included in the study to have a comprehensive analysis of aggregate formation in the HD mouse model, R6/2. Our results suggest that mHTT aggregates get to accumulate as early as 2 weeks in the striatum and cortex, whereas, in the hippocampus and cerebellum, mHTT aggregates were detected from 4 weeks of age. These results explain that aggregates start accumulating before the onset of symptoms and progressively accumulate and spread through the brain contributing to rapid disease progression in R6/2. Since aggregates form early in these mice, we next checked if there is any differential regulation in the overall ubiquitin profile of the cell. To our surprise, despite the presence of mHTT aggregates, there is no change in the ubiquitination pattern across different stages of disease progression in various regions of the brain.

Chapter 4 describes the results of Spatio-temporal analysis of basal autophagy in R6/2 mice. Many studies have reported that autophagy is impaired in HD and plays a significant role in the pathophysiology of the disease. In this regard, the expression of key autophagy related markers was assessed across the different stage of disease progression in various regions of the brain to understand the state of basal autophagy in R6/2. Interestingly, immunoblot results suggest that despite the early detection of mHTT aggregates in R6/2, there is no differential change in the expression of autophagy markers p62, LC3B, and GABARAPL2 at any given stage of disease progression (2, 4, 8, and 12 weeks) in various regions of the brain. Further, immunohistochemistry findings revealed that adapter protein p62 co-localises with mHTT aggregates and forms intranuclear inclusions in R6/2 mice compared to wild-type control mice. This kind of comprehensive analysis of basal autophagy has not been reported earlier in any of HD mouse models before, and this study is the first one to completely characterise the dynamics

of mHTT aggregate formation and state of basal autophagy in R6/2. Our results would aid in manoeuvring novel therapeutic strategies to ameliorate the disease pathology in HD.

Chapter 5 reviews the results of Nilotinib (TasignaTM) efficacy in inducing autophagy and clearing mHTT aggregates in R6/2 mice. Recent studies have proved that Tasigna is neuroprotective in preclinical models of PD and is currently in the clinical trials for PD and HD. Since its efficacy was not tested in any of HD mouse models to date, we evaluated its potency in inducing autophagy and clearing mHTT aggregates in R6/2 mice. Our findings suggest that the concentration of the Tasigna used in the study is not sufficient to induce autophagy and is inefficient in increasing the expression of autophagy markers in both wild-type and R6/2 mice at any stage of disease progression in different regions of the brain. Due to its inefficiency in inducing autophagy, we found that there is no clearance of mHTT aggregates in R6/2, thereby unable to delay the disease progression.

Chapter 6 evaluates the behaviour results and Tasigna inefficacy in improving the motor functions in R6/2 mice. Since our molecular experiments suggest that Tasigna is unable to induce autophagy and clear mHTT aggregates in R6/2, we performed motor functions tests, to see if the drug has any effect in improving the behavioral phenotypes. Our results indicate that Tasigna is unable to improve the bodyweight nor the survival rate in R6/2 compared to wild-type control mice. Motor function tests such as open-field locomotion and rotarod test were not improved after Tasigna treatment, and the hind-limb clasping test reveals that Tasigna is unable to delay the disease progression in R6/2 mice. The findings in this study suggest that Tasigna, which is in clinical trials for PD and HD, is not neuroprotective and does not ameliorate the disease phenotype in a pre-clinical model of HD, R6/2 mice.

Chapter 7 illustrates the overall results and discussion of the study carried out in this thesis. The results summarise that mHTT aggregates accumulate early in R6/2 mice, and basal autophagy is spatio-temporally maintained across different stages of disease progression in various regions of the brain in R6/2 mice compared to wild-type control littermates. Tasigna is ineffective in inducing autophagy and improving the motor functions in R6/2 mice. This kind of comprehensive study (different age groups and from different regions of the brain) has not been carried out in any of the HD mouse models and also in other NDDs to date. The results presented in this study would provide insights into understanding the mHTT aggregate formation and its consequences on autophagy dysfunction. Moreover, considering the fact the Tasigna is in the clinical trials for PD, and HD patients, to date, its potency is not studied in

any pre-clinical models of HD. This is the first study to be reported and to comment on the effect of Tasigna in the R6/2 mice model. In this regard, this study would be of interest to the researchers working on NDDs, focusing on autophagy dysfunction and also provide valuable insights to develop therapeutic strategies to design novel drugs. Moreover, all the limitations and conclusions drawn out of this study are discussed in this section. This chapter is completed by proposing future experiments to understand further the autophagy-related issues associated with HD.

References

- 1 Balch, W. E., Morimoto, R. I., Dillin, A. & Kelly, J. W. Adapting proteostasis for disease intervention. *Science* **319**, 916-919, doi:10.1126/science.1141448 (2008).
- 2 Yerbury, J. J., Ooi, L., Dillin, A., Saunders, D. N., Hatters, D. M., Beart, P. M., Cashman, N. R., Wilson, M. R. & Ecroyd, H. Walking the tightrope: proteostasis and neurodegenerative disease. *J Neurochem* **137**, 489-505, doi:10.1111/jnc.13575 (2016).
- 3 Sheikh, S., Safia, Haque, E. & Mir, S. S. Neurodegenerative Diseases: Multifactorial Conformational Diseases and Their Therapeutic Interventions. *J Neurodegener Dis* **2013**, 563481, doi:10.1155/2013/563481 (2013).
- 4 Gestwicki, J. E. & Garza, D. Protein quality control in neurodegenerative disease. *Prog Mol Biol Transl Sci* **107**, 327-353, doi:10.1016/B978-0-12-385883-2.00003-5 (2012).
- 5 Kulkarni, A., Chen, J. & Maday, S. Neuronal autophagy and intercellular regulation of homeostasis in the brain. *Curr Opin Neurobiol* **51**, 29-36, doi:10.1016/j.conb.2018.02.008 (2018).
- 6 Menzies, F. M., Fleming, A., Caricasole, A., Bento, C. F., Andrews, S. P., Ashkenazi, A., Fullgrabe, J., Jackson, A., Jimenez Sanchez, M., Karabiyik, C., Licitra, F., Lopez Ramirez, A., Pavel, M., Puri, C., Renna, M., Ricketts, T., Schlotawa, L., Vicinanza, M., Won, H., Zhu, Y., Skidmore, J. & Rubinsztein, D. C. Autophagy and Neurodegeneration: Pathogenic Mechanisms and Therapeutic Opportunities. *Neuron* **93**, 1015-1034, doi:10.1016/j.neuron.2017.01.022 (2017).
- 7 Rubinsztein, D. C., Gestwicki, J. E., Murphy, L. O. & Klionsky, D. J. Potential therapeutic applications of autophagy. *Nat Rev Drug Discov* **6**, 304-312, doi:10.1038/nrd2272 (2007).
- 8 Kaur, J. & Debnath, J. Autophagy at the crossroads of catabolism and anabolism. *Nat Rev Mol Cell Biol* **16**, 461-472, doi:10.1038/nrm4024 (2015).
- 9 Cortes, C. J. & La Spada, A. R. The many faces of autophagy dysfunction in Huntington's disease: from mechanism to therapy. *Drug Discov Today* **19**, 963-971, doi:10.1016/j.drudis.2014.02.014 (2014).
- 10 Menzies, F. M., Fleming, A. & Rubinsztein, D. C. Compromised autophagy and neurodegenerative diseases. *Nat Rev Neurosci* **16**, 345-357, doi:10.1038/nrn3961 (2015).
- 11 Finkbeiner, S. Huntington's Disease. *Cold Spring Harb Perspect Biol* **3**, doi:10.1101/cshperspect.a007476 (2011).
- 12 Vonsattel, J. P. & DiFiglia, M. Huntington disease. *J Neuropathol Exp Neurol* **57**, 369-384 (1998).
- 13 Vonsattel, J. P., Myers, R. H., Stevens, T. J., Ferrante, R. J., Bird, E. D. & Richardson, E. P., Jr. Neuropathological classification of Huntington's disease. *J Neuropathol Exp Neurol* **44**, 559-577, doi:10.1097/00005072-198511000-00003 (1985).

- 14 Waelter, S., Boeddrich, A., Lurz, R., Scherzinger, E., Lueder, G., Lehrach, H. & Wanker, E. E. Accumulation of mutant huntingtin fragments in aggresome-like inclusion bodies as a result of insufficient protein degradation. *Mol Biol Cell* **12**, 1393-1407, doi:10.1091/mbc.12.5.1393 (2001).
- 15 Landles, C. & Bates, G. P. Huntingtin and the molecular pathogenesis of Huntington's disease. Fourth in molecular medicine review series. *EMBO Rep* **5**, 958-963, doi:10.1038/sj.embor.7400250 (2004).
- 16 Metcalf, D. J., Garcia-Arencibia, M., Hochfeld, W. E. & Rubinsztein, D. C. Autophagy and misfolded proteins in neurodegeneration. *Exp Neurol* **238**, 22-28, doi:10.1016/j.expneurol.2010.11.003 (2012).
- 17 Nixon, R. A. The role of autophagy in neurodegenerative disease. *Nat Med* **19**, 983-997, doi:10.1038/nm.3232 (2013).
- 18 Martin, D. D., Ladha, S., Ehrnhoefer, D. E. & Hayden, M. R. Autophagy in Huntington disease and huntingtin in autophagy. *Trends Neurosci* **38**, 26-35, doi:10.1016/j.tins.2014.09.003 (2015).
- 19 Ravikumar, B. & Rubinsztein, D. C. Role of autophagy in the clearance of mutant huntingtin: a step towards therapy? *Molecular aspects of medicine* **27**, 520-527 (2006).
- 20 Park, H., Kang, J.-H. & Lee, S. Autophagy in neurodegenerative diseases: A hunter for aggregates. *International journal of molecular sciences* **21**, 3369 (2020).
- 21 Nixon, R. A. The role of autophagy in neurodegenerative disease. *Nature medicine* **19**, 983-997 (2013).
- 22 Corti, O., Blomgren, K., Poletti, A. & Beart, P. M. Autophagy in neurodegeneration: New insights underpinning therapy for neurological diseases. *Journal of neurochemistry* **154**, 354-371 (2020).
- 23 Li, J. Y., Popovic, N. & Brundin, P. The use of the R6 transgenic mouse models of Huntington's disease in attempts to develop novel therapeutic strategies. *NeuroRx* **2**, 447-464, doi:10.1602/neurorx.2.3.447 (2005).
- 24 Mangiarini, L., Sathasivam, K., Seller, M., Cozens, B., Harper, A., Hetherington, C., Lawton, M., Trotter, Y., Lehrach, H. & Davies, S. W. Exon 1 of the HD gene with an expanded CAG repeat is sufficient to cause a progressive neurological phenotype in transgenic mice. *Cell* **87**, 493-506 (1996).
- 25 Hickey, M., Gallant, K., Gross, G., Levine, M. & Chesselet, M.-F. Early behavioral deficits in R6/2 mice suitable for use in preclinical drug testing. *Neurobiology of disease* **20**, 1-11 (2005).
- 26 Carter, R. J., Lione, L. A., Humby, T., Mangiarini, L., Mahal, A., Bates, G. P., Dunnett, S. B. & Morton, A. J. Characterization of progressive motor deficits in mice transgenic for the human Huntington's disease mutation. *Journal of Neuroscience* **19**, 3248-3257 (1999).
- 27 Abushouk, A. I., Negida, A., Elshenawy, R. A., Zein, H., Hammad, A. M., Menshawy, A. & Mohamed, W. M. C-Abl inhibition; a novel therapeutic target for Parkinson's disease. *CNS & Neurological Disorders-Drug Targets (Formerly Current Drug Targets-CNS & Neurological Disorders)* **17**, 14-21 (2018).
- 28 Saglio, G., Kim, D.-W., Issaragrisil, S., Le Coutre, P., Etienne, G., Lobo, C., Pasquini, R., Clark, R. E., Hochhaus, A. & Hughes, T. P. Nilotinib versus imatinib for newly diagnosed chronic myeloid leukemia. *New England Journal of Medicine* **362**, 2251-2259 (2010).

List of publications

1. **Kumar MJV**, Shah D, Giridharan M, Yadav N, Manjithaya R, Clement JP. Spatiotemporal analysis of soluble aggregates and autophagy markers in the R6/2 mouse model. *Sci Rep.* 2021;11(1):96.
2. Chakraborty R, **Vijay Kumar MJ**, Clement JP. Critical aspects of neurodevelopment. *Neurobiol Learn Mem.* 2021;180:107415
3. Reversing developmental switch of GABA evoked chloride ion current flow corrects synaptic and behavioural deficits in *Syngap1*^{+/-} mice. Verma V, **M J Vijay Kumar**, Kavita Sharma, Sridhar Rajaram, Ravi Muddashetty, Ravi Manjithaya, Thomas Behnisch, Clement JP (under revision in eNeuro).

Chapter- 1 Introduction

The brain is the centre of our pleasures, joys, laughter, jests, and as well as our sorrows, pain, grief, and tears. It makes us think, walk, see, hear, and perform various everyday activities. Although understanding the function of the brain is still in its infancy, archaeological evidence suggests that ‘trepanation’, a form of primitive brain surgery that involved boring a hole through the skull, was widely practised in the prehistoric era.^{1,2} Old cave paintings from the stone age hint at people believing such practices would aid in healing migraines, mental disorders, and epileptic seizures in the conviction that surgery would allow evil spirits to escape.

Over the years, research has made enormous progress in deciphering the mystery of how the brain with 86 billion neurons and 85 billion non-neuronal cells create a network of connections and, potentially, stores and process more information than a supercomputer^{3,4}. Considering that the brain is the principal organ of the central nervous system which controls, and coordinates most of the activities of the body by processing, and integrating various signals received by the sensory systems, as mentioned earlier, one of the most critical functions is to balance and coordinate different muscular activities such as walking, writing, or holding a glass of water. The region of the brain that controls and regulates these activities is the motor cortex^{5,6}. The motor cortex facilitates the motor functions with associated regions such as the striatum, substantia nigra, and thalamus. The impairment in the function of these regions results in neurodegenerative diseases (NDDs) such as Parkinson’s disease (PD), Amyotrophic Lateral Sclerosis (ALS), and Huntington’s disease (HD)⁷⁻¹⁰. Studies have shown that the accumulation of misfolded proteins such as β -AMYLOID, α -SYNUCLEIN, and HUNTINGTIN are due to defects in protein homeostasis and is the primary cause for many age-related neurodegenerative disorders^{11,12}. Therefore, maintaining proteostasis is essential for healthy neuronal connections which facilitates proper motor function and coordination. The work carried out in this thesis, is mainly centred on how proteostasis dysfunction plays a role in the pathophysiology of HD, mainly focussing on autophagy dysfunction.

1.1 Protein homeostasis

Protein homeostasis (proteostasis) is regulated by maintaining the balance between the synthesis and degradation of proteins¹¹. Many complex and extensive signalling pathways play a vital role in safeguarding the cells from proteotoxic stress. Thus, the proteostasis network acts as a quality control check that regulates the biogenesis, folding, trafficking, subcellular localisation, and degradation of proteins. Many processes mediate this proteostasis network

^{13,14}. For example, the chaperone-mediated mechanism ensures the proper folding of the protein into its native functional conformational state, and protein degradation pathways such as ubiquitin-proteasome system (UPS) and autophagy degrade the misfolded and toxic form of proteins ¹⁵. The regulation of all these processes is critical for a cell to maintain a functional proteome and to reduce the toxicity associated with various mutations that lead to misfolded/damaged proteins. Removal of the toxic form of proteins (misfolded/aggregates) is crucial for all the cell types, but it is indispensable and significant in post-mitotic cells, such as neurons which cannot be replaced and cannot remove the aggregates retaining them in the parent cell during the process of cell division ¹⁶. Neurons are more susceptible to detrimental age-related metabolic changes than any other cell types and several interrelated factors contribute to this susceptibility. In the adult brain, damaged neurons are not replaced and after injury central axons do not regenerate completely ¹⁷. Although neurogenesis can take place in certain areas of the hippocampus and olfactory bulb, this process eventually slows down with ageing and the integration of newly formed neurons into functional networks becomes limited ^{18,19}. During pregnancy and infancy, the human brain grows fast, the size and the volume increases significantly, and such changes are often associated with very large energy demands. During childhood, the brain may account for up to ~60 % of the body basal energy requirements ^{20,21}. Moreover, local protein synthesis at synapses requires high energy and neuronal ATP requirements increase with ageing. These increased ATP requirements with ageing are possibly due to the reduction in the efficiency of energy utilization by aged neurons, however, the precise reason is not yet understood ²².

The production of ATP by oxidative phosphorylation leads to the release of oxidative free radicals that progressively damage neuronal DNA, proteins, and lipids. Therefore, in the absence of neuronal turnover, oxidative damage accumulates with ageing making the neurons more vulnerable to death ^{23,24}. In addition, chaperones such as heat shock proteins have a higher threshold for activation and show low expression levels in neurons compared to other cell types. For example, induction of HSP 70 by HSF1 is lower in neurons than non-neuronal cells ^{25,26}. Protein degradation by UPS is highly dependent on ATP ²⁷. Age-related changes in neuronal ATP balance/requirement are likely to have a significant effect on the capacity of the UPS. Additionally, mitochondrial proteins and components of energy metabolic pathways are substrates of UPS indicating a significant cross-talk between neuronal energy metabolism and protein turnover ²⁸⁻³⁰. Therefore, maintenance of protein homeostasis in neurons is essential for

healthy ageing, and any imbalance or dysregulation leads to neurodegenerative diseases ^{11,31} (Figure 1-1).

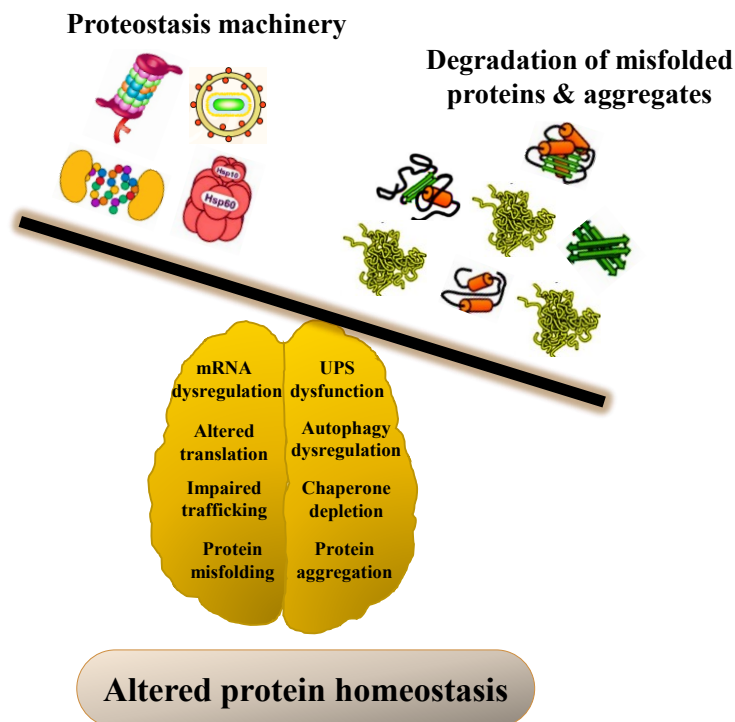


Figure 1-1 Diagram illustrating the intraneuronal proteostasis network

All the cellular processes like protein biogenesis, folding, trafficking and degradation are controlled regulated inside the cell to maintain protein homeostasis. Any imbalance in the protein homeostasis due to degradation pathways leads to the accumulation of misfolded proteins forming aggregates. Image source: adapted from ^{11,32}.

1.2 Protein aggregation in neurodegenerative diseases

Protein aggregates are defined as an association of two or more protein complex molecules in a non-native conformation state and comprise a broad range of structures from amorphous assemblies to higher ordered amyloid fibrils with crosslinked β -structures ^{33,34}. The propensity of a specific protein to form aggregates is primarily driven by the chemical properties of its amino acid sequence, the native conformational stability of its folded state, and its cellular concentration ^{33,34}. High protein concentration inside the cells results in excluded-volume effects and substantially increasing the tendency of non-native protein molecules to aggregate. Approximately 30 % of proteins in higher eukaryotes contain intrinsically unstructured regions, and these proteins often exist in metastable conformational states forming toxic aggregates as seen in neurodegenerative diseases such as α -SYNUCLEIN in Parkinson's disease (PD),

amyloid- β , and TAU in Alzheimer's disease (AD) and HUNTINGTIN in Huntington's disease (HD) ^{33,35,36}.

Cellular dysfunction and neuronal death in neurodegenerative diseases happen to be mainly caused by a subset of highly toxic aggregate species, including diffusible, oligomeric forms that lack ordered fibrillar topology ³⁴. These aggregate species are dynamic and structurally ill-defined and expose hydrophobic residues on unpaired β -strands that provide sticky surfaces for aberrant interactions with other cellular proteins and membranes ³⁴. Multiple endogenous proteins that are often newly synthesised containing extensive disordered regions and certain chaperones are sequestered with toxic aggregate species in many neurodegenerative diseases ³⁶. Notably, there is an increasing body of evidence that sequestration of oligomers into large insoluble deposits are neuroprotective, presumably by reducing the interaction with the solvent-exposed surface of the aggregate molecules ³⁷. However, inclusion body formation may be actively advocated by the proteostasis network in aged cells, these deposits are highly unlikely to be entirely harmless ³⁵. The causative reasons for aggregate formation in neurodegenerative diseases are not only the result of insufficient proteostasis capacity of the neuronal cells but also the imbalance in the proteostasis network by overburdening the chaperone activity and degradation pathways, leading to proteostasis collapse and neuronal death ^{14,38}. The failure of the neuronal cells to maintain proteostasis does not appear to be random; there are spatial and temporal patterns of inclusion body formation during the disease progression and the overall load of aggregates connects very well with the advancement and increased severity of pathological changes. ^{11,38,39}.

Studies have shown that different cell types and distinct brain regions vary in their proteostasis capacity and their ability to respond to different forms of stress ⁴⁰. A precise characterisation of these differences could facilitate understanding why neurons are more vulnerable to aberrant protein folding than others and why ubiquitously expressed proteins aggregate only in certain tissues. Pharmacological intervention to upregulate proteostasis capacity may begin to have new opportunities to combat neurodegeneration and cell death. This may be achieved by enhancing the protein degradation pathway such as autophagy ⁴¹. In any circumstance, restoring proteostasis balance should occur at an early stage of the disease before the manifestation of severe cellular dysfunction ⁴².

1.3 Autophagy

Autophagy is an intracellular degradative pathway that involves the delivery of cytoplasmic cargo sequestered inside double-membrane vesicles to the lysosomes⁴³. This cellular process of self-digestion not only provides energy supplements to maintain vital physiological functions during conditions such as starvation but also to get rid of toxic, superfluous, components such as damaged organelles, misfolded protein aggregates and pathogenic microorganisms⁴⁴⁻⁴⁶.

Identified by Christian de Duve in the 1950s, the lysosome is a membrane-bound organelle that contains various hydrolytic enzymes that drives the degradation process under an acidic pH^{47,48}. In the mid-1990s, Ohsumi and his colleagues uncovered the process of macroautophagy in yeast and were awarded the 2016 noble prize in Physiology and medicine^{49,50}. The delivery of the cargo into the lysosomal lumen is mediated by two trafficking pathways: Endocytosis transports extracellular, transmembrane bound cellular constituents; and autophagy transports cytosolic substrates using three different pathways: microautophagy, chaperone-mediated autophagy (CMA), and macroautophagy⁵¹⁻⁵³. Neurons were one of the first cell types used in the identification and ultrastructural characterisation of the macroautophagy pathway^{54,55}. The molecular machinery of this pathway is currently composed of more than 30 autophagy-related (ATG) genes in yeast, of which 18 have mammalian homologs⁵⁶⁻⁵⁸.

The autophagy mechanism starts with the initial steps of formation (vesicle nucleation) and expansion (vesicle elongation) of an isolation membrane called a phagophore. The edges of the phagophore eventually fuse (vesicle completion) to form autophagosomes, a double membraned structure that capture the cytoplasmic constituents. This step is followed by the fusion of autophagosomes with the lysosomes to form autolysosomes, where the captured cargo is degraded by acid hydrolases, and the building blocks thus generated are recycled back to the cytoplasm^{56,59} (**Figure 1-2**).

The primary process in autophagy is the synthesis of double-membrane autophagosomes which is divided into three steps: induction and nucleation, expansion, and maturation⁴³. The autophagy related proteins play a role in each of these steps and can be categorised into six functional groups: the ULK1 protein kinase complex, the BECLIN1-ATG14L-VPS34 lipid kinase complex, the PI3P (phosphatidylinositol-3-monophosphate) binding proteins, ATG9, and the two ubiquitin-like conjugation systems.

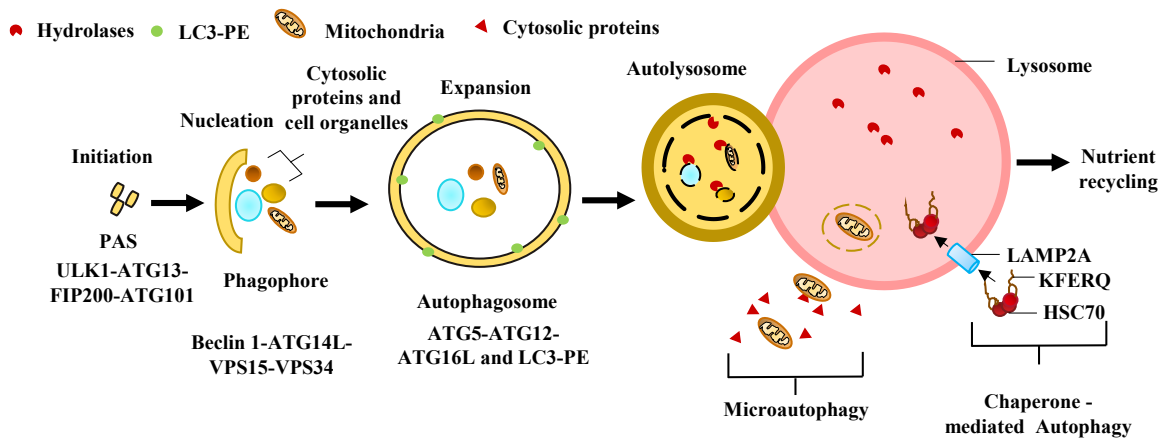


Figure 1-2 Overview of the autophagy pathway

The process of autophagy starts with the formation of a phagophore assembly site (PAS). This is mediated by the ULK1 complex consisting of ULK1, ATG13, FIP200, and ATG101. Nucleation requires the class III PI3K complex comprising of VPS34 along with ATG14L, VPS15, and BECLIN1. Phagophore membrane elongation and autophagosome maturation require two ubiquitin-like conjugation pathways. In the initial step, ATG5-ATG12 conjugate, which leads to the formation of a multimeric complex with ATG16L followed by conjugation of phosphatidylethanolamine (PE) to LC3. LC3-PE is required for the expansion of autophagosome membranes and their ability to recognise autophagic cargoes and the fusion of autophagosomes with lysosomes. The resulting autophagosome fuses with lysosomes forming autolysosome. In microautophagy, substrates are directly engulfed at the boundary of the lysosomal membrane. In CMA, substrates with pentapeptide motif KFERQ are selectively recognised by HSC70 chaperone and translocated to lysosomes in a LAMP2A dependent manner. PI3K - Phosphoinositide 3-kinase; LC3 – Light chain 3; CMA – Chaperone-mediated autophagy; LAMP2A – Lysosome-associated membrane protein 2A. Image source: Modified with permission from Copyright Clearance Center, Inc. Elsevier. ⁶⁰

The induction of autophagy is regulated by the phosphorylation status of the ULK1 complex, which drives the nucleation of the isolation membrane or the phagophore ⁵⁹. In the next step, the BECLIN1-ATG14L-VPS34 lipid kinase complex enriches the site with PI3P to recruit the PI3P binding proteins such as WIP1 and DFCP1 ⁵⁹. At present, the source for isolation membrane is heavily debated, however, the membrane origin differs depending on the type of autophagy that is induced or the cell type that is studied ⁶¹⁻⁶³. Once the isolation membrane is formed, the membrane expands and captures the cargo. This process requires the functions of the final three groups: ATG9 and two ubiquitin-like conjugation systems. How ATG9 promotes in elongation process is still unclear, but the membrane-spanning protein that shuttles across the different vesicles, and toward different membrane sources contribute to the autophagosome expansion ⁵⁹.

The two ubiquitin-like conjugation systems elongate the forming autophagosome membrane by driving a key reaction: lipidation of LC3 and its homologs to the PE (phosphatidylethanolamine) to the autophagosome membrane. The lipidation process is completed by two distinct reactions: the first forms an E3-ubiquitin ligase known as the ATG12-ATG5-ATG16L complex, and the second converts cytosolic ATG8 to its lipidated form. As the autophagosome membrane formation completes, the ATG12-ATG5-ATG16L complex leaves the outer membrane, with ATG8 bound to the autophagosome membrane. The presence of ATG16L on the vesicles originating from the plasma membrane suggests another membrane source for the elongation but how ATG16L associates with the membrane are not known⁶⁴. The ATG8 mammalian homolog LC3 (microtubule-associated protein 1 light chain 3) is the only marker for autophagosome membrane. The mammalian cells have multiple ATG8 homologs, and all facilitate the lipidation of the autophagosomes. The LC3 family has three isoforms A, B, and C of which LC3B is first identified and LC3C is only present in humans⁶⁵⁻⁶⁷.

The GABA(A) receptor-associated proteins family has three members that include GABARAP, GABARAP-like protein 1 (GABARAPL1), GABARAP-like protein 2 (GABARAPL2). LC3B, LC3C, and all GABARAPs are highly expressed in the brain⁶⁸. As the name implies, GABARAP proteins interact with GABA(A) receptors and regulate their trafficking in the neuronal cells. In the next step, the autophagosomes deliver their cargo to the lysosomes for degradation⁵⁹. Mammalian autophagosomes fuse into the endolysosomal system to form an amphisome and then an autolysosome. Amphisome formation depends on the proteins that are implicated in the biogenesis of multivesicular bodies (MVBs), specialised late endosomes that sort endocytic proteins for lysosomal degradation⁶⁹. The dependence on MVBs has led to the hypothesis that amphisome formation may increase the efficiency of lysosome-mediated degradation. Especially in neuronal cells, amphisome formation may be valid since autophagosomes need to travel long distances along the axons before the degradation occur^{70,71}.

1.4 Aggrephagy: The selective degradation of aggregates

The accumulation of ubiquitinated protein aggregates is the hallmark of many adult-onset severe neurodegenerative diseases and many seminal studies have proposed the role of aggrephagy to intervene in disease progression and prevention^{59,72,73}. Aggrephagy is a form of macroautophagy where it selectively degrades accumulated and aggregated intracellular

ubiquitinated proteins. Aggrephagy relies on the adaptor proteins such as p62/SQSTM1, (Sequestosome-1) NBR1 (Neighbour of BRCA1), and ALFY (Autophagy-linked FYVE protein), the only identified selective adaptor protein^{65,74}. ALFY is a highly conserved domain protein across the species that mediates the interaction of the p62 and NBR1 positive proteins to the ATG12-ATG5 and PI3P complex. ALFY is most abundantly expressed in the brain⁷⁵ and its overexpression can promote the degradation of aggregates in the primary cortical neurons⁶⁵. Studies have also shown that ALFY promotes autophagic clearance of misfolded proteins in mouse models of HD and ALS^{72,76}. OPTN (Optineurin) has been recently implicated in the aggregate turnover and recognises protein aggregates with its c-terminal coiled-coil domain in a ubiquitin independent manner⁷⁷. Moreover, the recent study conducted using cortico-striatal slice cultures reported that protein aggregates can be cleared in a macroautophagy-dependent manner and that aggregating proteins are preferentially degraded over bulk cytoplasm⁷⁸. Together, these studies strongly indicate that aggrephagy play a crucial role in maintaining the proteome of the neuronal cells^{56,65,74}.

1.5 Neuronal autophagy

All forms of autophagy were detected under starvation conditions and the resulting biochemical studies revealed that, at the cellular level, starvation is translated into signalling through the large, serine/threonine kinase mTOR (mammalian target of rapamycin)^{59,79,80}. mTOR is found in two different complexes: mTORC1 and mTORC2 and mTORC1 act as a negative regulator of autophagy. Autophagic response to mTORC1 inhibition is robust and profound in most organs, but the response in the brain is very limited⁸¹. One of the studies has shown that autophagy in the brain is highly regulated and cannot be modulated as observed in other peripheral tissues. Acute starvation in the transgenic mice expressing GFP-LC3 (green fluorescent protein-tagged Light Chain 3) triggers a rapid increase in the GFP-LC3 positive autophagosomes in the liver, muscle, heart, but rarely in the brain, despite the strong expression in the neuronal cells and glia⁸². The differential response to mTORC1 reflects the physiology of the vertebrate brain in comparison with peripheral organs such as the liver. The brain is the highest consumer of energy, glucose metabolism is tightly regulated in the neuronal cells^{83,84}. Under nutrient deprivation conditions, hepatocytes account for as much as 75 % of protein breakdown, but whereas in the brain, it is very minimal⁸⁵⁻⁸⁷. Therefore, the brain's drive to degrade proteins in response to mTORC1 inhibition is reduced. Biochemical measures that are used to scale the LC3 lipidation are difficult to detect in the neural tissue⁸⁸. The two possible

reasons for the scarcity of autophagosomes in healthy neurons are (i) autophagy activity is maintained at a low level in the brain and (ii) the other reason is that autophagic degradation is so efficient that autophagosomes cannot be accumulated in healthy neurons at a detectable level⁸⁸.

Genetic studies have firmly established that basal autophagy is essential for the development of a healthy brain. Many seminal studies have shown that deletion of core autophagy genes such as *Atg5* and *Atg7* in brain-specific knockout mouse models resulted in the accumulation of toxic intra-neuronal aggregates⁸⁹⁻⁹¹. Knockout of *Atg7* resulted in the loss of Purkinje neurons of the cerebral and cerebellar cortices⁹⁰ and loss of *Beclin-1*, *Atg5*, and *Atg7* resulted in the degeneration of individual Rhodopsin neurons of the retina^{92,93}. Further, deletion of core ATG genes resulted in reduced survival with early-onset and progressive loss of neuronal cells across different regions of the brain^{89,90}. In addition, as mentioned earlier, brain-specific knockout of *Atg5* causes neurodegeneration in mice, whereas overexpression of *Atg5* increases the life span⁹⁴. The lifespan extension after autophagy induction has also been corroborated in a knock-in *Beclin1* mouse model, where they show a clear increase in life span⁹⁵. One of the studies has shown that wild-type mice under starvation conditions, can survive for approximately 20 hrs after birth. Whereas *Atg5* knock out mice die within 12 hrs after birth, indicating that under starvation conditions, autophagy is essential for the survival of the mice. Most importantly, when *Atg5* is expressed only in the brain under a neuron-specific promoter, mice survived with abnormalities in the organs⁹⁶. So, these studies imply that maintenance of autophagy in the neurons is essential for the basic physiology and survival of an individual and is compromised in many NDD's.

Apart from protecting the neuronal cells from degeneration, autophagy plays a crucial role in neurogenesis. Autophagy is highly active during development from early preimplantation and maintains postnatal neural stem cells and promotes neurogenesis during the embryonic period^{56,97}. Essential ATG proteins BECLIN-1 and AMBRA1 were highly expressed in SVZ from early neurulation onwards, and deletion of one of the alleles for the *Beclin-1* gene resulted in decreased cell proliferation in-vitro⁹⁸. Heterozygosis of *Beclin-1* resulted in increased apoptotic cell death and augmented the sensitivity to DNA-damaged induced cell death⁹⁸. In the adult brain, neural stem cells (NSCs) within the subgranular zone (SGZ) of the dentate gyrus and sub-ventricular zone (SVZ) of the lateral ventricle can produce new functional neuronal cells in response to physiological and pathological stimulus⁹⁹. Deletion of *Atg5* in adult NSCs in dentate gyrus also resulted in impairment in neuronal maturation, thereby,

affecting the survival rate ¹⁰⁰. In supporting these studies, upregulation of autophagy is found to be protective in *C. elegans* in different contexts like nutrient restriction ¹⁰¹, and mitochondrial turnover ¹⁰². Overexpression of essential *atg* gene, *dmeI/atg8a*, in *Drosophila* resulted in extended lifespan ¹⁰³, and overexpression of *Atg5* in mice extended lifespan with increased insulin sensitivity and improved motor function ⁹⁴. In Huntington's disease (HD), for example, deletion of polyglutamine expansion from endogenous HTT-coding gene was found to be beneficial with an increase in autophagosome biogenesis with a significant increase in lifespan ¹⁰⁴. Thus, upregulation of basal autophagy in animals is observed to be effective and beneficial in protecting the neuronal cells from dying during ageing.

1.6 Autophagy in neurodegenerative diseases

There is an increasing body of evidence for the physiological importance of autophagy in neuronal health raising the possibility that autophagy dysfunction may play a significant role in the pathogenesis of neurodegenerative diseases (NDDs) ¹⁰⁵⁻¹⁰⁷. This is further supported by the fact that intraneuronal aggregates of misfolded proteins are the substrates for autophagic degradation. Most of the NDDs do not follow a simple, monogenic pattern of inheritance. However, in all major NDDs, a division of cases are associated with the inherited genetic mutations. These familial forms of disease provide an insight into the disease-causing mechanisms that enable delineating the pathways responsible for autophagy dysfunction ^{105,108}. Investigation of disease-associated genes and investigations into their functions indicate that many affect the autophagy process (**Figure 1-3**). Since many NDDs are late-onset, even small perturbations in the protein turnover may have cumulative effects that manifest later in life ¹⁰⁹. Since the autophagy pathway is complex with multiple steps and modes of regulation, it would be challenging to ascertain the exact cause for autophagy dysfunction in various NDDs ¹¹⁰.

1.6.1 Alzheimer's disease

The pathological hallmarks of AD are the accumulation of intracellular TAU tangles and extracellular β -amyloid plaques ¹¹¹. There is a complex interplay between β -amyloid ($A\beta$) and autophagy and studies have shown that upregulation of autophagy reduces the level of $A\beta$ in many cellular and rodent model systems ¹¹²⁻¹¹⁵. However, $A\beta$ is generated in autophagosomes which contains both amyloid precursor protein (APP) and PRESENILIN-1 (PS-1), an enzyme implicated in the cleavage of APP to $A\beta$ ^{112,116}.

Studies have shown that deletion of *Atg7* in APP transgenic mice significantly reduced the extracellular secretion of A β and plaque formation¹¹⁷. Genetic studies have implicated the role of phosphatidylinositol-binding clathrin assembly protein (PICALM) in AD, where differential changes in the expression of this protein have been observed in patients with AD¹¹⁸⁻¹²¹. PICALM is a clathrin adaptor protein essential for the endocytosis of soluble NSF attachment protein receptors (SNAREs), and loss of this function has been shown to disrupt autophagy at multiple steps, including autophagosome formation and maturation¹²². Altered trafficking of these SNAREs is likely to affect other vesicle trafficking pathways, that contribute to the disease pathogenesis. PICALM forms a complex with assembly polypeptide 2 (AP2) and acts as an autophagy receptor interacting with LC3, thereby targeting APP into autophagosomes¹²³.

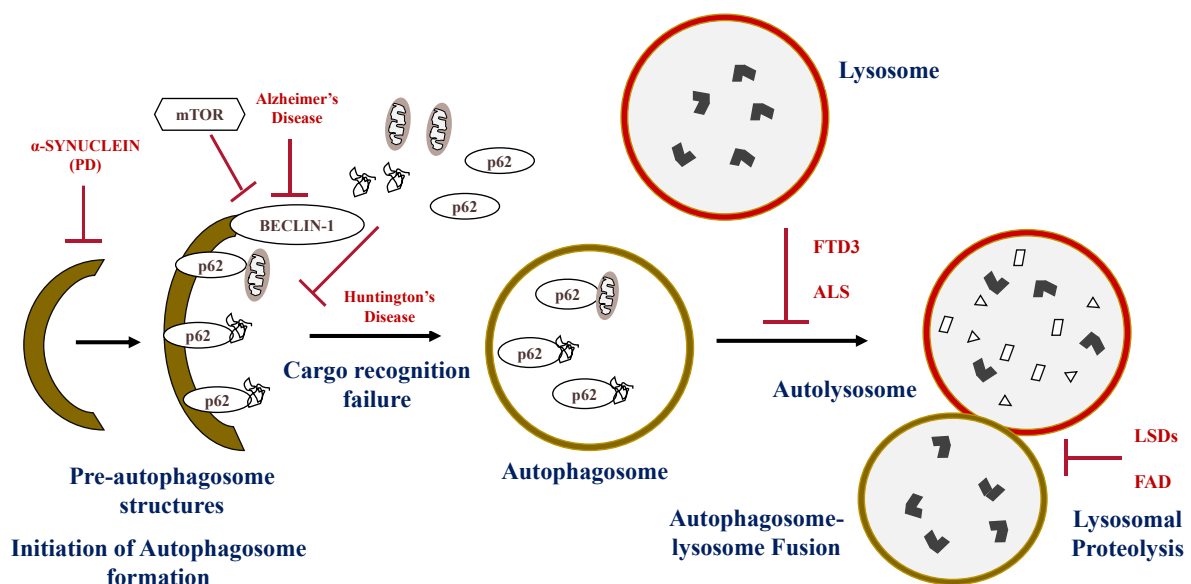


Figure 1-3 Impaired autophagy mechanism in neurodegenerative diseases

This diagram illustrates how autophagy is compromised at different steps in various neurodegenerative diseases. In PD, autophagy is impaired at the initiation of phagophore formation level. Cargo recognition failure in HD, and incomplete formation of autophagosomes in AD. In FTD3, and ALS, autophagy is dysfunctional at the fusion state of autophagosomes with lysosomes and in LSDs and FAD, lysosomal proteolysis is affected. All these factors contribute to the accumulation of specific protein aggregates associated with several neurodegenerative diseases. Image source: Adapted from¹²⁴

Mutations in PS-1 cause familial AD and have been shown that these mutations change according to the processing of APP protein contributing to disease pathogenesis¹²⁵. PS-1 function as an ER chaperone for the V0A1 subunit of lysosomal v-ATPase and mutations in PS-1 lead to decreased maturation of lysosomal ATPase, thereby increasing the lysosomal pH which reduces autophagosome clearance¹²⁶⁻¹²⁸. Post-mortem brain samples from patients with AD show reduced levels of *Beclin 1* mRNA and protein and are thought to be decreased due to the increased activity of CASPASE-3 in the brains of AD patients affecting the autophagy pathway^{129,130}.

Accumulation of TAU protein into intracellular tangles is one of the characteristic features of AD pathogenesis and is observed in a group of neurological disorders termed tauopathies, which include frontotemporal dementia (FTD), supranuclear palsy (PSP), and cortico-basal degeneration (CBD)¹³¹. Hyperphosphorylated TAU co-localises with LC3-positive vesicles and autophagy cargo-receptor p62 in PSP and CBD patients rendering their activity¹³². Moreover, aberrant TAU disrupts axonal vesicle transport by impairing the dynein-dynactin complex, thus increasing the number of autophagosomes, and contributing to TAU-induced toxicity in AD and FTDs^{133,134}. It has also been reported that TAU binds to lysosomal membranes perturbing the lysosomal permeability in vitro and an AD mouse model^{135,136}. AD patients show defective lysosomal membrane integrity and studies have shown increased levels of lysosomal-associated membrane protein-1 (LAMP1) and cathepsin D in PSP and CBD patients¹³².

In the AD brain, dystrophic and degenerating neurites have an excess of autophagosomes, which is a major intracellular reservoir of toxic peptide¹³⁷. This leads to massive accumulation of immature autophagosome vesicles within the senile neurons, including increased initiation of autophagy flux, retrograde transport of vesicles and their defects in the lysosome maturation^{111,112,138}. The accumulation of autophagosomes in dystrophic neurons contributes to the generation of A β peptides which is attained by increased turnover of APP and enrichment of γ -secretase complex. However, in the APP/PS1 double transgenic mouse model, the formation, and accumulation of autophagosome vesicles is mediated by activation of AMPK^{111,112,138}.

Enhancement of autophagy reduces AD-related phenotypes in animal models. Rapamycin treatment resulted in a reduction of A β deposition and extended longevity in AD mouse models^{139,140}. For example, in Tg2567 mice, rapamycin treatment reduces the A β burden and restore synaptic and cognitive functions¹⁴¹. Trehalose, an mTOR independent autophagy enhancer

decreases TAU aggregates in a neuronal cell model of tauopathy and suppresses the accumulation of A β aggregates^{142,143}.

1.6.2 Parkinson's disease

PD is characterised by the presence of toxic α -SYNUCLEIN (α -SYN) inclusions leading to the loss of dopaminergic neurons in the substantia nigra pars compacta (SNpc)¹⁴⁴. In neurons with α -SYN inclusions, although the lysosomal function is unaffected, they show reduced autophagosome maturation and fusion with lysosomes resulting in decreased protein degradation by autophagy¹⁴⁵. It is shown that the alteration in vesicle trafficking is not from non-physical blockade of axons by inclusions but, rather specific inhibition of endocytic and autophagic vesicles¹⁴⁶. Irrespective of the formation of inclusion bodies, elevated levels of α -SYN in cell and mouse models led to mislocalisation of ATG9 impairing the autophagy flux¹⁴⁷. Mutations in vacuolar protein sorting-associated protein 35 (VPS35) causes ATG9 mislocalisation and autophagy impairment. VPS35 is a component of the retromer complex, that recruits the actin nucleation-promoting WASP and Scar homolog (WASH) complex to endosomes. D620N mutation in VPS35 prevents this recruitment causing abnormal trafficking of ATG9¹⁴⁸. Extensive research has provided enough evidence for the role of dysfunctional autophagy as a causative factor in PD¹⁴⁹.

The autosomal recessive familial form of early-onset PD is associated with mutations in genes encoding E3 ubiquitin ligase Parkin and phosphatase and tensin homolog-induced putative kinase 1 (PINK1)^{150,151}. PARKIN and PINK1 function in the same pathway to promote mitophagy. PINK1 is stabilised on the outer membrane of damaged mitochondria, leading to the recruitment and activation of PARKIN, and ultimately sequestration of damaged mitochondria into autophagosomes^{152,153}. Several mouse models have been generated to elucidate the function of the proteins associated with mitophagy in the brain. The activity of mitochondria in the striatal neuron was impaired in *Parkin* knock out (KO) mice with no gross behavioural changes and also display a deficit in evoked dopamine release response and striatal synaptic plasticity in the striatum¹⁵⁴⁻¹⁵⁶. Deletion of PINK1 resulted in increased sensitivity to oxidative stress and also shown reduced ATP production¹⁵⁷. Moreover, dopaminergic neurons derived from PINK1 KO mice show defective morphology with reduced activity¹⁵⁸. PINK1 interacts with BECLIN-1 and significantly enhances basal, and starvation-induced autophagy¹⁵⁹. A recent study presented that upon mitochondrial depolarization, PINK1 interacts and phosphorylates BCL-XL, an anti-apoptotic protein shown to inhibit autophagy through its

binding to BECLIN-1. PINK1-BCL-XL interaction safeguards cell from death by hindering the pro-apoptotic cleavage of BCL-XL, suggesting a novel cell survival mechanism ¹⁶⁰.

Loss-of-function mutations in P-type ATP13A2 cause early-onset parkinsonism ¹⁶¹. Mutations in ATP13A2 increases the lysosomal pH, impairing the fusion of autophagosomes with lysosomes leading to the accumulation of α -SYN inclusions thus contributing to disease pathogenesis in the familial form of PD ¹⁶². Depletion of ATP13A2 leads to decreased levels of PD-associated gene SYNAPTOTAGMIN 11 (SYT11) that causes lysosomal dysfunction and impaired autophagosome degradation. Overexpression of SYT11 in ATP32A knockdown cells has been shown to rescue autophagy defects, demonstrating that they both act in the same pathway ¹⁶³. Mutant forms of α -SYN (A30P and A53T) have been shown to inhibit chaperone-mediated autophagy and display a high binding capacity to lysosomal-associated membrane protein 2A (LAMP-2A) than wild-type α -SYN ^{144,164,165}. It has also been reported that activation of autophagy in primary cortical neurons expressing mutant A53T α -SYN leads to loss of mitochondria leading to severe energy deficit causing neuronal degeneration. This data suggests that overactivation of mitochondria degradation by autophagy could be one of the causative factors that leads to the mitochondrial loss observed in PD models ¹⁶⁶. Another study showed that the lysosomal binding of several pathogenic mutant LRRK2 proteins disrupted the organisation of the CMA translocation complex, resulting in defective CMA. These studies demonstrate that the defects in both autophagy activation and lysosomal clearance contribute to the pathogenesis in PD models ^{105,106}.

1.6.3 Amyotrophic Lateral Sclerosis (ALS)

ALS is a rapidly progressing severe form of neurodegenerative disorder that selectively target motor neurons with uncertain pathogenesis ^{167,168}. Several studies on transgenic mouse models and human post-mortem brain tissues demonstrate that the degeneration process of motor neuron comprises of multiple pathological events such as glutamate excitotoxicity, neuroinflammation, mitochondrial degeneration, oxidative stress, cytoskeletal abnormalities, abnormalities in growth factors and formation of protein aggregates leading to cell death ¹⁶⁹⁻¹⁷¹. Amongst these disease-causing mechanisms, plentiful aberrant protein species gets accumulate in the affected neuron due to the disturbances in the protein homeostasis and imply that impaired autophagy pathway may be involved in the pathogenesis of ALS ^{172,173}. Many ALS-associated genes are implicated in autophagy/lysosomal functions ¹⁰⁵. Indeed, accumulation of autophagosomes was detected in the spinal cord of sporadic ALS patients

suggesting autophagy dysfunction in ALS patients ¹⁷⁴. In addition, a recent study has reported that autophagic impairment in ALS is seen at an early stage of the disease progression and becomes profound at the terminal stage. For example, in the transgenic SOD1G93A mice, increased autophagy is detected during the presymptomatic stage (<90 days) and then become prominent at the age of 120 days ¹⁷⁵.

Haplosufficient BECLIN-1 display neuroprotective effects in mutant SOD 1 transgenic mice ¹⁷⁶. In the early symptomatic stage of disease, mutant SOD1 (G93A) transgenic mice, show increased expression of TFEB and BECLIN-1, whereas the levels of these proteins are decreased in the mid and end-stage of disease progression ¹⁷⁷. Trehalose treatment in mutant SOD1 (G93A) mice efficiently induced autophagy and cleared aggregate complexes of SOD1 and p62 thereby rescuing mitochondrial degeneration ¹⁷⁸. Moreover, Trehalose extended the life span and delayed the disease progression by enhancing the expression of key autophagy proteins such as ATG5, BECLIN-1, LC3, and p62, although the improvement of the disease may be due to the chaperone effect of Trehalose reducing aggregation of mutant SOD1 ¹⁷⁹. ALS tissues show abnormal accumulation of cytoplasmic aggregates of TDP-43 and many autophagy inducers such as tamoxifen, rapamycin, carbamazepine, and spermidine helped in the clearance of toxic TDP-43 aggregates and improve the motor functions in transgenic mice of ALS ¹⁸⁰. Other major mutations in ALS include hexanucleotide repeat expansions of GGGGCC in C9ORF72. This gene is involved in RAB dependent regulation of endosomal trafficking in autophagy and studies have shown that deletion of C9ORF72 impairs endocytosis and autophagy and contributes to disease pathogenesis in ALS ¹⁸¹.

Mutant SOD1 protein impairs axonal transport through inhibition of dynein/dynactin function in ALS mouse model with dynein mutation ¹⁸². Mutations in dynein or dynactin can impair autophagosome trafficking in the motor neurons. For instance, a mutation in DCTN1 encoding dynactin regulating the efficiency of dynein motor function has been implicated in the autosomal dominant form of lower motor neuron diseases ¹⁸³. Moreover, familial-ALS associated gene variants have provided enough evidence about the underlying pathological mechanisms and these causative/associated genes such as SOD1, SQSTM1 (p62), DCTN1, DYNC1H1 for motor neuron diseases are functionally linked to autophagy ¹⁸⁴⁻¹⁸⁷. It is now well accepted that as the disease progresses, there is increased accumulation of SOD1 mutants thereby causing autophagy dysfunction ¹⁸⁸. Autophagic clearance of SOD1 has been proven to be beneficial for motor neuron loss where heat-shock protein HSPB8 enhances the clearance of SOD1 by initiating autophagy in ALS mouse models ¹⁸⁹.

1.6.4 Huntington's disease (HD)

HD is an autosomal-dominant neurodegenerative disorder caused by an expansion of CAG repeats encoding a polyglutamine (polyQ) tract in the HUNTINGTIN (HTT) protein. Dysfunction of cellular proteolytic systems has been extensively linked to HD pathogenesis. The detection of different proteasome subunits in inclusion bodies of mutant HTT (mHTT) aggregates was one of the first links connecting HD with alterations in the proteolytic system¹⁹⁰. Defective macroautophagy has been ascribed in HD and upregulation of basal autophagy acts as a compensatory mechanism for both UPS and macroautophagy dysfunction¹⁹¹⁻¹⁹⁴.

mHTT protein forms intranuclear and perinuclear cytoplasmic inclusions in the neurons of HD patients and these can be targeted to degradation through autophagy pathway¹⁹⁵. Several studies have revealed that induction of autophagy leads to enhanced clearance of both aggregated and soluble monomeric species of mHTT and alleviates their toxicity in various cellular and mouse models of HD¹⁹⁶⁻¹⁹⁸. The role of autophagy in HD is strongly supported by the studies that show sequestration of mTOR by mHTT aggregates in the various cell, and transgenic mouse models, including humans, results in the decrease of mTOR activity and then induction of the autophagy pathway^{196,199}. The combined inhibition of mTORC1 and mTORC2 complexes is required for autophagy induction and degradation of mHTT aggregates, suggesting that multiple components of the mTOR pathway modulate HD pathogenesis²⁰⁰.

Moreover, the dysfunction of macroautophagy may enhance the chaperone-mediated autophagy (CMA) pathway in the early stages of HD (where the mHTT aggregate formation is not aggravated and the symptoms are not severe in 12 weeks¹¹¹Qhtt mice), but the efficiency of this compensatory mechanism may be decreased during ageing contributing to the cellular dysfunctions and the onset of pathologic manifestations of the disease phenotype^{193,201}. Despite the neuroprotective role of autophagy in HD models, the precise mechanisms underlying autophagy dysfunctions remains enigmatic. Cargo recognition failure has been shown to be responsible for impaired autophagy in HD. In these HD mouse models, and the neurons from HD patients, however, the rate of formation of autophagosome vesicle and fusion with lysosomes were normal, but the inability of autophagosomes to recognise and capture the cargo resulted in mHTT aggregate accumulation inside the neurons¹⁹¹. In addition, sequestration of essential autophagy proteins such as BECLIN-1 by mHTT aggregates results in impaired autophagy, and it has also been suggested that age-dependent reduction in BECLIN-1 expression result in the decreased autophagic activity aiding to autophagy dysfunction²⁰². It

has also been reported there is up-regulation and accumulation of adapter protein p62 in HD mouse model R6/2 and suggest that mHTT aggregates sequester p62 leading to both proteasome and autophagy dysfunction in HD ²⁰³ (Figure 1-4).

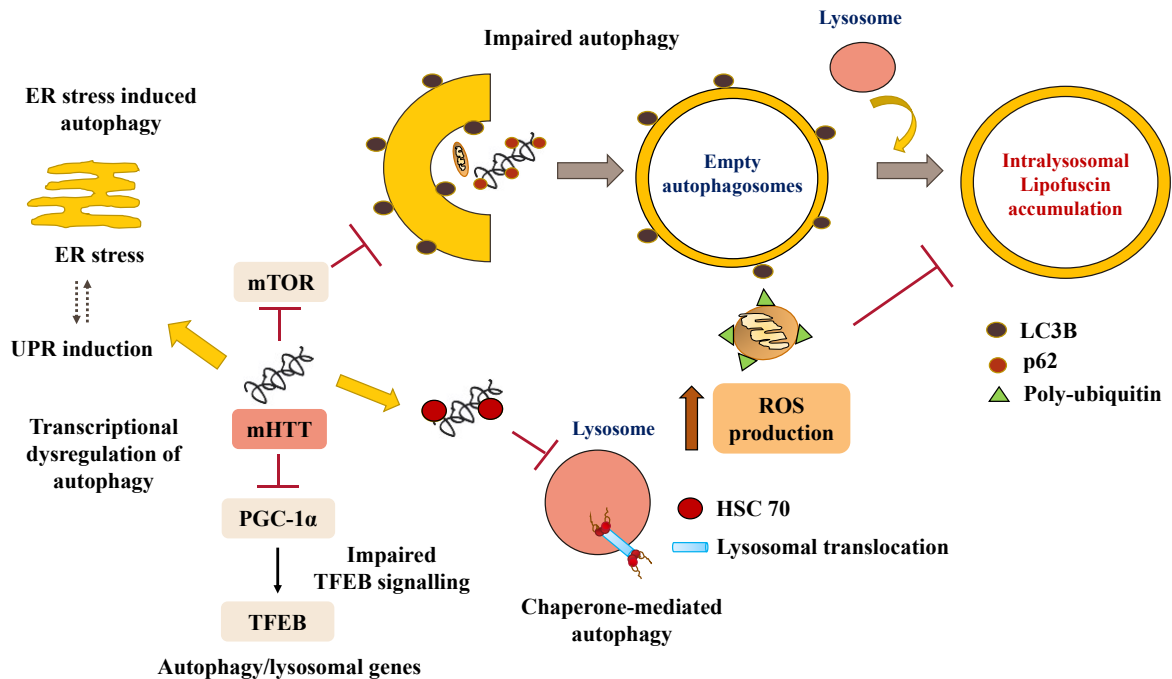


Figure 1-4 Autophagy dysfunction in Huntington’s disease

In HD, mHTT protein forms aggregate inside the neuronal cells and elicit an ER stress response and activation of ER-stress induced activation of autophagy. mHTT aggregates sequester mTOR resulting in disinhibition of autophagy, however, mHTT impairs recognition and loading of cargo leading to the accumulation of empty autophagosomes. Lysosomal activity is reduced in HD due to an increase in ROS and accumulation of non-degraded lipofuscin in lysosomes. mHTT interfere with proliferator-activated receptor gamma coactivator 1- α (PGC-1 α) and leads to impaired TFEB transactivation of lysosomal genes. mHTT interacts with HSC 70 and the lysosomal translocation machinery resulting in impaired chaperone-mediated autophagy in HD. Image source: Modified with permission from Copyright Clearance Center, Inc. Elsevier ²⁰⁴.

While mHTT protein can be degraded both by UPS and lysosomes under normal physiological conditions, it is preferentially degraded by autophagy when it undergoes mutation and forms toxic intracellular aggregates. The clearance of mHTT aggregates by autophagy can be modulated by various post-translational modifications such as ubiquitination, SUMOylation, and acetylation that drive the process of degradation by autophagy ^{195,205-207}. Moreover, studies have shown that genetic and pharmacological inhibition of macroautophagy in HD mouse models worsens the disease phenotype, while the activation facilitates and enhances the

clearance of toxic forms of mHTT protein thereby improving the symptoms and ameliorating the pathology^{196,208,209}.

HTT plays a vital role in autophagy degradation and several groups have reported alterations in autophagy as a consequence of toxic gain of function of polyQ tract^{210,211}. The changes in the mRNA expression of different autophagy-related genes were observed in the brain samples of HD patients²¹². HTT is associated with RAB5 which is present in late endosomes and is also involved in the early stage of autophagosome formation²¹³. HTT protein forms a part of the multi-protein complex that acts as an adapter between the specific cargo and autophagosome and is crucial for cargo recognition during selective autophagy and this process is impaired in HD^{191,211}. HTT protein shares structural similarities with ATG11 and ATG23 that are involved in selective autophagy and forms part of the ATG1/ULK1 complex which is involved in the initiation of autophagosome formation²¹⁴.

The role of HTT as a scaffold protein for selective autophagy has been affected in HD thus contributing to autophagy dysfunction leading to the accumulation of toxic mHTT aggregate species²¹⁴. HTT protein plays a role in vesicular trafficking and fusion and directly binds to the microtubule-dependent motor protein dynein, dynactin and kinesin-1 that promote bidirectional transport of vesicles including lysosomes, autophagosomes and endosomes. Recently, it has been shown that HTT along with HAP1 is crucial for retrograde axonal transport of autophagosomes toward soma and allow fusion with lysosomes. mHTT interacts and sequester essential components of microtubule protein complexes thereby impairing the vesicular transport causing cellular dysfunction²¹⁵⁻²¹⁸.

1.7 Pathophysiology of Huntington's disease

HD is an autosomal dominant trinucleotide repeat disorder caused by an unstable expansion of CAG repeats in the exon 1 on the short arm of chromosome 4, that codes for HUNTINGTIN protein²¹⁹. The disease progression is directly linked to the number of CAG repeats. The normal individual has CAG repeats ranging from 8-24, and the individual with CAG repeats above 40 are most likely affected with HD (**Figure 1-5**). The extended polyglutamine tract forms intranuclear and cytoplasmic aggregates leading to neurodegeneration characterised by loss of efferent medium spiny neurons in the striatum of the basal ganglia²²⁰. However, degeneration also occurs in other cortical regions of the brain²²¹. Thus, the presence of toxic HUNTINGTIN aggregates in the neurons is responsible for the failure of many fundamental

cellular processes characterised by severe motor dysfunction, dementia, and cognitive impairment²²²⁻²²⁴ (Table 1-1).

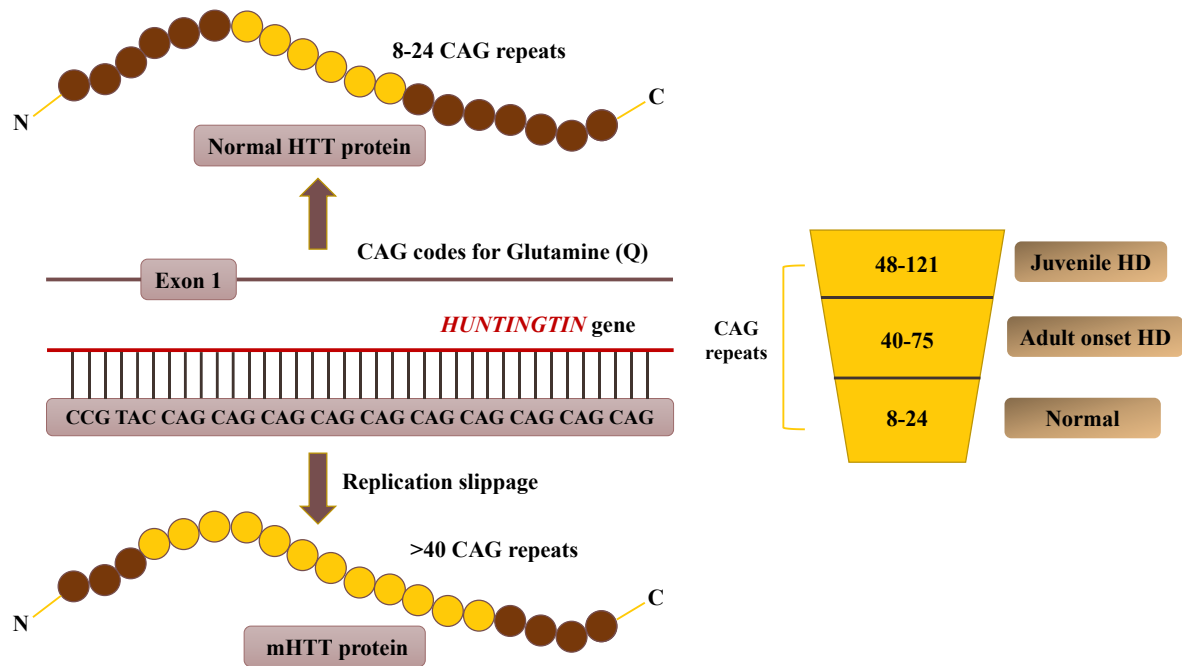


Figure 1-5 Genetics of Huntington’s disease (HD)

Huntington’s disease, a trinucleotide repeat disorder is highly polymorphic with the unstable expansion of CAG repeats in the exon 1 of the HTT gene. CAG repeats codes for the amino acid glutamine. The expanded polyQ are the characteristic feature of the mutant HTT protein. The disease progression is directly linked to the number of CAG repeats. Normal individuals’ express CAG repeats in the range of 8-24, and the individual with CAG repeats above 40 are most likely affected with HD. In juvenile HD, CAG repeats are in the range of 48-121 and the onset of symptoms is much early. Image source: adapted from^{198,225,226}.

Motor deficits are the major characteristic sign of HD and indeed used as primary diagnostic criteria. The motor impairments can be divided into voluntary and involuntary symptoms^{221,227}. The involuntary symptoms typically follow a biphasic pattern. They initially display mild hyperkinetic movements or imbalance. As the disease progresses, chorea develops, which involves uncontrolled dance-like movements of the limbs and torso. In later stages, bradykinesia prevails, eventually progressing to hypokinesia and a rigid-akinetic state. The voluntary impairments correlate to progressive changes in gait, fine motor movements, and ocular/oral control^{225,227}.

The hyperkinetic movement in HD is caused by disruptions in the basal ganglia pathway. The excitatory input to the GPi (Globus pallidus internal) is lost resulting in less inhibition of

VA/VL of the thalamus. Thus, the activity of VA/VL and motor cortex is increased causing hyperactivity of the motor system in HD. Huntington's chorea is characterised by uncontrolled involuntary choreiform movements which show as rapid purposeless jerks of irregular changes in the body ²²⁸. These movements are spontaneous and cannot be inhibited, controlled, or directed by the patient. The initial cause of these uncontrolled movements is the loss of GABAergic neurons in the striatum that project to GPe (Globus pallidus external) that direct the indirect pathway of basal ganglia ^{229,230}.

The loss of this inhibition on the indirect pathway, leads to activation of the VA/VL of the thalamus and the motor cortex, leading to uncontrollable hyperactivity of the motor neurons. In addition to the loss of striatal GABAergic neurons of the indirect pathway, cholinergic interneurons also start degenerating in the striatum. The loss of both the cell types elevates the activity of VA/VL and show increased motor output ²³¹. Hyperkinesia can be alleviated by bringing both direct and indirect pathways into balance. Moreover, the direct pathway is mediated by dopamine receptor 1 (D1) expressing neurons, while the striatal neurons driving the indirect pathway express D2 receptors ²³². Both these populations are GABA-expressing medium spiny neurons (MSNs) and makeup approximately 95 % of the striatum ²³³. In HD, the D2-MSNs of the indirect pathway degenerate first causing the onset of involuntary movements, such as chorea. As the disease progresses, the D1-MSNs of the direct pathway and other cortical afferents start degenerating, leading to the loss of voluntary movements ²³⁴ (**Figure 1-6**). The striatum is extensively connected to the frontal cortex and limbic system that play a significant role in cognitive and emotional processing. The degeneration of the striatum leads to the subsequent dysfunction resulting in the cognitive and affective symptoms that include memory impairment in HD ²³⁴.

In 1985, neuropathologist Jean-Paul from Columbia University assessed and classified the severity of HD degeneration by grading system (0-4) ²³⁵. Grade 0 is normal and indistinguishable from the healthy brain with no gross or microscopic abnormalities. Grade 1 shows neuronal loss, atrophy, and astrogliosis. Severe loss of striatal neurons characterises grade 2 and 3. Grade 4 includes the most severe case of HD with atrophy of striatum up to 95% neuronal loss ²³⁵. Apart from the striatum, regions of the cerebral cortex, globus pallidus, thalamus, subthalamic nucleus, substantia nigra, white matter, and cerebellum were affected. Due to this, HD is well characterised by a reduction in the volume and size in almost all brain structures mainly in the striatal and cortical regions at the end stage of disease progression ^{235,236}.

Table 1-1 Overview of different stages of Huntington’s disease and its varied symptoms

Symptoms	Early-stage HD	Middle-stage HD	Late-stage HD
Motor	Chorea, restlessness, agitation, changes in facial expression, difficulty in walking	Chorea worsens, loss of coordination, difficulty in speech, dystonia	Parkinsonism (slowness, stiffness, abnormal limb posture, forceful eye closure, teeth grinding, walking difficulty)
Cognitive	Memory loss, executive dysfunction, loss of mental flexibility, perseveration, impulsivity, poor attention, slow processing speed, trouble organising and planning,	Suicidal tendency, decreasing physical independence, frustration, social isolation, loss of driving, employment	Processing time is increased, difficulty in speech, social isolation, attention deficit, avoidance behaviour, hallucinations, delusions.
Psychiatric disorders	Anxiety and depression, irritability, apathy, impulsive behaviour, obsessions/compulsions	Irritability, anxiety, impulsiveness, lack of insight, poor sleep	Significant confusion and screaming, less aggression

In accordance with the cortico-striatal neuropathology of HD, there are multiple peripheral manifestations of the disease that are not clearly defined compared to CNS dysfunction. HUNTINGTIN (HTT) gene is widely expressed throughout the body, and there exists much evidence suggesting that neuropathological processes are evoked by the expression of mutant HTT in the peripheral tissues. However, it remains plausible that degeneration of the neurons is the primary driving force for peripheral pathology associated with HD. For example, the risk of cardiac events and cardiomyopathy are elevated in patients with HD, although it remains unclear to what extent it can be attributed to CNS dysfunction²³⁷. Likewise, metabolic changes that are manifested as dysregulation of body weight, loss of appetite, insulin homeostasis and liver function may be partially ascribed to hypothalamic dysfunction. Apparently, skeletal muscle pathology may be more clearly correlated to the deficits in cellular energy metabolism and mitochondrial dysfunction observed in HD²³⁷.

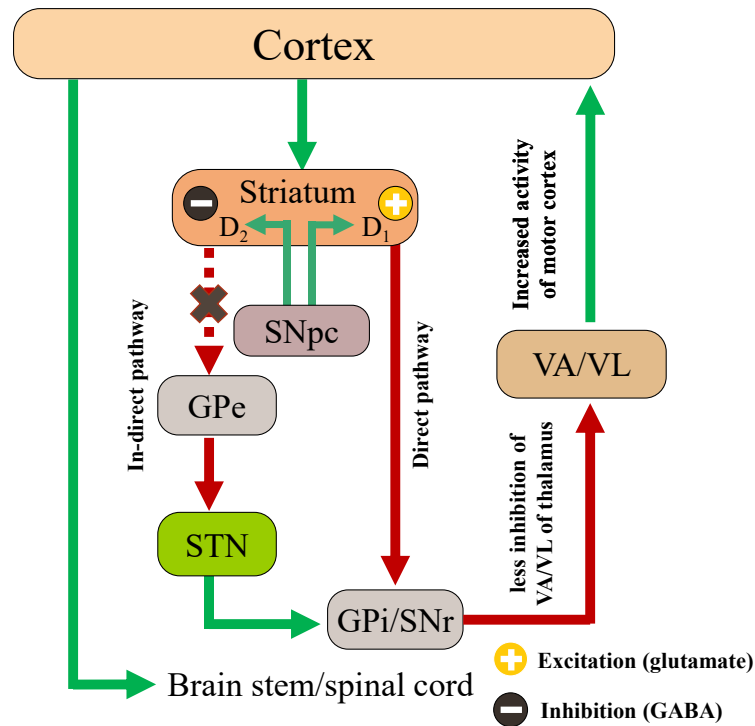


Figure 1-6 Pathway illustrating disruption in basal ganglia circuitry in Huntington’s disease

In hyperkinetic disorder like HD, the projections from the striatum to the GPe are diminished. This effect increases the tonic inhibition from the GPe to the STN, making the excitatory STN less effective in opposing the action of the direct pathway. Thus, thalamic excitation of the cortex is increased, leading to greater inappropriate motor activity. Moreover, the D2-MSNs of the indirect pathway degenerate first causing inhibition of the indirect pathway leading to the onset of involuntary movements, such as chorea. As the disease progresses, the D1-MSNs of the direct pathway and other cortical afferents start degenerating, leading to the loss of voluntary movements. Glutamatergic and dopaminergic synapses are denoted in green arrows, GABAergic MSNs are labelled in red arrows. D1, D2 – Dopaminergic receptors; SNpc – Substantia nigra pars compacta; GPe – Globus pallidus external; STN – Subthalamic nucleus; GPi – Globus pallidus internal; SNr – Substantia nigra reticulata; VA/VL – Ventral anterior/ventral lateral nucleus of the thalamus. Image source: adapted from ^{229,234}

1.7.1 Functions of HUNTINGTIN (HTT) protein

HUNTINGTIN is highly conserved among vertebrates and shares no sequence homology across the species ²¹¹. Its molecular mass is around 347 kDa with 3142 amino acids. In healthy individuals, the normal HTT protein contains 8-24 glutamine residues at its N-terminus, and the number may go up to 40-75 glutamine residues in HD patients. HTT is ubiquitously expressed all over the body, and in the brain, it concentrates mostly in the neocortex, cerebellar

cortex, striatum and hippocampus²³⁸. HTT expresses during embryonic stages [2.5 days post coitum – E1.0]²³⁹, and *Htt* knock-out mice die at embryonic day 7.5²⁴⁰⁻²⁴². The COOH-terminal nuclear export signal (NES) sequence and a nuclear localisation signal (NLS) of HTT protein are involved in transporting molecules from the nucleus to the cytoplasm²⁴³.

HTT is enriched in consensus sequences called HEAT repeats (HUNTINGTIN, elongation factor 3, protein phosphatase 2A and TOR1) that are organised in functional protein domains which play an important role in protein-protein interactions^{211,244}. HEAT repeats are ~40 amino acids long and occur downstream of the polyQ. The polyQ stretch of glutamine residues forms a polar zipper structure, and its physiological function is to bind transcription factors that contain a polyQ region²¹¹. PolyQ tract is a key regulator of HTT and interacts with a large number of partners such as HTT-interacting protein 1 (HIP1), HTT associated protein 1 (HAP1), Src homology region 3-containing Grb2-like protein 3, protein kinase, and Casein kinase substrate in neurons 1, and postsynaptic density-95 (PSD95)²⁴⁴⁻²⁴⁸. HUNTINGTIN interacting proteins (HIP) play diverse cellular roles like apoptosis, vesicular transport, cell signalling, clathrin-mediated endocytosis, morphogenesis and transcriptional regulation²¹¹.

HAP1 is expressed in the brain and interacts with the p150 subunit of dynactin, thus involved in intracellular transport²⁴⁹. HIP1 binds to α -ADAPTIN and CLATHRIN and is implicated in endocytosis and cytoskeleton assembly²⁵⁰. HTT interacts with PSD95 through its Src homology-3 (SH3) sequences regulating the expression of NMDA and Kainite (KA) receptors to the postsynaptic membrane. mHTT protein with its polyglutamine expansion interferes with the ability of HTT to interact with PSD95 and causes sensitization of NMDA receptors thereby promoting neuronal apoptosis induced by glutamate²⁴⁵. HTT also promotes the expression of brain-derived neurotrophic factor (BDNF) which is essential for the survival of striatal neurons and the activity of the cortico-striatal synapses²⁵¹. The striatal cells do not produce BDNF and depend on the BDNF delivered by cortico-striatal afferents. HTT facilitates the transcription of BDNF and promotes the axonal transport and delivery of vesicles containing BDNF to cortico-striatal synapse²⁵²⁻²⁵⁴. BDNF co-localizes with HTT cortical neurons that project to the striatum. Loss or reduction in HTT activity diminishes BDNF production, thus contributing to the degeneration of neurons²⁵¹.

Apart from these, HTT has a prosurvival role. Wildtype HTT protects neuroblastoma and kidney cells from death triggered by the mHTT protein²⁵⁵. Wild-type HTT blocks apoptosis by physically interacting with active caspase-3, thereby, inhibiting its proteolytic activity²⁵⁶.

HTT regulates the balance between neuronal death and survival and modulates neuronal sensitivity to excitotoxic neurodegeneration^{211,257}. HTT is also involved in the fast axonal trafficking of mitochondria in mammalian neurons²⁵⁸. It regulates axonal transport by participating in the assembly of the motor complex on microtubules. It enables retrograde and anterograde transport by interacting with the p150 subunit of dynactin via HAP1²⁵⁹. HTT interacts with cytoskeletal and synaptic vesicle proteins essential for exocytosis and endocytosis at synaptic terminals thus controlling synaptic activity in neurons²⁶⁰. These interactions depend on the length of the polyglutamine repeat and are enhanced by the presence of an expanded CAG, leading to the impairment of synaptic transmission in HD²⁶⁰.

1.8 Mouse models to study Huntington's disease

The study of genetics and disease pathogenesis of HD provided a wealth of information on the process of disease-causing mechanisms and have driven the development of a vast array of genetically modified mouse models. The generous use of experimental preclinical models has shed light only on the partial aspects of the disorder, thereby preventing and limiting a fair translation into new therapeutics, diagnostics, and prevention; although preclinical results were often promising and encouraging, the results were not implicated, and the enthusiasm raised were eventually faded when the new strategy was tested in the clinical trials. However, the limiting factor is that these mouse models do not readily develop the full neuropathological and clinical symptoms that are observed in humans, yet have proven to be effective in dissecting the basic disease-causing mechanisms and also in screening compounds of therapeutic importance in designing effective treatment options for the human welfare²⁶¹.

The importance of any given mouse model of human diseases is often evaluated based on three broad measures of validity: construct validity, face validity, and predictive validity²⁶².

Construct validity

Construct validity relates to how closely the mouse model reconstructs and reproduces the pathogenic features that manifest the disease in humans^{262,263}. In the context of Huntington's disease (HD), the construct validity of mouse models expressing full-length human mutant *HUNTINGTIN (HTT)* gene is greater than those expressing full-length mouse mutant *Htt*²⁶⁴. Similarly, models that express full-length genomic sequences of mutant *HTT* (with exons and introns) have higher construct validity than those with full-length mutant *HTT* cDNA models or only expressing N-terminal fragments of *HTT* (only exon 1 of mutant *HTT* is expressed)²⁶⁵. The mouse models in which full-length mutant *HTT* or a fragment is expressed under the

control of *HTT* promoter exhibit greater construct validity than the models in which the same coding sequence is expressed under a non-*HTT* promoter²⁶⁶

Face validity

Face validity corresponds to the extent to which a mouse model mimics the symptoms and the phenotypes that are associated with the human disease²⁶². For HD, models with high face validity would reproduce and imitate progressive motor and cognitive deficits along with psychiatric disturbances. Moreover, neuroanatomically and histologically, the HD mouse models would exhibit selective, age-dependent striatal and cortical neuronal loss and severe atrophy with intranuclear inclusions with neuropile aggregate²⁶⁷.

Predictive validity

The predictive validity of a mouse model is assessed based on how closely the mice respond and show improvements to the treatment that corresponds and relate or predict improvements in human patients²⁶². For treatable conditions, the predictive validity of a mouse model may be tested but for diseases such as HD with no effective treatment available, assessment of the predictive validity is challenging and currently not possible.

The list of various mouse models for HD detailing the number of CAG repeats, neuropathological and behavioural features are mentioned in **(Table 1-2)**.

1.9 Detailed insights into HD mouse model – R6/2

The R6/2 mouse is the first transgenic model to be generated for HD. It is the most robust and commonly used mouse model to study the pathogenesis of HD. Bates et al had created this transgenic murine line by inserting a 1.9kb fragment derived from the 5' end of the human *HTT* gene into the mouse genome²⁶⁸. This fragment consists of only exon 1 of the *HTT* gene and expresses approximately 144 CAG repeats. The truncated mutant *HTT* gene is randomly inserted into the mouse genome and expresses three copies of the *HTT* gene: one copy of the mutant human gene and two copies of the wildtype *HTT* mouse gene. The expression of the mutant *HTT* gene is driven by a human *HTT* promoter and is the strong promoter with maximum expression levels. The mutant gene is expressed in all cells and tissues of the mouse at 75 % expression of wild-type gene²⁶⁸. Due to a large number of CAG repeats, the R6/2 mice correspond to a juvenile-onset of HD symptoms in humans.

R6/2 mouse model has a very severe and aggressive behavioural phenotype and develops symptoms as early as 4-5 weeks of age with a very low survival rate of 12-14 weeks. Motor

symptoms include chorea-like movements, resting tremors, stereotypic involuntary grooming movements, and dystonia of the limbs when suspended by its tail typically called hind-limb clasping^{268,269}. The mice show a progressive decline on the rotarod test as early as 40 days of age and by 12 weeks, mice are unable to move or maintain their balance even for 10 seconds²⁷⁰. In the open-field test, R6/2 mice show increased locomotor and exploratory behaviour compared to wild-type mice at 3 weeks. This hyperactivity progressively declines and by the age of 8-10 weeks, they become hypoactive relative to wild-type mice²⁶⁸.

The R6/2 mice also suffer from epileptic seizures and spontaneous shuddering movements. As the diseases progress, there is a significant reduction in the body weight and the size of the body is almost reduced to half compared to wild-type mice²⁶⁸. They also display cognitive deficits as early as 3.5 weeks before the onset of overt motor symptoms²⁷¹. The R6/2 mice exhibit deficits in the spatial learning task in the Morris water maze test, and by the time mice reach 7-8 weeks, they completely lose the ability to learn the task, partly due to severe motor impairment as the mice lose the ability to swim. A deficit in the spatial learning task may be due to the accumulation of mHTT aggregates in the hippocampus. Although the cognitive deficits seen in R6/2 mice are quite evident compared to wild-type control mice, it is unclear whether they are related to those seen in HD patients. In contrast, the cognitive deficits seen in HD patients are typically frontostriatal and are typically characterised by loss in executive function, procedural memory, and psychomotor skills²⁷²⁻²⁷⁴.

The R6/2 mice typically display time-dependent changes with respect to brain volume, striatal volume, and striatal neuronal counts^{268,275}. The mice showed a time-dependent reduction in brain weight and brain volume starting at postnatal days 30 and 60, respectively. Pathological modifications were associated with changes in body weight, grip strength, rotarod performance, and dystonia²⁷⁵. Studies have shown a significant reduction in the number of enkephalin-expressing neurons in the striatum at 12 weeks without any change in the number of substance P-expressing neurons. Moreover, the enkephalin projections to the globus pallidus show significant degeneration while substance P projections to the pallidus and substantia nigra are relatively spared²⁷⁶. mHTT inclusions initially appear in the region cortex and hippocampus (CA1 before CA3) and then eventually spread to the striatum^{269,277}. The exact mechanism of cell death is unknown, but one study reported the presence of 'dark neurons' resembling those in the human HD brain in R6/2 mice brain tissues. This type of neuronal cell death seems to be neither necrotic nor apoptotic and occurs in the striatum, cerebellum, and cingulate cortex²⁷⁸.

Table 1-2 Mouse models of Huntington’s disease

The summary of different rodent models of HD expressing N-terminal fragments of human HD, knock-in models, and full-length transgenic models. These models vary with the expression of the number of CAG repeats and associated pathological changes with distinct behavioural differences.

Huntington’s Disease (HD)

Rodent model	CAG repeats	Behaviour	Neuropathology	Survival	References
R6/1	116	Significant weight loss at 22 weeks, motor deficits at 4-5 months	Neuronal atrophy, reduced brain volume by 18 weeks, reduced dopamine levels, presence of mHTT aggregates at 2 months	Normal life span	268,279
R6/2	144-150	Hind-limb claspings by 6 weeks, progressive weight loss, rotarod deficit, seizures, diabetes	Significant brain weight loss by 30 days, neuronal atrophy, mHTT aggregate formation, astrogliosis by day 90, reduced dopamine levels	12-14 weeks	268-270,275,279,280
N171-82Q	82	Weight loss, motor deficits and claspings by 11 weeks	Gross brain atrophy, striatal neuron atrophy, presence of mHTT aggregate by 16 weeks, enlarged ventricles	130-180 days	267,279
Hdh/Q72-80	72-80	No weight loss, Rotarod impairment, aggressive behaviour	mHTT aggregates by 28 weeks and nuclear inclusions by 96 weeks. No neuronal loss or reactive astrogliosis	Normal life span	281
HdhQ111	109-111	Gait abnormality by 96 weeks	Diffuse mHTT aggregates by 6 weeks, nuclear inclusions by 48 weeks, neuropil aggregates by 68 weeks, astrogliosis by 96 weeks	Normal life span	282

Rodent model	CAG repeats	Behaviour	Neuropathology	Survival	References
CAG140	140	Weight loss, gait abnormalities by 48 weeks, increased hyperactivity by 12 weeks	Nuclear and neuropil aggregates by 8 months, diffuse mHTT aggregates by 8 weeks	Normal life span	265
CAG150	150	Weight loss, rotarod deficit, gait abnormalities, and beam balance by 20-23 months	Striatal mHTT reactivity by 28 weeks, nuclear inclusions by 37 weeks, reactive astrogliosis at 56 weeks	Normal life span	283
YAC128	128	Progressive motor and cognitive deficits	Selective striatal and cortical atrophy by 12 months	Normal life span	284-286
BACHD	97	Progressive motor and cognitive deficits	Selective striatal and cortical atrophy by 12 months	Normal life span	264,286

Before the onset of symptoms in R6/2 mice, there is a loss of different neurotransmitter receptors such as type 1 metabotropic glutamate receptor, D1 and D2 dopamine receptors, and muscarinic cholinergic receptors similar to that seen in adult HD²⁸⁷. It has been shown that at specific stages of disease progression in R6/2 mice, there is reduced capacity to synthesize neurotransmitters such as dopamine and serotonin, alterations in the levels of synaptic proteins, changes in the glial transport system thereby impairing the extracellular glutamate uptake leading to excitotoxicity²⁸⁸⁻²⁹⁰. There is a severe malfunction of the neuronal circuitry in R6/2 mice, where striatal neurons exhibit more depolarised resting potentials and show increased intracellular calcium levels compared to wild-type control mice. These mice also display significant changes in the firing patterns of cortico-striatal fibres and all these events contribute to excitotoxicity in R6/2 mice²⁹¹⁻²⁹³. Under normal physiological conditions, there is a reduction in the extracellular dopamine levels in the striatum and an increase in extracellular striatal glutamate levels following stimulation, but at the later stages, as the disease progresses, the dopamine levels in the striatum are considerably reduced in R6/2 mice^{294,295}.

Several studies have reported that R6/2 mice gradually develop diabetes and display impaired glucose tolerance. As the disease progresses, insulin production fails and eventually the mice are hyperglycemic even under starvation conditions^{270,280,296}. Studies have also suggested that there is a reduction in the number of neurons expressing gonadotropin-releasing hormone in the hypothalamus and this can lead to gonadal atrophy causing infertility in adult R6/2 mice

²⁹⁷. In the R6/2 striatum, the cell bodies, and dendritic fields of medium-sized spiny neurons have been shown to shrink by around 20 % and similar reductions in neuronal size have been reported in the striatum and substantia nigra of R6/1 mice as well ²⁹⁸⁻³⁰⁰.

R6/2 mice show significant changes in the gene expression in the striatum and cortex as early as 6 weeks and become more pronounced as the mice age ³⁰¹. The expression of numerous genes has been shown to be altered and specifically striatal signalling genes induced by cAMP and retinoid are downregulated, whereas genes associated with cell stress and inflammation are upregulated. However, these expression changes do not appear to be brain region-specific that are classically affected in HD but are also detected in the cerebellum and other peripheral tissues in the body such as muscle and liver ³⁰². The R6/2 mice show a significant increase in the markers for oxidative damage and show impaired mitochondrial function. In addition, there is increased NOS activity in the striatum of the R6 lines ³⁰³⁻³⁰⁵. The striatal neurons from R6/2 mice show increased autophagic vacuoles in response to oxidative stress than in control cells, suggesting a change in the fundamental mechanisms related to cell response ³⁰⁶.

1.10 Autophagy as a therapeutic strategy for HD

Autophagy is a lysosomal-dependent cellular mechanism for the degradation of toxic waste inside the cell, thereby maintaining cellular homeostasis ⁵⁹. As mentioned earlier, dysregulation of autophagy has been closely linked to many disease pathology, including a severe form of neurodegenerative diseases ¹⁰⁹. Therefore, targeting autophagy has been implicated as a promising therapeutic strategy to identify scalable drug targets for many diseases. Most of the compounds have multiple targets associated with many complex cellular metabolic pathways, and proteins, which has very limited scope for the evaluation of therapeutic value ³⁰⁷. Therefore, the identification and development of specific active modulators of autophagy is necessary and is highly beneficial for clinical interventions ³⁰⁸. Identification of novel small molecules of autophagy modulators has gain importance for the past 15 years and many reports have shown that autophagy can be regulated at each step with the interventions of small molecules and has high therapeutic value for the treatment of many severe forms of diseases including neurodegenerative diseases ³⁰⁹. Therapeutic manipulation of autophagy in vivo, either by pharmacological or genetic means have shown promising results in mouse models of HD, resulting in an amelioration of disease phenotypes ³⁰⁹.

The autophagy-modulating agents that are used in pre-clinical trials in various models of NDDs are multifactorial and have diverse mechanisms of action. Our understanding of how these

agents elicit their function is not completely understood, however, they are divided into mTOR dependent and mTOR independent modulators ³¹⁰.

1.10.1 mTOR dependent modulators

The mammalian target of rapamycin (mTOR) signalling pathway integrates both intracellular and extracellular signals and functions as a central regulator of cell growth, proliferation, and survival ⁷⁹. mTOR exists in two different functional complexes, mTORC1 (a negative regulator of autophagy) and mTORC2 (a positive regulator of autophagy) ⁸³. The allosteric regulator rapamycin was the first drug to be identified as an autophagy inducer that inhibits the mTORC1 complex ^{311,312}. Rapamycin forms a complex with FK506-binding protein 12 (FKBP12) and inhibits the kinase activity of mTORC1 ³¹³. mTOR dependent agents induce autophagy by repressing the activity of mTOR and these can be ATP competitive such as Torin and non-ATP competitive Rapamycin. Inhibition of the mTORC1 complex induces autophagosome formation as this kinase phosphorylates and inhibits core autophagy proteins such as ULK1/2 and ATG13 ^{314,315}.

Even though the mTOR pathway is involved in a wide range of cellular functions, the therapeutic effect of rapamycin is predominantly autophagy-mediated and is found to be neuroprotective in various neurodegenerative diseases such as HD, AD, PD, and FTD ^{316,317}. Due to limited absorption of rapamycin, many so-called analogues of rapamycin have been developed such as temsirolimus (CC-779), everolimus (RAD001), and ridaforolimus (AP23573) ³¹⁸. David C Rubinsztein and his group were the first ones to report that inducing macroautophagy could indeed have beneficial effects in HD. In this study, rapamycin analogue, CCI-779, a known mTOR kinase inhibitor, reduced polyglutamine aggregate load and improved motor functions in HD transgenic mice by inducing autophagy ²⁰⁸. PI103 is a dual class-I PI3K/mTORC1 modulator that induces autophagy by inhibiting both mTOR and AKT pathways, but due to its rapid in vivo metabolism, this drug is currently unsuitable as a therapy for neurodegenerative diseases ³¹⁹.

There are other classes of drugs that function by indirectly inhibit the mTOR pathway. For example, metformin (type 2 diabetes drug) inhibits mTOR activity by regulating the AMPK pathway can upregulate autophagy in an mTOR-independent manner ³²⁰. Another drug Nilotinib which is a receptor tyrosine kinase inhibitor can induce autophagy via AMPK activation and is shown to be neuroprotective in a mouse model of PD and is currently in a

phase-II clinical trial for PD therapy^{321,322}. In this thesis, Nilotinib (Tasigna™) has been used to test its efficacy in ameliorating the disease pathogenesis in HD mouse model R6/2.

1.10.2 mTOR independent modulators

mTOR has diverse functions that are autophagy-independent which include cellular metabolism and ribosome biogenesis⁸⁴. mTOR being the central regulator of various physiological functions, long-term usage of drugs dependent on mTOR inhibition could have significant toxic effects on a cell such as impaired wound healing and immunosuppression. In this scenario, several studies have been carried out to identify and screen FDA-approved drugs that induce autophagy in an mTOR independent manner. These drugs are proven to be effective in ameliorating neurodegenerative disease pathology in the various cell, rodent, Drosophila, and Zebrafish models of HD³²³. These compounds regulate autophagy by involving two cyclical pathways namely Ca²⁺/calpain/Gsα pathway and the cAMP/EPAC/PLCε/Ins(1,4,5)P3 pathway³²³. Rilmenidine, an mTOR independent autophagy inducer acts via inhibiting imidazoline receptors that are abundantly distributed in the brain to reduce the levels of cAMP. It has been shown to be a neuroprotective and lowered level of toxic mHTT fragment and attenuated motor phenotypes in HD 171-82Q transgenic mice³²⁴. Rilmenidine is currently undergoing safety clinical trials for HD (**EudraCT number 2009-018119-14**). Other drugs that induce autophagy through the cyclical pathway include lithium³²⁵, valproic acid, and carbamazepine. Valproic acid and carbamazepine inhibit inositol synthesis, whereas lithium inhibits inositol monophosphate to decrease Ins(1,4,5)P3 levels thereby inducing autophagy without mTOR inhibition³²³. Several FDA approved drugs that modulate Ca²⁺/calpain/Gsα pathway such as nitrendipine, verapamil, and amiodarone have been shown to promote the clearance of aggregate-prone proteins by inducing autophagy³²⁰.

There are many other compounds that modulate autophagy with therapeutic potential in HD. Trehalose, a disaccharide showed to induce autophagy, reduced polyglutamine toxicity, ameliorate motor deficits and extended the life span in R6/2 transgenic mice³²⁶. Congo red preferably binds to β-sheets with amyloid fibrils and when administered to HD mice, it enhanced the clearance of expanded polyQ and inhibited the formation of polyglutamine oligomers by disrupting the preformed oligomers³²⁷. Studies have shown that Compound C2-8 inhibits the formation of polyglutamine aggregates in cell cultures and brain slices. When treated in HD mouse model R6/2, it decreased neuronal atrophy, reduced accumulation of mHTT aggregates and thereby improving the motor functions^{328,329}. Studies have also

demonstrated that CMA might preferentially target soluble, N-terminal fragments of polyQ-HTT for degradation³³⁰. Apparently, in an R6/2 mouse model, the CMA-targeting adaptor molecule has been used against polyQ-HTT and found to be effective in increasing the life span of the mice and so far, it has been the most significant single-molecule pre-clinical trials reported so far in an HD mouse model, R6/2^{193,197}.

The crucial factor for autophagy induction in HD is the timing of the intervention. Early activation of autophagy would aid in the clearance of aggregate prone mHTT species thereby conferring a neuroprotective role and preventing neuronal death. However, with more complex disease-causing mechanisms, lysosome and proteasome abnormalities become more apparent in HD, and these defects could undermine the efficacy of autophagy induction. Therapies that concurrently activate autophagy and modulate HTT protein post-translational modifications could yield different isoforms of mHTT protein, which neurons will be inefficient in turning over. Given the fact that patients with HD can be diagnosed at presymptomatic disease stages through genetic testing, therapeutic modulation of autophagy before the onset of symptoms is not only beneficial in delaying the disease progression but also because autophagy induction in symptomatic patients could worsen the disease phenotypes. For example, drugs that increase the autophagy flux in advanced HD patients are only effective when the underlying cargo recognition defects are corrected in the autophagy pathway. Therefore, understanding the precise molecular players that lead to autophagy dysfunction such as cargo recognition failure is important to develop novel therapeutics for HD. It would also be ideal to understand the physiological role of HTT with respect to autophagy pathway, membrane dynamics, and trafficking before pushing forward with therapeutic modulation of autophagy because the loss of HTT function has been implicated in autophagy dysfunction in HD. Eventually, identifying specific steps that are affected in the autophagy pathway in HD will be key for the development of novel rational drugs for the treatment of HD and other neurodegenerative diseases.

1.11 Nilotinib (Tasigna™)

Nilotinib (Tasigna™) is a second-generation BCR-ABL1 tyrosine kinase inhibitor approved by the US Food and Drug Administration (FDA) for the treatment of adult patients with chronic and accelerated phase (AP) Philadelphia chromosome-positive (Ph+) chronic myelogenous leukaemia (CML)³³¹. Studies have shown that inhibition of BCR-ABL1 tyrosine kinase by Nilotinib protects neurons from dying against MPTP (1-methyl-4-phenyl-1,2,3,6-tetrahydropyridine) toxicity in the preclinical mouse model of PD and enhances the clearance

of α -SYNUCLEIN^{322,332}. Mice treated with Nilotinib have shown increased expression of autophagy related proteins such as BECLIN-1, and ATG12, thereby enhancing the clearance of toxic α -SYNUCLEIN aggregates in the brain³²². BCR-ABL is activated by phosphorylation and its levels are increased in the nigrostriatal region of PD patients, and BCR-ABL inhibition has proven to be efficient in preventing the neurons from dying in PD mouse models³³³. Therefore, the increased activity of BCR-ABL may be associated with disease pathology in various other neurodegenerative disorders including PD, HD, ALS, and multiple system atrophy (MSA).

Nilotinib is also a potent inhibitor of Discoidin Domain Receptors (DDR 1 and 2)^{334,335}. DDRs are receptor tyrosine kinases that are found to be overexpressed in the midbrain of post-mortem patients with PD³³⁶. Partial or complete deletion or inhibition of DDR1 by Nilotinib increases autophagy and reduces inflammation and load of neurotoxic aggregates in mouse models of neurodegenerative diseases³³⁷. Oral treatment of Nilotinib increases dopamine levels and reduced p-tau levels in a dosage-dependent manner³³⁸⁻³⁴⁰. It has also been shown to attenuate hippocampal atrophy and reduces cerebrospinal fluid (CSF) amyloid and plaque concentration in AD, which is independent of BCR-ABL inhibition^{338,339}. Recently, in a small 12 patient pilot study, Nilotinib was found to be potentially effective in treating the patients of PD with motor and non-motor symptoms and dementia with Lewy bodies. The treatment seemed to affect surrogate disease biomarkers such as dopamine metabolism and the load of α -SYNUCLEIN³⁴¹. One of the recent studies has reported that Nilotinib treatment reduces BCR-ABL phosphorylation, improves autophagy, thereby reducing the A β levels in the Tg2576 AD mouse model. Chronic treatment of Nilotinib prevents degeneration and preserves the functional and morphological alteration in dopamine neurons of the VTA. The drug prevents the reduction of dopamine outflow to the hippocampus and ameliorates the hippocampal-related cognitive functions in Tg2576 AD mouse model³⁴².

However, no reports have shown the state of BCR-ABL activation via phosphorylation and its inhibition by Nilotinib in HD mouse models. Therefore, it would be ideal and promising to study the phosphorylation state of BCR-ABL and the effectiveness of Nilotinib in inducing autophagy and clearing the toxic HTT aggregates in mouse models of HD. Interestingly, Nilotinib (TasignaTM) is in clinical trials for Parkinson's disease and Huntington's disease, but its potency has not been evaluated in any of the rodent models of HD³⁴³⁻³⁴⁶. Therefore, we assessed the efficacy of Nilotinib (TasignaTM) in ameliorating physiological and behavioural deficits and extending the lifespan of the R6/2 mouse.

1.12 Aim and scope of the study

Hypothesis:

Most neurodegenerative diseases such as AD, PD, and HD show distinct phenotypic differences and are caused due to the accumulation of specific protein aggregates leading to severe brain atrophy. Restoring proteostasis balance by enhancing autophagy may be potentially useful in clearing toxic neuronal aggregates thereby rescuing the behavioural defects and improving the life span of an individual. Since neurodegenerative diseases are age-related and the efficiency of the neurons in maintaining the basal autophagy levels is compromised over time, it is crucial to identify the stage at which autophagy has to be induced. To address this, the HD mouse model, R6/2 was used as a model system to understand the dynamics of aggregate formation and autophagy dysfunction in neurodegenerative diseases.

With this backdrop, the aims and objectives of this study are:

- To understand the rate at which mHTT aggregates accumulate and the state of basal autophagy in R6/2 mice across different stages of disease progression in various regions of the brain.
- To restore the proteostasis balance by inducing autophagy and see if it clears mHTT aggregates and improve motor functions in R6/2 mice.

Scope of the study:

The study carried out in this manuscript is systematic and is the first report made to evaluate the expression of mHTT aggregates and autophagy related proteins at different stages of disease progression in R6/2 mice across various regions of the brain, i.e., cortex, hippocampus, striatum, and cerebellum. This kind of comprehensive study (different age groups and from different regions of the brain) has not been carried out in any of the HD mouse models and also in other neurodegenerative diseases to date. The results presented in this thesis would provide insights into understanding the mHTT aggregate formation and its consequences on autophagy dysfunction. Moreover, considering the fact the Tasigna is in the clinical trials for PD, and HD patients, to date, its potency is not studied in pre-clinical models of HD. This would be the first study to be reported to comment on the effect of Tasigna in the R6/2 mice model. In this regard, this study would be of interest to the researchers working on neurodegenerative diseases focusing on autophagy dysfunction and also provide valuable insights to develop therapeutic strategies to design novel drugs.

Chapter- 2 Material and Methods

2.1 Mouse studies

All experimental mice were maintained and bred in the animal house facility at JNCASR under 12-hour light and dark cycle. Food and water were available ad libitum. All the experiments and the protocols used in the study were approved by the institutional ethical committee and were performed according to the guidelines of the Institutional Animal Ethical Committee (IAEC), and the Committee for Control and Supervision of Experiments on Animals (CPCSEA). Huntington's disease mouse model, R6/2 (B6CBA-Tg(HDexon1)62Gpb/3J; <https://www.jax.org/strain /006494>) was procured from Prof. Nihar Ranjan Jana, National Brain Research Centre (NBRC), New Delhi, India (approved by Jackson's laboratory) and bred and maintained with C57BL/6 background wild-type mice. Separate C57BL/6 wild-type colony were maintained for breeding R6/2 mice. R6/2 male mice were allowed to breed with 3 C57BL/6 wild-type females in a 1:3 ratio. Hemizygous R6/2 females were infertile, and hence, not used for breeding strategies.

2.2 Genotyping

All the experimental mice were tagged on one of the ears at PND 9-12 using Monel ear tags (Cat # 1005-1 MONEL, Kent Scientific, U.S.A) with a hand-held ear tag applicator (Cat # INS1005-5LS, MONEL, Kent Scientific, U.S.A). Mice tail ~1-inch long was clipped at the time of tagging. Forceps and scissors were used for tail clipping and were heat sterilised using a germinator (Cat # 5-1460; CellPoint Scientific Inc. U.S.A) and to seal the wound caused during clipping of the tail. Animals were genotyped for wild-type and R6/2 mice. Genomic DNA isolation was performed by chopping mice tail into small pieces (~2.5-5 mm in length) using a scalpel (sterilised using 70 % ethanol before using it on every tail), and pieces were added to a 1.5 ml microcentrifuge tube. (~1-inch-long tail was clipped, half of the tail was used for DNA isolation, and the rest of the tail was stored in -20°C for the second round of genotype confirmation). Tailpieces were mixed with 180 µl of 50 mM NaOH (GRM467, HIMEDIA) solution, vortexed for a few seconds and heated in the dry bath at 95°C for 10 minutes. NaOH being a strong alkali helps in the alkaline lysis of the tail samples and ruptures the cell membrane, thereby DNA gets precipitated. Then, 20 µl of 1 M Tris-HCl (pH – 8.0) (Tris: 15965, Thermo Fisher Scientific; HCl: HC301585, Merck) was added to each tube to dissolve the DNA, and the samples were centrifuged at 12000 RPM for 10 minutes. Tris-HCL acts as a buffering agent and plays an important role in maintaining pH and cell lysis. The speed and duration mentioned above for centrifugation is optimum for efficient sedimentation of cell

debris and extraction of DNA. After the centrifugation step, the supernatant was aliquoted into fresh microcentrifuge tubes, and pellets were discarded. Further, genotyping was done using Polymerase Chain Reactions (PCR) in Thermocycler (Master cycler Nexus GX2, Eppendorf) with these DNA samples. (Approximately 2 μ L of DNA was used for PCR and the rest of the DNA samples were stored in -20°C for further usage). Following primers (procured from Sigma Aldrich) were used to determine the genotype for R6/2: Forward primer: 5' CCGCTCAGGTTC TGCTTTTA 3'; Reverse primer: 5' TGGAAGGACTTGAGGGACTC 3'. Experimenters were not blind to the genotype and injection regimen used in the study. Detailed protocol setup for PCR is shown in (Table 2-1). A representative image for the *Htt* PCR result is shown in (Figure 2-1).

Table 2-1 PCR protocol for *Htt* (R6/2) genotyping

Step	Temperature (°C)	Duration	Cycles
Initial denaturation	95	3 minutes	1
Cycle denaturation	95	30 seconds	35
Annealing	55	45 seconds	
Extension	72	35 seconds	
Final extension	72	1 minute	1
Hold	4	∞	

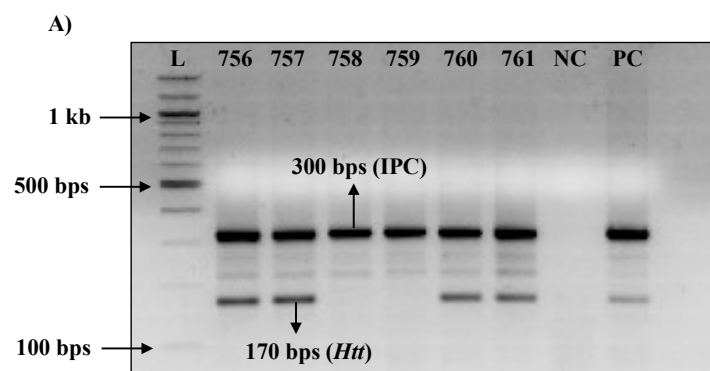


Figure 2-1 Representative image for *Htt* (R6/2) PCR

A) DNA samples were separated on 2 % Agarose gel (1X TAE) at a constant 120 V for ~ 45-50 minutes. The image was obtained from Gel Doc (Bio-Rad). L = 100 bps ladder; 756-761 = Tag No. for R6/2 mice. 300 bps band corresponds to an internal positive control (IPC) and 170 bps band to *Htt* (R6/2). NC = Negative control; PC = Positive control. Kb = Kilo bases; bps = Base pairs.

2.3 Injection regimen

Nilotinib (TasignaTM), procured commercially from medical stores, was dissolved in saline and mice were injected intraperitoneally every day, from 2 to 12 weeks of age at a dosage of 20 mg/kg body weight in C57BL/6 wild-type and R6/2 mice. Control littermates were injected with saline for both the genotypes. Mice were habituated by the experimenter from the day of tagging (PND 9-12) and were acclimatised to the conditions of the experiment performed. The detailed experimental paradigm is shown in (Figure 2-2).

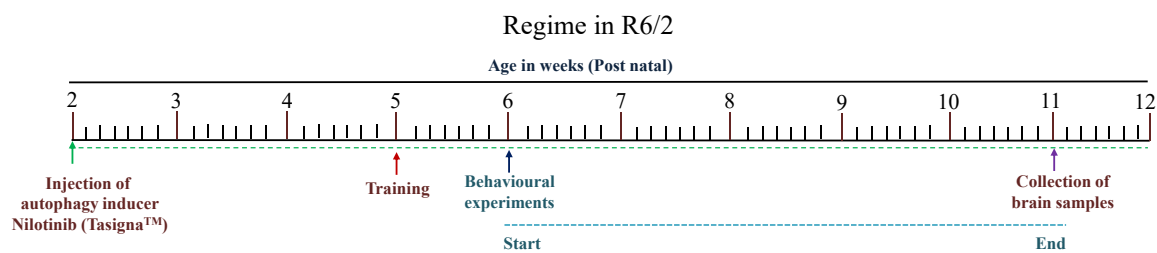


Figure 2-2 Injection regime in R6/2 mice

Image representing different stages of disease progression in R6/2, starting from 2 to 12 weeks. Autophagy inducer Nilotinib (TasignaTM), was injected intraperitoneally from 2 weeks, and training for behaviour experiments was performed from 5th week, and testing was done every week from 6th to 11th week. Brain samples for molecular analysis, of immunoblotting and immunohistochemistry, were collected every week at different time points, i.e., from 6 to 12 weeks.

2.4 Bodyweight measurement and survival

All the experimental mice were weighed using a weighing machine (Cat# DS-450 series, Essae-Teraoka, India) on alternate days before the start of injections from 2 weeks onwards, and dosage was calculated according to the weight of the mouse. Bodyweight across weeks was plotted by averaging weights measured on three alternate days.

2.5 Behavioural Studies

All the behavioural experiments were done in the behaviour room in the Institute's animal facility. HD transgenic mouse model R6/2 and wild-type C57BL/6 littermates were used for the experiments from 5-6 weeks of age and tests were done until 11-12 weeks of age. All the mice were acclimatised to the conditions and the experimenter before the start of injections, i.e., from PND 9-12 (day of tagging the mice). All the animals used for the behaviour were subjected to the habituation in the behaviour room for approximately 30 minutes before the

start of the experiment every week (since tests are done once per week starting from 6 weeks). The light intensity was maintained at 100 LUX throughout the experiment and on all days.

2.5.1 Open Field Test

Open Field Test was done to study the locomotion and exploratory behaviour of animals. The open-field arena of 50×50×45 cm was custom-made at JNCASR using plywood, and the internal surface was coated with odourless white polish (**Figure 2-3**). During testing, the mouse was allowed to explore the arena for 5 minutes by introducing the mouse in the periphery zone, and movement was recorded using a SONY video camera (Model no. SSC-G118, India), and a Sony HD camera (HDR-CX405). After the stipulated time of 5 minutes, the mouse was returned to its respective home cage. The open-field arena was then cleaned with 70 % ethanol and was allowed to air-dry before placing the next mouse in the arena. Distance travelled was calculated off-line by the experimenter using SMART v3.0.04 software (Panlab Harvard Apparatus, U.S.A). The videos recorded with a Sony camera (SSC-G118) were analysed using in-built automatic software in the SMART module. In parallel to this, the behaviour of mice from a different set of batches was also recorded using a Sony HD camera (HDR-CX405) and videos from this were analysed manually using SMART software. These differences in recording and analysing the behaviour data helped us to rule out the possibility of errors arising due to jerky and epileptic movements of the mice.

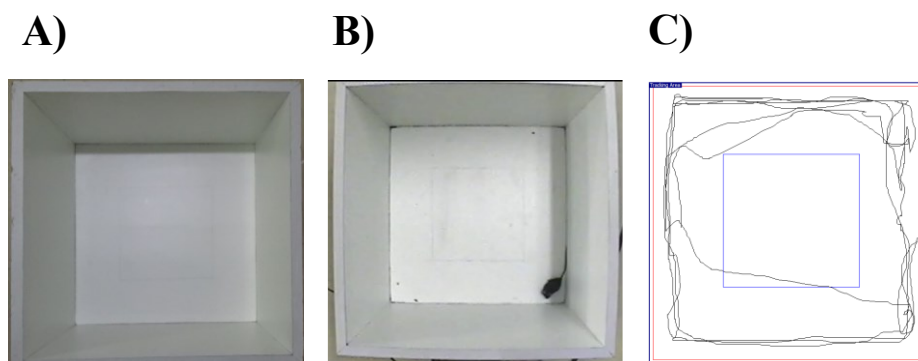


Figure 2-3 Representative images showing Open-field arena and trajectory

A) Open-field arena (50 X 50 X 45 cm) without the mouse. **B)** Open-field arena with the mouse showing boundaries drawn for centre and periphery. **C)** Example of one of the trajectories showing mouse movement in the marked regions.

All the data from both sets were pooled together to make any interpretations and conclusions of the results thereafter. After recording, videos were loaded onto the SMART module, details of the experimental conditions were given, and boundaries were marked for periphery and centre. A test run was carried out to ensure that all the parameters were checked and correct, and software can track the mouse movement. A maximum of 5 minutes was given to explore the arena, and once the run was completed, trajectories were exported as a JPEG image for reference and the total distance travelled by the mice in the open field arena was calculated by the software.

2.5.2 Rotarod test

The rotarod test was performed to assess the balance and motor coordination in R6/2 mice. The Rotarod instrument was custom-made at the mechanical workshop at National Centre for Biological Sciences, Bengaluru, India. The diameter of the rotating rod was 3.3 cm made of Delrin and textured to enhance the grip of the animal. The rotating rod was fixed at the height of 30 cm from the platform, and the rod was partitioned into 3 areas at a 9.3 cm gap between each partition using discs made of Teflon of 40 cm diameter. A representative image showing the rotarod is depicted in **(Figure 2-4)**. Mice were trained for 5 consecutive days at different revolutions per minute (RPM) accelerated at 1 RPM/5 second, except on day-4 and -5, for 3 trials. A detailed protocol is given in **(Table 2-2)**. During testing, mice were given 3 trials at 15 rpm for 60 seconds. After the trial/testing, each mouse was returned to its respective home cage. The rotating rod was wiped with 70 % ethanol and was allowed to dry completely before placing the next animal on the rotating rod. All the trials were recorded using a Sony HD camera (HDR-CX405), and videos were analysed to score the latency to fall manually. Latency to fall was calculated by averaging the time spent on the rotarod from three trials.

Table 2-2 Protocol followed during training in rotarod on different days

RPM	Day
5-10	1
11-15	2
16-20	3
20	4
20	5

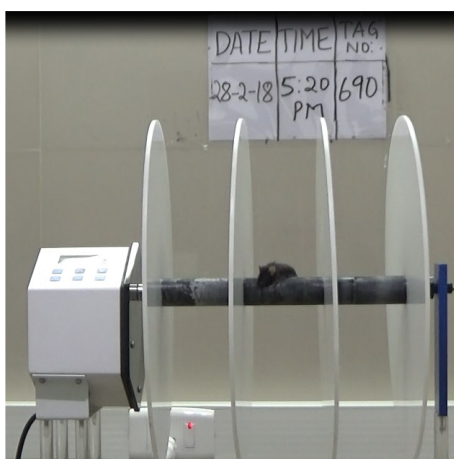


Figure 2-4 Image representing Rotarod apparatus

A picture depicting the mice placed on the rotarod at 15 RPM. The experimental trials were captured using a Sony HD camera and videos were later analysed manually to calculate the latency to fall. Latency to fall was scored by calculating the average time spent on the rotarod from three trials.

2.5.3 Hind-limb clasping

Hind-limb clasping was performed to assess the motor coordination and stages of disease progression in R6/2. Mice were suspended in the air by holding their tail for a maximum of 60 seconds, and videos were recorded using a Sony HD camera (HDR-CX405). A representative image depicting hind-limb clasping is shown in **(Figure 2-5)**. The recorded videos were then analysed manually based on the Racine scale. Depending on its hind-limb movements, scores were calculated accordingly. Lower the score better the performance of the mice. The method for scoring hind-limb clasping is mentioned in **(Table 2-3)**.

Table 2-3 Protocol showing the method to score based on Racine scale

Score	Time taken to Clasp
Zero	No clasping
One	Clasping in 31-60 seconds
Two	Clasping in 16-30 seconds
Three	Clasping in 11-15 seconds
Four	Clasping in 6-10 seconds
Five	Clasping in 1-5 seconds

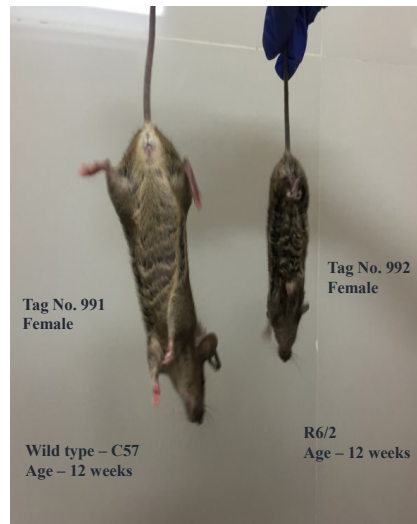


Figure 2-5 Image representing typical hind-limb clasping phenotype in R6/2 mice

The R6/2 was suspended by its tail in the air for a maximum of 60 seconds and its movement was recorded using a camera. The videos were analysed manually based on the Racine scale to determine the progress of disease severity.

2.6 Immunoblot Analysis

2.6.1 Lysate preparation

Mice were sacrificed by cervical dislocation and lysates from different regions of the brain, i.e., cortex, hippocampus, striatum, and cerebellum were considered for immunoblot analysis. Studies have shown that mHTT aggregates get accumulated throughout the brain (as explained in Chapter 3 introduction), it is important to validate and check for the major areas affected by mHTT aggregate accumulation. Besides, the above-mentioned brain regions are responsible for effective motor, cognitive functions, memory, and balance which are thereby impaired in R6/2 as the disease progresses^{10,277}.

These different regions were carefully separated from whole brain and lysates were prepared in Dounce tissue homogenizer - 7 mL (Cat# D9063, Sigma, India), and 15 mL (Cat# D9938, Sigma, India) in modified RIPA (Radio-Immunoprecipitation Assay) lysis buffer: 150 mM NaCl (Cat# S6191, Sigma, India), 50 mM Tris-HCl, pH 7.4 (Tris – Cat# 15965, Fisher Scientific, India; HCl – Cat# HC301585, Merck, India), 5 mM EDTA (Cat# RM1195, HiMedia, India), 0.25 % sodium deoxycholate (Cat# D6750-100G, Sigma, India), 0.1 % Triton X (Cat# 845, HiMedia, India), 0.1 % SDS (Cat# 161-0302, Bio-Rad, India), with protease

inhibitor (Cat# 11836170001, Sigma, India), and phosphatase inhibitor cocktails (Cat# P2850 – Cocktail 1, P5726 – Cocktail 2, P0044 – cocktail 3 Sigma, India).

Functions of the components of RIPA lysis buffer are mentioned in **(Table 2-4)**. Homogenates were centrifuged at 14,000 rpm at 4°C for 30 minutes, and the supernatant was collected for a soluble fraction. The centrifugation speed and time is optimum for the separation of the soluble fraction of proteins, and insoluble fractions will get sediment in the form of pellet as inclusion bodies. Centrifugation at 4°C will prevent the proteins from degradation. These steps were followed for all the lysate preparations used in the study.

Table 2-4 Functions of components of RIPA buffer.

Components	Function
150 mM NaCl	Prevents non-specific protein aggregation
Tris-HCl, pH 7.4	Buffering agent and prevents protein denaturation
5 mM EDTA	Chelates divalent cations and inhibit protease activity
0.25% sodium deoxycholate	The ionic detergent used to disrupt protein interactions
0.1% Triton X	Used to lyse cells and extract proteins
protease inhibitor	Inhibits various proteases; prevents protein degradation
phosphatase inhibitor	Inhibits various phosphatases; prevents protein degradation

2.6.2 Protein estimation

Proteins were estimated by Bradford assay using Bradford reagent (Cat # 5000006 from Bio-Rad, India). Bradford assay is a sensitive technique used to measure the total protein concentration in the given sample. Bradford reagent is commonly called Coomassie G-250 or Coomassie Blue. Under acidic conditions, the dye is cationic, protonated and is red. It binds stably to proteins and the protein-dye complex shifts the absorbance maximum from 465 nm to 595 nm. The colour changes from red to blue upon binding to protein and is measured spectroscopically at 595 nm. The increase in absorbance at 595 nm is directly proportional to the amount of dye bound to the protein present in the sample.

Protein standards with range (0.5 µg - 10 µg/µL) were assayed using Bovine Serum Albumin (BSA) (Cat # TC194 from HIMEDIA, India) as a standard and concentration of the protein samples were measured by taking absorbance at 595 nm against BSA as a standard reference using ELISA reader – (Versamax Molecular devices). A representative graph for Bradford assay is shown in (Error! Reference source not found.).

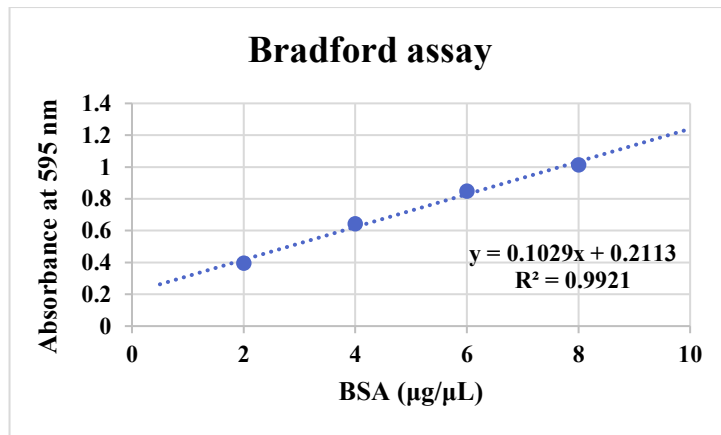


Figure 2-6 Graph depicting Bradford assay to measure protein concentration

The protein concentration was calculated using BSA as a standard reference range (0.5 µg - 10 µg/µL) by measuring absorbance maximum at 595 nm using an ELISA plate reader. The standard curve is plotted using linear regression and the relationship between the standard is described by linear relationship ($R^2 = 0.9921$). The grey line shows the linear plot, and the equation is $y=0.1029x+0.2113$. Solving for x value against the absorbance value gives the protein concentration.

2.6.3 SDS-PAGE and immunoblotting

Proteins were separated and electrophoresed in SDS-PAGE (Sodium Dodecyl Sulphate-Polyacrylamide Gel Electrophoresis) using Bio-Rad electrophoresis apparatus (Mini-PROTEAN Tetra Cell – Cat # 1658005). Proteins were separated based on their molecular masses. After treatment with reducing agent and SDS, all the proteins are in their primary structure and attains a uniform negative charge, thereby the shape and charge of the protein do not affect the separation. Therefore, proteins are separated based on their molecular weights. 5 % stacking was used for all the experiments, while 12 % for autophagy related proteins (LC3B, p62, and GABARAPL2), 8 % for Ub and 6 % resolving were used mHTT aggregates (EM48) respectively for ~2 hours at 90V. The separated proteins were transferred onto PVDF (Polyvinylidene fluoride; Cat# 162-0177, Bio-Rad, India) membrane for 2 or 24 hours at 90V approximately for autophagy related proteins, UBIQUITIN (Ub), and HTT aggregates at 4°C, respectively. (PVDF membrane is preferred over nitrocellulose as it has high protein binding capacity and offers high sensitivity. Moreover, PVDF membrane is less fragile than nitrocellulose and is a better choice for experiments that require stripping and re-probing of the membrane). Since mHTT aggregates are dynamic and larger in size with higher-order oligomeric structures, the transfer was set up for 24 hours for efficient transfer of aggregates

onto PVDF membrane. Whereas autophagy related proteins and Ub chain have a molecular weight of less than 180 kDa, transfer was set up for 2 hours at 4°C. After transfer, blots were blocked in 5 % skimmed milk (Cat# M530, Hi-Media, India) for one hour and washed thrice in PBST (Phosphate Buffered Saline Tween; 0.1 % Tween-20 (Cat# 28599, Sisco research laboratories, India) in 1X PBS). Skimmed milk was used for blocking as it effectively prevents the non-specific binding of primary antibodies to the PVDF membrane. PBST as a buffering and washing agent was used in all the washing steps for western blotting. It maintains the pH of the solution, washes any residual leftover, thereby preventing non-specific interactions with primary and secondary antibodies. Proteins were then probed for autophagy related proteins, Ub, and mHTT aggregates. A detailed list of primary and secondary antibodies used in the study are provided in (**Table 2-5**). After incubation, blots were washed thrice for ~10 minutes in PBST and incubated in secondary antibodies conjugated with Horse-radish-peroxidase in 1 % skimmed milk for ~1 hour at room temperature. Proteins were detected using ECL (Enhanced-Luminol-based chemiluminescent substrate; Cat# 1705060, Bio-Rad, India) and visualised using an I-Bright CL1000 Chemidoc system (Thermofisher). ECL assay depends on the emission of light as a product of the chemical reaction used to detect proteins. The secondary antibody is conjugated to the horseradish peroxidase (HRP) enzyme which reacts with the HRP substrate luminol. This reaction emits light at 428 nm and the signal is captured by a digital imager. Luminol emits light weakly, therefore enhancers are used to amplify the signal. This enhancement of a luminol-based signal is commonly referred to as Enhanced Chemiluminescence (ECL). Blots were quantified using ImageJ software (v1.52a, National Institutes of Health (NIH), U.S.A).

2.7 Histology

2.7.1 Perfusion

All the experimental mice were transcardially perfused with ice-cold (PBS) Phosphate Buffered Saline, pH – 7.4 (NaH₂PO₄·2H₂O – Cat # 14105; Na₂HPO₄·2H₂O – Cat # 27785; NaCl – Cat # 15915 from Fisher Scientific, India) and were fixed with 4 % PFA (Cat # 158127) in 0.1 M Sodium Phosphate buffer, pH – 7.4. A peristaltic pump (Cat# RH-P110S-25, Ravel Hitek PVT LTD, India) was used to perfuse the animals and the flow rate was constantly maintained at 10.2 mL per minute. After perfusion, brains were subjected to post-fixation in 4 % PFA overnight and transferred to 30 % sucrose with 0.1 % Sodium Azide to prevent bacterial and fungal contamination (Cat # TC048 from Hi-Media, India) and were preserved at 4°C for

further procedures. Functions of the buffer and reagent components used for perfusion and IHC are mentioned in (Table 2-6).

Table 2-5 Details of primary and secondary antibodies used in the study to check the expression of autophagy related proteins, Ub, and mHTT aggregates

Antibody	Dilution	Host	Catalogue No.
LC3B	1:1000	Rabbit	L7543, Sigma, India
GABARAPL2	1:1000	Rabbit	PAJ288Hu01, Cloud-Clone, India
p62	1:1000	Rabbit	P0067, Sigma
Anti-HTT (EM48)	1:500	Mouse	MAB5374, Merck, India
Anti-UBIQUITIN	1:1000	Mouse	P4D1-BML-PW0930-0100, ENZO Life Sciences, India
β-ACTIN	1:10000	Rabbit	PA116889, Thermo Fischer Scientific
Anti-rabbit	1:10000		1721019, Bio-Rad, India
Anti-mouse	1:10000		1706516, Bio-Rad, India

Table 2-6 Functions of the solutions used for perfusion and IHC

Components	Function
Phosphate Buffered Saline, pH – 7.4	Used as a buffer to maintain constant pH
4 % PFA	PFA fixes the tissue and preserves cell components and morphology
Sodium citrate buffer	Used to disrupt cross-linking between fixative and antigens (proteins)
PBSTx	The buffer used as a washing solution to remove leftover residues
0.1 % Triton-X-100	Used to lyse cells and extract proteins
2 % BSA	Used for blocking to prevent non-specific binding of antibodies to tissue or Fc receptors
1 % goat serum	Used as a blocking agent to prevent non-specific binding of primary antibody
1 % horse serum	Used as a blocking agent to prevent non-specific binding of primary antibody

2.7.2 Slide coating

Slides used for taking sections were soaked in 1N HCl (Cat # 29505 from Fischer Scientific, India) overnight and rinsed with double distilled water, and air-dried. Slides are treated with HCl to degrease the surface and to remove unwanted minute dust particles from the slides that are used for the coating to avoid cross-contamination. Slides were coated with 3 % gelatin [3 g gelatin (Cat # GRM019 from Hi-Media, India), and 0.05 g Chromium potassium sulphate dodecahydrate (Cat # GRM3042 from Hi-Media, India) in 100 mL of water]. Gelatin is an adhesive substance and slides coated with it are widely used since they are highly reliable and can hold the tissue sections effectively, thereby prevent them from falling off the slides. Chromium potassium sulphate dodecahydrate is used along with Gelatin to impart a positive charge to the slides so that tissues that are negatively charged are attracted to the opposite charge and can effectively attach to the surface of the slides. Gelatin coated slides were allowed to dry overnight at 60°C in a hot air oven and stored at room temperature for further use.

2.7.3 Cryosectioning

Sucrose-treated brains were embedded in OCT (Optimal Cutting Temperature) – Tissue freezing medium (Cat # 14020108926 from Leica Biosystems, India) on the chuck and was placed inside the cryostat (Cat # CM3050s from Leica, India) chamber. OCT is a water-soluble resin that provides a suitable matrix for sectioning the tissues at very low temperatures using a cryostat. Moreover, OCT leaves no residues after it is cleaned and prevents any undesirable background during staining. Internal chamber temperature (CT) in the cryostat was maintained at -20°C and Object Temperature (OT) at -22°C throughout the procedure. 40 µm thick coronal sections were taken on gelatin-coated slides. 5-6 sections were taken on each slide sequentially from the cortex, hippocampus, and striatum. Slides with sections were stored and preserved at 4°C till further usage. For all the brain tissues processed, experimental procedures were maintained constant throughout the study.

2.8 Immunohistochemistry

For Immunohistochemistry, the antigen retrieval was done by treating the sections with 10 mM Sodium citrate buffer (Cat# 6132-4-3, Fisher Scientific, India). The citrate buffer disrupts the protein cross-linking created by PFA, therefore, unmasking the antigens and epitopes. This will enhance the efficient binding of primary antibodies and increase the signal to noise ratio during imaging. The sections were then permeabilised with PBSTx (0.1 M PBS and 0.1 % Triton-X-

100) followed by blocking for ~4 hours at room temperature with 2 % BSA (Bovine Serum Albumin) and 1 % goat serum, and 1 % horse serum diluted in PBSTx. Functions of the components of the solutions used are mentioned in Table 2.6. Sections were incubated with primary antibodies for 48 hours at 4°C after 2 hours of incubation at room temperature. A cocktail of antibodies was diluted 300 times in 2 % BSA prepared in PBSTx. The antibodies used were anti-LC3B, anti-GABARAPL2, anti-p62, anti-HTT – EM48. After primary incubation, sections were probed with secondary antibodies for ~4 hours at room temperature in the dark. A cocktail of secondary antibodies was diluted 300 times in 2 % BSA, 1 % goat serum prepared in PBSTx. Complete details of primary and secondary antibodies were mentioned in (Table 2-7). After incubation, sections were mounted with Vecta-Shield containing DAPI (4',6-diamidino-2-phenylindole; Cat# H-1200, Vector Laboratories, CA, U.S.A) and were used for imaging. Images were obtained using confocal microscopy LSM 880 Airy Scan (Zeiss, India), and Delta Vision (Model#, GE Healthcare Ltd, India).

Table 2-7 Details of the list of primary and secondary antibodies used for immunostaining

Antibody	Dilution	Host	Catalogue No.
Anti-LC3B	1:300	Rabbit	L7543, Sigma, India
Anti-GABARAPL2	1:300	Rabbit	PAJ288Hu01, Cloud-Clone, India
anti-p62	1:300	Guinea-pig	GP62-C, iProgen Scientific
anti-HTT	1:300	Mouse	MAB5374, Merck, India
Atto Flour 550	1:300	Rabbit	43328, Sigma, India
Alexa flour 647	1:300	Guinea-pig	A-21450, Thermo Fisher Scientific, India
Alexa flour 488	1:300	Mouse	62197, Sigma, India

2.9 Cell culture experiments

HeLa cells were maintained in a growth medium composed of DMEM (Dulbecco's Modified Eagle Medium) (Cat# D5648, Sigma-Aldrich) supplemented with 3.7 g/l sodium bicarbonate (Cat# S5761, Sigma-Aldrich) plus 10 % Fetal Bovine Serum (FBS) (Cat#10270-106, Life Technologies). (FBS is used as a growth supplement for cell culture media because of its high content of embryonic growth-promoting factors and very low levels of antibodies) and 100 U/ml penicillin and streptomycin (Cat#15140-122, Life Technologies) at 5 % CO₂ and 37°C.

Upon confluence, the cells were passaged with 0.05 % Trypsin-EDTA (Cat#59418C, Sigma-Aldrich). (Trypsin-EDTA is a mixture of proteases used for cell dissociation and breaks down the proteins which enable the cells to adhere to the culture plates. Trypsinization is often used to passage cells to a new plate.

The drugs used in this study for the cell-culture experiments were – Nilotinib (Tasigna™) procured commercially, 6-bromoindirubin-3'-oxime, (6BIO) (Cat# B1686, Sigma-Aldrich, India) and Bafilomycin A1, (BafA1) (Cat#11038, Cayman chemicals)

2.9.1 Autophagy Assay

To perform Autophagy assays, 1.0×10^6 HeLa cells were seeded per well on 6-well plates and were allowed to attach for 24 hours. Autophagy was induced using Nilotinib(Tasigna™) dissolved in saline (5, 25, 50, 100, 250 μ M, and 1 mM), 6BIO (10 μ M) and BafA1 (100 nM) for ~2 hours. 6BIO and BafA1 were used as positive and negative control of autophagy modulators, respectively³⁴⁷.

Following treatments, cells were washed with ice-cold PBS. Cells were then lysed in 100 μ l of sample buffer [10 % w/v SDS, 10 mM dithiothreitol (reducing agent to breakdown protein disulfide bonds), 20 % vol/vol glycerol, 0.2 M Tris-HCl (pH 6.8), 0.05 % w/v bromophenol blue] and then collected using a cell scraper. Immunoblot was performed to check the expression of LC3B, and a similar procedure was followed, as mentioned in section 2.6.3.

2.10 Statistics

All the graphs were plotted using Microsoft office 365, and Graph Pad Prism 7 (for Survival graph). Data are presented as Mean \pm Standard Error of Mean (SEM). One-way, Two-way and Three-way ANOVA were applied, followed by appropriate post-hoc analysis (Bonferroni and Tukey), to test statistical significance as appropriate unless otherwise stated.

Chapter- 3
**Characterisation of mutant HUNTINGTIN aggregate
formation in R6/2 mice**

3.1 Introduction

HD is caused by a mutation in the *HUNTINGTIN* gene resulting in the expansion of polyQ in the HUNTINGTIN protein²²⁶. mHTT protein is prone to form amyloid fibrils and triggers the formation of the aggregation process. The rate of formation of aggregates from amyloid fibrils and oligomers depends on the length of polyQ leading to the presence of cytoplasmic and intranuclear inclusions, the most distinctive pathological hallmarks of Huntington's disease³⁴⁸. These inclusions consisting of toxic polyglutamine aggregates trigger mutant HUNTINGTIN dependent neuronal dysfunction. The mechanism of aggregate formation could account for many aspects of pathogenesis and the rate at which disease progresses in HD. Initiation of aggregation requires a critical concentration of oligomeric precursors and is also associated with a lag time, which may contribute and account for late-onset of the disease³⁴⁹. The process of nucleation leading to neuronal inclusions is very complex, and many intracellular factors play a determining role³⁵⁰.

The critical concentration of aggregate precursor in a given neuronal cell depends on cellular factors such as the ability of the cell to divide, transcriptional profile, post-processing of mHTT protein, cell-specific expression levels of key proteins, subcellular localisation, and compartmentalisation^{211,236,244,348,351}. The neuropathological hallmark of HD is the presence of N-terminal mHTT fragments in the form of inclusion bodies in cell culture models, animal models, and human post-mortem brain samples^{350,352-355}. The concept of N-terminal mHTT fragments as a part of inclusion bodies has been supported by many studies where antibodies have stained neuronal inclusions against the N-terminal part of mHTT but not the C-terminal³⁵⁴⁻³⁵⁹. Moreover, many mouse models have been generated where HD progression has been accelerated by overexpression of N-terminal mHTT fragment compared to full-length mHTT protein^{268,279,360-363}. One such mouse model is R6/2, where exon 1 of the human mHTT gene is expressed under the human *HTT* promoter, which recapitulates HD-like phenotype²⁶⁸. Therefore, as mentioned earlier, the post-processing of mHTT protein plays a very important role in the pathogenesis of HD.

The age-related decline in the capacity of neurons to maintain protein homeostasis also contributes to the accumulation of toxic inclusion bodies that may explain the late onset of many protein conformation-based diseases, including HD^{11,15,31,364}. However, the role of inclusion bodies in HD has been challenged and proposed that mHTT aggregate bodies can be neuroprotective^{37,365}. Interestingly, studies have shown that mHTT aggregates from cell-line-

based models, mouse models, and human post-mortem brain samples are positive for UBIQUITIN, indicating the role of proteasome degradation pathway and autophagy in maintaining the protein quality control in neuronal cells ^{350,352,366}. Studies have shown that wild-type HTT and mHTT can be ubiquitinated at its N-terminal domain, suggesting specific UBIQUITIN-mediated degradation by cellular clearance mechanisms such as UPS and autophagy pathways ^{207,367-370}. Besides the direct role of UPS and autophagy in diluting the mHTT oligomers and aggregates, the impairment of these pathways by polyQ expanded mHTT protein determine the HD-related pathological changes. ^{7,15,106}.

Therefore, it is essential to understand the process of mHTT aggregate formation and intracellular ubiquitination pattern to get detailed insights into the pathophysiology of HD. To date, many studies have been carried out to understand the mechanisms of aggregate formation in various cellular and mouse models, but at what stage of disease progression these aggregates start accumulating and whether the presence of mHTT aggregates affects the ubiquitination pattern is not investigated. In this regard, the HD mouse model, R6/2, has been used to study the accumulation of toxic mHTT aggregates across different stages of disease progression in various regions of the brain such as the cortex, hippocampus, striatum, and cerebellum.

3.2 Methods

Brain lysates from different regions such as cortex, hippocampus, striatum, and cerebellum from wild-type and R6/2 mice were prepared in a modified RIPA lysis buffer. Four age groups 2, 4, 8, and 12 weeks were considered for the analysis corresponding to different stages of disease progression in R6/2. mHTT aggregates were detected by probing with mEM48 primary antibody, which reacts explicitly with HUNTINGTIN protein that expresses a different number of polyglutamine repeats and detects toxic mHTT protein. Ubiquitin profile was checked by staining with PAN-Ubiquitin antibody, which detects a stretch of native ubiquitin molecules. [Note: Detailed experimental procedures were mentioned in chapter 2: Methods and materials section].

3.3 Results

3.3.1 Mutant HUNTINGTIN aggregates were detected as early as 2 weeks in R6/2 mice

Many studies have been carried out to understand the dynamics of mHTT aggregate formation and have been shown that aggregates exist in multiple different conformations inside the cells leading to neuronal toxicity^{349,350,356,371}. Based on the intrinsic properties and post-processing of HTT protein with polyQ, aggregates exist as soluble monomers, oligomers, and higher-order annular and amyloid fibril like structures, thereby forming inclusion bodies inside the neuronal cells^{211,368}. Immunohistochemical analysis has shown that UBIQUITIN positive mHTT aggregates are present as early as PND 1 (Post Natal Day) in neostriatum and hippocampus of R6/2 mice, and they increase in number and size as the disease progresses²⁶⁹.

To further understand the aggregate formation in R6/2 mice, expression of mHTT aggregates was assayed by immunoblotting at the end stage of disease progression, i.e., at 12 weeks from the cortex, hippocampus, striatum, cerebellum. Results suggest that, compared to wild-type control mice, mHTT aggregates were detected by mEM48 from all four brain regions in R6/2 mice (**Figure 3-1A, B**). Furthermore, to understand at what stage of disease progression mHTT aggregates accumulate inside the neuronal cells, expression was assayed by immunoblotting from 2-, 4-, 8-, and 12-weeks brain lysates from the cortex, hippocampus, striatum, and cerebellum. Remarkably, mHTT aggregates were detected from 2 weeks of age in the cortex, and striatum (**Figure 3-2A, B** for Striatum; **Figure 3-2C, D** for Cortex), whereas in the hippocampus, and cerebellum, mHTT aggregates were detected from 4 weeks (**Figure 3-2E, F** for Hippocampus; **Figure 3-2G, H** for Cerebellum).

Due to the early presence of mHTT aggregates, there is a disruption in cortico-striatal connections making neurons vulnerable to degeneration^{235,269,372}. These results propose and support the fact that striatum and cortex are affected early, leading to cognitive and motor dysfunctions in R6/2. These findings suggest that seed nucleation starts early during development to form large mHTT aggregates. mHTT aggregates increase in concentration and spread gradually across different regions of the brain, thereby contributing to rapid disease progression leading to neuronal death in R6/2.

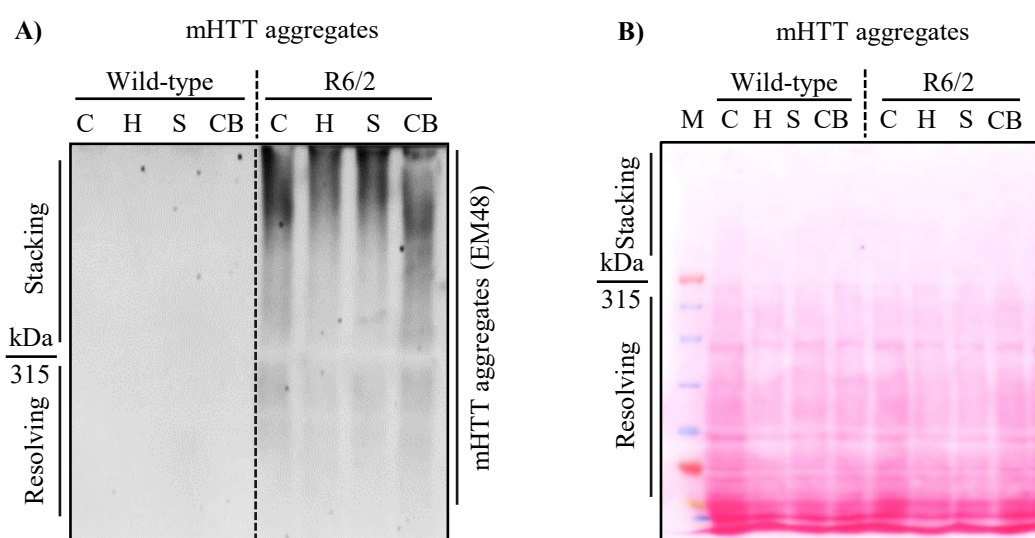


Figure 3-1 Detection of mHTT aggregates at different regions of the brain in R6/2 mice from 12 weeks of age

A) Representative immunoblot showing mHTT aggregates at 12 weeks of age in R6/2 compared to wild-type control littermates across different regions of the brain. mHTT aggregates were detected by EM48 antibody, which specifically detects polyglutamine aggregates. **B)** Representative ponceau S staining for the blot represented to the left. Vertical black dashed lines separate the genotypes. N=12 (Male). C=Cortex, H=Hippocampus, S=Striatum, CB=Cerebellum; WT=Wild-type; kDa=kiloDaltons.

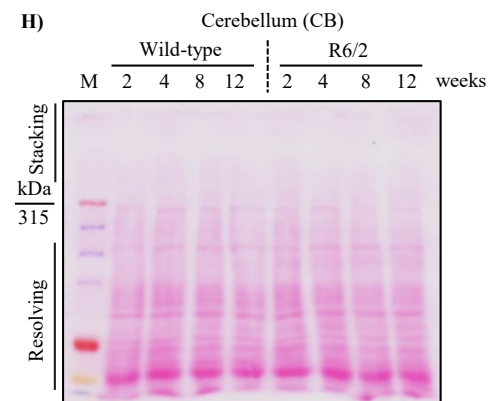
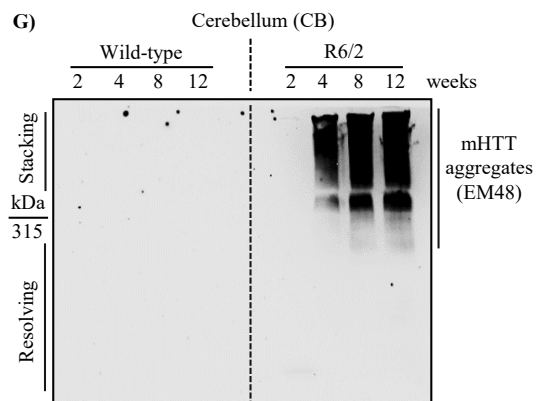
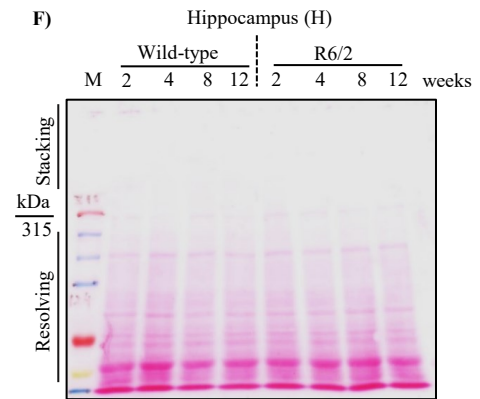
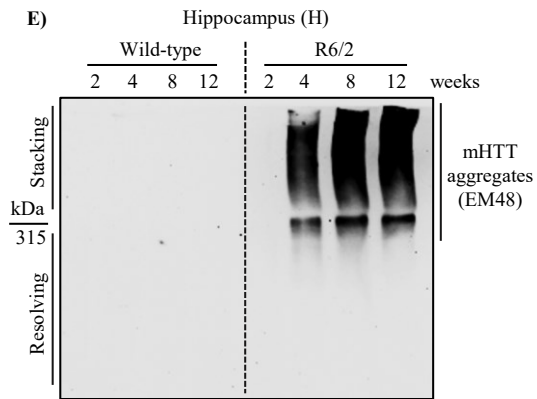
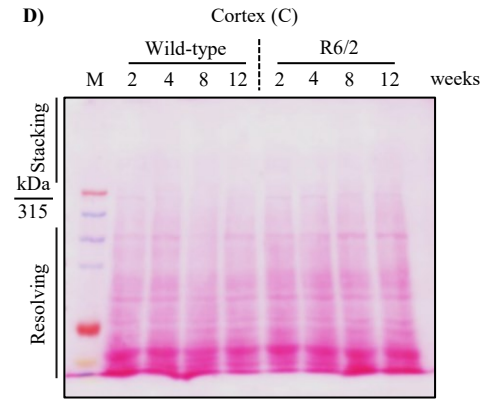
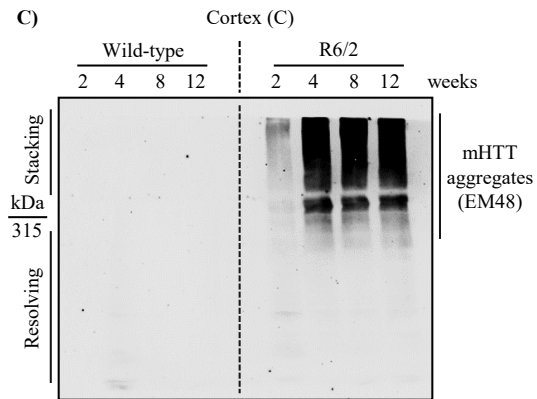
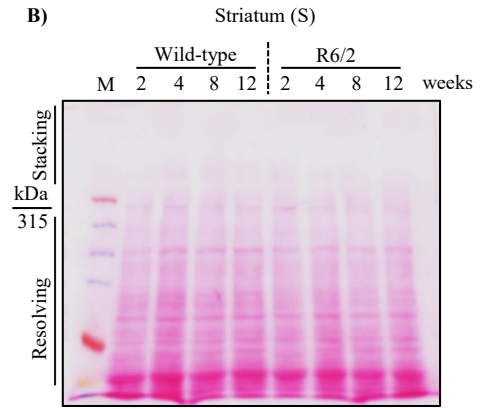
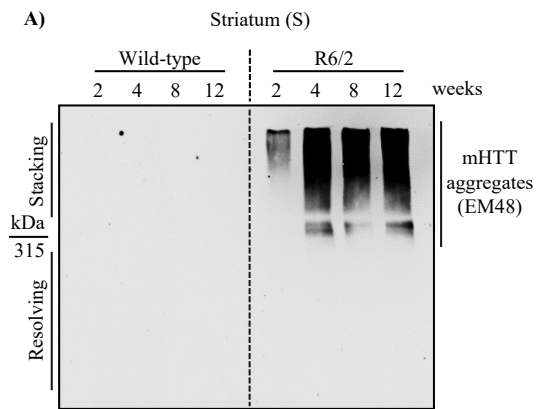


Figure 3-2 Dynamics of mHTT aggregate formation across different stages of disease progression in R6/2 mice

A) Representative immunoblot showing early accumulation of mHTT aggregates in the striatum at 2 weeks of age in R6/2 compared to wild-type control littermates. **B)** Representative image showing ponceau S staining for the striatum blot represented to the left. **C)** Representative image of an immunoblot showing accumulation of mHTT aggregates in the cortex at 2 weeks in R6/2. **D)** Blot showing ponceau S staining for the cortex. **E)** Representative blot showing detection of mHTT aggregates in the hippocampus at 4 weeks of age in R6/2 compared to wild-type mice. **F)** Image showing ponceau S staining for the region hippocampus. **G)** Representative immunoblot showing accumulation of mHTT aggregates in the region cerebellum at 4 weeks in R6/2. **H)** Representative image showing ponceau S staining for the cerebellum blot. Mouse monoclonal EM48 antibody was used to detect mHTT aggregates in R6/2. Vertical black dashed lines separate the genotypes. N=5 for 2 weeks, N=7 for 4 and 8 weeks, and N=12 for 12 weeks. N=number of mice. C=Cortex, H=Hippocampus, S=Striatum, CB=Cerebellum; kDa=kiloDaltons.

3.3.2 Ubiquitination is increased in the striatum at the end stage of disease progression in R6/2 mice

Labelling a chain of UBIQUITIN molecules to the protein is essential for a wide range of cellular activities such as degradation and localisation³⁷³. Covalent attachment of a series of UBIQUITIN molecules to a lysine residue side chain of a targeted protein is a multistep process for degradation by UPS and autophagy machinery³⁷³. Different enzymatic components such as a UBIQUITIN-activating enzyme (E1), UBIQUITIN-conjugating enzyme (E2), and UBIQUITIN-ligating enzyme (E3) are required for labelling the proteins to be degraded³⁷³. mHTT gets ubiquitinated at its N-terminal domain-containing polyQ by specific E3 UBIQUITIN ligases suggesting UBIQUITIN-mediated degradation by cellular mechanisms such as UPS and autophagy pathways^{369,374}. Since there is an early accumulation of mHTT aggregates in R6/2, it is interesting to find out if there are any noticeable changes in the overall ubiquitination pattern in the neuronal cell. In this regard, the UBIQUITIN profile of the cell was checked by staining with Pan-UBIQUITIN antibody, which identifies the chain of native UBIQUITIN molecules binding to aggregates.

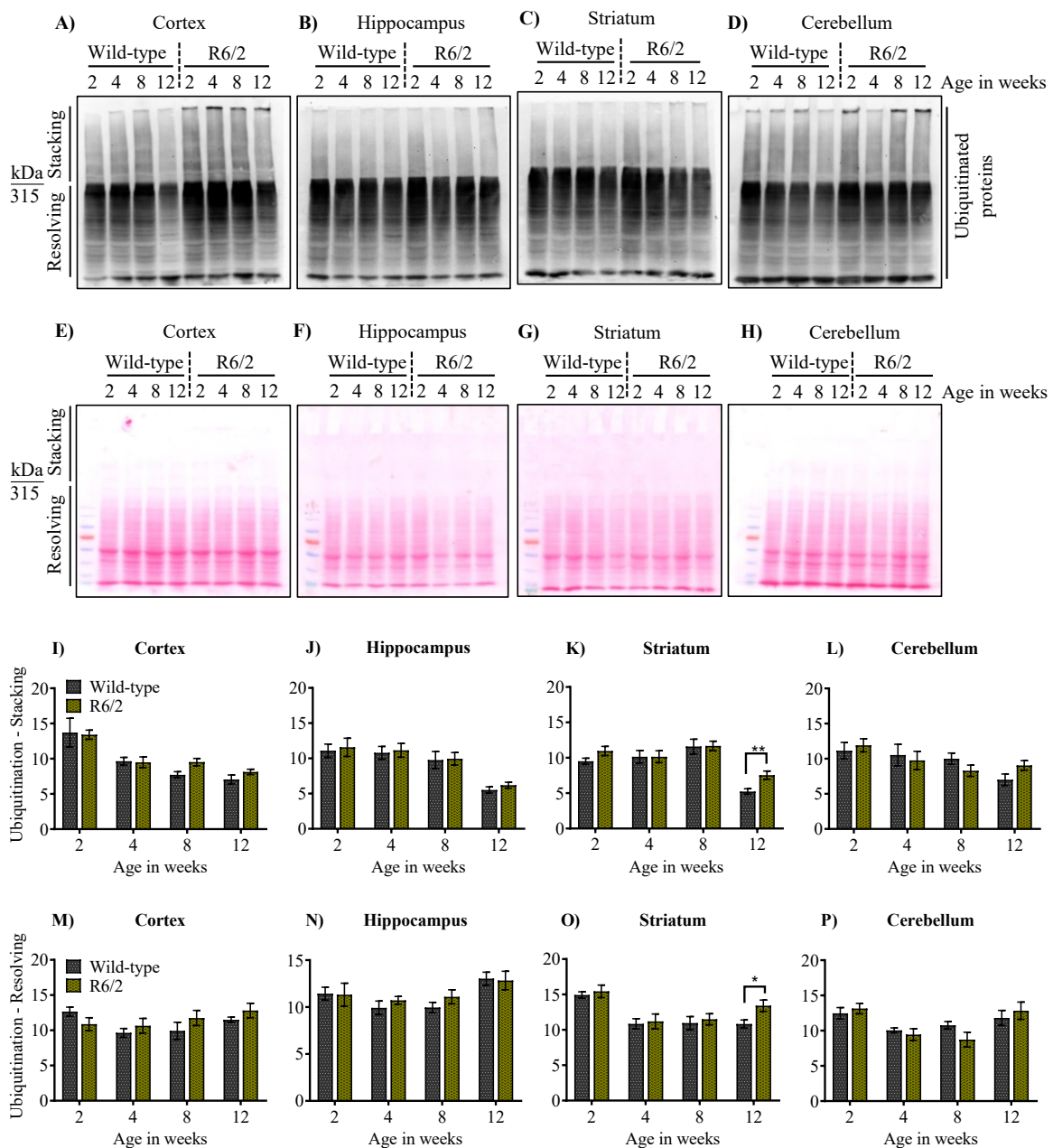


Figure 3-3 Ubiquitination is increased in the striatum at the end-stage of disease progression in R6/2 mice

A, B, C and D. Representative immunoblot for UBIQUITIN profile from 2, 4, 8, and 12 weeks in the cortex, hippocampus, striatum, and cerebellum, respectively. **E – H.** Representative ponceau S-stained blot for UBIQUITIN profile from 2, 4, 8, and 12 weeks in the cortex, hippocampus, striatum, and cerebellum, respectively. **I – L.** Quantified bar graphs for UBIQUITIN profile (Stacking) for cortex: Age x Genotype ($F_{(3,54)}=0.82$, $p=0.48$), hippocampus: Age x Genotype ($F_{(3,54)}=0.04$, $p=0.98$), striatum: Age x Genotype ($F_{(3,54)}=1.49$, $p=0.22$), and cerebellum: Age x Genotype ($F_{(3,54)}=1.57$, $p=0.20$), respectively. **M – P.** Quantified bar graphs for UBIQUITIN profile (Resolving) for cortex: Age x Genotype ($F_{(3,54)}=1.095$, $p=0.35$), hippocampus: Age x Genotype ($F_{(3,54)}=0.31$, $p=0.81$), striatum: Age x

Genotype ($F_{(3,54)}=1.08$, $p=0.36$), and cerebellum: Age x Genotype ($F_{(3,54)}=0.89$, $p=0.44$), respectively. $N=5$ for 2 weeks, $N=7$ for 4 and 8 weeks, and $N=12$ for 12 weeks for both the genotypes wild-type and R6/2. Error bars indicate \pm SEM. N =number of mice. The genotypes are separated by vertical dashed lines. Statistical analysis was done by Two-way ANOVA followed by Bonferroni post-hoc test. * $p\leq 0.05$; ** $p\leq 0.01$.

Since mHTT aggregates were detected at the early stages of disease progression in R6/2, we checked for any alteration in the global ubiquitination profiles across different brain regions. Considering that mHTT aggregates are of high molecular weight, we observed aggregates only in the stacking gel in western blot analysis (**Figure 3-3 (A-H)**). In view of this, to identify the detectable changes, we assayed the ubiquitination profiles in both stacking and resolving gels from different regions of the brain across various stages of disease progression (**Figure 3-3**). There was a significant increase in the ubiquitination pattern in both stacking and resolving in the region striatum in R6/2, compared to wild-type controls at 12 weeks of age. (**Figure 3-3C, G, K, O**). Interestingly, despite the presence of mHTT aggregates, there was no significant difference observed in the ubiquitination pattern in the other regions of the brain such as the cortex (**Figure 3-3A, E, I, M**), hippocampus (**Figure 3-3B, F, J, N**), and cerebellum (**Figure 3-3D, H, L, P**) across different stages of disease progression in R6/2. These results explain that due to the presence of mHTT aggregates, there is increased Ubiquitination in the striatum, which is the most affected region of the brain in HD. These findings correlate with previous studies suggesting the presence of intracellular ubiquitinated HUNTINGTIN aggregates in inclusion bodies^{269,355,375-377}.

3.4 Discussion

The results discussed in this chapter suggest that mHTT aggregates accumulate inside the neuronal cells as early as 2 weeks of age and contribute to disease pathogenesis in R6/2. This study is the first to characterise the complete developmental profile of mHTT aggregate formation in R6/2 across different stages of disease progression from various regions of the brain. It has been shown that mHTT aggregates accumulate from 2 weeks in the striatum and the cortex, whereas in the hippocampus and cerebellum, mHTT aggregates were detected from 4 weeks of age. The N-terminal specific antibody mEM48, which specifically identifies toxic polyQ human HUNTINGTIN fragments, was used to detect mHTT aggregates³⁵². The accumulation of mHTT aggregates was assayed only in the soluble fractions because studies have shown that soluble fractions are toxic and disrupt many cellular processes leading to

pathogenicity in HD ³⁷⁸⁻³⁸³. Moreover, it would be interesting to study the properties of different oligomeric species of mHTT aggregates. In this regard, in future studies, the A11 antibody can be used that detects explicitly soluble toxic amyloid polyglutamine aggregates.

The study also characterised the UBIQUITIN expression profile and shown that it is differentially regulated across different regions of the brain in R6/2 mice. The expression of the UBIQUITIN profile was increased in both stacking and resolving in the region striatum at 12 weeks in R6/2 compared to wild-type, suggesting that there was no defect in labelling mHTT aggregates by UBIQUITIN molecules. However, despite the early accumulation of mHTT aggregates in R6/2, there was no change observed in the global ubiquitination profile of the cell across different stages of disease progression in the cortex, hippocampus, and cerebellum. These results suggest that mHTT aggregates were detected and labelled by UBIQUITIN molecules, but the accumulation is due to the defects in intracellular clearance pathways such as UPS and autophagy. In conclusion, mHTT aggregates are complex and dynamic and get accumulated starting from 2 weeks of age in R6/2, thereby contributing to rapid disease progression.

Chapter- 4
Spatio-temporal analysis of autophagy and its efficiency
in clearing polyglutamine aggregates in R6/2 mice

4.1 Introduction

Autophagy is a highly conserved catabolic process that degrades and recycles cellular constituents such as proteins, protein complexes, and damaged organelles⁶⁰. Aggrephagy is a major pathway through which many aggregates that are implicated in neurodegenerative disorders like PD, AD, ALS, and HD are degraded. Due to increasing evidence for the physiological importance of autophagy in neuronal cells, impairment in autophagy may play a vital role in the progression of many severe forms of age-related neurodegenerative diseases^{105,106,124,384-386}. For example, defect in cargo recognition and loading has been implicated in HD and is mediated through the interaction of mHTT aggregates with p62/SQSTM1, and can affect autophagy in many ways, such as impairing vesicle trafficking^{387,388}.

mHTT interacts with cytoskeletal proteins, thereby disrupting autophagosome motility and subsequently preventing the autophagosome fusion with lysosomes²¹⁸. It is known that lysosomal enzyme activity is reduced in HD, because of the accumulation of reactive oxygen species, given the fact that neuronal cells with mHTT aggregates contain markedly increased numbers of lysosomes containing non-degraded lipofuscin^{204,389}. After post-processing of mHTT protein, N-terminal fragment of polyQ-HTT translocate into the nucleus and has been shown to interact with various transcriptional factors such as TFEB, which encode the proteins required for autophagosome assembly, autophagosome-lysosome fusion, and lysosomal degradative enzyme activity^{204,351,358}. Given all the compelling evidence to support autophagy dysfunction in NDD's including HD, yet the state of basal autophagy in these diseases is unclear. In this study, the HD mouse model, R6/2, was used to understand and evaluate the Spatio-temporal expression of key autophagy related proteins from various brain regions such as the cortex, hippocampus, striatum, and cerebellum across different stages of disease progression.

4.2 Methods

For immunoblotting, brain lysates from different regions of the brain such as the cortex, hippocampus, striatum, and cerebellum were collected from four age groups, 2, 4, 8, and 12 corresponding to different stages of disease progression from wild-type and R6/2 mice. For immunohistochemistry analysis, PFA fixed brain sections were taken from 12-week-old wild-type and R6/2 mice. For both the analysis, proteins were detected by probing with primary

antibodies such as anti-LC3B, anti-p62, anti-GABARAPL2, anti-HTT (EM48), and anti- β -ACTIN.

[Note: Detailed experimental procedures were mentioned in Chapter 2: Methods and materials section].

4.3 Results

4.3.1 Basal autophagy is unaltered and spatiotemporally maintained in R6/2 mice

Autophagy in the brain is tightly controlled and regulated, and its dysfunction plays a very important role in the pathophysiology of HD ^{210,364,386,390,391}. To investigate the state of basal autophagy in R6/2 mice, the expression of key autophagy related proteins, p62/SQSTM1, LC3B, and GABARAPL2, was assessed by immunoblotting technique. Four different age groups, i.e., 2, 4, 8, 12 weeks, from different stages of disease progression, were considered for temporal analysis and diverse brain regions such as the cortex, hippocampus, striatum, and cerebellum were considered for spatial analysis. p62/SQSTM1, a UBIQUITIN-LC3 binding protein, one of the most abundantly expressed adapter molecule in the neuronal cell, binds to the aggregates and drives its degradation by autophagy. There was no significant difference observed in the levels of p62/SQSTM1 in the cortex (**Figure 4-1A, B**), hippocampus (**Figure 4-2A, B**), striatum (**Figure 4-3A, B**), and cerebellum (**Figure 4-4A, B**) in all the four age groups in R6/2 mice compared to wild-type control mice. Further, out of 5 isoforms of MAPLC3 (Microtubule Associated Protein Light Chain 3), 2 of them, LC3B and GABARAPL2, were used to assess the autophagy flux in R6/2. LC3B and GABARAPL2 were considered autophagosome markers that label the double membrane mature autophagosomes and exist in both lipidated (phosphatidylethanolamine conjugated) and non-lipidated (unconjugated) forms, the former being the active one. No significant difference observed in the levels of LC3B in the cortex (**Figure 4-1A, C, and D**), hippocampus (**Figure 4-2A, C, and D**), striatum (**Figure 4-3A, C, and D**), and cerebellum (**Figure 4-4A, C, and D**) in all the four age groups, except for 12 weeks, where there was a significant decrease in the expression of LC3B-I in the cortex. This differential regulation of expression at later stages of disease progression in R6/2 might be due to the loss of function of LC3B, where there might be a defect in the conversion rate of LC3B-I form to LC3B-II form, which is the functional one, for active autophagy flux. However, another autophagosome marker, GABARAPL2,

showed a significant increase in the cortex only at 8 weeks (**Figure 4-1A, E**), whereas the expression is unaltered in the hippocampus (**Figure 4-2A, E**), striatum (**Figure 4-3A, E**), and cerebellum (**Figure 4-4A, E**) in all four age groups in R6/2 compared to wild-type control mice. In all the experimental conditions, house-keeping protein β -ACTIN was used as a loading control to normalise the expression of all key autophagy related proteins used in the study. Despite the build-up of toxic mHTT aggregates in these brain regions, as early as 2 weeks of age, the basal level of autophagy was not altered during the developmental stages in R6/2. These findings validate an earlier study in the BACHD (Bacterial Artificial Chromosome Huntington's Disease) mouse model of HD in which the basal autophagy remained unaltered in the hypothalamus and cortical regions of the brain despite metabolic dysfunction³⁹². In conclusion, western blot analysis showed no significant changes observed in the expression of key autophagy related proteins p62/SQSTM1, LC3B-II, GABARAPL2-II in different regions of the brain across various stages of disease progression in R6/2 mice. The only significant difference found in levels of LC3B-I and GABARAPL2-II in 12 and 8 weeks in the cortex, respectively, might suggest an impairment in the formation and maturation of the autophagosome. However, these results are inconclusive and need to be further validated by different autophagy assays. Moreover, the study carried out in this thesis is the first to provide evidence to show that basal autophagy is spatiotemporally maintained in R6/2 and would provide critical insights in understanding autophagy dysfunction in other age-related neurodegenerative diseases including HD.

4.3.2 mHTT aggregates form intranuclear inclusions and co-localise with p62/SQSTM1 in R6/2 mice

Many studies have shown that mHTT protein at its N-terminal domain-containing polyQ forms intracytoplasmic and nuclear inclusions depending on the post-processing of HTT protein. mHTT protein undergoes a series of proteolytic cleavage by various caspases and undergoes nuclear translocation, thereby forming intranuclear inclusions. mHTT aggregates inside the nucleus, sequester many essential transcriptional factors, thus impairing the expression of key proteins for cell survival. Since immunoblotting results suggest no change in the expression of key autophagy related proteins in R6/2, it is important to study the expression pattern and co-localisation of key autophagy related proteins p62/SQSTM1, LC3B, GABARAPL2, with each other and with mHTT aggregates. In this regard, their expression was checked by immunohistochemistry at 12 weeks in the striatum of wild-type and R6/2 mice. In accordance

with previous studies, mHTT aggregates formed intranuclear inclusions and were co-localised with an adaptor protein, p62/SQSTM1, where distinct punctate-like structures were observed inside the nucleus in R6/2, whereas diffused pattern was observed in wild-type mice (**Figure 4-5A, B**). There was no change in the expression pattern of autophagosome markers, LC3B and GABARAPL2, in R6/2 at 12 weeks in the striatum compared to the wild-type counterparts. However, LC3B and GABARAPL2 did not completely co-localise with neither p62/SQSTM1 nor mHTT aggregates, indicating impairment in cargo recognition and loading, suggesting autophagy dysfunction in R6/2 (**Figure 4-5A, B**)

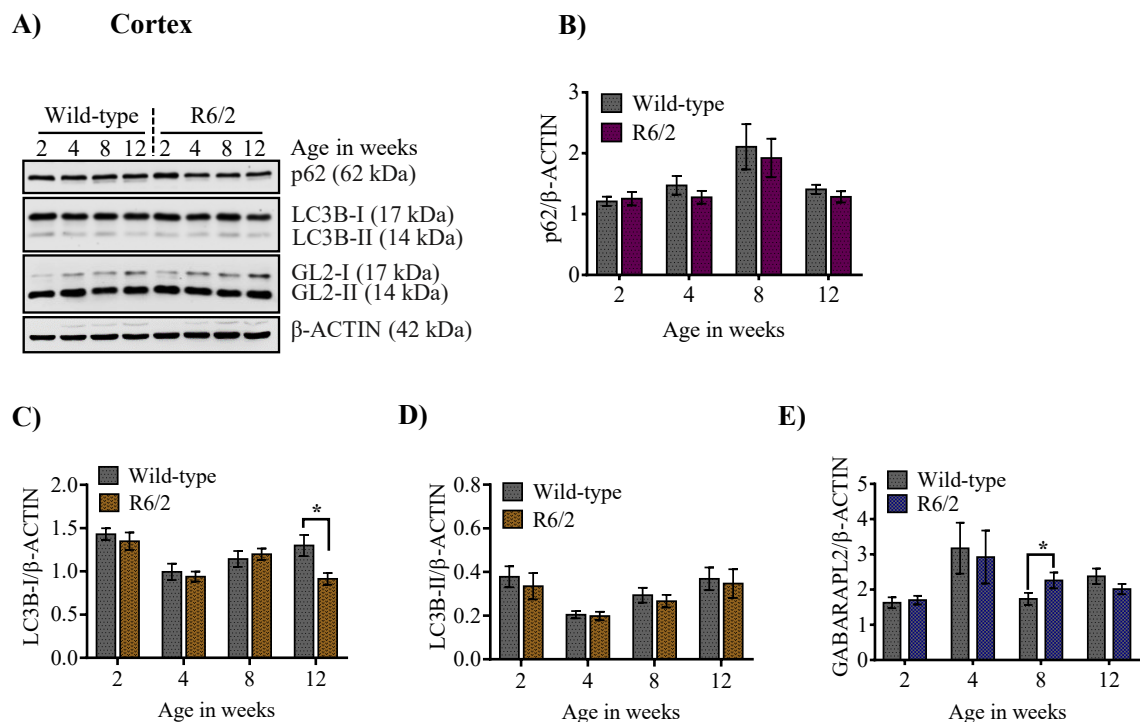
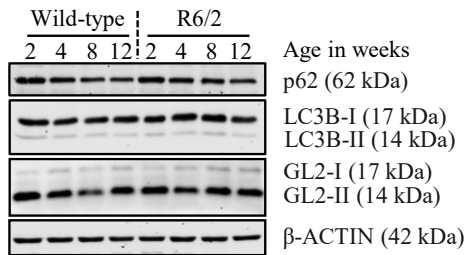


Figure 4-1 Basal autophagy is not altered in Cortex across different stages of disease progression in R6/2 mice

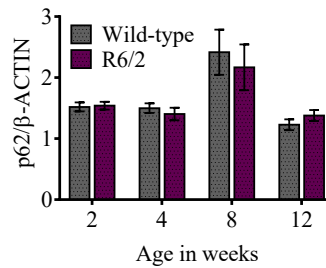
A) Representative immunoblots for autophagy related proteins: p62/SQSTM1, LC3B, GAPARAPL2 from the region cortex across different stages of disease progression in wild-type and R6/2 mice. β -ACTIN was used as a loading control for normalisation. **B)** Quantified bar graphs showing no significant difference in the expression levels of p62/SQSTM1 in R6/2 compared to wild-type mice across different age groups; Age x Genotype ($F_{(3,54)}=0.1322$, $p=0.94$). **C)** Pooled quantified bar graphs showing a significant difference in the expression levels of LC3B-I at 12 weeks in R6/2 compared to wild-type control mice; Age x Genotype ($F_{(3,54)}=2.380$, $p=0.07$); (12 weeks: $*p<0.05$). **D)** Compiled quantified bar graphs representing no change in the expression of LC3B-II across different stages of disease progression in R6/2; Age x Genotype ($F_{(3,54)}=0.03193$, $p=0.99$). **E)** Quantified bar graphs showing a significant difference in the expression of autophagosome marker GABARAPL2 (GL2) at 8 weeks in R6/2; Age x Genotype ($F_{(3,54)}=0.5814$, $p=0.62$); (8 weeks: $*p<0.05$). N=5 for 2 weeks, N=7 for 4 and 8 weeks, and N=12 for 12 weeks for both the genotypes wild-type and R6/2. Statistical

analysis was done by Two-way ANOVA followed by Bonferroni *post-hoc* test. Error bars indicate \pm SEM. N=number of mice. Vertical dashed lines separate the genotypes.

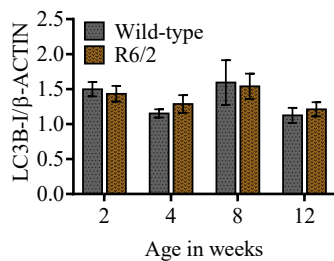
A) Hippocampus



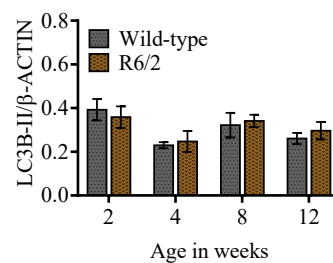
B)



C)



D)



E)

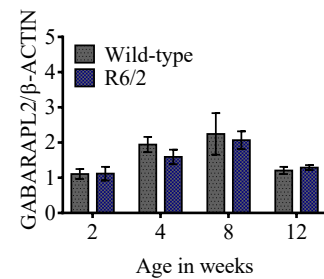


Figure 4-2 Basal autophagy is unaltered in R6/2 mice across different stages of disease progression in the region hippocampus

A) Representative immunoblots for autophagy related proteins: p62/SQSTM1, LC3B, GAPARAPL2 from the region hippocampus across different disease progression stages in wild-type and R6/2 mice. β -ACTIN was used as a loading control for normalisation. **B)** Quantified bar graphs showing no significant difference in the expression levels of p62 in R6/2 compared to wild-type mice across different age groups; Age x Genotype ($F_{(3,54)}=0.4656$, $p=0.70$). **C)** Pooled quantified bar graphs showing no significant change in the expression levels of LC3B-I in R6/2 compared to wild-type control mice; Age x Genotype ($F_{(3,54)}=0.1890$, $p=0.90$). **D)** Compiled quantified bar graphs representing no change in the expression of LC3B-II across different stages of disease progression in R6/2; Age x Genotype ($F_{(3,54)}=0.2341$, $p=0.87$). **E)** Summary of quantified bar graphs showing no difference in the expression of GABARAPL2 (GL2) in R6/2 across different age groups; Age x Genotype ($F_{(3,54)}=0.3486$, $p=0.79$). N=5 for 2 weeks, N=7 for 4 and 8 weeks, and N=12 for 12 weeks for both the genotypes wild-type and R6/2. Statistical analysis was done by Two-way ANOVA followed by Bonferroni *post-hoc* test. Error bars indicate \pm SEM. N=number of mice. Vertical dashed lines separate the genotypes.

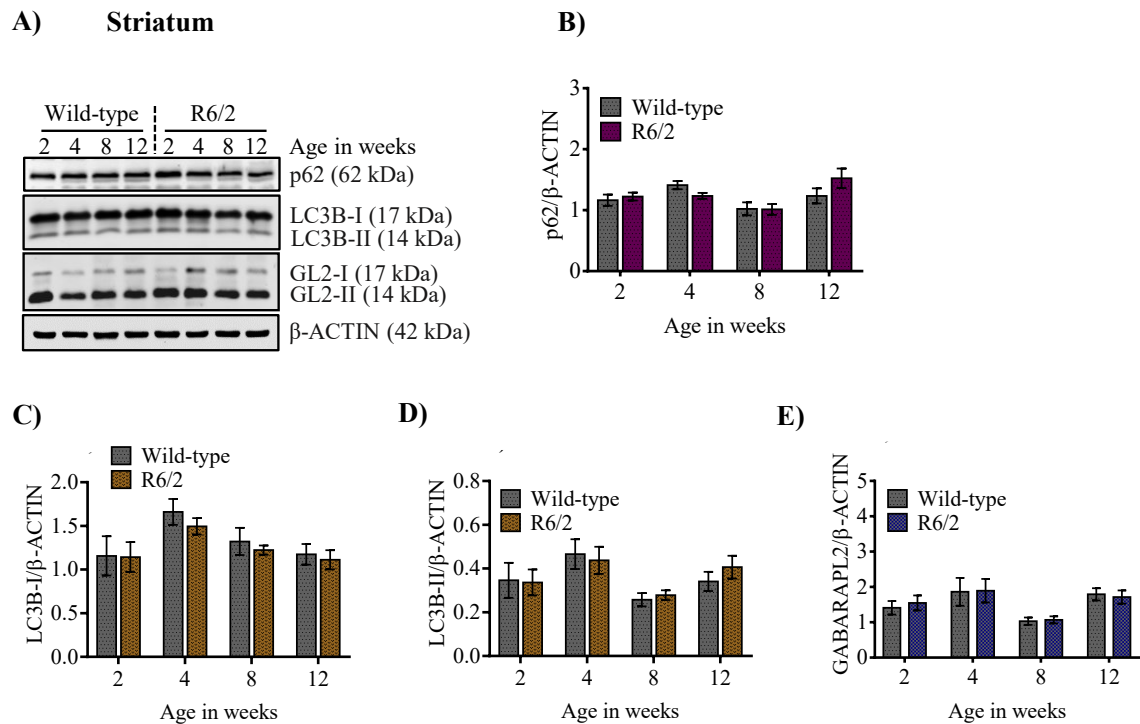


Figure 4-3 Spatio-temporal regulation of autophagy related proteins in striatum across different stages of disease progression in R6/2 mice

A) Representative immunoblots for autophagy related proteins: p62/SQSTM1, LC3B, GABARAPL2 across different disease progression stages in wild-type and R6/2 mice. β -ACTIN was used as a loading control for normalisation. **B)** Quantified bar graphs showing no significant difference in the expression levels of p62/SQSTM1 in R6/2 compared to wild-type mice across different age groups; Age x Genotype ($F_{(3,54)}=1.394$, $p=0.25$). **C)** Compiled quantified bar graphs representing no change in the expression of LC3B-I across different stages of disease progression in R6/2; Age x Genotype ($F_{(3,54)}=0.09385$, $p=0.96$). **D)** Summary of quantified bar graphs showing no change in the expression of LC3B-II in R6/2 across different stages of disease progression; Age x Genotype ($F_{(3,54)}=0.3311$, $p=0.80$). **E)** Pooled quantified bar graphs showing no significant change in the expression of GABARAPL2 (GL2) in R6/2 across different age groups; Age x Genotype ($F_{(3,54)}=0.07321$, $p=0.97$). $N=5$ for 2 weeks, $N=7$ for 4 and 8 weeks, and $N=12$ for 12 weeks for both the genotypes wild-type and R6/2. Statistical analysis was done by Two-way ANOVA followed by Bonferroni *post-hoc* test. Error bars indicate \pm SEM. N =number of mice. Vertical dashed lines separate the genotypes.

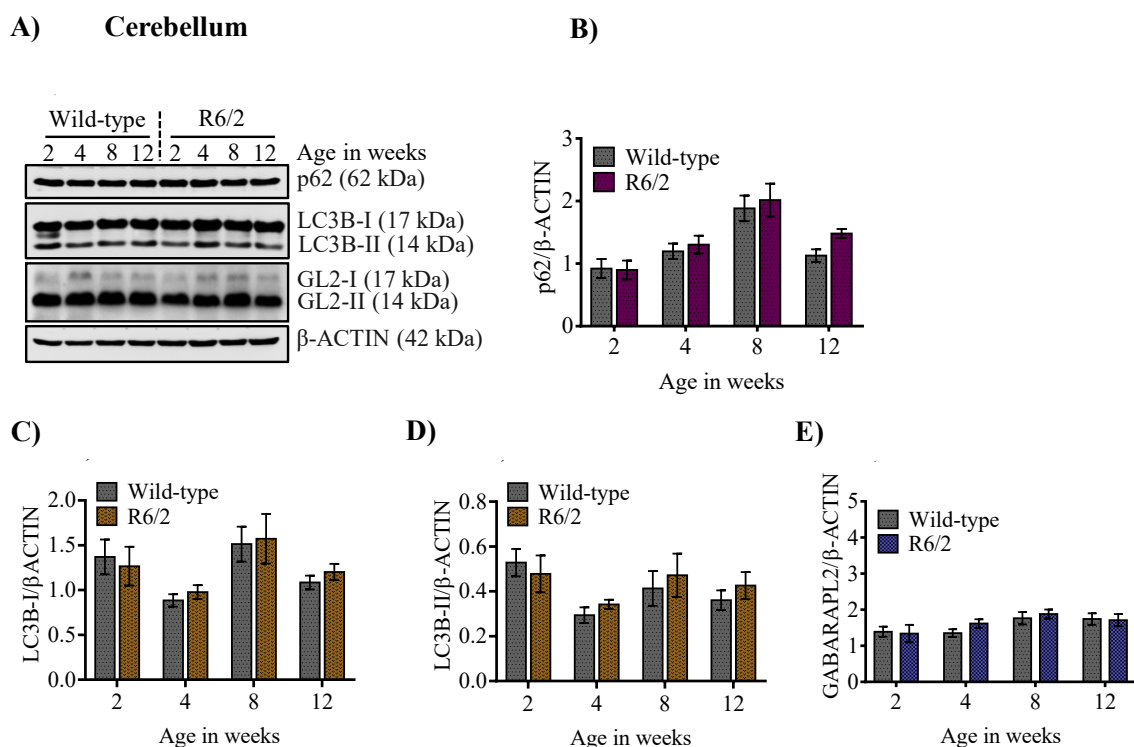


Figure 4-4 Autophagy protein expression is unaltered in cerebellum across different stages of disease progression in R6/2 mice

A) Representative immunoblots for autophagy related proteins: p62/SQSTM1, LC3B, GABARAPL2 from the region cerebellum across different disease progression stages in wild-type and R6/2 mice. β-ACTIN was used as a loading control for normalisation. **B)** Quantified bar graphs showing no significant difference in the expression levels of p62/SQSTM1 in R6/2 compared to wild-type mice across different age groups; Age x Genotype ($F_{(3,54)}=0.6080$, $p=0.61$). **C)** Pooled quantified bar graphs showing no difference in the expression levels of LC3B-I in R6/2 compared to wild-type control mice; Age x Genotype ($F_{(3,54)}=0.1832$, $p=0.90$). **D)** Compiled quantified bar graphs representing no change in the expression of LC3B-II across different stages of disease progression in R6/2; Age x Genotype ($F_{(3,54)}=0.2769$, $p=0.84$). **E)** Quantified bar graphs showing no difference in the expression of autophagosome marker GABARAPL2 (GL2) in R6/2 across different age groups; Age x Genotype ($F_{(3,54)}=0.3691$, $p=0.77$). N=5 for 2 weeks, N=7 for 4 and 8 weeks, and N=12 for 12 weeks for both the genotypes wild-type and R6/2. Statistical analysis was done by Two-way ANOVA followed by Bonferroni *post-hoc* test. Error bars indicate \pm SEM. N=number of mice. Vertical dashed lines separate the genotypes.

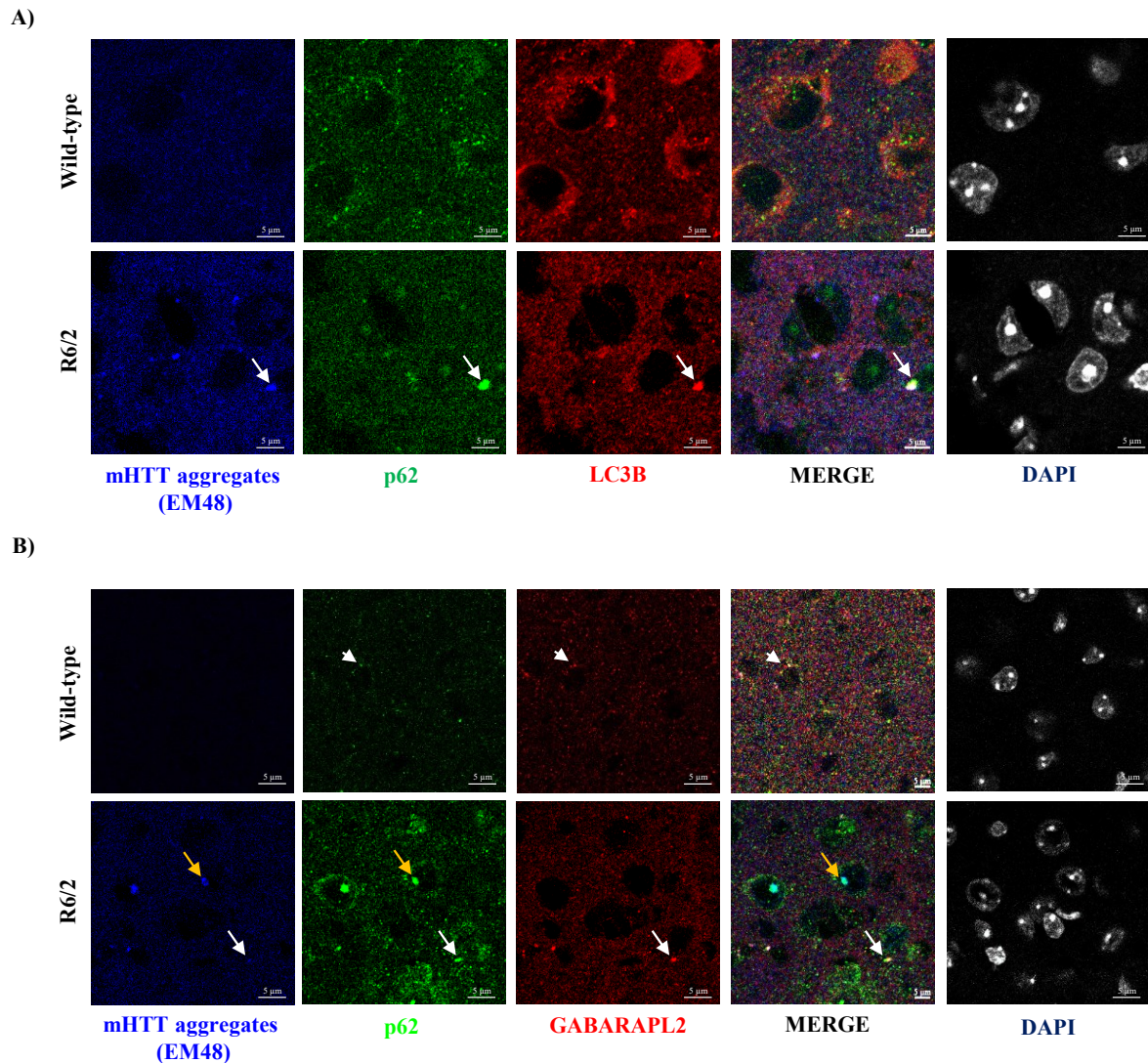


Figure 4-5 mHTT aggregates form intranuclear inclusions and get co-localised with p62/SQSTM1 in R6/2 mice in the striatum at 12 weeks

A) Representative images of immunohistochemistry labelling mHTT aggregates by EM48, and autophagy related proteins p62/SQSTM1, LC3B from wild-type and R6/2 mice. p62/SQSTM1 is labelled in green, LC3B in red, and mHTT (EM48) in Blue. B. Representative images of immunohistochemistry labelling mHTT aggregates by EM48, and autophagy related proteins p62/SQSTM1, and GABARAPL2 from wild-type and R6/2 mice. p62/SQSTM1 is labelled in green, GABARAPL2 in red, and mHTT (EM48) in Blue. Scale bar = 5 μ m; Magnification = 63X. N=3 [1M, 2F]; White arrow indicates co-localisation of mHTT (EM48) aggregates with autophagy markers. White arrowheads indicate co-localisation of p62/SQSTM1 with GABARAPL2. Yellow arrows indicate co-localisation of mHTT (EM48) aggregates with p62/SQSTM1. M=Males, F=Females. N=number of mice.

4.4 Discussion

In this chapter, it has been shown that basal autophagy is functional and is spatiotemporally regulated across different stages of disease progression in R6/2. Immunoblotting results suggest no differential change in the expression of key autophagy related proteins:

p62/SQSTM1, LC3B, and GABARAPL2 from different regions of the brain at 2, 4, 8, and 12 weeks in R6/2 compared to wild-type control mice. It is interesting to note that, despite the early presence of mHTT aggregates, and given that autophagy related proteins get sequestered in inclusion bodies, there was no differential change observed in the expression of autophagy related proteins in R6/2 at any stage of disease progression. To date, there are no studies in any of the neurodegenerative mouse models explaining the status of basal autophagy across disease progression. The study performed in this thesis would be the first to report unaltered basal autophagy in R6/2, which is the most severe and robust mouse model for HD. This study can be correlated with other age-related neurodegenerative diseases and would provide valuable insights into the pathophysiology of the disease, focusing primarily on autophagy dysfunction.

The study hypothesises that, as the age progresses, the efficiency of the neuronal cell to cope up with a build-up of toxic mHTT aggregates is compromised, and the basal autophagy functioning at a steady-state level was insufficient to clear it, thereby unable to prevent the neuronal death. Moreover, in addition to this, autophagy dysfunction with protein level being unaffected involves a deficit in the functionalities of autophagy related proteins rather than in their levels. The results imply that there is a significant change in the expression of LC3B-I and GABARAPL2 in the cortex at 12 and 8 weeks, respectively, suggesting a possible defect in the conversion rate of autophagosome markers. Another possible hypothesis is impairment in the expression of autophagy related genes, and the studies shown so far have conflicting results. Considering the fact that HTT plays a role in autophagy pathway^{211,248,351,393}, it is of no surprise that in HD patients, there is clear evidence that gene expression of the autophagy pathway is altered³⁹⁴. In one of the studies, the expression levels of autophagy mRNA and proteins are unaltered in the HD mouse model despite the presence of metabolic dysfunction³⁹⁵.

Similar results from immunohistochemistry suggest that mHTT aggregates co-localised with adaptor protein p62/SQSTM1, but not with autophagosome markers LC3B and GABARAPL2, signifying aggrephagy dysfunction in R6/2 mice. In conclusion, the results described in this chapter suggest that basal autophagy is unaltered in R6/2, and thus inducing autophagy at an early stage of disease progression might be beneficial, where newly expressed functional autophagy related proteins might potentially enhance the clearance of mHTT aggregates in neurons (Thus, autophagy induction by small molecules and its impact on the clearance of mHTT aggregates will be discussed in the next two chapters).

Chapter- 5

Nilotinib (Tasigna™) is ineffective in inducing autophagy and clearing mHTT aggregates in R6/2 mice

5.1 Introduction

Autophagy, an intracellular catabolic process that maintains the protein homeostasis, has been in the limelight in the pathophysiology of many late-onset proteinopathies such as AD, PD, HD, and ALS^{364,384,386}. Many misfolded proteins and their aggregates contribute to disease pathology through diverse mechanisms, and in recent times due to the increasing evidence of the importance of autophagy, there has been a focus on its role in understanding the pathologic mechanisms, and as a therapeutic target in many neurodegenerative diseases^{7,106}. In HD, the first evidence for the role of autophagy was made by the observations of elevated levels of key autophagy related markers in the brains of mouse models and patients with HD^{192,396,397}. Studies have shown that key autophagy regulator mTOR is sequestered in mHTT aggregates in cell models, transgenic mice, and human brain samples, resulting in decreased mTOR activity, thereby inducing autophagy^{196,205,385}. However, this inactivation of mTOR signalling suggests an autophagy upregulation in HD, but the situation may be more complicated due to the dynamic nature of mHTT aggregate formation and sequestration of other downstream signalling proteins³⁹⁸.

Given the therapeutic potential of autophagy upregulation in clearing mHTT aggregates in HD, there is a need to develop and design more specific autophagy modulators where they can act at every step of the process involved with more defined mechanisms of action. This would enable the efficient counteraction of the autophagy defects present in the specific neurodegenerative disease pathology. In this study, the efficacy of Nilotinib (TasignaTM) was tested in enhancing the clearance of mHTT aggregates and ameliorating behavioural deficits that extend the lifespan of the R6/2 mouse. Studies have shown that inhibition of BCR-ABL1 tyrosine kinase by Nilotinib (TasignaTM) protects neurons from dying against MPTP toxicity in a pre-clinical mouse model of PD and enhances the clearance of α -SYN^{322,332}. BCR-ABL is activated by phosphorylation, and its levels are increased in the nigrostriatal region of PD patients, and its inhibition has proven to be efficient in preventing the neurons from dying in PD mouse models³³³. Mice treated with Nilotinib have shown to induce autophagy and increased the expression of BECLIN-1, and ATG12, thereby enhancing the clearance of toxic α -SYN aggregates in the brain³²². Therefore, its efficacy is tested in a more severe model of HD, R6/2 in alleviating the disease phenotypes.

5.2 Methods

For immunoblotting, brain lysates from different regions of the brain such as the cortex, hippocampus, striatum, and cerebellum were collected from four age groups, 6, 8, 10, and 12 weeks from saline and Tasigna treated wild-type and R6/2 mice. For immunohistochemistry analysis, PFA fixed brain sections were taken from 12-week-old saline and Tasigna treated wild-type and R6/2 mice. For both the analysis, proteins were detected by probing with primary antibodies such as anti-LC3B, anti-p62, anti-GABARAPL2, anti-Ub, anti-HTT (EM48), and anti- β -ACTIN.

An autophagy assay was done in HeLa cells to test the efficacy of Tasigna in inducing autophagy in a dosage-dependent manner. 6BIO and Bafilomycin A1 were used as positive and negative modulators of autophagy, respectively.

[Note: Detailed experimental procedures were mentioned in chapter 2: Methods and materials section].

5.3 Results

5.3.1 Nilotinib (TasignaTM) induces autophagy in HeLa cells

Autophagy is the process of sequestering the cargo into the double membrane autophagic vesicles and fusing them with lysosomes, thereby degrading the cytoplasmic contents. To validate the efficiency of Tasigna in inducing autophagy, HeLa cells were treated with varying concentrations of the drug for 2 hours and observed that Tasigna induced autophagy in a dosage-dependent manner. Tasigna (1 mM) treatment induced autophagy compared to controls, as revealed by the significant increase in the expression of LC3B-II. Immunoblot results suggest that Tasigna enhanced the conversion of LC3B-I to LC3B-II compared to the control treatment in a dosage-dependent manner. Treatment with bafilomycin A₁ and 6BIO was used as a negative and positive modulator of autophagy, respectively. These results suggest that Nilotinib (TasignaTM) induces autophagy (**Figure 5-1**).

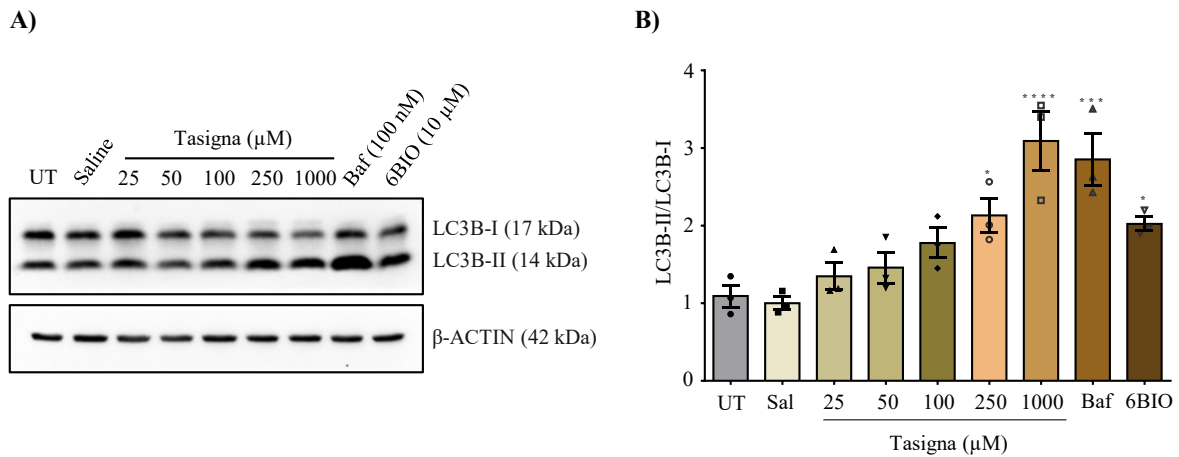


Figure 5-1 Nilotinib (Tasigna™) induces autophagy in HeLa cells in a dosage-dependent manner

A. Representative western blot showing an increase in the expression of autophagy related protein LC3B upon treatment with Nilotinib (Tasigna™). β -ACTIN was used as a loading control. **B.** Quantified bar graphs showing induction of autophagy (ratio of LC3B-II/LC3B-I) in a dosage-dependent manner. ($F_{(8,18)} = 10.91$, $p < 0.0001$). Bafilomycin (100 nM), and 6BIO (10 μ M) were used as negative and positive autophagy controls, respectively. $n=3$. Error bars indicate \pm SEM. n =number of biological replicates. Statistical analysis was done by One-way ANOVA followed by Bonferroni *post-hoc* test. * ≤ 0.05 ; *** ≤ 0.001 ; **** ≤ 0.0001 .

5.3.2 Nilotinib (Tasigna™) is ineffective in inducing autophagy in Wild-type and R6/2 mice

Nilotinib is a BCR-ABL tyrosine kinase inhibitor and was proved to be effective in the clearance of α -SYNUCLEIN aggregates by inducing autophagy, thereby preventing the neurons from dying and rescuing them the behavioural defects in the MPTP mouse model of PD³²². The efficacy of this small molecule was tested in the more severe form of the mouse model, R6/2. Tasigna was dissolved in saline, and mice were injected intraperitoneally every day, from 2 to 12 weeks of age at a dosage of 20 mg/kg body weight in C57BL/6 wild-type and R6/2 mice (see methods). Post-injection of Tasigna, brain samples from mice were collected for immunoblotting and immunohistochemical analyses at various disease progression stages, from the cortex, hippocampus, striatum, and cerebellum from both wild-type and R6/2 mice. To investigate the induction of autophagy, the expression of key autophagy related proteins, p62, LC3B, GABARAPL2 was assessed by immunoblotting technique. In all the experimental conditions, house-keeping protein β -ACTIN was used as a loading control to normalise the expression of all key autophagy related proteins used in the study. Results showed that Tasigna had failed to induce autophagy in wild-type control mice, as there was no significant change observed in the expression of p62, LC3B, and GABARAPL2 in all the four

age groups in the cortex [Figure 5-2 (A-E)], hippocampus [Figure 5-3 (A-E)], striatum [Figure 5-4 (A-E)], and cerebellum [Figure 5-5 (A-E)] respectively, except for p62 in the cerebellum where there was a significant decrease in the expression level at 8 weeks and for GABARAPL2 in the cortex where its expression significantly increased at 10 weeks. In accordance with this, Tasigna did not affect autophagy induction in R6/2 mice as well, as the expression of autophagy related proteins, p62, LC3B, and GABARAPL2 remained unaltered in all the 4 age groups in the cortex [Figure 5-6 (A-E)], hippocampus [Figure 5-7 (A-E)], striatum [Figure 5-8 (A-E)], and cerebellum [Figure 5-9 (A-E)]. Immunoblotting results suggest that Tasigna did not modulate the autophagy flux in both wild-type and R6/2 mice across different stages of disease progression, which further validates and explains the lack of improvement in motor function in R6/2 (see chapter 6).

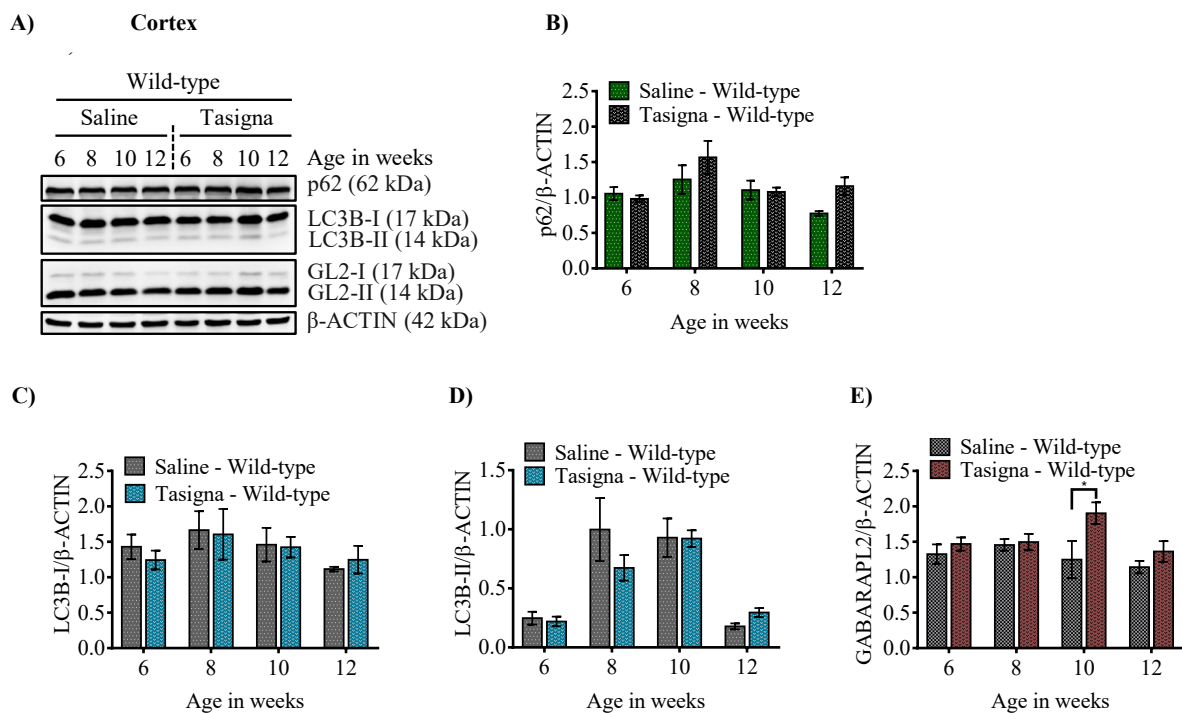


Figure 5-2 Tasigna is ineffective in inducing autophagy in Cortex across different age groups in wild-type mice

A) Representative immunoblots for autophagy related proteins: p62, LC3B, GAPARAPL2 from the region cortex in wild-type mice. β -ACTIN was used as a loading control for normalisation. B) Quantified bar graphs showing no significant difference in the expression levels of p62 in Tasigna treated group compared to saline in wild-type mice across different age groups; Age x treatment ($F_{(3,12)}=2.32$, $p=0.12$). C) Pooled quantified bar graphs showing no significant difference in the expression levels of LC3B-I in Tasigna treated group compared to saline in wild-type mice across different age groups; Age x treatment ($F_{(3,12)}=0.59$, $p=0.63$). D) Compiled quantified bar graphs representing no change in the expression of LC3B-II in

Tasigna treated group compared to saline in wild-type mice; Age x treatment ($F_{(3,12)}=1.65$, $p=0.22$). E) Quantified bar graphs showing a significant difference in the expression of autophagosome marker GABARAPL2 (GL2) at 10 weeks in wild-type mice in Tasigna treated group compared to saline; Age x treatment ($F_{(3,12)}=1.86$, $p=0.18$); (10 weeks: $*p < 0.05$). $N = 3$ [1M, 2F] for all the age groups 6, 8, 10, and 12 weeks. Statistical analysis was done by Two-way ANOVA followed by Bonferroni *post-hoc* test. Error bars indicate \pm SEM. N =number of mice, M =Males, F =Females. Vertical dashed lines separate the drug treatment groups.

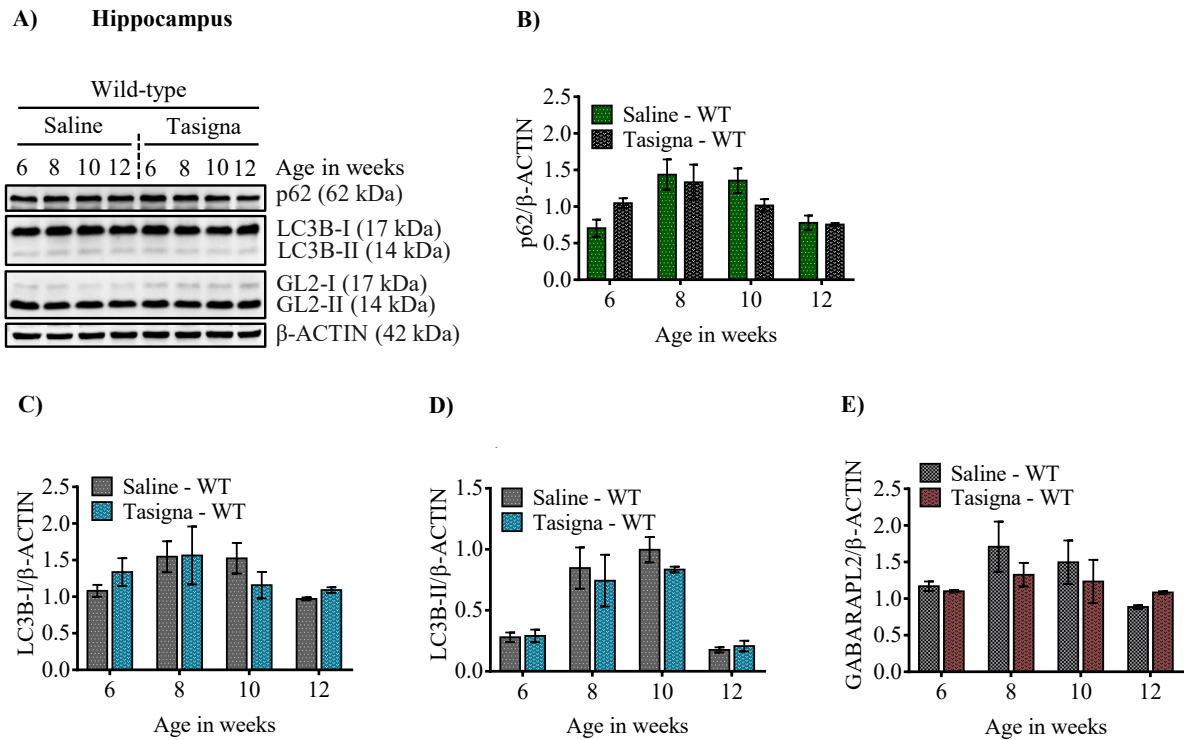


Figure 5-3 Tasigna is unable to induce autophagy in Hippocampus in wild-type mice

A) Representative immunoblots for autophagy related proteins: p62, LC3B, GAPARAPL2 from the region hippocampus in wild-type mice. β -ACTIN was used as a loading control for normalisation. **B)** Quantified bar graphs showing no significant difference in the expression levels of p62 in Tasigna treated group compared to saline in wild-type mice across different age groups; Age x treatment ($F_{(3,12)}=1.87$, $p=0.18$). **C)** Pooled quantified bar graphs showing no significant change in the expression levels of LC3B-I in Tasigna treated group compared to saline in wild-type mice across different age groups; Age x treatment ($F_{(3,12)}=1.72$, $p=0.21$); **D)** Compiled quantified bar graphs representing no change in the expression of LC3B-II across different age groups in Tasigna treated group compared to saline in wild-type mice; Age x treatment ($F_{(3,12)}=0.57$, $p=0.64$). **E)** Summary of quantified bar graphs showing no difference in the expression of GABARAPL2 (GL2) in Tasigna treated group compared to saline in wild-type mice across different age groups; Age x treatment ($F_{(3,12)}=1.01$, $p=0.42$). $N = 3$ [1M, 2F] for all the age groups 6, 8, 10, and 12 weeks. Statistical analysis was done by Two-way

ANOVA followed by Bonferroni *post-hoc* test. Error bars indicate \pm SEM. N=number of mice, M=Males, F=Females. Vertical dashed lines separate the drug treatment groups.

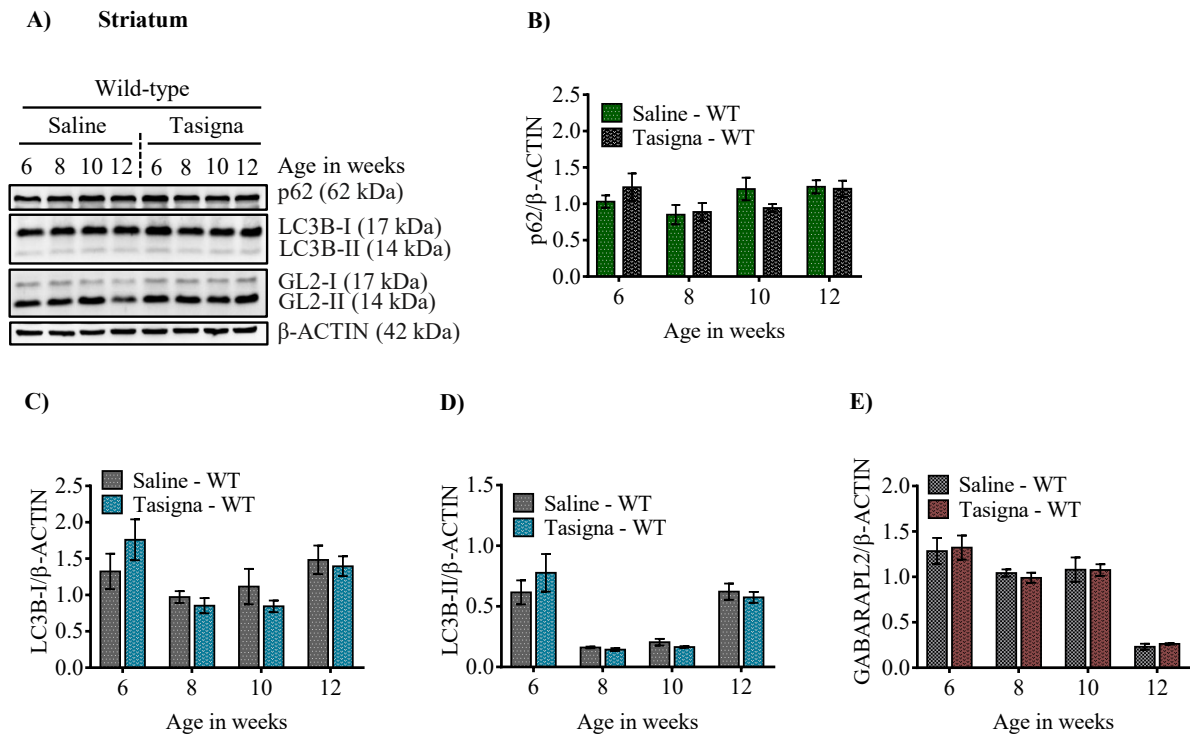


Figure 5-4 Tasigna is ineffective in inducing autophagy in the striatum in wild-type across different age groups

A) Representative immunoblots for autophagy related proteins: p62, LC3B, GAPARAPL2 across different age groups in wild-type mice. β -ACTIN was used as a loading control for normalisation. **B)** Quantified bar graphs showing no significant difference in the expression levels of p62 in Tasigna treated group compared to saline in wild-type mice across different age groups; Age x treatment ($F_{(3,12)}=0.99$, $p=0.42$). **C)** Compiled quantified bar graphs representing no change in the expression of LC3B-I across different age groups in wild-type in Tasigna treated group compared to saline; Age x treatment ($F_{(3,12)}=1.13$, $p=0.37$). **D)** Summary of quantified bar graphs showing no change in the expression of LC3B-II in wild-type mice across different age groups in Tasigna treated group compared to saline; Age x treatment ($F_{(3,12)}=1.22$, $p=0.34$). **E)** Pooled quantified bar graphs showing no significant change in the expression of GABARAPL2 (GL2) in wild-type mice in Tasigna treated group compared to saline; Age x treatment ($F_{(3,12)}=0.08$, $p=0.96$). N = 3 [1M, 2F] for all the age groups 6, 8, 10, and 12 weeks. Statistical analysis was done by Two-way ANOVA followed by Bonferroni *post-hoc* test. Error bars indicate \pm SEM. N=number of mice, M=Males, F=Females. Vertical dashed lines separate the drug treatment groups.

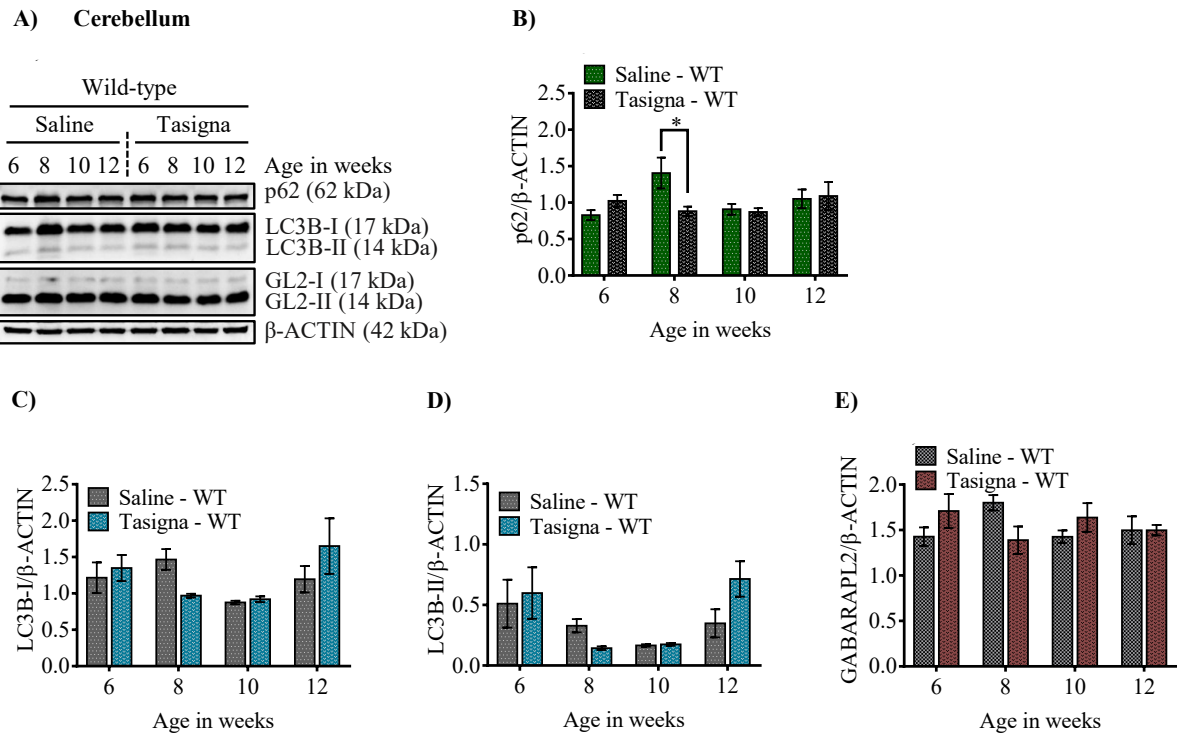


Figure 5-5 Tasigna is ineffective in inducing autophagy in the cerebellum across different age groups in wild-type mice

A) Representative immunoblots for autophagy related proteins: p62, LC3B, GAPARAPL2 from the region cerebellum across different age groups in wild-type mice. β-ACTIN was used as a loading control for normalisation. **B)** Quantified bar graphs showing no significant difference in the expression levels of p62 in Tasigna treated group compared to saline in wild-type mice across different age groups; Age x treatment ($F_{(3,12)}=5.40$, $p=0.01$); (8 weeks: $*p < 0.01$). **C)** Pooled quantified bar graphs showing no difference in the expression levels of LC3B-I in wild-type mice in the Tasigna treated group compared to saline across different age groups; Age x treatment ($F_{(3,12)}=3.06$, $p=0.06$). **D)** Compiled quantified bar graphs representing no change in the expression of LC3B-II across various age groups in Tasigna treated group compared to saline; Age x treatment ($F_{(3,12)}=2.22$, $p=0.13$). **E)** Quantified bar graphs showing no difference in the expression of autophagosome marker GABARAPL2 (GL2) in wild-type mice across different age groups; Age x treatment ($F_{(3,12)}=3.74$, $p=0.04$). $N = 3$ [1M, 2F] for all the age groups 6, 8, 10, and 12 weeks. Statistical analysis was done by Two-way ANOVA followed by Bonferroni *post-hoc* test. Error bars indicate \pm SEM. N=number of mice, M=Males, F=Females. Vertical dashed lines separate the drug treatment groups.

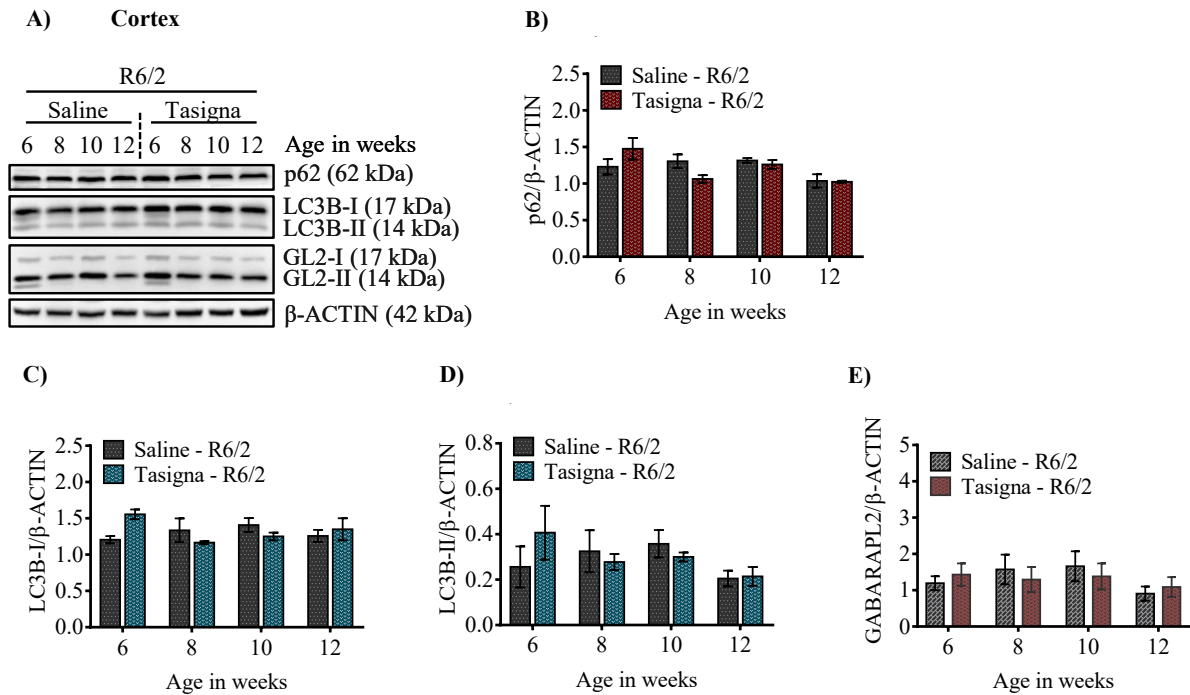


Figure 5-6 Tasigna is ineffective in inducing autophagy in the cortex across different stages of disease progression in R6/2 mice

A) Representative immunoblots for autophagy related proteins: p62, LC3B, GAPARAPL2 from the region cortex in R6/2 mice. β-ACTIN was used as a loading control for normalisation. **B)** Quantified bar graphs showing no significant difference in the expression levels of p62 in Tasigna treated group compared to saline in R6/2 mice across different age groups; Age x treatment ($F_{(3,12)}=2.29$, $p=0.12$). **C)** Pooled quantified bar graphs showing no significant difference in the expression levels of LC3B-I in Tasigna treated group compared to saline in R6/2 mice across different age groups; Age x treatment ($F_{(3,12)}=3.27$, $p=0.05$). **D)** Compiled quantified bar graphs representing no change in the expression of LC3B-II in Tasigna treated group compared to saline in R6/2 mice; Age x treatment ($F_{(3,12)}=0.91$, $p=0.46$). **E)** Quantified bar graphs showing no significant difference in the expression of autophagosome marker GABARAPL2 (GL2) in R6/2 mice in Tasigna treated group compared to saline; Age x treatment ($F_{(3,12)}=3.30$, $p=0.05$). $N = 3$ [1M, 2F] for all the age groups 6, 8, 10, and 12 weeks. Statistical analysis was done by Two-way ANOVA followed by Bonferroni *post-hoc* test. Error bars indicate \pm SEM. N =number of mice, M =Males, F =Females. The drug treatment groups are separated by vertical dashed lines.

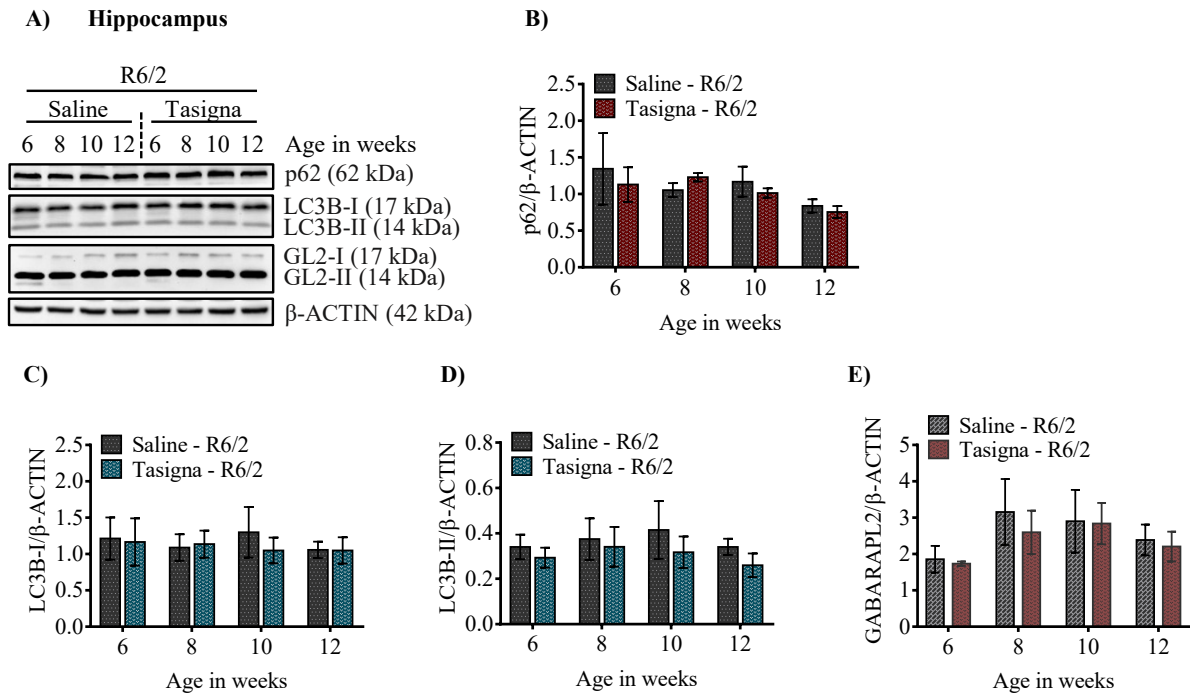


Figure 5-7 Tasigna is ineffective in inducing autophagy in Hippocampus across different stages of disease progression in R6/2 mice

A) Representative immunoblots for autophagy related proteins: p62, LC3B, GAPARAPL2 from the region hippocampus in R6/2 mice. β-ACTIN was used as a loading control for normalisation. **B)** Quantified bar graphs showing no significant difference in the expression levels of p62 in Tasigna treated group compared to saline in R6/2 mice across different age groups; Age x treatment ($F_{(3,12)}=0.28$, $p=0.83$). **C)** Pooled quantified bar graphs showing no significant change in the expression levels of LC3B-I in Tasigna treated group compared to saline in R6/2 mice across different age groups; Age x treatment ($F_{(3,12)}=0.27$, $p=0.84$); **D)** Compiled quantified bar graphs representing no change in the expression of LC3B-II across different age groups in Tasigna treated group compared to saline in R6/2 mice; Age x treatment ($F_{(3,12)}=0.13$, $p=0.93$). **E)** Summary of quantified bar graphs showing no difference in the expression of GABARAPL2 (GL2) in Tasigna treated group compared to saline in R6/2 mice across different age groups; Age x treatment ($F_{(3,12)}=0.20$, $p=0.88$). $N = 3$ [1M, 2F] for all the age groups 6, 8, 10, and 12 weeks. Statistical analysis was done by Two-way ANOVA followed by Bonferroni *post-hoc* test. Error bars indicate \pm SEM. N=number of mice, M=Males, F=Females. Vertical dashed lines separate the drug treatment groups.

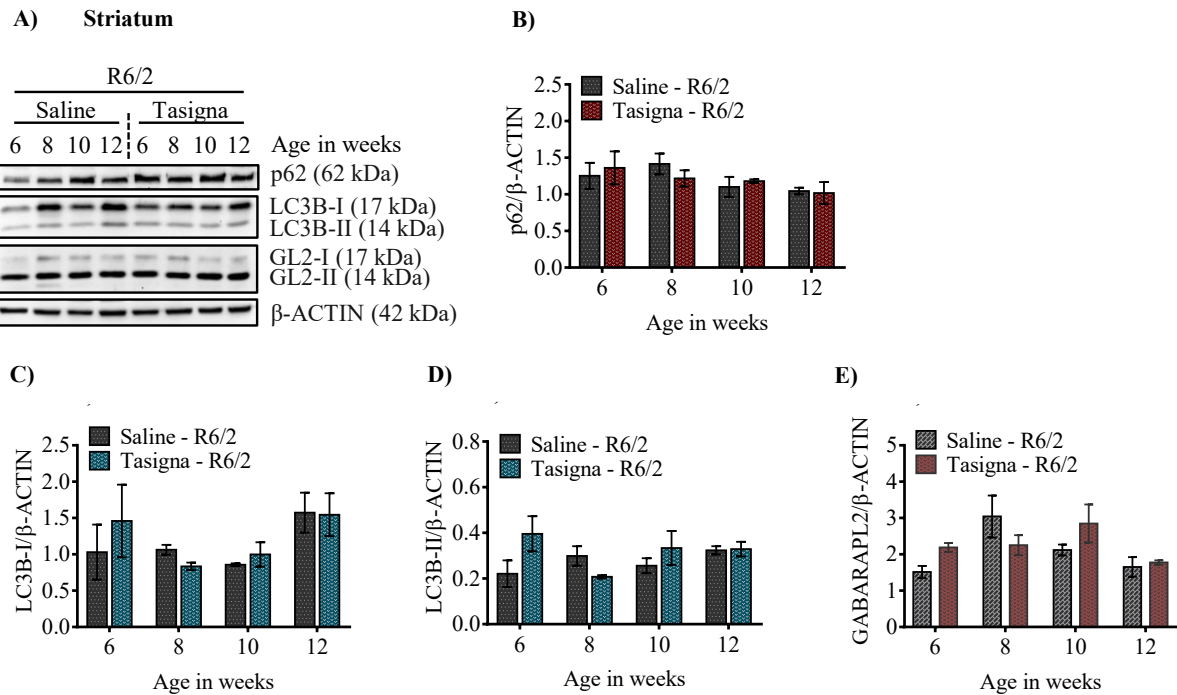


Figure 5-8 Tasigna is ineffective in inducing autophagy in striatum across different stages of disease progression in R6/2 mice

A) Representative immunoblots for autophagy related proteins: p62, LC3B, GAPARAPL2 across different age groups in R6/2 mice. β-ACTIN was used as a loading control for normalisation. **B)** Quantified bar graphs showing no significant difference in the expression levels of p62 in Tasigna treated group compared to saline in R6/2 mice across different age groups; Age x treatment ($F_{(3,12)}=0.39$, $p=0.76$). **C)** Compiled quantified bar graphs representing no change in the expression of LC3B-I across different age groups in R6/2 in Tasigna treated group compared to saline; Age x treatment ($F_{(3,12)}=0.85$, $p=0.49$). **D)** Summary of quantified bar graphs showing no change in the expression of LC3B-II in R6/2 mice across different age groups in Tasigna treated group compared to saline; Age x treatment ($F_{(3,12)}=4.68$, $p=0.02$). **E)** Pooled quantified bar graphs showing no significant change in the expression of GABARAPL2 (GL2) in R6/2 mice in Tasigna treated group compared to saline; Age x treatment ($F_{(3,12)}=3.09$, $p=0.06$). $N = 3$ [1M, 2F] for all the age groups 6, 8, 10, and 12 weeks. Statistical analysis was done by Two-way ANOVA followed by Bonferroni *post-hoc* test. Error bars indicate \pm SEM. N=number of mice, M=Males, F=Females. Vertical dashed lines separate the drug treatment groups.

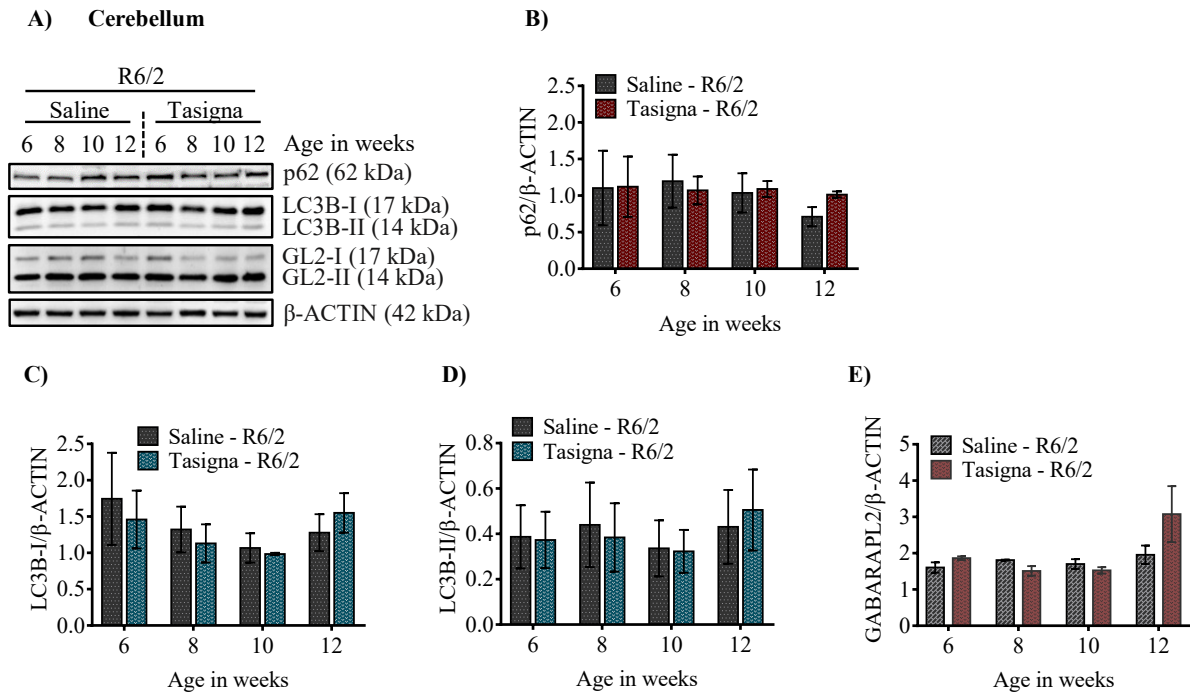


Figure 5-9 Tasigna is ineffective in inducing autophagy in Cerebellum across different stages of disease progression in R6/2 mice

A) Representative immunoblots for autophagy related proteins: p62, LC3B, GAPARAPL2 from the region cerebellum across different age groups in R6/2 mice. β -ACTIN was used as a loading control for normalisation. **B)** Quantified bar graphs showing no significant difference in the expression levels of p62 in Tasigna treated group compared to saline in R6/2 mice across different age groups; Age x treatment ($F_{(3,12)}=0.27$, $p=0.84$). **C)** Pooled quantified bar graphs showing no difference in the expression levels of LC3B-I in R6/2 mice in Tasigna treated group compared to saline across different age groups; Age x treatment ($F_{(3,12)}=0.55$, $p=0.65$). **D)** Compiled quantified bar graphs representing no change in the expression of LC3B-II across various age groups in Tasigna treated group compared to saline; Age x treatment ($F_{(3,12)}=0.43$, $p=0.73$). **E)** Quantified bar graphs showing no difference in the expression of autophagosome marker GABARAPL2 (GL2) in R6/2 mice across different age groups; Age x treatment ($F_{(3,12)}=2.24$, $p=0.13$). $N = 3$ [1M, 2F] for all the age groups 6, 8, 10, and 12 weeks. Statistical analysis was done by Two-way ANOVA followed by Bonferroni *post-hoc* test. Error bars indicate \pm SEM. N=number of mice, M=Males, F=Females. Vertical dashed lines separate the drug treatment groups.

5.3.3 Nilotinib (TasignaTM) is unable to clear mHTT aggregates in R6/2 mice

Despite the inability of Tasigna in inducing autophagy in wild-type and R6/2 mice and given the severity and accelerated disease progression in R6/2, Tasigna may increase the clearance of mHTT aggregates to an extent. To test the efficacy of Tasigna, expression of mHTT aggregates was assayed by immunoblotting from 6-, 8-, 10-, and 12-weeks brain lysates from the cortex, hippocampus, striatum, and cerebellum. Results of immunoblot assays further

validated the earlier observations on the inability of Tasigna to clear mHTT aggregates in Tasigna treated group compared to saline across all four age groups in R6/2 in the cortex [Figure 5-10 (A-C)], hippocampus [Figure 5-11 (A-C)], striatum [Figure 5-12 (A-C)], and cerebellum [Figure 5-13 (A-C)]. In addition to the investigation of mHTT expression, the global UBIQUITINATION profile of different brain regions in wild-type and R6/2 mice was checked for any observable changes. Tasigna treatment showed no significant change in the UBIQUITINATION pattern compared to saline in wild-type control mice in all the age groups in the cortex [Figure 5-14 (A-B)], hippocampus [Figure 5-14 (C-D)], striatum [Figure 5-15 (A-B)], and cerebellum [Figure 5-15 (C-D)], except for 8th week, where a significant decrease was observed in Tasigna treated group in the cerebellum. Since, Tasigna was inefficient in inducing autophagy and clearance of mHTT aggregates in R6/2, we did not check the ubiquitin pattern in stacking gels for Tasigna treated group. Similarly, Tasigna failed to change the ubiquitination pattern irrespective of the stage of disease progression in all the age groups in R6/2 in the cortex [Figure 5-16 (A-B)], hippocampus [Figure 5-16 (C-D)], striatum [Figure 5-17 (A-B)], and cerebellum [Figure 5-17 (C-D)].

For immunohistochemistry, the expression of autophagy markers in the striatum was checked in both wild-type and R6/2 mice at 12 weeks. Tasigna did not modulate the expression of autophagy related proteins p62, LC3B, and GABARAPL2 at 12 weeks in the striatum in wild-type control mice [Figure 5-18 (A-B)]. Moreover, as Tasigna did not induce autophagy in R6/2, there was no change observed in the expression of p62, LC3B, and GABARAPL2 in Tasigna treated group compared to saline-treated at 12 weeks in the striatum [Figure 5-18 (C-D)]. Compared to the saline-treated group, Tasigna treatment did not affect the clearance of mHTT aggregates in R6/2 [Figure 5-18 (C-D)]. Overall, immunoblotting and immunohistochemical analysis suggest that Tasigna was ineffective in inducing autophagy in both wild-type and R6/2 mice and did not increase the clearance of mHTT aggregates at any given stage of disease progression, thereby it might not improve the motor functions in R6/2 (see chapter 6).

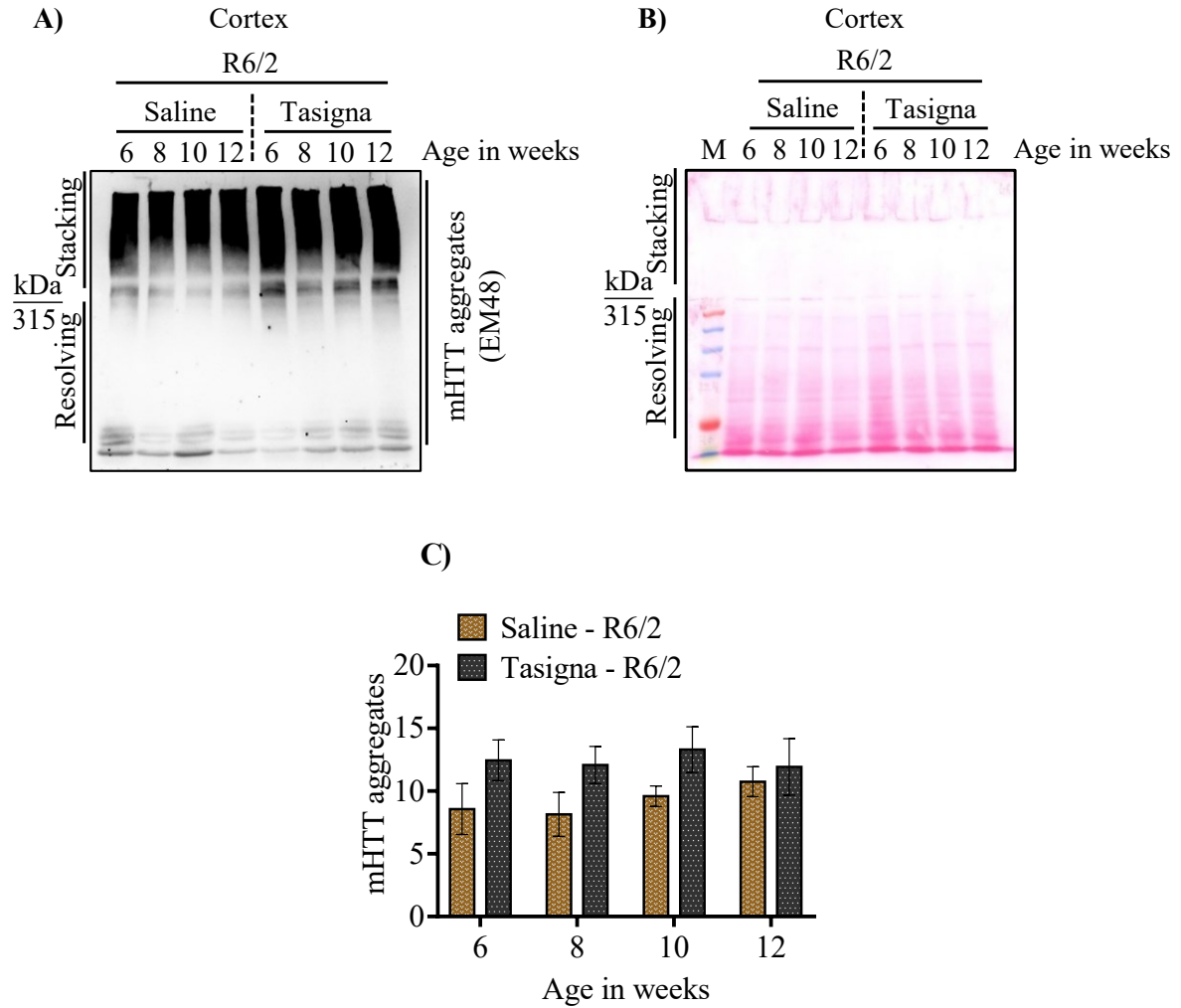


Figure 5-10 Tasigna is ineffective in clearing mHTT aggregates in Cortex across different stages of disease progression in R6/2 mice

A) Representative immunoblot showing no effect of Tasigna in clearing mHTT aggregates (EM48) from 6, 8, 10, and 12 weeks in the cortex in R6/2. **B)** Representative Ponceau S-stained blot for mHTT aggregates from 6, 8, 10, and 12 weeks in the cortex. **C)** Pooled quantified bar graphs for mHTT aggregates for cortex (6, 8, 10, 12 weeks: $p > 0.05$). $N = 3$ [1M, 2F]; (R6/2-Saline), and (R6/2-Tasigna) for all the 4 age groups 6, 8, 10, and 12 weeks. Error bars indicate \pm SEM. N =number of mice, M =Males, F =Females. Vertical dashed lines separate the treatment groups. Statistical analysis was done by Two-way ANOVA followed by Bonferroni *post-hoc* test. Vertical dashed lines separate the drug treatment groups.

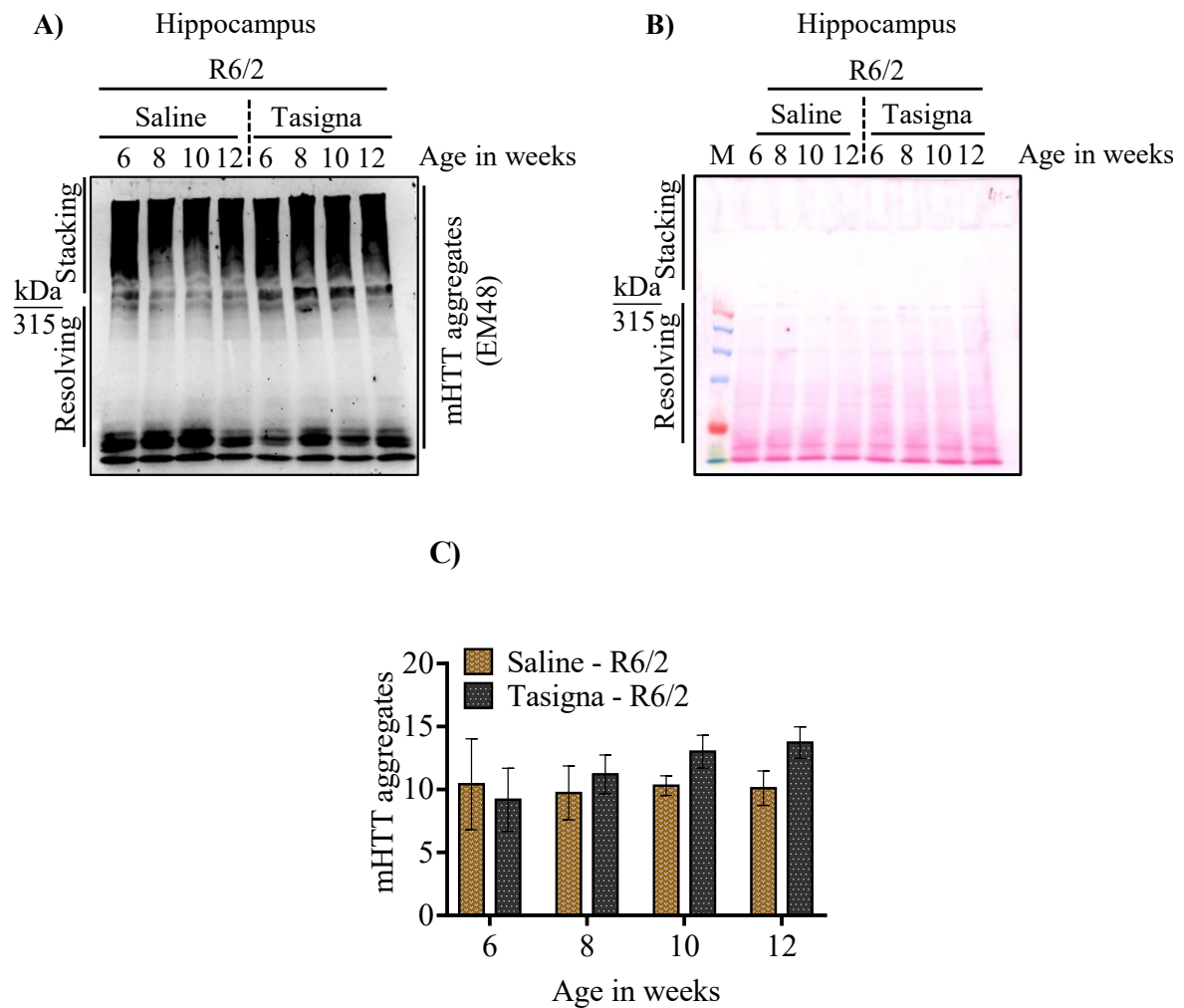


Figure 5-11 Tasigna is ineffective in clearing mHTT aggregates in the hippocampus across different stages of disease progression in R6/2 mice

A) Representative immunoblot showing no effect of Tasigna in clearing mHTT aggregates (EM48) from 6, 8, 10, and 12 weeks in the hippocampus in R6/2. **B)** Representative Ponceau S-stained blot for mHTT aggregates from 6, 8, 10, and 12 weeks in the hippocampus. **C)** Pooled quantified bar graphs for mHTT aggregates for the hippocampus (6, 8, 10, 12 weeks: $p > 0.05$). $N = 3$ [1M, 2F]; (R6/2-Saline), and (R6/2-Tasigna) for all the 4 age groups 6, 8, 10, and 12 weeks. Error bars indicate \pm SEM. N =number of mice, M =Males, F =Females. Vertical dashed lines separate the treatment groups. Statistical analysis was done by Two-way ANOVA followed by Bonferroni *post-hoc* test. Vertical dashed lines separate the drug treatment groups.

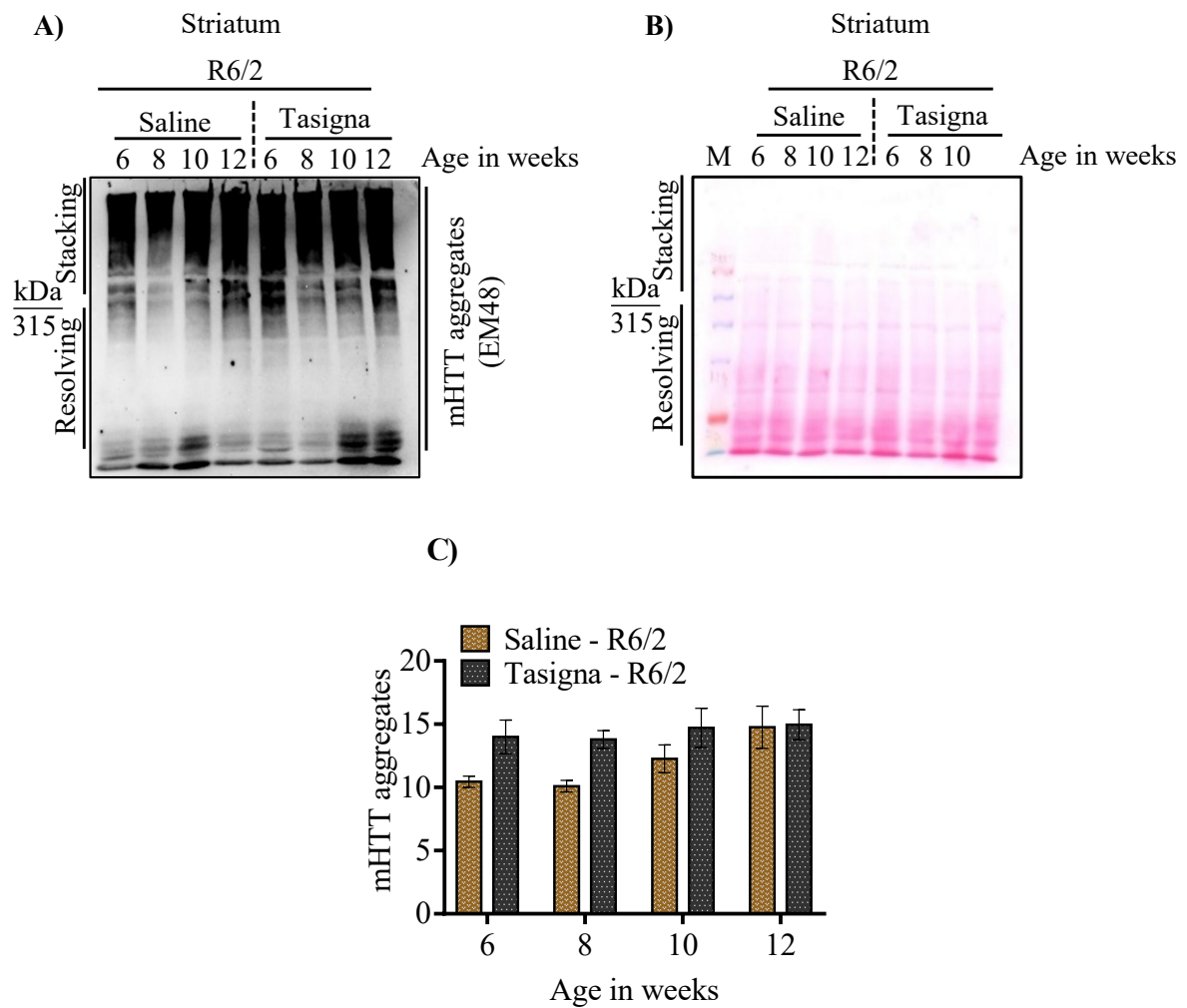


Figure 5-12 Tasigna is ineffective in clearing mHTT aggregates in striatum across different stages of disease progression in R6/2 mice

A) Representative immunoblot showing no effect of Tasigna in clearing mHTT aggregates (EM48) from 6, 8, 10, and 12 weeks in the Striatum in R6/2. **B)** Representative Ponceau S-stained blot for mHTT aggregates from 6, 8, 10, and 12 weeks in the striatum. **C)** Pooled quantified bar graphs for mHTT aggregates for striatum (6, 8, 10, 12 weeks: $p > 0.05$). $N = 3$ [1M, 2F]; (R6/2-Saline), and (R6/2-Tasigna) for all the 4 age groups 6, 8, 10, and 12 weeks. Error bars indicate \pm SEM. N =number of mice, M =Males, F =Females. Vertical dashed lines separate the treatment groups. Statistical analysis was done by Two-way ANOVA followed by Bonferroni *post-hoc* test. Vertical dashed lines separate the drug treatment groups.

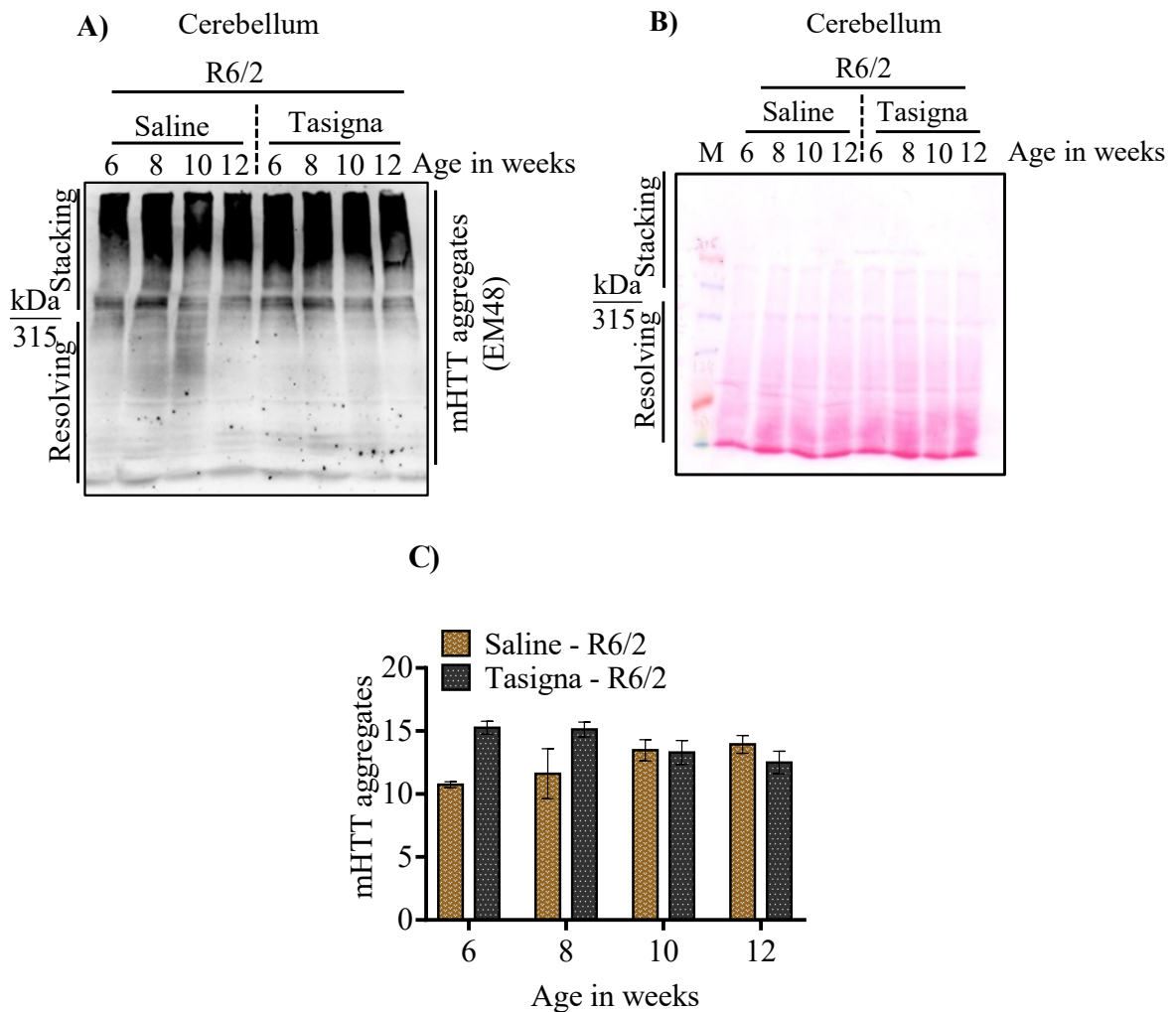


Figure 5-13 Tasigna is ineffective in clearing mHTT aggregates in the cerebellum across different stages of disease progression in R6/2 mice

A) Representative immunoblot showing no effect of Tasigna in clearing mHTT aggregates (EM48) from 6, 8, 10, and 12 weeks in the cerebellum in R6/2. **B)** Representative Ponceau S-stained blot for mHTT aggregates from 6, 8, 10, and 12 weeks in the cerebellum. **C)** Pooled quantified bar graphs for mHTT aggregates for cerebellum (6, 8, 10, 12 weeks: $p > 0.05$). $N = 3$ [1M, 2F]; (R6/2-Saline), and (R6/2-Tasigna) for all the 4 age groups 6, 8, 10, and 12 weeks. Error bars indicate \pm SEM. N=number of mice, M=Males, F=Females. Vertical dashed lines separate the treatment groups. Statistical analysis was done by Two-way ANOVA followed by Bonferroni *post-hoc* test. Vertical dashed lines separate the drug treatment groups.

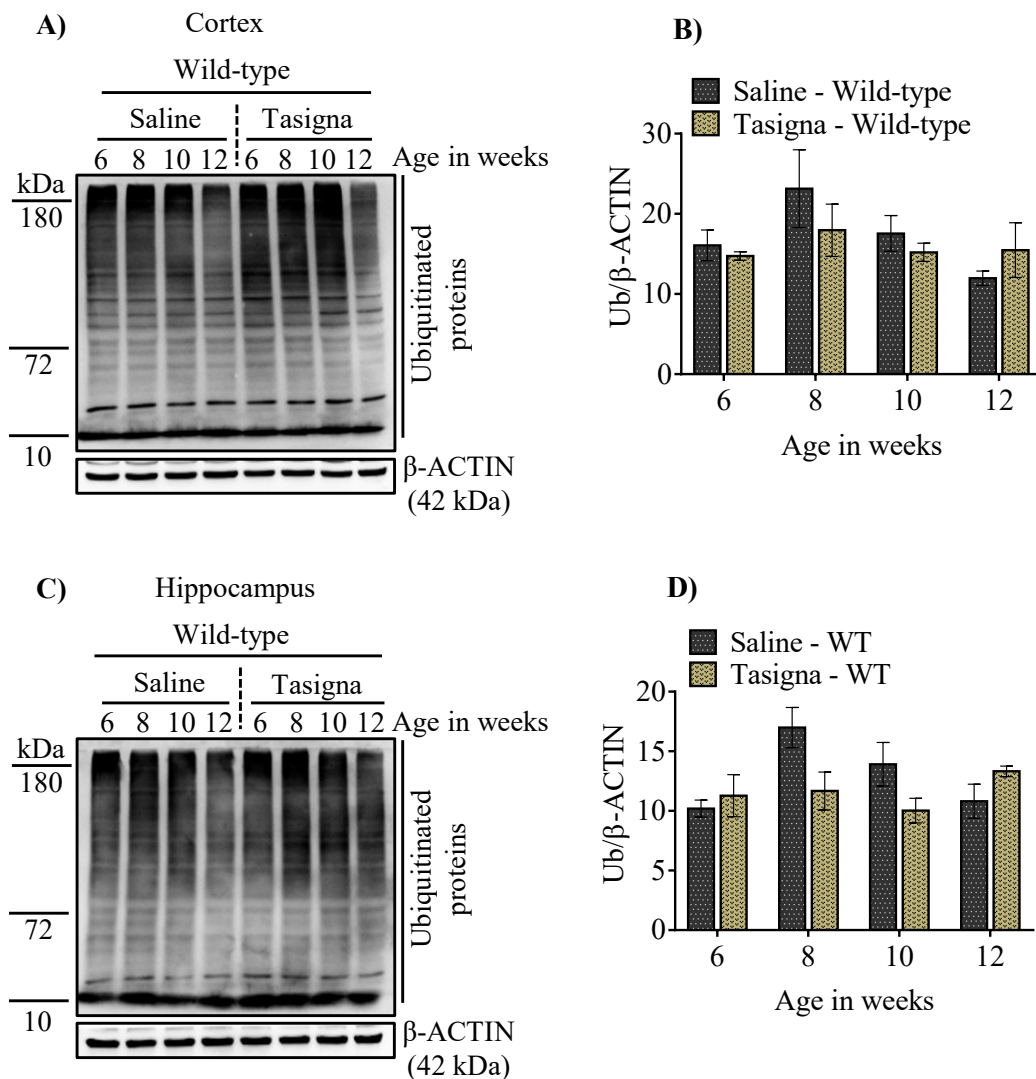


Figure 5-14 UBIQUITIN profile of the cell is unchanged in cortex and hippocampus across different age groups in wild-type mice

A) Representative blot of UBIQUITIN profile for the region cortex in wild-type across different age groups. **B)** Pooled quantified bar graphs showing no significant difference in UBIQUITIN profile for the region cortex in wild-type; Age x treatment ($F_{(3,12)}=2.24$, $p=0.13$). **C)** Representative Immunoblot for the region hippocampus showing no change in the UBIQUITIN profile in wild-type in Tasigna treated group compared to saline across different age groups. **D)** Quantified bar graphs representing no difference in UBIQUITIN profile for the region hippocampus in wild-type across different age groups; Age x treatment ($F_{(3,12)}=5.70$, $p=0.01$). β -ACTIN is used as a loading control in all the experimental conditions. $N = 3$ [1M, 2F] for all the age groups 6, 8, 10, and 12 weeks. Statistical analysis was done by Two-way ANOVA followed by Bonferroni *post-hoc* test. Error bars indicate \pm SEM. N=number of mice, M=Males, F=Females. Vertical dashed lines separate the drug treatment groups.

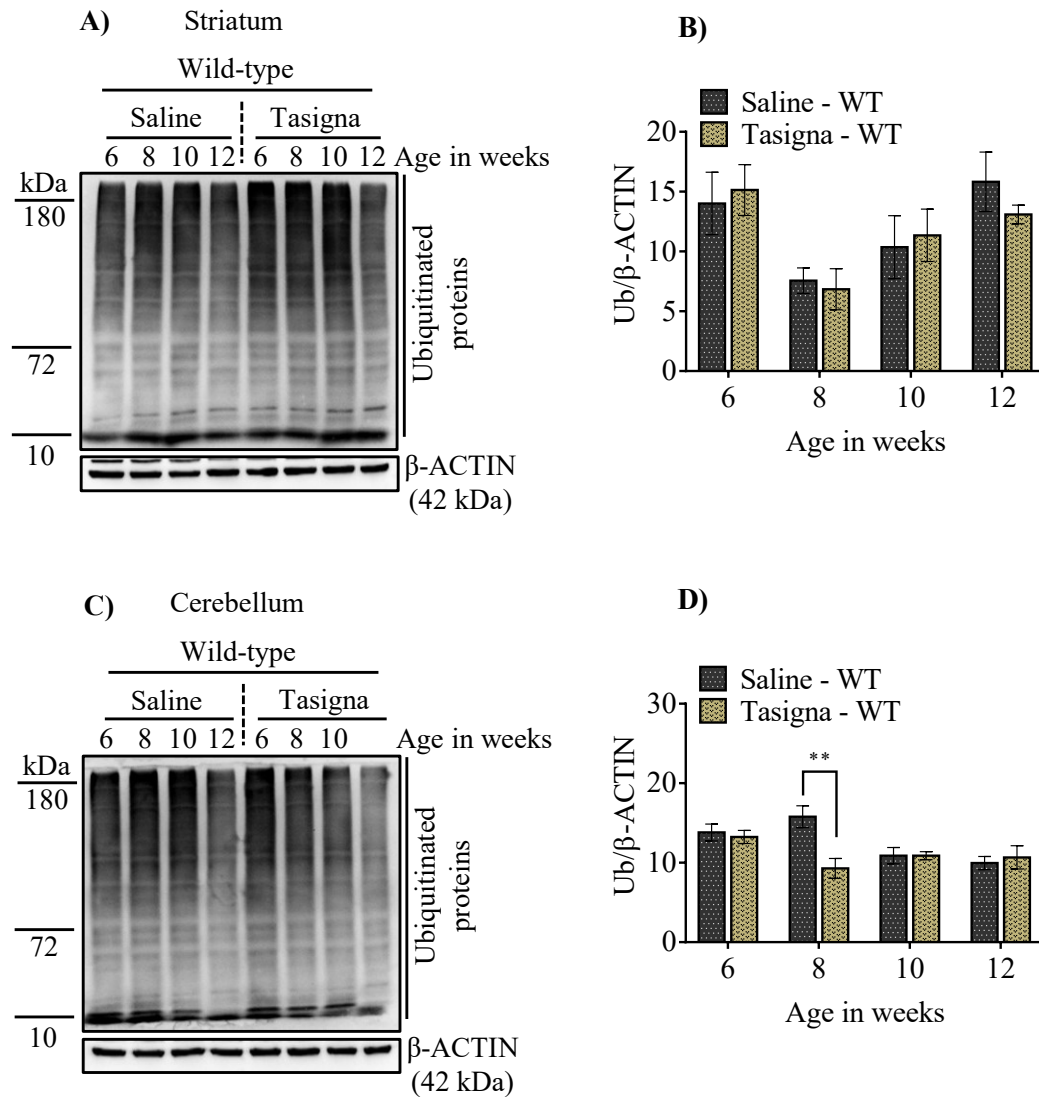


Figure 5-15 UBIQUITIN profile of the cell is unchanged in striatum and cerebellum across different age groups in wild-type mice

A) Representative blot of UBIQUITIN profile for the region Striatum in wild-type mice across different age groups. **B)** Pooled quantified bar graphs showing no significant difference in UBIQUITIN profile for the region Striatum in wild-type; Age x treatment ($F_{(3,12)}=0.31$, $p=0.81$). **C)** Representative Immunoblot for the region cerebellum showing no change in the UBIQUITIN profile in wild-type mice across different age groups. **D)** Quantified bar graphs representing the significant difference in UBIQUITIN profile for the region cerebellum in wild-type at 8 weeks of age; Age x treatment ($F_{(3,12)}=4.48$, $p=0.02$); (8 weeks: $**p<0.01$). β -ACTIN is used as a loading control in all the experimental conditions. $N = 3$ [1M, 2F] for all the age groups 6, 8, 10, and 12 weeks. Statistical analysis was done by Two-way ANOVA followed by Bonferroni *post-hoc* test. Error bars indicate \pm SEM. N =number of mice, M =Males, F =Females. Blue bar graphs show saline and black for Tasigna. Vertical dashed lines separate the drug treatment groups.

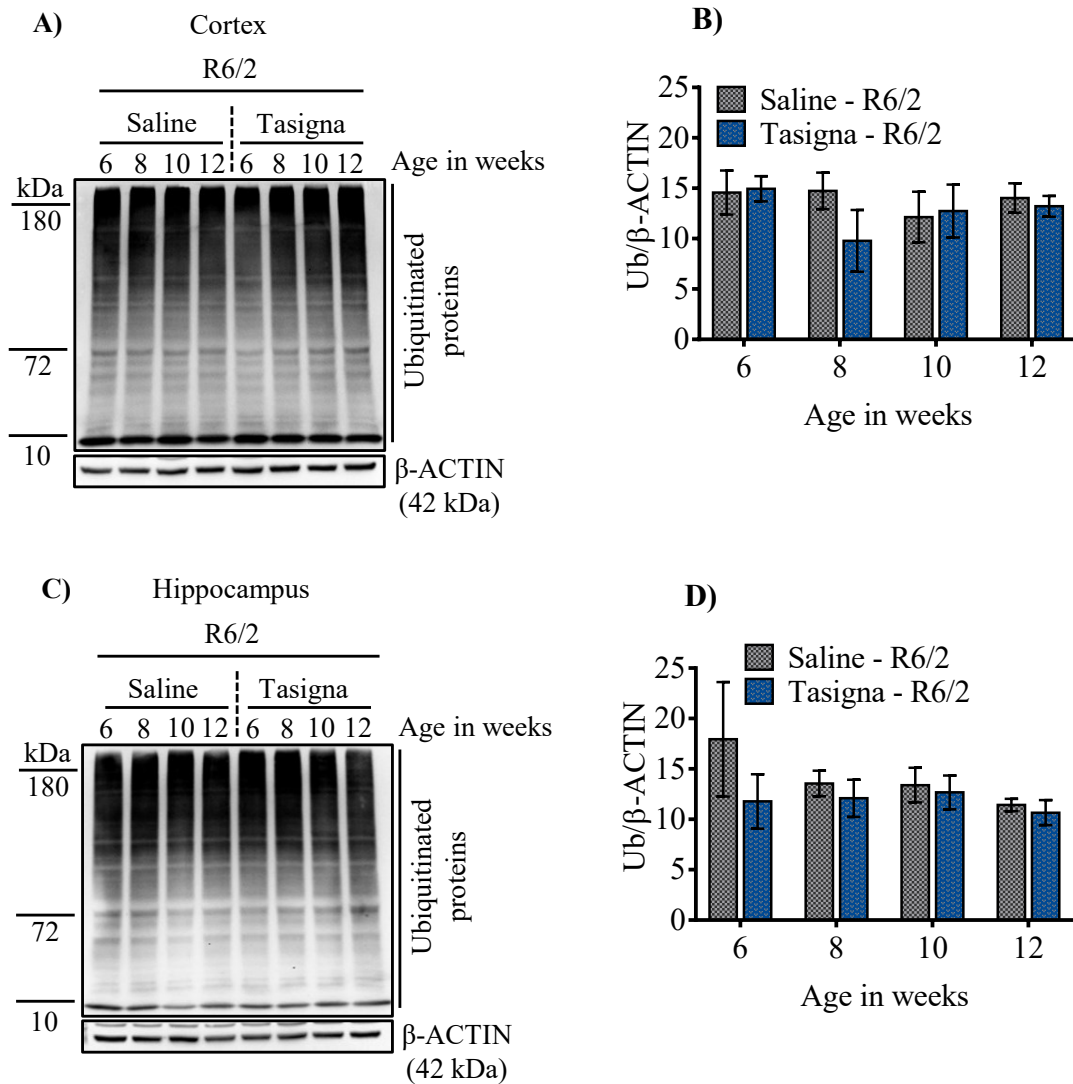


Figure 5-16 UBIQUITIN profile of the cell is unchanged despite the presence of mHTT aggregates in cortex and hippocampus across different stages of disease progression in R6/2 mice

A) Representative blot of UBIQUITIN profile for the region cortex in R6/2 mice across different age groups. **B)** Pooled quantified bar graphs showing no significant difference in UBIQUITIN profile for the region cortex in R6/2; Age x treatment ($F_{(3,12)}=2.40$, $p=0.11$). **C)** Representative immunoblot for the region hippocampus showing no change in the UBIQUITIN profile in R6/2 in Tasigna treated group compared to saline across different stages of disease progression. **D)** Quantified bar graphs representing no difference in UBIQUITIN profile for the region hippocampus in R6/2 across different age groups; Age x treatment ($F_{(3,12)}=0.58$, $p=0.63$). β -ACTIN is used as a loading control in all the experimental conditions. $N = 3$ [1M, 2F] for all the age groups 6, 8, 10, and 12 weeks. Statistical analysis was done by Two-way ANOVA followed by Bonferroni *post-hoc* test. Error bars indicate \pm SEM. N =number of mice, M =Males, F =Females. Vertical dashed lines separate the drug treatment groups.

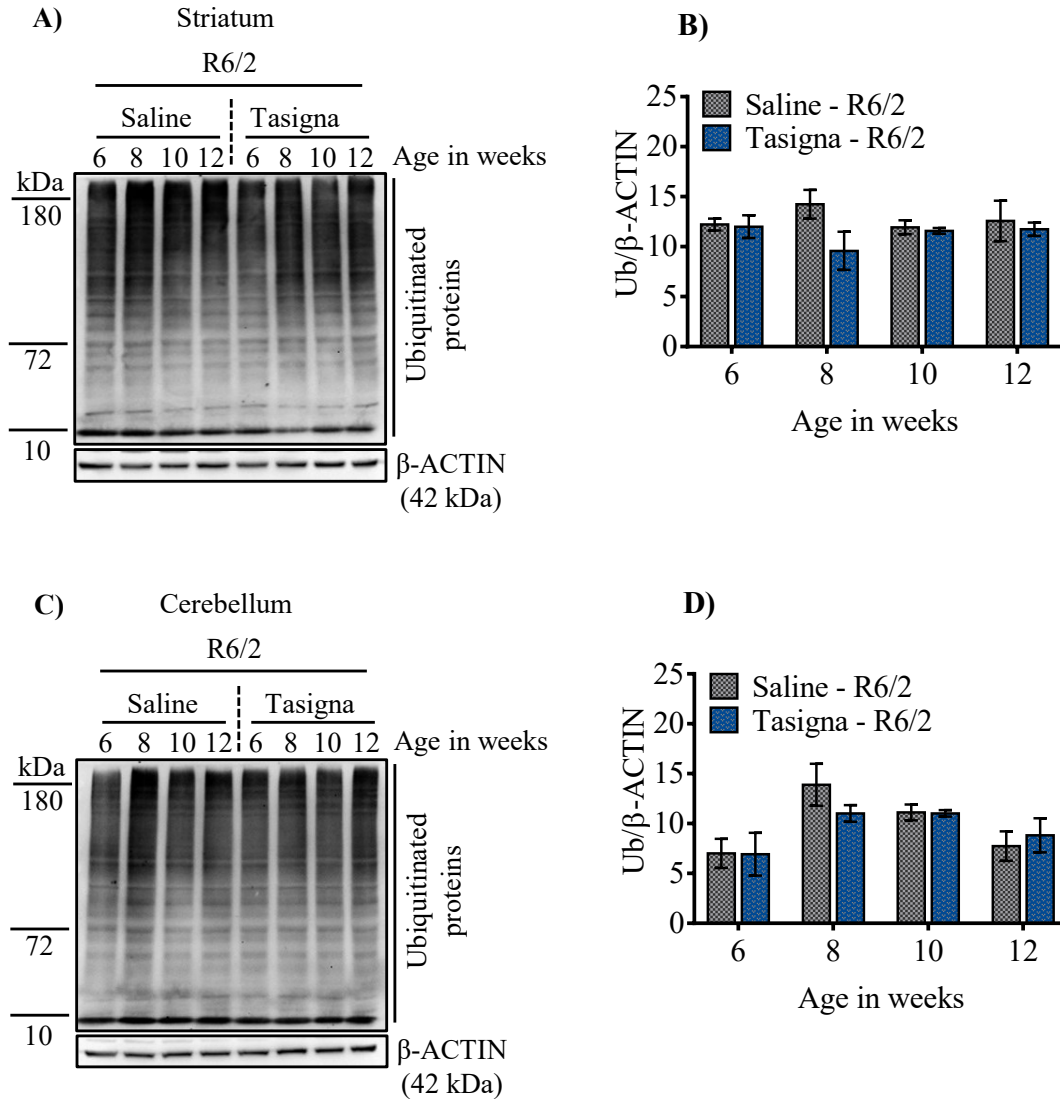


Figure 5-17 UBIQUITIN profile of the cell is unchanged despite the presence of mHTT aggregates in striatum and cerebellum across different stages of disease progression in R6/2 mice

A) Representative blot of UBIQUITIN profile for the region Striatum in R6/2 mice across different age groups. **B)** Pooled quantified bar graphs showing no significant difference in UBIQUITIN profile for the region Striatum in R6/2; Age x treatment ($F_{(3,12)}=1.42$, $p=0.28$). **C)** Representative Immunoblot for the region Cerebellum showing no change in the UBIQUITIN profile in R6/2 in Tasigna treated group compared to saline across different stages of disease progression. **D)** Quantified bar graphs representing no difference in UBIQUITIN profile for the region Cerebellum in R6/2 across different age groups; Age x treatment ($F_{(3,12)}=0.62$, $p=0.61$). β -ACTIN is used as a loading control in all the experimental conditions. $N = 3$ [1M, 2F] for all the age groups 6, 8, 10, and 12 weeks. Statistical analysis was done by Two-way ANOVA followed by Bonferroni *post-hoc* test. Error bars indicate \pm SEM. N=number of mice, M=Males, F=Females. Vertical dashed lines separate the drug treatment groups.

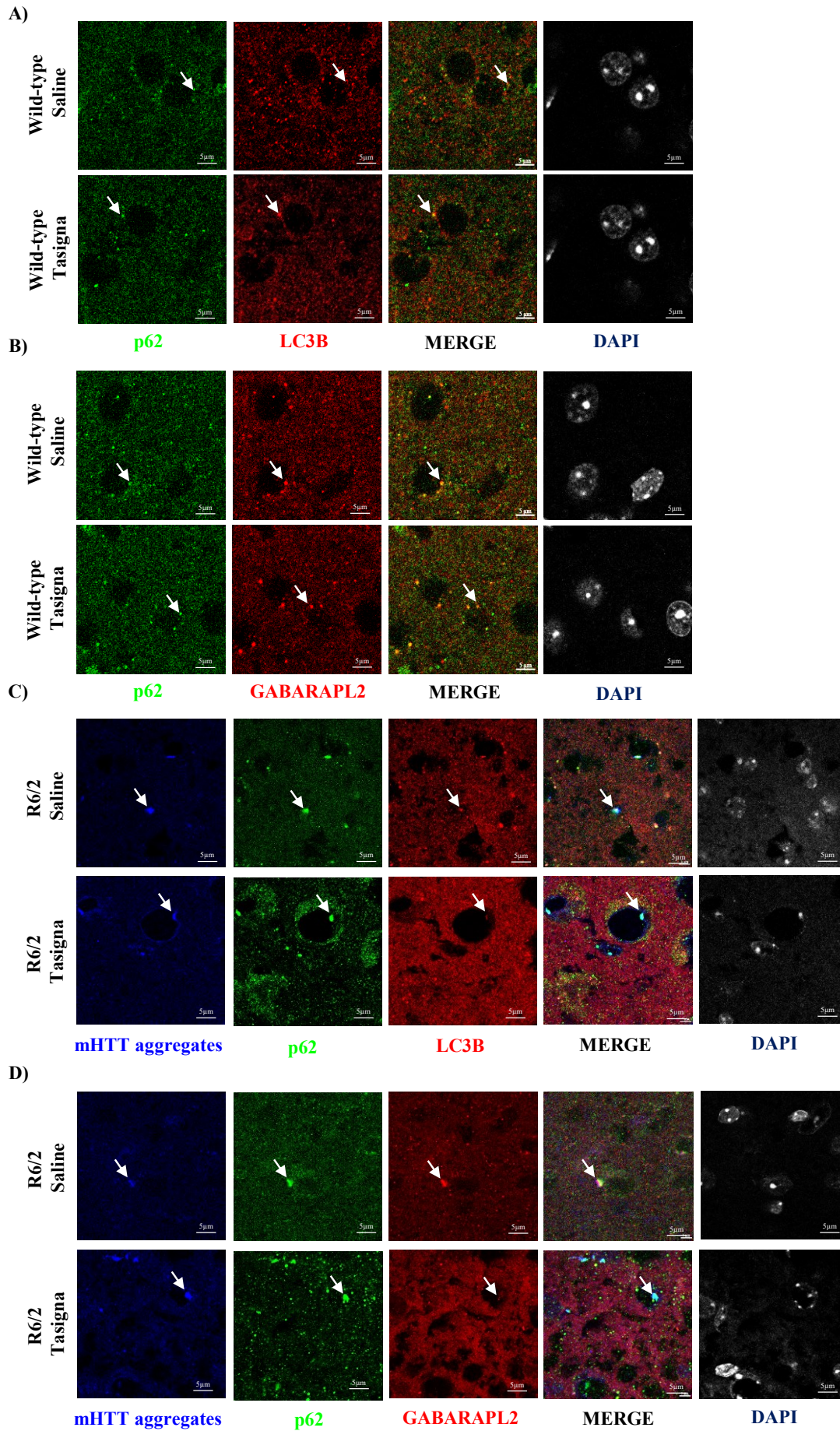


Figure 5-18 Nilotinib (Tasigna™) does not affect the expression of autophagy related proteins and clearance of mHTT aggregates at 12 weeks in Striatum in R6/2 mice

A. Representative images of immunohistochemistry for labelling autophagy related proteins p62, LC3B from WT-Saline and WT-Tasigna treated mice in the striatum at 12 weeks. p62 labelled in green, LC3B in red. **B.** Representative images of immunohistochemistry for labelling autophagy related proteins p62, GABARAPL2 from WT-Saline and WT-Tasigna treated mice in the striatum at 12 weeks. p62 labelled in green, GABARAPL2 in red. **C.** Representative images for immunohistochemistry for labelling mHTT aggregates by EM48, and autophagy related proteins p62, LC3B from R6/2-Saline and R6/2-Tasigna treated mice in the striatum at 12 weeks. mHTT (EM48) aggregates are labelled in Blue, p62 in green, and LC3B in red. **D.** Representative images for immunohistochemistry for labelling of mHTT aggregates by EM48, and autophagy related proteins p62, and GABARAPL2 from R6/2-Saline and R6/2-Tasigna treated mice in the striatum at 12 weeks. mHTT (EM48) aggregates are labelled in Blue, p62 in green, and GABARAPL2 in red. Magnification = 63X. Scale bar = 5 μ m. N=3 [1M, 2F]; WT-Saline, and WT-Tasigna; N=3 [1M, 2F]; R6/2-Saline, and R6/2-Tasigna. N=number of mice, M=Males, F=Females. White arrows indicate co-localisation of mHTT (EM48) aggregates with p62, LC3B or GABARAPL2.

5.4 Discussion

The HD mouse model, R6/2, was one of the first and extensively used models in pre-clinical drug trials to target autophagy³⁶¹. Small molecule modulators of autophagy effectively induce the process in several models of neurodegenerative diseases, including HD^{193,399}. Our lab has previously shown that inducing autophagy was proven beneficial in clearing toxic α -SYNUCLEIN aggregates, thereby rescuing behavioural phenotypes in a pre-clinical mouse model of PD^{400,401}. Tasigna induces autophagy and was proven to be neuroprotective in the MPTP mouse model of PD^{322,332}. Currently, Tasigna is in clinical trials to study the tolerance of the drug in PD, and HD patients, although not validated using a pre-clinical model for the latter. Therefore, we tested the efficacy of Tasigna in the more severe and robust form of the HD mouse model, R6/2.

Immunoblotting and immunohistochemical results suggest no differential change in the expression of key autophagy related proteins: p62, LC3B, and GABARAPL2 from different regions of the brain at 6, 8, 10, and 12 weeks in Tasigna treated wild-type and R6/2 mice. These results have been further validated and supported, showing that Tasigna is inefficient in clearing mHTT aggregates in R6/2 at any given stage of disease progression. The study carried out in this thesis will be the first one to report its inefficacy in ameliorating disease pathology in the HD mouse model, R6/2. There might be several reasons accounting for discrepancies observed regarding a model-based bias ineffectiveness. It is possible that dosage optimisation might give an insight into the efficacy of this drug in inducing autophagy, but it is also plausible

that Tasigna effectively induces autophagy in the presymptomatic stage when the aggregate load is not overwhelming. For therapeutic benefit, the desired levels of Tasigna in inducing autophagy in R6/2 mice may not be achieved by the concentration used in this study due to the severity and rapid progression of the disease. Therefore, studying the effect of Tasigna at higher concentrations could clarify the appropriate dosage and effectiveness of the drug.

Studies so far carried out to exhibit the effect of Tasigna as an active therapeutic molecule for NDDs are in concern with C-ABL inhibition and some are also focused on autophagic clearance of α -SYNUCLEIN and amyloid aggregates in PD and AD, respectively. It has been previously established that C-ABL kinase levels are upregulated in PD ^{321,341,402}. However, concerning HD, there are no reports of over-expression of C-ABL and its interaction with HTT protein in any of the HD mouse models to date. The levels of C-ABL kinase in HD and its modulation after treatment with Tasigna needs to be elucidated.

Chapter- 6
**Nilotinib (Tasigna™) is not neuroprotective and is
unable to rescue motor functions in R6/2 mice**

6.1 Introduction

Huntington's disease is an autosomal dominant, fatal, progressive neurodegenerative disorder caused by an expansion of trinucleotide CAG repeats in the gene coding for *HUNTINGTIN*^{236,403}. Despite enormous progress, a direct causative pathway/mechanism from HD gene mutation to various neuronal dysfunction and death has not yet been clearly elucidated. One of the major advances in understanding the pathophysiology of the disease has been the development of multiple rodent models that replicate many of the molecular, cellular, neuropathological, and clinical events in HD patients^{279,360}. Various mouse models have played a significant role in providing accurate, rapid, and experimentally accessible systems to study and understand the multiple aspects of the disease pathogenesis and test and validate potential therapeutic strategies to ameliorate the disease phenotypes³⁶⁰. Moreover, understanding how the disease progresses over a period of time has become vital in identifying pharmacotherapy and success in clinical trials. To date, there is no clinically proven treatment or drug that can halt or ameliorate the inexorable disease progression for HD.

Since the identification of the disease-causing mutation for HD in 1993, various genetically modified mouse models of HD have been generated^{404,405}. The first transgenic mouse model R6/2 remained the best characterised and widely used robust model to study the pathogenesis of HD and also to test and validate novel therapeutic strategies. In terms of behavioural changes, brain pathology, and age of death, the rapid disease progression makes these mice relatively faster to study the disease pathophysiology of HD²³⁶. In this study, R6/2 mice were used to understand the proteostasis defects concerning pathological significance in autophagy dysfunction. As discussed earlier, results presented in this study suggested that mHTT aggregates form early in R6/2, and basal autophagy is spatio-temporally maintained across different stages of disease progression in various regions of the brain (refer to chapter 3 & 4).

Moreover, Nilotinib (TasignaTM) is in clinical trials for PD and HD, but its potency has not been evaluated in any rodent models neurodegenerative illnesses^{345,346}. Although our results suggest that Nilotinib (TasignaTM) is ineffective in inducing autophagy and clearing mHTT aggregates in R6/2, (discussed in chapter 5) we, assessed to check if Tasigna would be able to ameliorate and improve subtle behavioural deficits and extend the lifespan of the R6/2 mouse.

6.2 Methods

6.2.1 Behavioural studies

All the experiments were done in the behaviour room in the Institute's animal facility. HD mouse model, R6/2, and wild-type littermates (all males) were used for the experiments from 5-6 to 12-13 weeks of age. Mice used for the tests were habituated in the behaviour room for approximately 30 minutes before the start of the experiment. The light intensity was maintained at 100 LUX. Behavioural experiments such as open-field, rotarod, hind-limb clasping were conducted to assess the motor function tests in R6/2 mice. The bodyweight of the mice was measured and monitored through the experimental paradigm. [Note: Detailed experimental procedures were mentioned in chapter 2: Methods and materials section].

6.3 Results

6.3.1 Nilotinib (TasignaTM) is ineffective in improving the body weight and survival rate in R6/2 mice

Tasigna was dissolved in saline, and mice were injected intraperitoneally every day, from 2 to 12 weeks of age at a dosage of 20 mg/kg body weight in C57BL/6 wild-type and R6/2 mice. The control littermates were treated with saline. All the experimental mice were weighed on alternate days before the start of injections, and dosage was calculated according to the weight of the mouse. The mice were trained at 5 weeks of age and all the behaviour experiments were performed every week from 6 to 12 weeks of age. Tasigna treatment neither affected body weight (**Figure 6-1A**) nor the survival rate of WT and R6/2 (**Figure 6-1B**). Our results imply that Tasigna is safe, tolerable, and non-toxic, as we observe no significant changes in the health and behaviour of the wild-type control littermates.

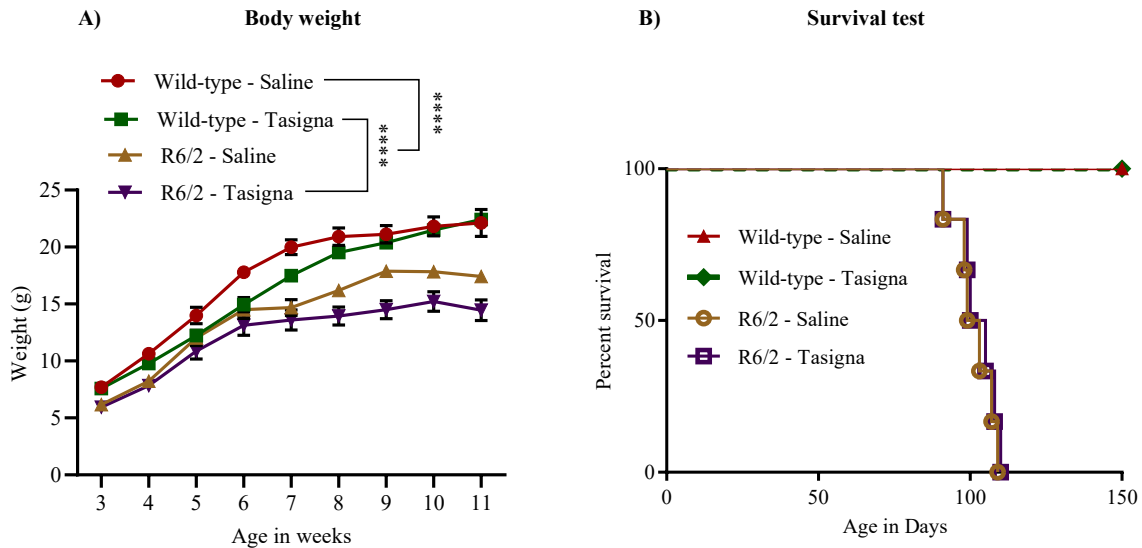


Figure 6-1 Nilotinib is unable to improve the body weight and survival rate in R6/2 mice

A. Line graph showing no effect of Tasigna on weight gain in R6/2 compared to wild-type control mice (saline and Tasigna) across different disease progression stages. R6/2-Saline: N=12 (M); R6/2-Tasigna: N=12 (M); WT-Saline: N=12 (M); WT-Tasigna: N=12 (M); Age x Treatment x Genotype ($F_{(8, 8)}=2.079, p=0.03$). **B.** Kaplan-Meier survival curve showing no increase in life span in Tasigna treated R6/2 mice compared to saline-treated mice (R6/2 - Saline: N=12 (M); R6/2-Tasigna: N=12 (M)).

6.3.2 Nilotinib (TasignaTM) is unable to ameliorate motor functions in R6/2 mice

The next question asked was whether administering Tasigna would alleviate motor dysfunction in R6/2 in the open-field and rotarod test. An open-field test was done to assess the exploratory and locomotory behaviour of the R6/2 mice. The results imply that there is no improvement in locomotor activity in R6/2 mice treated with Tasigna compared to wild-type littermates (**Figure 6-2A, B**). Following, the rotarod test was performed to check the motor coordination in mice by calculating the latency time to fall on the rotating rod in R6/2 mice. Tasigna treated mice showed no signs of improvement in drug-treated groups and their motor coordination had progressively deteriorated across different stages of disease progression. (**Figure 6-2C**). These results confirm that Tasigna is not effective in rescuing behavioural impairments in R6/2, which led us to verify by checking the hind-limb clasp phenotype in R6/2. Tasigna treatment failed to restore hind-limb clasp issues in R6/2 to WT levels, suggesting no delay in disease progression in Tasigna treated group compared to saline-treated R6/2 animals (**Figure 6-2D**).

Therefore, Tasigna was ineffective in rescuing or delaying the onset of behavioural symptoms in R6/2, suggesting that the drug is not a potent therapeutic molecule in the R6/2 mouse model of HD.

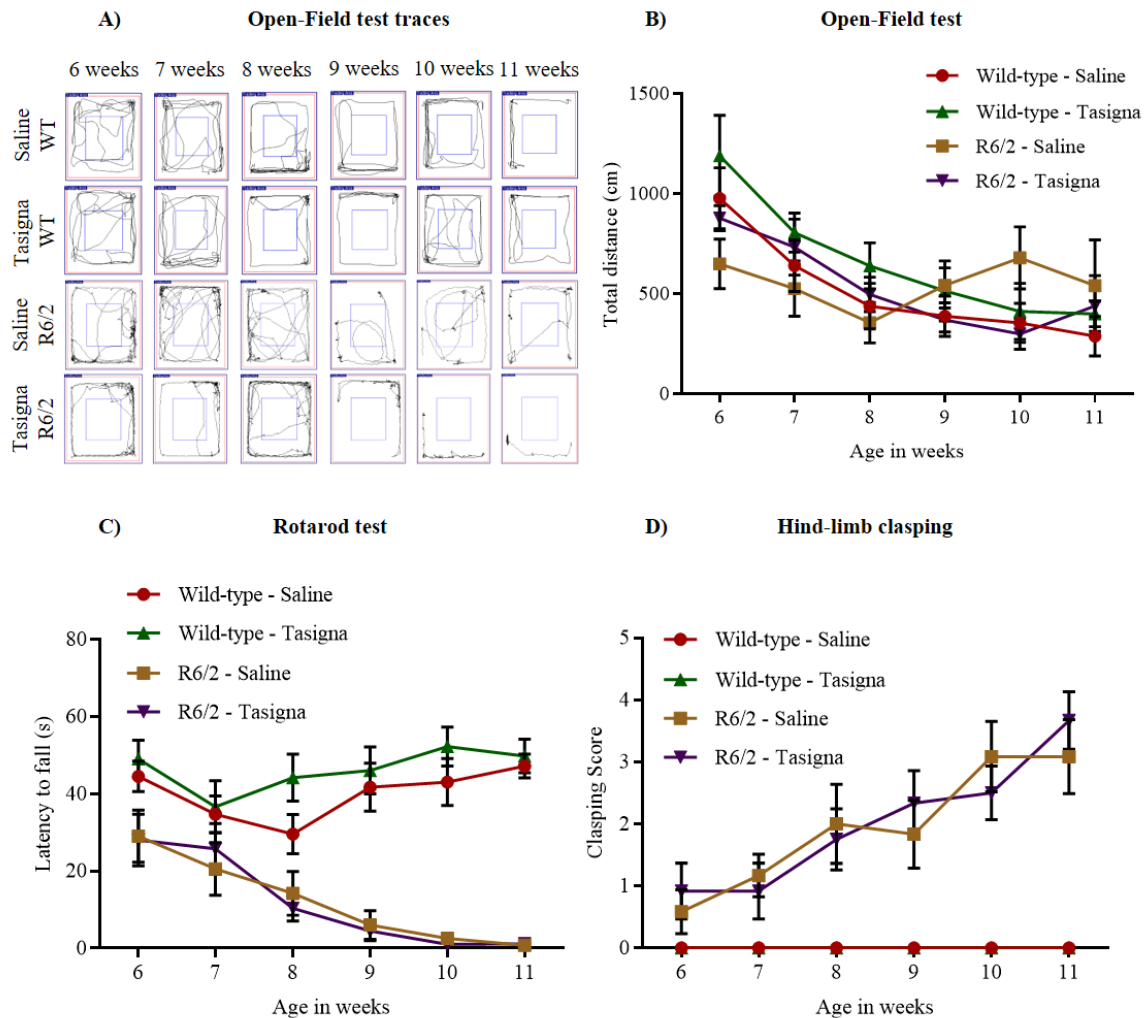


Figure 6-2 Nilotinib (TasignaTM) is ineffective in rescuing the motor functions in R6/2 mice

A. Representative traces showing no significant improvement in the distance travelled in the Open-Field test in Tasigna treated group in R6/2 compared to the saline-treated group from 6 to 11 weeks. WT-Saline and WT-Tasigna groups also showing no significant difference in the distance travelled. **B.** Line graph depicting total distance travelled in Open-field test from 6 to 11 weeks in Tasigna and saline-treated ones in both the genotypes. R6/2-Saline: N=12 (M); R6/2-Tasigna: N=12 (M); WT-Saline: N=12 (M); WT-Tasigna: N=12 (M); Age x Treatment x Genotype ($F_{(5, 5)}=0.560$, $p=0.73$). **C.** Line graph showing no significant improvement in latency to fall in Rotarod test in R6/2 from 6 to 11 weeks in Tasigna-treated group compared to saline-treated. Tasigna does not affect WT control mice from 6 to 11 weeks. R6/2-Saline: N=12 (M); R6/2-Tasigna: N=12 (M); WT-Saline: N=12 (M); WT-Tasigna: N=12 (M); Age x Treatment x Genotype ($F_{(5, 5)}=0.5618$, $p=0.72$). **D.** Line graph showing Tasigna having no

significant effect in delaying the onset of hind-limb clasping symptom in R6/2 from 6 to 11 weeks. WT control mice were showing no effect on Tasigna treatment. Scores were plotted based on the Racine scale from 0-5, as explained in the methods section. R6/2-Saline: N=12 (M); R6/2-Tasigna: N=12 (M); WT-Saline: N=12 (M); WT-Tasigna: N=12 (M); Age x Treatment x Genotype ($F_{(5,5)}=0.4634$, $p=0.80$). Error bars indicate \pm SEM. N=number of mice, M=Males. Statistical analysis was done by 3-way ANOVA followed by Tukey *post-hoc* test.

6.4 Discussion

The R6/2 mice are considered a robust mouse model to screen small molecule modulators of autophagy and to develop novel therapeutic strategies for HD^{193,399}. Our lab has previously shown that inducing autophagy by small molecules cleared α -SYNUCLEIN aggregates, thereby improving the behavioural phenotypes in an MPTP mouse model of PD^{400,401}. Currently, Tasigna is in clinical trials for PD, and HD is not yet validated for its efficacy in any of the HD mouse models. Therefore, we assessed the potency of Tasigna in improving the motor phenotypes in an HD mouse model, R6/2.

The results from a battery of behavioural tests suggested that Tasigna is ineffective in improving the bodyweight or extending lifespan and unable to rescue the motor functions in R6/2 mice. Due to the aggressive and penetrant phenotypes of R6/2, subtle improvements caused by Tasigna treatment at the molecular level might have masked any observable changes in behaviour phenotypes. Due to the severity of disease progression in R6/2, Tasigna when administered at higher doses might throw some clarity on the effectiveness of the drug in delaying the onset of symptoms and improving the life span.

Apart from R6/2, many HD mouse models have been developed by expressing full-length HTT gene containing a variable number of polyQ such as BACHD, YAC128 transgenic mouse models or CAG140, CAG150 knock-in mouse models^{279,360,362}. These mouse models exhibit less severe and modest behaviour phenotypes⁴⁰⁶. Moreover, since R6/2 expresses only exon 1, but not the complete *HTT* gene, it is often considered as a polyglutamine toxicity model rather than an HD model. However, pathogenicity and symptoms in R6/2 are correlated with juvenile HD. So, considering R6/2 as a model system for HD or for polyglutamine toxicity is a debatable topic. Therefore, Tasigna, when tested in these mouse models or at a higher dose, may prove to be effective in rescuing the motor functions and ameliorate the disease phenotype.

Chapter- 7
Discussion and future directions

Protein homeostasis refers to a highly complex and interconnected set of cellular processes that affect and determine the levels and conformational stability of proteins inside the cell ¹². Maintenance of optimal protein homeostasis especially in neurons is critical for its viability, growth, and function ³². The functions of the normal proteins are determined by their precise three-dimensional structures, which are defined by their amino acid sequences during the process of protein folding that is regulated by a special class of proteins called chaperones ⁴⁰⁷. Mutations, external stress-related factors, and inherent instability of proteins contribute to the failure of maintaining the correct conformational structure causing them to misfold and aggregate ¹⁴. Protein homeostatic processes combat these problems by stabilising proteins that carry out beneficial functions or by degrading the misfolded proteins and aggregates that are detrimental to the neuronal cell ¹⁴. Impairment in the protein degradation pathways such as UPS and autophagy leads to the accumulation of intracellular mutant protein aggregates in the form of inclusion bodies. The presence of such toxic proteinaceous bodies inside the neuronal cells is the characteristics of protein conformational disorders or proteinopathies ¹¹. Proteinopathies encompass a class of family of neurodegenerative diseases such as AD, PD, HD, and ALS. The signature hallmark of all these groups of devastating diseases is the presence of specific mutant protein aggregates/inclusions inside the brain ¹¹.

Neurodegenerative diseases are severe forms of neurological aberrations due to the progressive degeneration of neurons ³⁹. The neuropathology of protein misfolding diseases is primarily linked to the toxic gain-of-function mechanisms, and one way of combatting disease is to reduce the levels of such proteins inside the neuronal cells ^{12,39}. The aggregate-prone neurodegenerative disease-associated proteins are autophagy substrates, including mutant HTT, α -SYNUCLEIN, and TAU ^{105,106}. Increasing evidence has firmly certified the fact that neuronal autophagy is an essential anchor for delaying ageing and pathophysiology of NDDs ^{310,408}. The evidence supporting a pathogenic role for autophagy impairment in several major proteinopathies is becoming persuasive and provides a strong rationale for developing novel therapeutics to modulate autophagy in these disorders ¹⁰⁶. As promising as these beginnings are, the nutshell has barely been cracked on understanding the regulation of autophagy, especially in the broader context of proteostasis and general metabolic regulation with respect to NDDs ¹⁰⁹.

Dynamics of mHTT aggregate formation and state of basal autophagy in R6/2 mice

In this study, the HD mouse model, R6/2 was used to study the proteostasis defects concerning pathological significance in autophagy dysfunction. The molecular mechanisms underlying the pathogenesis of HD are very complex and are not completely understood. The presence of intranuclear and cytoplasmic accumulation of mutant N-terminal HTT fragments is well established, but their role in disease pathogenesis is still controversial^{352,409,410}. However, mHTT aggregate formation plays a direct role in the induction of neuronal dysfunction and death thereby contributing to disease progression in HD³⁵². Our understanding of the complex molecular process of mHTT aggregate formation in HD mouse models are very limited and only a few studies have characterised its role in disease pathogenesis^{352,411,412}. In this thesis, a comprehensive study was carried out to investigate the mHTT aggregate formation in the R6/2 mouse model across different stages of disease progression in certain regions of the brain.

mHTT aggregates were detected at a very early stage of disease progression (before the onset of symptoms), i.e., from 2 weeks in the region cortex and striatum, and 4 weeks in the hippocampus and cerebellum. This early accumulation of toxic N-terminal mHTT aggregates implies that the striatum and cortex are primarily affected leading to the disruption of cortico-striatal signalling impairing the motor and cognitive functions such as mood, and attention. As the disease progresses, the aggregate formation increases and spread to the other regions of the brain thereby impairing and causing more severe deficits in the executive and motor functions in R6/2 mice. The accumulation of noxious HTT aggregates sequesters and impairs the functions of many cellular proteins including that of autophagy pathways contributing to disease pathogenesis^{375,413-415}.

The degradation of mHTT aggregates by autophagy involves the identification and labelling of aggregates by a chain of UBIQUITIN molecules^{59,416}. In this regard, the UBIQUITIN expression of the cell was checked for any alteration as the disease progresses in R6/2. The ubiquitination pattern was increased in both stacking and resolving gels only in the region striatum at 12 weeks in R6/2 mice compared to wild-type control littermates. There was no differential change observed in other regions of the brain in R6/2 indicating that mHTT aggregates are being detected and labelled by UBIQUITIN molecules. These results are supported by initial findings that ubiquitinated N-terminal mHTT fragments are detected in intracellular aggregates and are targeted to degradation^{352,355,416}. However, the accumulation of aggregates inside the neuronal cells might be due to the impairment in downstream

signalling processes of the autophagy pathway and these facets have to be considered seriously for the critical investigation to identify the factors associated with disease-causing mechanisms.

Our knowledge of the intricate molecular mechanisms of autophagy impairment in neurodegenerative diseases is far from complete and may lead to variable outcomes. Although, autophagy in the brain is tightly controlled and regulated, it is challenging to modulate autophagy flux inside the neuronal cells^{390,391}. To assess the regulation of autophagy in R6/2 mice, the state of basal autophagy was studied by investigating the expression of key autophagy related markers such as p62/SQSTM1, LC3B and GABARAPL2 from the cortex, hippocampus, striatum, and cerebellum across different stages of disease progression. Despite the early accumulation of toxic mHTT aggregates, there is no differential change in the expression of autophagy related markers at any given stage of disease progression, indicating that basal autophagy in R6/2 mice is spatio-temporally maintained. These results substantiate earlier findings that indicate no change in basal autophagy despite metabolic dysfunction in HD mouse model³⁹². Moreover, contrary to the earlier report, the study performed in this thesis comprehensively examined the basal autophagy levels in major regions of the brain during various stages of disease progression in an R6/2 mouse model.

mHTT aggregates exist in multiple different conformational states and their pathogenicity is dependent on the number of CAG repeats, the solubility of the aggregates, and the precise accumulation of intranuclear, cytoplasmic and perinuclear inclusion bodies^{348,417}. Many studies have proved that soluble mHTT aggregates are highly toxic and disrupt many cellular processes leading to pathogenicity in HD³⁷⁸⁻³⁸³. These soluble mHTT aggregates undergo various proteolytic cleavages by various caspases and form a prime seedling to generate higher-order oligomers. During this process, mHTT aggregates sequester many functional proteins including that of autophagy pathways rendering its toxicity^{198,211}.

In this regard, the study performed in this project involves the evaluation of mHTT aggregate formation and state of basal autophagy only in the soluble fractions of the R6/2 brain lysates. On the contrary, there are other few studies, which propose that insoluble mHTT aggregates formed and accumulated as inclusion bodies are neuroprotective. One of the landmark paper published in Nature by Steve Finkbeiner group has shown that the formation of inclusion bodies reduces the toxicity and load of mHTT aggregates, thereby protecting the neurons from dying⁴¹⁸. In the aid of this report, few other groups have also shown the neuroprotective role of mHTT aggregates in inclusion bodies^{419,420}. However, some of the studies contradict the

function of inclusion bodies as neuroprotective in HD ⁴²¹⁻⁴²⁴. Contemplating these results, the role of mHTT aggregates as inclusion bodies in HD is debatable and inconclusive; therefore, further studies have to be carried out to understand its role in neurodegenerative diseases.

The results discussed in this thesis hypothesise that the functioning of the steady-state basal autophagy in neurons does not cope with the rapid accumulation of mHTT aggregates. The rate at which aggregates getting cleared by basal autophagy is not sufficient to maintain proteostasis balance to prevent/delay neuronal death. Another conceivable theory for autophagic dysfunction without the protein level being affected involves a deficit in the functionalities of autophagy related proteins, rather than in their levels. This hypothesis supports the findings as there is a significant change in the expression of LC3B-I form in the cortex at 12 weeks, suggesting a possible defect in the conversion rate of LC3B, implying aggrephagy dysfunction in R6/2 mice. Moreover, impairment in the expression of autophagy related genes may add to the autophagy dysfunction and studies carried out so far has conflicting results. Considering the fact that HTT plays a crucial role in autophagy pathway ^{211,248,351,393}, it is of no surprise that in HD patients, there is clear evidence that gene expression of the autophagy pathway is altered ³⁹⁴. However, in one of the study, the expression levels of mRNA and proteins of the autophagy pathway are unaffected in the HD mouse model despite the metabolic dysfunction ³⁹⁵. Therefore, to ascertain the reasons for autophagy impairment, a wide-ranging analysis of gene expression of various autophagy related proteins needs to be investigated across different stages of disease progression in R6/2 mice.

Inducing autophagy as a potential therapeutic strategy to alleviate the disease phenotypes in R6/2 mice

The HD mouse model, R6/2, is considered as one of the severe pre-clinical models to study the potency of the drugs that modulate the autophagy pathway in neurodegenerative diseases ³⁶¹. Autophagy induction by small molecules was established as a potential disease-modifying strategy in enhancing the clearance of toxic aggregates, thereby rescuing the molecular and behavioural phenotypes, and increasing the lifespan in several neurodegenerative diseases including HD ^{326,329,399,400,425}. Recently, our lab has extensively contributed to screening and testing the potency of various small molecules and have reported that inducing autophagy cleared toxic α -SYNUCLEIN aggregates and rescued behavioural phenotypes in a pre-clinical MPTP mouse model of PD ^{400,401}.

Tasigna is a BCR-ABL receptor tyrosine kinase inhibitor and was shown to be effective in inducing autophagy and clearing α -SYNUCLEIN aggregates thereby preventing neurons from dying and improving the motor functions in a pre-clinical mouse model of PD^{322,332}. Currently, Tasigna is already in phase-II clinical trials to study the tolerance of the drug for PD and HD patients, but no pre-clinical study has been carried out to validate its potency in inducing autophagy in any of the HD mouse models. Therefore, in this thesis, the efficacy of Tasigna was studied in a more severe and robust HD mouse model, R6/2. The results from a battery of behavioural experiments indicate that Tasigna treatment is neither effective in rescuing the motor functions nor extending the lifespan in R6/2 mice. Immunoblotting and immunohistochemistry results suggest that Tasigna is unable to induce autophagy, as the expression of key autophagy related markers remained unchanged in both wild-type and R6/2 mice. Due to the inability of Tasigna treatment in increasing autophagy flux, mHTT aggregates are not cleared at any given stage of disease progression in R6/2 mice.

Based on the results, there might be multiple reasons accounting for discrepancies observed involving a model-based bias ineffectiveness of Tasigna treatment. Due to the severe, aggressive, and penetrant phenotypes of R6/2, the subtle improvements caused by Tasigna at the molecular level might have masked any observable changes in the behavioural phenotype. Moreover, due to the rapid disease progression in R6/2, the desired levels of Tasigna in inducing autophagy may not be achieved by the concentration used in this study. It is most likely that optimization of the drug dosage may give an insight into the efficacy of Tasigna in inducing autophagy, however, it is also conceivable that the drug effectively induces autophagy in the presymptomatic stage when the aggregate load is not overwhelming.

Studies so far reported the effectiveness of Tasigna as an active therapeutic agent for NDDs is in interest with the C-ABL inhibition^{322,332}. Some groups have also focused on autophagic clearance of α -SYNUCLEIN and amyloid aggregates in PD and AD, respectively^{322,332}. Given the lack of detailed investigations related to the potency of Tasigna in inducing autophagy and based on a study showing that Tasigna induces autophagy unconventionally through a non-canonical pathway in hepatocellular carcinoma cells⁴²⁶, a thorough study has to be carried out to ascertain the use of Tasigna in HD patients by using appropriate pre-clinical models. Some studies have shown that levels of C-ABL kinase are elevated in PD^{321,341,402}. However, with respect to HD disease, there are no reports of over-expression of C-ABL and its interaction with HTT protein in any of the HD mouse models to date. The levels of C-ABL kinase in HD

and its modulation after treatment with Tasigna needs to be investigated to ascertain its efficacy.

However, given that Tasigna is in Phase-II clinical trials for PD, and HD, researchers have expressed serious concerns about its safety in PD, despite a recent study suggesting its promise in treating certain symptoms ³³⁹. Recently, a clinical trial conducted with 76 PD patients was completed and results have shown that dopamine metabolites were not altered in CSF of Tasigna recipients. Therefore, authors have concluded that drug treatment was safe but was ineffective for the treatment of PD and should not be considered as a potential therapeutic agent for further studies ⁴²⁷. These reports and the results presented in this thesis suggest that Tasigna is ineffective in ameliorating the disease pathogenesis in severe models of neurodegenerative diseases such as PD and HD.

Future directions

- 1) In this study, the expression of mHTT aggregates was evaluated only in the soluble fractions considering the fact that soluble mHTT aggregates are toxic. However, as mentioned earlier, there is a discrepancy and healthy debate about the role of mHTT aggregates as inclusion bodies in HD ^{418-420 421-424}. To understand the toxicity of N-terminal mutant HTT aggregates, it is essential to investigate the expression in insoluble fractions as well. The process of formation and accumulation of mHTT aggregates from seed nucleation to higher-order oligomers might start early in HD, but it requires a critical concentration inside the neuronal cells to get detected by various N-terminal specific antibodies ^{10,198}. In this study, N-terminal specific antibody mEM48, which specifically identifies toxic polyglutamine HUNTINGTIN fragments, was used to detect mHTT aggregates. It would be interesting to study the properties of other different oligomeric species of mHTT aggregates by using different conformation-specific antibodies which identifies the toxic form of mHTT aggregates. Soluble amyloid oligomers are considered as the potentially pathogenic species and are involved in the pathogenesis of many NDDs including HD. A11 polyclonal antibody identifies amino acid independent oligomers of amyloidogenic polypeptides. This antibody can be used to identify the toxic amyloid oligomers in R6/2 across different stages of disease progression.
- 2) The mHTT aggregates undergo various proteolytic cleavages and sequester many functional proteins related to the autophagy pathway and form inclusion bodies that are mostly insoluble ^{10,198}. In this study, the expression of autophagy related markers was assessed only in the soluble fractions. It is quite surprising that despite the early presence of mHTT aggregates, there is no differential change in the expression of key autophagy markers in R6/2 mice. Apart from p62, LC3B, and GABARAPL2, there are many autophagy related markers that play a very important role in regulating the autophagy flux, and many of them have been implicated in neurodegenerative diseases. To ascertain the reasons for autophagy dysfunction in R6/2, it would be ideal for checking the expression levels of these markers in both soluble and insoluble fractions

to understand the state of basal autophagy across different stages of disease progression in R6/2 mice.

- 3) The concentration of the Tasigna used in this study might not be sufficient to induce autophagy. Therefore, studying the potency of Tasigna in a dosage-dependent manner or at higher concentrations could throw clarity on the appropriate dosage and effectiveness of the drug in R6/2 mice. Moreover, inducing autophagy at an early stage of disease progression might be beneficial, where newly expressed, functional autophagy related proteins might potentially enhance the clearance of mHTT aggregates in neurons. Additionally, a thorough examination of the expression of autophagy genes also needs to be investigated to conclusively assert the effects of Tasigna in pre-clinical models of HD.
- 4) It is critical to understand the precise autophagy mechanism that helps to evaluate the therapeutic value of various small molecules of autophagy modulators in neurodegenerative diseases. Since the autophagy pathway is impaired at multiple steps in HD, multiple autophagy modulators (6BIO, XCT, and Tasigna) can be used in combination where it can have multiple effects in inducing autophagic flux, thereby enhancing the clearance of toxic aggregates in an R6/2 mouse model. This attempt to target autophagy in the brain brings tremendous excitement for the development of novel therapeutic strategies for several NDDs. Yet, it is also necessary to elucidate the complexity of autophagy and its signalling pathways to limit the potential side effect for detrimental outcomes. Moreover, future studies must also focus on the disease-causing mechanisms by which aberrant protein aggregates impair the autophagy pathway and on the exploration of therapeutic strategies to prevent their toxicity.
- 5) Studies have shown that overexpression of *Atg5* in mice resulted in increased basal autophagy, which correlated strongly with an extended lifespan, increased insulin sensitivity and improved motor function ⁹⁴. Interestingly, the neonatal lethality of systemic deletion of *Atg5* is rescued even when it is re-expressed only in neurons ⁹⁶. The lifespan extension after autophagy induction has also been corroborated in a knock-in *Beclin1* mouse model, where they show an apparent increase in the life span ⁹⁵. Thus, upregulation of basal autophagy in these mouse models protects the neuronal cells from age-mediated death. Therefore, it would be ideal to restore proteostasis balance in R6/2

by crossing *Atg5* transgenic mice or induce autophagy in R6/2 by overexpressing *Atg5/Atg7* genes by AAV mediated gene transfer.

References

- 1 Verano, J. W. Differential diagnosis: Trepanation. *Int J Paleopathol* **14**, 1-9, doi:10.1016/j.ijpp.2016.04.001 (2016).
- 2 Mahoney, D. E. & Green, A. L. Psychosurgery: History of the Neurosurgical Management of Psychiatric Disorders. *World Neurosurg* **137**, 327-334, doi:10.1016/j.wneu.2020.01.212 (2020).
- 3 Azevedo, F. A., Carvalho, L. R., Grinberg, L. T., Farfel, J. M., Ferretti, R. E., Leite, R. E., Jacob Filho, W., Lent, R. & Herculano-Houzel, S. Equal numbers of neuronal and nonneuronal cells make the human brain an isometrically scaled-up primate brain. *J Comp Neurol* **513**, 532-541, doi:10.1002/cne.21974 (2009).
- 4 Silbereis, J. C., Pochareddy, S., Zhu, Y., Li, M. & Sestan, N. The Cellular and Molecular Landscapes of the Developing Human Central Nervous System. *Neuron* **89**, 248-268, doi:10.1016/j.neuron.2015.12.008 (2016).
- 5 Papale, A. E. & Hooks, B. M. Circuit changes in motor cortex during motor skill learning. *Neuroscience* **368**, 283-297, doi:10.1016/j.neuroscience.2017.09.010 (2018).
- 6 Svoboda, K. & Li, N. Neural mechanisms of movement planning: motor cortex and beyond. *Curr Opin Neurobiol* **49**, 33-41, doi:10.1016/j.conb.2017.10.023 (2018).
- 7 Sheikh, S., Safia, Haque, E. & Mir, S. S. Neurodegenerative Diseases: Multifactorial Conformational Diseases and Their Therapeutic Interventions. *J Neurodegener Dis* **2013**, 563481, doi:10.1155/2013/563481 (2013).
- 8 McColgan, P., Joubert, J., Tabrizi, S. J. & Rees, G. The human motor cortex microcircuit: insights for neurodegenerative disease. *Nat Rev Neurosci* **21**, 401-415, doi:10.1038/s41583-020-0315-1 (2020).
- 9 O'Callaghan, C., Bertoux, M. & Hornberger, M. Beyond and below the cortex: the contribution of striatal dysfunction to cognition and behaviour in neurodegeneration. *J Neurol Neurosurg Psychiatry* **85**, 371-378, doi:10.1136/jnnp-2012-304558 (2014).
- 10 Illarioshkin, S. N., Klyushnikov, S. A., Vigont, V. A., Seliverstov, Y. A. & Kaznacheyeva, E. V. Molecular Pathogenesis in Huntington's Disease. *Biochemistry (Mosc)* **83**, 1030-1039, doi:10.1134/S0006297918090043 (2018).
- 11 Balch, W. E., Morimoto, R. I., Dillin, A. & Kelly, J. W. Adapting proteostasis for disease intervention. *Science* **319**, 916-919, doi:10.1126/science.1141448 (2008).
- 12 Kurtishi, A., Rosen, B., Patil, K. S., Alves, G. W. & Moller, S. G. Cellular Proteostasis in Neurodegeneration. *Mol Neurobiol* **56**, 3676-3689, doi:10.1007/s12035-018-1334-z (2019).
- 13 Zhong, M., Lee, G. M., Sijbesma, E., Ottmann, C. & Arkin, M. R. Modulating protein-protein interaction networks in protein homeostasis. *Curr Opin Chem Biol* **50**, 55-65, doi:10.1016/j.cbpa.2019.02.012 (2019).
- 14 Balchin, D., Hayer-Hartl, M. & Hartl, F. U. In vivo aspects of protein folding and quality control. *Science* **353**, aac4354, doi:10.1126/science.aac4354 (2016).
- 15 Hipp, M. S., Park, S. H. & Hartl, F. U. Proteostasis impairment in protein-misfolding and -aggregation diseases. *Trends Cell Biol* **24**, 506-514, doi:10.1016/j.tcb.2014.05.003 (2014).
- 16 Rujano, M. A., Bosveld, F., Salomons, F. A., Dijk, F., van Waarde, M. A., van der Want, J. J., de Vos, R. A., Brunt, E. R., Sibon, O. C. & Kampinga, H. H. Polarised asymmetric inheritance of accumulated protein damage in higher eukaryotes. *PLoS Biol* **4**, e417, doi:10.1371/journal.pbio.0040417 (2006).

- 17 Liu, K., Tedeschi, A., Park, K. K. & He, Z. Neuronal intrinsic mechanisms of axon regeneration. *Annu Rev Neurosci* **34**, 131-152, doi:10.1146/annurev-neuro-061010-113723 (2011).
- 18 Kuhn, H. G., Dickinson-Anson, H. & Gage, F. H. Neurogenesis in the dentate gyrus of the adult rat: age-related decrease of neuronal progenitor proliferation. *J Neurosci* **16**, 2027-2033 (1996).
- 19 Overstreet-Wadiche, L. S., Bensen, A. L. & Westbrook, G. L. Delayed development of adult-generated granule cells in dentate gyrus. *J Neurosci* **26**, 2326-2334, doi:10.1523/JNEUROSCI.4111-05.2006 (2006).
- 20 Steiner, P. Brain Fuel Utilization in the Developing Brain. *Ann Nutr Metab* **75 Suppl 1**, 8-18, doi:10.1159/000508054 (2019).
- 21 Diemel, G. A. Brain Glucose Metabolism: Integration of Energetics with Function. *Physiol Rev* **99**, 949-1045, doi:10.1152/physrev.00062.2017 (2019).
- 22 Gabbita, S. P., Butterfield, D. A., Hensley, K., Shaw, W. & Carney, J. M. Aging and caloric restriction affect mitochondrial respiration and lipid membrane status: an electron paramagnetic resonance investigation. *Free Radic Biol Med* **23**, 191-201, doi:10.1016/s0891-5849(97)00043-9 (1997).
- 23 Hohn, A., Tramutola, A. & Cascella, R. Proteostasis Failure in Neurodegenerative Diseases: Focus on Oxidative Stress. *Oxid Med Cell Longev* **2020**, 5497046, doi:10.1155/2020/5497046 (2020).
- 24 Daniele, S., Giacomelli, C. & Martini, C. Brain ageing and neurodegenerative disease: The role of cellular waste management. *Biochem Pharmacol* **158**, 207-216, doi:10.1016/j.bcp.2018.10.030 (2018).
- 25 Marcuccilli, C. J., Mathur, S. K., Morimoto, R. I. & Miller, R. J. Regulatory differences in the stress response of hippocampal neurons and glial cells after heat shock. *J Neurosci* **16**, 478-485 (1996).
- 26 Manzerra, P., Rush, S. J. & Brown, I. R. Tissue-specific differences in heat shock protein hsc70 and hsp70 in the control and hyperthermic rabbit. *J Cell Physiol* **170**, 130-137, doi:10.1002/(SICI)1097-4652(199702)170:2<130::AID-JCP4>3.0.CO;2-P (1997).
- 27 Hershko, A., Ciechanover, A., Heller, H., Haas, A. L. & Rose, I. A. Proposed role of ATP in protein breakdown: conjugation of protein with multiple chains of the polypeptide of ATP-dependent proteolysis. *Proc Natl Acad Sci U S A* **77**, 1783-1786, doi:10.1073/pnas.77.4.1783 (1980).
- 28 Huang, Q., Wang, H., Perry, S. W. & Figueiredo-Pereira, M. E. Negative regulation of 26S proteasome stability via calpain-mediated cleavage of Rpn10 subunit upon mitochondrial dysfunction in neurons. *J Biol Chem* **288**, 12161-12174, doi:10.1074/jbc.M113.464552 (2013).
- 29 Heo, J. M. & Rutter, J. Ubiquitin-dependent mitochondrial protein degradation. *Int J Biochem Cell Biol* **43**, 1422-1426, doi:10.1016/j.biocel.2011.06.002 (2011).
- 30 Livnat-Levanon, N. & Glickman, M. H. Ubiquitin-proteasome system and mitochondria - reciprocity. *Biochim Biophys Acta* **1809**, 80-87, doi:10.1016/j.bbagr.2010.07.005 (2011).
- 31 Yerbury, J. J., Ooi, L., Dillin, A., Saunders, D. N., Hatters, D. M., Beart, P. M., Cashman, N. R., Wilson, M. R. & Ecroyd, H. Walking the tightrope: proteostasis and neurodegenerative disease. *J Neurochem* **137**, 489-505, doi:10.1111/jnc.13575 (2016).
- 32 Douglas, P. M. & Dillin, A. Protein homeostasis and aging in neurodegeneration. *J Cell Biol* **190**, 719-729, doi:10.1083/jcb.201005144 (2010).

- 33 Ciryam, P., Tartaglia, G. G., Morimoto, R. I., Dobson, C. M. & Vendruscolo, M. Widespread aggregation and neurodegenerative diseases are associated with supersaturated proteins. *Cell Rep* **5**, 781-790, doi:10.1016/j.celrep.2013.09.043 (2013).
- 34 Chiti, F. & Dobson, C. M. Protein misfolding, functional amyloid, and human disease. *Annu Rev Biochem* **75**, 333-366, doi:10.1146/annurev.biochem.75.101304.123901 (2006).
- 35 Olzscha, H., Schermann, S. M., Woerner, A. C., Pinkert, S., Hecht, M. H., Tartaglia, G. G., Vendruscolo, M., Hayer-Hartl, M., Hartl, F. U. & Vabulas, R. M. Amyloid-like aggregates sequester numerous metastable proteins with essential cellular functions. *Cell* **144**, 67-78, doi:10.1016/j.cell.2010.11.050 (2011).
- 36 Soto, C. & Pritzkow, S. Protein misfolding, aggregation, and conformational strains in neurodegenerative diseases. *Nat Neurosci* **21**, 1332-1340, doi:10.1038/s41593-018-0235-9 (2018).
- 37 Arrasate, M., Mitra, S., Schweitzer, E. S., Segal, M. R. & Finkbeiner, S. Inclusion body formation reduces levels of mutant huntingtin and the risk of neuronal death. *Nature* **431**, 805-810, doi:10.1038/nature02998 (2004).
- 38 Davis, A. A., Leyns, C. E. G. & Holtzman, D. M. Intercellular Spread of Protein Aggregates in Neurodegenerative Disease. *Annu Rev Cell Dev Biol* **34**, 545-568, doi:10.1146/annurev-cellbio-100617-062636 (2018).
- 39 Dugger, B. N. & Dickson, D. W. Pathology of Neurodegenerative Diseases. *Cold Spring Harb Perspect Biol* **9**, doi:10.1101/cshperspect.a028035 (2017).
- 40 Tsvetkov, A. S., Arrasate, M., Barmada, S., Ando, D. M., Sharma, P., Shaby, B. A. & Finkbeiner, S. Proteostasis of polyglutamine varies among neurons and predicts neurodegeneration. *Nat Chem Biol* **9**, 586-592, doi:10.1038/nchembio.1308 (2013).
- 41 Gidalevitz, T., Prahlad, V. & Morimoto, R. I. The stress of protein misfolding: from single cells to multicellular organisms. *Cold Spring Harb Perspect Biol* **3**, doi:10.1101/cshperspect.a009704 (2011).
- 42 Leitman, J., Ulrich Hartl, F. & Lederkremer, G. Z. Soluble forms of polyQ-expanded huntingtin rather than large aggregates cause endoplasmic reticulum stress. *Nat Commun* **4**, 2753, doi:10.1038/ncomms3753 (2013).
- 43 Noda, N. N. & Inagaki, F. Mechanisms of Autophagy. *Annu Rev Biophys* **44**, 101-122, doi:10.1146/annurev-biophys-060414-034248 (2015).
- 44 Dikic, I. & Elazar, Z. Mechanism and medical implications of mammalian autophagy. *Nat Rev Mol Cell Biol* **19**, 349-364, doi:10.1038/s41580-018-0003-4 (2018).
- 45 Levine, B. & Klionsky, D. J. Development by self-digestion: molecular mechanisms and biological functions of autophagy. *Dev Cell* **6**, 463-477, doi:10.1016/s1534-5807(04)00099-1 (2004).
- 46 Glick, D., Barth, S. & Macleod, K. F. Autophagy: cellular and molecular mechanisms. *J Pathol* **221**, 3-12, doi:10.1002/path.2697 (2010).
- 47 de Duve, C. Lysosomes, a new group of cytoplasmic particles. *Subcellular particles* **60**, 128-159 (1959).
- 48 De Duve, C., Pressman, B. C., Gianetto, R., Wattiaux, R. & Appelmans, F. Tissue fractionation studies. 6. Intracellular distribution patterns of enzymes in rat-liver tissue. *Biochem J* **60**, 604-617, doi:10.1042/bj0600604 (1955).
- 49 Takeshige, K., Baba, M., Tsuboi, S., Noda, T. & Ohsumi, Y. Autophagy in yeast demonstrated with proteinase-deficient mutants and conditions for its induction. *J Cell Biol* **119**, 301-311, doi:10.1083/jcb.119.2.301 (1992).
- 50 Baba, M., Takeshige, K., Baba, N. & Ohsumi, Y. Ultrastructural analysis of the autophagic process in yeast: detection of autophagosomes and their characterization. *J Cell Biol* **124**, 903-913, doi:10.1083/jcb.124.6.903 (1994).

- 51 Ohsumi, Y. Historical landmarks of autophagy research. *Cell Res* **24**, 9-23, doi:10.1038/cr.2013.169 (2014).
- 52 Galluzzi, L., Baehrecke, E. H., Ballabio, A., Boya, P., Bravo-San Pedro, J. M., Cecconi, F., Choi, A. M., Chu, C. T., Codogno, P., Colombo, M. I., Cuervo, A. M., Debnath, J., Deretic, V., Dikic, I., Eskelinen, E. L., Fimia, G. M., Fulda, S., Gewirtz, D. A., Green, D. R., Hansen, M., Harper, J. W., Jaattela, M., Johansen, T., Juhasz, G., Kimmelman, A. C., Kraft, C., Ktistakis, N. T., Kumar, S., Levine, B., Lopez-Otin, C., Madeo, F., Martens, S., Martinez, J., Melendez, A., Mizushima, N., Munz, C., Murphy, L. O., Penninger, J. M., Piacentini, M., Reggiori, F., Rubinsztein, D. C., Ryan, K. M., Santambrogio, L., Scorrano, L., Simon, A. K., Simon, H. U., Simonsen, A., Tavernarakis, N., Tooze, S. A., Yoshimori, T., Yuan, J., Yue, Z., Zhong, Q. & Kroemer, G. Molecular definitions of autophagy and related processes. *EMBO J* **36**, 1811-1836, doi:10.15252/embj.201796697 (2017).
- 53 Morishita, H. & Mizushima, N. Diverse Cellular Roles of Autophagy. *Annu Rev Cell Dev Biol* **35**, 453-475, doi:10.1146/annurev-cellbio-100818-125300 (2019).
- 54 Dixon, J. S. "Phagocytic" lysosomes in chromatolytic neurones. *Nature* **215**, 657-658, doi:10.1038/215657a0 (1967).
- 55 Holtzman, E. & Novikoff, A. B. Lysosomes in the rat sciatic nerve following crush. *J Cell Biol* **27**, 651-669, doi:10.1083/jcb.27.3.651 (1965).
- 56 Mizushima, N. & Levine, B. Autophagy in mammalian development and differentiation. *Nat Cell Biol* **12**, 823-830, doi:10.1038/ncb0910-823 (2010).
- 57 Johnson, C. W., Melia, T. J. & Yamamoto, A. Modulating macroautophagy: a neuronal perspective. *Future Med Chem* **4**, 1715-1731, doi:10.4155/fmc.12.112 (2012).
- 58 Mizushima, N., Yoshimori, T. & Ohsumi, Y. The role of Atg proteins in autophagosome formation. *Annu Rev Cell Dev Biol* **27**, 107-132, doi:10.1146/annurev-cellbio-092910-154005 (2011).
- 59 Yu, L., Chen, Y. & Tooze, S. A. Autophagy pathway: Cellular and molecular mechanisms. *Autophagy* **14**, 207-215, doi:10.1080/15548627.2017.1378838 (2018).
- 60 Kaur, J. & Debnath, J. Autophagy at the crossroads of catabolism and anabolism. *Nat Rev Mol Cell Biol* **16**, 461-472, doi:10.1038/nrm4024 (2015).
- 61 Axe, E. L., Walker, S. A., Manifava, M., Chandra, P., Roderick, H. L., Habermann, A., Griffiths, G. & Ktistakis, N. T. Autophagosome formation from membrane compartments enriched in phosphatidylinositol 3-phosphate and dynamically connected to the endoplasmic reticulum. *J Cell Biol* **182**, 685-701, doi:10.1083/jcb.200803137 (2008).
- 62 Ge, L., Melville, D., Zhang, M. & Schekman, R. The ER-Golgi intermediate compartment is a key membrane source for the LC3 lipidation step of autophagosome biogenesis. *Elife* **2**, e00947, doi:10.7554/eLife.00947 (2013).
- 63 Hamasaki, M., Furuta, N., Matsuda, A., Nezu, A., Yamamoto, A., Fujita, N., Oomori, H., Noda, T., Haraguchi, T., Hiraoka, Y., Amano, A. & Yoshimori, T. Autophagosomes form at ER-mitochondria contact sites. *Nature* **495**, 389-393, doi:10.1038/nature11910 (2013).
- 64 Ravikumar, B., Moreau, K., Jahreiss, L., Puri, C. & Rubinsztein, D. C. Plasma membrane contributes to the formation of pre-autophagosomal structures. *Nat Cell Biol* **12**, 747-757, doi:10.1038/ncb2078 (2010).
- 65 Filimonenko, M., Isakson, P., Finley, K. D., Anderson, M., Jeong, H., Melia, T. J., Bartlett, B. J., Myers, K. M., Birkeland, H. C., Lamark, T., Krainc, D., Brech, A., Stenmark, H., Simonsen, A. & Yamamoto, A. The selective macroautophagic degradation of aggregated proteins requires the PI3P-binding protein Alfy. *Mol Cell* **38**, 265-279, doi:10.1016/j.molcel.2010.04.007 (2010).

- 66 Nishimura, T., Kaizuka, T., Cadwell, K., Sahani, M. H., Saitoh, T., Akira, S., Virgin, H. W. & Mizushima, N. FIP200 regulates targeting of Atg16L1 to the isolation membrane. *EMBO Rep* **14**, 284-291, doi:10.1038/embor.2013.6 (2013).
- 67 Kabeya, Y., Mizushima, N., Ueno, T., Yamamoto, A., Kirisako, T., Noda, T., Kominami, E., Ohsumi, Y. & Yoshimori, T. LC3, a mammalian homologue of yeast Apg8p, is localized in autophagosome membranes after processing. *EMBO J* **19**, 5720-5728, doi:10.1093/emboj/19.21.5720 (2000).
- 68 Chakrama, F. Z., Seguin-Py, S., Le Grand, J. N., Fraichard, A., Delage-Mourroux, R., Despouy, G., Perez, V., Jouvenot, M. & Boyer-Guittaut, M. GABARAPL1 (GEC1) associates with autophagic vesicles. *Autophagy* **6**, 495-505, doi:10.4161/auto.6.4.11819 (2010).
- 69 Rusten, T. E., Filimonenko, M., Rodahl, L. M., Stenmark, H. & Simonsen, A. ESCRTing autophagic clearance of aggregating proteins. *Autophagy* **4**, 233-236 (2008).
- 70 Hollenbeck, P. J. Products of endocytosis and autophagy are retrieved from axons by regulated retrograde organelle transport. *J Cell Biol* **121**, 305-315, doi:10.1083/jcb.121.2.305 (1993).
- 71 Maday, S., Wallace, K. E. & Holzbaur, E. L. Autophagosomes initiate distally and mature during transport toward the cell soma in primary neurons. *J Cell Biol* **196**, 407-417, doi:10.1083/jcb.201106120 (2012).
- 72 Yamamoto, A. & Simonsen, A. The elimination of accumulated and aggregated proteins: a role for aggrephagy in neurodegeneration. *Neurobiol Dis* **43**, 17-28, doi:10.1016/j.nbd.2010.08.015 (2011).
- 73 Finkbeiner, S. The Autophagy Lysosomal Pathway and Neurodegeneration. *Cold Spring Harb Perspect Biol* **12**, doi:10.1101/cshperspect.a033993 (2020).
- 74 Kirkin, V., Lamark, T., Sou, Y. S., Bjorkoy, G., Nunn, J. L., Bruun, J. A., Shvets, E., McEwan, D. G., Clausen, T. H., Wild, P., Bilusic, I., Theurillat, J. P., Overvatn, A., Ishii, T., Elazar, Z., Komatsu, M., Dikic, I. & Johansen, T. A role for NBR1 in autophagosomal degradation of ubiquitinated substrates. *Mol Cell* **33**, 505-516, doi:10.1016/j.molcel.2009.01.020 (2009).
- 75 Isakson, P., Holland, P. & Simonsen, A. The role of ALFY in selective autophagy. *Cell Death Differ* **20**, 12-20, doi:10.1038/cdd.2012.66 (2013).
- 76 Han, H., Wei, W., Duan, W., Guo, Y., Li, Y., Wang, J., Bi, Y. & Li, C. Autophagy-linked FYVE protein (Alfy) promotes autophagic removal of misfolded proteins involved in amyotrophic lateral sclerosis (ALS). *In Vitro Cell Dev Biol Anim* **51**, 249-263, doi:10.1007/s11626-014-9832-4 (2015).
- 77 Korac, J., Schaeffer, V., Kovacevic, I., Clement, A. M., Jungblut, B., Behl, C., Terzic, J. & Dikic, I. Ubiquitin-independent function of optineurin in autophagic clearance of protein aggregates. *J Cell Sci* **126**, 580-592, doi:10.1242/jcs.114926 (2013).
- 78 Proenca, C. C., Stoehr, N., Bernhard, M., Seger, S., Genoud, C., Roscic, A., Paganetti, P., Liu, S., Murphy, L. O., Kuhn, R., Bouwmeester, T. & Galimberti, I. Atg4b-dependent autophagic flux alleviates Huntington's disease progression. *PLoS One* **8**, e68357, doi:10.1371/journal.pone.0068357 (2013).
- 79 Switon, K., Kotulska, K., Janusz-Kaminska, A., Zmorzynska, J. & Jaworski, J. Molecular neurobiology of mTOR. *Neuroscience* **341**, 112-153, doi:10.1016/j.neuroscience.2016.11.017 (2017).
- 80 Stavoe, A. K. H. & Holzbaur, E. L. F. Autophagy in Neurons. *Annu Rev Cell Dev Biol* **35**, 477-500, doi:10.1146/annurev-cellbio-100818-125242 (2019).
- 81 Efeyan, A., Zoncu, R. & Sabatini, D. M. Amino acids and mTORC1: from lysosomes to disease. *Trends Mol Med* **18**, 524-533, doi:10.1016/j.molmed.2012.05.007 (2012).

- 82 Mizushima, N., Yamamoto, A., Matsui, M., Yoshimori, T. & Ohsumi, Y. In vivo analysis of autophagy in response to nutrient starvation using transgenic mice expressing a fluorescent autophagosome marker. *Mol Biol Cell* **15**, 1101-1111, doi:10.1091/mbc.e03-09-0704 (2004).
- 83 Munson, M. J. & Ganley, I. G. mTOR, PIK3C3, and autophagy: Signaling the beginning from the end. *Autophagy* **11**, 2375-2376, doi:10.1080/15548627.2015.1106668 (2015).
- 84 Zoncu, R., Efeyan, A. & Sabatini, D. M. mTOR: from growth signal integration to cancer, diabetes and ageing. *Nat Rev Mol Cell Biol* **12**, 21-35, doi:10.1038/nrm3025 (2011).
- 85 Mortimore, G. E., Poso, A. R. & Lardeux, B. R. Mechanism and regulation of protein degradation in liver. *Diabetes Metab Rev* **5**, 49-70, doi:10.1002/dmr.5610050105 (1989).
- 86 Seglen, P. O. & Bohley, P. Autophagy and other vacuolar protein degradation mechanisms. *Experientia* **48**, 158-172, doi:10.1007/BF01923509 (1992).
- 87 Goodman, M. N., Lowell, B., Belur, E. & Ruderman, N. B. Sites of protein conservation and loss during starvation: influence of adiposity. *Am J Physiol* **246**, E383-390, doi:10.1152/ajpendo.1984.246.5.E383 (1984).
- 88 Mizushima, N., Yoshimori, T. & Levine, B. Methods in mammalian autophagy research. *Cell* **140**, 313-326, doi:10.1016/j.cell.2010.01.028 (2010).
- 89 Hara, T., Nakamura, K., Matsui, M., Yamamoto, A., Nakahara, Y., Suzuki-Migishima, R., Yokoyama, M., Mishima, K., Saito, I., Okano, H. & Mizushima, N. Suppression of basal autophagy in neural cells causes neurodegenerative disease in mice. *Nature* **441**, 885-889, doi:10.1038/nature04724 (2006).
- 90 Komatsu, M., Waguri, S., Chiba, T., Murata, S., Iwata, J., Tanida, I., Ueno, T., Koike, M., Uchiyama, Y., Kominami, E. & Tanaka, K. Loss of autophagy in the central nervous system causes neurodegeneration in mice. *Nature* **441**, 880-884, doi:10.1038/nature04723 (2006).
- 91 Komatsu, M., Waguri, S., Koike, M., Sou, Y. S., Ueno, T., Hara, T., Mizushima, N., Iwata, J., Ezaki, J., Murata, S., Hamazaki, J., Nishito, Y., Iemura, S., Natsume, T., Yanagawa, T., Uwayama, J., Warabi, E., Yoshida, H., Ishii, T., Kobayashi, A., Yamamoto, M., Yue, Z., Uchiyama, Y., Kominami, E. & Tanaka, K. Homeostatic levels of p62 control cytoplasmic inclusion body formation in autophagy-deficient mice. *Cell* **131**, 1149-1163, doi:10.1016/j.cell.2007.10.035 (2007).
- 92 Chen, Y., Sawada, O., Kohno, H., Le, Y. Z., Subauste, C., Maeda, T. & Maeda, A. Autophagy protects the retina from light-induced degeneration. *J Biol Chem* **288**, 7506-7518, doi:10.1074/jbc.M112.439935 (2013).
- 93 Zhou, Z., Doggett, T. A., Sene, A., Apte, R. S. & Ferguson, T. A. Autophagy supports survival and phototransduction protein levels in rod photoreceptors. *Cell Death Differ* **22**, 488-498, doi:10.1038/cdd.2014.229 (2015).
- 94 Pyo, J. O., Yoo, S. M., Ahn, H. H., Nah, J., Hong, S. H., Kam, T. I., Jung, S. & Jung, Y. K. Overexpression of Atg5 in mice activates autophagy and extends lifespan. *Nat Commun* **4**, 2300, doi:10.1038/ncomms3300 (2013).
- 95 Fernandez, A. F., Sebt, S., Wei, Y., Zou, Z., Shi, M., McMillan, K. L., He, C., Ting, T., Liu, Y., Chiang, W. C., Marciano, D. K., Schiattarella, G. G., Bhagat, G., Moe, O. W., Hu, M. C. & Levine, B. Disruption of the beclin 1-BCL2 autophagy regulatory complex promotes longevity in mice. *Nature* **558**, 136-140, doi:10.1038/s41586-018-0162-7 (2018).
- 96 Yoshii, S. R., Kuma, A., Akashi, T., Hara, T., Yamamoto, A., Kurikawa, Y., Itakura, E., Tsukamoto, S., Shitara, H., Eishi, Y. & Mizushima, N. Systemic Analysis of Atg5-

- Null Mice Rescued from Neonatal Lethality by Transgenic ATG5 Expression in Neurons. *Dev Cell* **39**, 116-130, doi:10.1016/j.devcel.2016.09.001 (2016).
- 97 Wang, C., Liang, C. C., Bian, Z. C., Zhu, Y. & Guan, J. L. FIP200 is required for maintenance and differentiation of postnatal neural stem cells. *Nat Neurosci* **16**, 532-542, doi:10.1038/nn.3365 (2013).
- 98 Yazdankhah, M., Farioli-Vecchioli, S., Tonchev, A. B., Stoykova, A. & Cecconi, F. The autophagy regulators Ambra1 and Beclin 1 are required for adult neurogenesis in the brain subventricular zone. *Cell Death Dis* **5**, e1403, doi:10.1038/cddis.2014.358 (2014).
- 99 Gage, F. H. Mammalian neural stem cells. *Science* **287**, 1433-1438 (2000).
- 100 Xi, Y., Dhaliwal, J. S., Ceizar, M., Vaculik, M., Kumar, K. L. & Lagace, D. C. Knockout of Atg5 delays the maturation and reduces the survival of adult-generated neurons in the hippocampus. *Cell Death Dis* **7**, e2127, doi:10.1038/cddis.2015.406 (2016).
- 101 Hansen, M., Chandra, A., Mitic, L. L., Onken, B., Driscoll, M. & Kenyon, C. A role for autophagy in the extension of lifespan by dietary restriction in *C. elegans*. *PLoS Genet* **4**, e24, doi:10.1371/journal.pgen.0040024 (2008).
- 102 Palikaras, K., Lionaki, E. & Tavernarakis, N. Coordination of mitophagy and mitochondrial biogenesis during ageing in *C. elegans*. *Nature* **521**, 525-528, doi:10.1038/nature14300 (2015).
- 103 Simonsen, A., Cumming, R. C., Brech, A., Isakson, P., Schubert, D. R. & Finley, K. D. Promoting basal levels of autophagy in the nervous system enhances longevity and oxidant resistance in adult *Drosophila*. *Autophagy* **4**, 176-184 (2008).
- 104 Zheng, S., Clabough, E. B., Sarkar, S., Futter, M., Rubinsztein, D. C. & Zeitlin, S. O. Deletion of the huntingtin polyglutamine stretch enhances neuronal autophagy and longevity in mice. *PLoS Genet* **6**, e1000838, doi:10.1371/journal.pgen.1000838 (2010).
- 105 Menzies, F. M., Fleming, A., Caricasole, A., Bento, C. F., Andrews, S. P., Ashkenazi, A., Fullgrabe, J., Jackson, A., Jimenez Sanchez, M., Karabiyik, C., Licitra, F., Lopez Ramirez, A., Pavel, M., Puri, C., Renna, M., Ricketts, T., Schlotawa, L., Vicinanza, M., Won, H., Zhu, Y., Skidmore, J. & Rubinsztein, D. C. Autophagy and Neurodegeneration: Pathogenic Mechanisms and Therapeutic Opportunities. *Neuron* **93**, 1015-1034, doi:10.1016/j.neuron.2017.01.022 (2017).
- 106 Nixon, R. A. The role of autophagy in neurodegenerative disease. *Nat Med* **19**, 983-997, doi:10.1038/nm.3232 (2013).
- 107 Mizushima, N. & Levine, B. Autophagy in Human Diseases. *N Engl J Med* **383**, 1564-1576, doi:10.1056/NEJMra2022774 (2020).
- 108 Park, H., Kang, J. H. & Lee, S. Autophagy in Neurodegenerative Diseases: A Hunter for Aggregates. *Int J Mol Sci* **21**, doi:10.3390/ijms21093369 (2020).
- 109 Wong, E. & Cuervo, A. M. Autophagy gone awry in neurodegenerative diseases. *Nat Neurosci* **13**, 805-811, doi:10.1038/nn.2575 (2010).
- 110 Guo, F., Liu, X., Cai, H. & Le, W. Autophagy in neurodegenerative diseases: pathogenesis and therapy. *Brain Pathol* **28**, 3-13, doi:10.1111/bpa.12545 (2018).
- 111 Nixon, R. A. & Yang, D. S. Autophagy failure in Alzheimer's disease--locating the primary defect. *Neurobiol Dis* **43**, 38-45, doi:10.1016/j.nbd.2011.01.021 (2011).
- 112 Boland, B., Kumar, A., Lee, S., Platt, F. M., Wegiel, J., Yu, W. H. & Nixon, R. A. Autophagy induction and autophagosome clearance in neurons: relationship to autophagic pathology in Alzheimer's disease. *J Neurosci* **28**, 6926-6937, doi:10.1523/JNEUROSCI.0800-08.2008 (2008).
- 113 Spilman, P., Podlitskaya, N., Hart, M. J., Debnath, J., Gorostiza, O., Bredesen, D., Richardson, A., Strong, R. & Galvan, V. Inhibition of mTOR by rapamycin abolishes

- cognitive deficits and reduces amyloid-beta levels in a mouse model of Alzheimer's disease. *PLoS One* **5**, e9979, doi:10.1371/journal.pone.0009979 (2010).
- 114 Tian, Y., Bustos, V., Flajolet, M. & Greengard, P. A small-molecule enhancer of autophagy decreases levels of Aβ and APP-CTF via Atg5-dependent autophagy pathway. *FASEB J* **25**, 1934-1942, doi:10.1096/fj.10-175158 (2011).
- 115 Vingtdeux, V., Chandakkar, P., Zhao, H., d'Abramo, C., Davies, P. & Marambaud, P. Novel synthetic small-molecule activators of AMPK as enhancers of autophagy and amyloid-beta peptide degradation. *FASEB J* **25**, 219-231, doi:10.1096/fj.10-167361 (2011).
- 116 Yu, W. H., Cuervo, A. M., Kumar, A., Peterhoff, C. M., Schmidt, S. D., Lee, J. H., Mohan, P. S., Mercken, M., Farmery, M. R., Tjernberg, L. O., Jiang, Y., Duff, K., Uchiyama, Y., Naslund, J., Mathews, P. M., Cataldo, A. M. & Nixon, R. A. Macroautophagy--a novel Beta-amyloid peptide-generating pathway activated in Alzheimer's disease. *J Cell Biol* **171**, 87-98, doi:10.1083/jcb.200505082 (2005).
- 117 Nilsson, P., Loganathan, K., Sekiguchi, M., Matsuba, Y., Hui, K., Tsubuki, S., Tanaka, M., Iwata, N., Saito, T. & Saido, T. C. Aβ secretion and plaque formation depend on autophagy. *Cell Rep* **5**, 61-69, doi:10.1016/j.celrep.2013.08.042 (2013).
- 118 Harold, D., Abraham, R., Hollingworth, P., Sims, R., Gerrish, A., Hamshere, M. L., Pahwa, J. S., Moskvina, V., Dowzell, K., Williams, A., Jones, N., Thomas, C., Stretton, A., Morgan, A. R., Lovestone, S., Powell, J., Proitsi, P., Lupton, M. K., Brayne, C., Rubinsztein, D. C., Gill, M., Lawlor, B., Lynch, A., Morgan, K., Brown, K. S., Passmore, P. A., Craig, D., McGuinness, B., Todd, S., Holmes, C., Mann, D., Smith, A. D., Love, S., Kehoe, P. G., Hardy, J., Mead, S., Fox, N., Rossor, M., Collinge, J., Maier, W., Jessen, F., Schurmann, B., Heun, R., van den Bussche, H., Heuser, I., Kornhuber, J., Wiltfang, J., Dichgans, M., Frolich, L., Hampel, H., Hull, M., Rujescu, D., Goate, A. M., Kauwe, J. S., Cruchaga, C., Nowotny, P., Morris, J. C., Mayo, K., Sleegers, K., Bettens, K., Engelborghs, S., De Deyn, P. P., Van Broeckhoven, C., Livingston, G., Bass, N. J., Gurling, H., McQuillin, A., Gwilliam, R., Deloukas, P., Al-Chalabi, A., Shaw, C. E., Tsolaki, M., Singleton, A. B., Guerreiro, R., Muhleisen, T. W., Nothen, M. M., Moebus, S., Jockel, K. H., Klopp, N., Wichmann, H. E., Carrasquillo, M. M., Pankratz, V. S., Younkin, S. G., Holmans, P. A., O'Donovan, M., Owen, M. J. & Williams, J. Genome-wide association study identifies variants at *CLU* and *PICALM* associated with Alzheimer's disease. *Nat Genet* **41**, 1088-1093, doi:10.1038/ng.440 (2009).
- 119 Jun, G., Naj, A. C., Beecham, G. W., Wang, L. S., Buross, J., Gallins, P. J., Buxbaum, J. D., Ertekin-Taner, N., Fallin, M. D., Friedland, R., Inzelberg, R., Kramer, P., Rogava, E., St George-Hyslop, P., Alzheimer's Disease Genetics, C., Cantwell, L. B., Dombroski, B. A., Saykin, A. J., Reiman, E. M., Bennett, D. A., Morris, J. C., Lunetta, K. L., Martin, E. R., Montine, T. J., Goate, A. M., Blacker, D., Tsuang, D. W., Beekly, D., Cupples, L. A., Hakonarson, H., Kukull, W., Foroud, T. M., Haines, J., Mayeux, R., Farrer, L. A., Pericak-Vance, M. A. & Schellenberg, G. D. Meta-analysis confirms *CR1*, *CLU*, and *PICALM* as Alzheimer disease risk loci and reveals interactions with *APOE* genotypes. *Arch Neurol* **67**, 1473-1484, doi:10.1001/archneurol.2010.201 (2010).
- 120 Ando, K., Brion, J. P., Stygelbout, V., Suain, V., Authelet, M., Dedecker, R., Chanut, A., Lacor, P., Lavaur, J., Sazdovitch, V., Rogava, E., Potier, M. C. & Duyckaerts, C. Clathrin adaptor *CALM/PICALM* is associated with neurofibrillary tangles and is cleaved in Alzheimer's brains. *Acta Neuropathol* **125**, 861-878, doi:10.1007/s00401-013-1111-z (2013).

- 121 Ando, K., Tomimura, K., Sazdovitch, V., Suain, V., Yilmaz, Z., Authelet, M., Ndjim, M., Vergara, C., Belkouch, M., Potier, M. C., Duyckaerts, C. & Brion, J. P. Level of PICALM, a key component of clathrin-mediated endocytosis, is correlated with levels of phosphotau and autophagy-related proteins and is associated with tau inclusions in AD, PSP and Pick disease. *Neurobiol Dis* **94**, 32-43, doi:10.1016/j.nbd.2016.05.017 (2016).
- 122 Moreau, K., Fleming, A., Imarisio, S., Lopez Ramirez, A., Mercer, J. L., Jimenez-Sanchez, M., Bento, C. F., Puri, C., Zavodszky, E., Siddiqi, F., Lavau, C. P., Betton, M., O'Kane, C. J., Wechsler, D. S. & Rubinsztein, D. C. PICALM modulates autophagy activity and tau accumulation. *Nat Commun* **5**, 4998, doi:10.1038/ncomms5998 (2014).
- 123 Tian, Y., Chang, J. C., Fan, E. Y., Flajolet, M. & Greengard, P. Adaptor complex AP2/PICALM, through interaction with LC3, targets Alzheimer's APP-CTF for terminal degradation via autophagy. *Proc Natl Acad Sci U S A* **110**, 17071-17076, doi:10.1073/pnas.1315110110 (2013).
- 124 Metcalf, D. J., Garcia-Arencibia, M., Hochfeld, W. E. & Rubinsztein, D. C. Autophagy and misfolded proteins in neurodegeneration. *Exp Neurol* **238**, 22-28, doi:10.1016/j.expneurol.2010.11.003 (2012).
- 125 Citron, M., Westaway, D., Xia, W., Carlson, G., Diehl, T., Levesque, G., Johnson-Wood, K., Lee, M., Seubert, P., Davis, A., Kholodenko, D., Motter, R., Sherrington, R., Perry, B., Yao, H., Strome, R., Lieberburg, I., Rommens, J., Kim, S., Schenk, D., Fraser, P., St George Hyslop, P. & Selkoe, D. J. Mutant presenilins of Alzheimer's disease increase production of 42-residue amyloid beta-protein in both transfected cells and transgenic mice. *Nat Med* **3**, 67-72, doi:10.1038/nm0197-67 (1997).
- 126 Coffey, E. E., Beckel, J. M., Laties, A. M. & Mitchell, C. H. Lysosomal alkalization and dysfunction in human fibroblasts with the Alzheimer's disease-linked presenilin 1 A246E mutation can be reversed with cAMP. *Neuroscience* **263**, 111-124, doi:10.1016/j.neuroscience.2014.01.001 (2014).
- 127 Lee, J. H., Yu, W. H., Kumar, A., Lee, S., Mohan, P. S., Peterhoff, C. M., Wolfe, D. M., Martinez-Vicente, M., Massey, A. C., Sovak, G., Uchiyama, Y., Westaway, D., Cuervo, A. M. & Nixon, R. A. Lysosomal proteolysis and autophagy require presenilin 1 and are disrupted by Alzheimer-related PS1 mutations. *Cell* **141**, 1146-1158, doi:10.1016/j.cell.2010.05.008 (2010).
- 128 Wolfe, D. M., Lee, J. H., Kumar, A., Lee, S., Orenstein, S. J. & Nixon, R. A. Autophagy failure in Alzheimer's disease and the role of defective lysosomal acidification. *Eur J Neurosci* **37**, 1949-1961, doi:10.1111/ejn.12169 (2013).
- 129 Pickford, F., Masliah, E., Britschgi, M., Lucin, K., Narasimhan, R., Jaeger, P. A., Small, S., Spencer, B., Rockenstein, E., Levine, B. & Wyss-Coray, T. The autophagy-related protein beclin 1 shows reduced expression in early Alzheimer disease and regulates amyloid beta accumulation in mice. *J Clin Invest* **118**, 2190-2199, doi:10.1172/JCI33585 (2008).
- 130 Rohn, T. T., Wirawan, E., Brown, R. J., Harris, J. R., Masliah, E. & Vandenabeele, P. Depletion of Beclin-1 due to proteolytic cleavage by caspases in the Alzheimer's disease brain. *Neurobiol Dis* **43**, 68-78, doi:10.1016/j.nbd.2010.11.003 (2011).
- 131 Lee, V. M., Goedert, M. & Trojanowski, J. Q. Neurodegenerative tauopathies. *Annu Rev Neurosci* **24**, 1121-1159, doi:10.1146/annurev.neuro.24.1.1121 (2001).
- 132 Piras, A., Collin, L., Gruninger, F., Graff, C. & Ronnback, A. Autophagic and lysosomal defects in human tauopathies: analysis of post-mortem brain from patients with familial Alzheimer disease, corticobasal degeneration and progressive supranuclear palsy. *Acta Neuropathol Commun* **4**, 22, doi:10.1186/s40478-016-0292-9 (2016).

- 133 Butzlaff, M., Hannan, S. B., Karsten, P., Lenz, S., Ng, J., Vossfeldt, H., Prussing, K., Pflanz, R., Schulz, J. B., Rasse, T. & Voigt, A. Impaired retrograde transport by the Dynein/Dynactin complex contributes to Tau-induced toxicity. *Hum Mol Genet* **24**, 3623-3637, doi:10.1093/hmg/ddv107 (2015).
- 134 Majid, T., Ali, Y. O., Venkitaramani, D. V., Jang, M. K., Lu, H. C. & Pautler, R. G. In vivo axonal transport deficits in a mouse model of fronto-temporal dementia. *Neuroimage Clin* **4**, 711-717, doi:10.1016/j.nicl.2014.02.005 (2014).
- 135 Collin, L., Bohrmann, B., Gopfert, U., Oroszlan-Szovik, K., Ozmen, L. & Gruninger, F. Neuronal uptake of tau/pS422 antibody and reduced progression of tau pathology in a mouse model of Alzheimer's disease. *Brain* **137**, 2834-2846, doi:10.1093/brain/awu213 (2014).
- 136 Wang, Y., Martinez-Vicente, M., Kruger, U., Kaushik, S., Wong, E., Mandelkow, E. M., Cuervo, A. M. & Mandelkow, E. Tau fragmentation, aggregation and clearance: the dual role of lysosomal processing. *Hum Mol Genet* **18**, 4153-4170, doi:10.1093/hmg/ddp367 (2009).
- 137 Nixon, R. A., Wegiel, J., Kumar, A., Yu, W. H., Peterhoff, C., Cataldo, A. & Cuervo, A. M. Extensive involvement of autophagy in Alzheimer disease: an immuno-electron microscopy study. *J Neuropathol Exp Neurol* **64**, 113-122, doi:10.1093/jnen/64.2.113 (2005).
- 138 Li, L., Zhang, X. & Le, W. Autophagy dysfunction in Alzheimer's disease. *Neurodegener Dis* **7**, 265-271, doi:10.1159/000276710 (2010).
- 139 Rubinsztein, D. C., Marino, G. & Kroemer, G. Autophagy and aging. *Cell* **146**, 682-695, doi:10.1016/j.cell.2011.07.030 (2011).
- 140 Singh, A. K., Kashyap, M. P., Tripathi, V. K., Singh, S., Garg, G. & Rizvi, S. I. Neuroprotection Through Rapamycin-Induced Activation of Autophagy and PI3K/Akt1/mTOR/CREB Signaling Against Amyloid-beta-Induced Oxidative Stress, Synaptic/Neurotransmission Dysfunction, and Neurodegeneration in Adult Rats. *Mol Neurobiol* **54**, 5815-5828, doi:10.1007/s12035-016-0129-3 (2017).
- 141 Caccamo, A., De Pinto, V., Messina, A., Branca, C. & Oddo, S. Genetic reduction of mammalian target of rapamycin ameliorates Alzheimer's disease-like cognitive and pathological deficits by restoring hippocampal gene expression signature. *J Neurosci* **34**, 7988-7998, doi:10.1523/JNEUROSCI.0777-14.2014 (2014).
- 142 Kruger, U., Wang, Y., Kumar, S. & Mandelkow, E. M. Autophagic degradation of tau in primary neurons and its enhancement by trehalose. *Neurobiol Aging* **33**, 2291-2305, doi:10.1016/j.neurobiolaging.2011.11.009 (2012).
- 143 Liu, R., Barkhordarian, H., Emadi, S., Park, C. B. & Sierks, M. R. Trehalose differentially inhibits aggregation and neurotoxicity of beta-amyloid 40 and 42. *Neurobiol Dis* **20**, 74-81, doi:10.1016/j.nbd.2005.02.003 (2005).
- 144 Kalia, L. V. & Lang, A. E. Parkinson's disease. *Lancet* **386**, 896-912, doi:10.1016/S0140-6736(14)61393-3 (2015).
- 145 Tanik, S. A., Schultheiss, C. E., Volpicelli-Daley, L. A., Brunden, K. R. & Lee, V. M. Lewy body-like alpha-synuclein aggregates resist degradation and impair macroautophagy. *J Biol Chem* **288**, 15194-15210, doi:10.1074/jbc.M113.457408 (2013).
- 146 Volpicelli-Daley, L. A., Gamble, K. L., Schultheiss, C. E., Riddle, D. M., West, A. B. & Lee, V. M. Formation of alpha-synuclein Lewy neurite-like aggregates in axons impedes the transport of distinct endosomes. *Mol Biol Cell* **25**, 4010-4023, doi:10.1091/mbc.E14-02-0741 (2014).
- 147 Winslow, A. R., Chen, C. W., Corrochano, S., Acevedo-Arozena, A., Gordon, D. E., Peden, A. A., Lichtenberg, M., Menzies, F. M., Ravikumar, B., Imarisio, S., Brown, S.,

- O'Kane, C. J. & Rubinsztein, D. C. alpha-Synuclein impairs macroautophagy: implications for Parkinson's disease. *J Cell Biol* **190**, 1023-1037, doi:10.1083/jcb.201003122 (2010).
- 148 Zavodszky, E., Seaman, M. N., Moreau, K., Jimenez-Sanchez, M., Breusegem, S. Y., Harbour, M. E. & Rubinsztein, D. C. Mutation in VPS35 associated with Parkinson's disease impairs WASH complex association and inhibits autophagy. *Nat Commun* **5**, 3828, doi:10.1038/ncomms4828 (2014).
- 149 Cerri, S. & Blandini, F. Role of Autophagy in Parkinson's Disease. *Curr Med Chem* **26**, 3702-3718, doi:10.2174/0929867325666180226094351 (2019).
- 150 Valente, E. M., Abou-Sleiman, P. M., Caputo, V., Muqit, M. M., Harvey, K., Gispert, S., Ali, Z., Del Turco, D., Bentivoglio, A. R., Healy, D. G., Albanese, A., Nussbaum, R., Gonzalez-Maldonado, R., Deller, T., Salvi, S., Cortelli, P., Gilks, W. P., Latchman, D. S., Harvey, R. J., Dallapiccola, B., Auburger, G. & Wood, N. W. Hereditary early-onset Parkinson's disease caused by mutations in PINK1. *Science* **304**, 1158-1160, doi:10.1126/science.1096284 (2004).
- 151 Kitada, T., Asakawa, S., Hattori, N., Matsumine, H., Yamamura, Y., Minoshima, S., Yokochi, M., Mizuno, Y. & Shimizu, N. Mutations in the parkin gene cause autosomal recessive juvenile parkinsonism. *Nature* **392**, 605-608, doi:10.1038/33416 (1998).
- 152 Matsuda, N., Sato, S., Shiba, K., Okatsu, K., Saisho, K., Gautier, C. A., Sou, Y. S., Saiki, S., Kawajiri, S., Sato, F., Kimura, M., Komatsu, M., Hattori, N. & Tanaka, K. PINK1 stabilized by mitochondrial depolarization recruits Parkin to damaged mitochondria and activates latent Parkin for mitophagy. *J Cell Biol* **189**, 211-221, doi:10.1083/jcb.200910140 (2010).
- 153 Narendra, D., Tanaka, A., Suen, D. F. & Youle, R. J. Parkin is recruited selectively to impaired mitochondria and promotes their autophagy. *J Cell Biol* **183**, 795-803, doi:10.1083/jcb.200809125 (2008).
- 154 Goldberg, M. S., Fleming, S. M., Palacino, J. J., Cepeda, C., Lam, H. A., Bhatnagar, A., Meloni, E. G., Wu, N., Ackerson, L. C., Klapstein, G. J., Gajendiran, M., Roth, B. L., Chesselet, M. F., Maidment, N. T., Levine, M. S. & Shen, J. Parkin-deficient mice exhibit nigrostriatal deficits but not loss of dopaminergic neurons. *J Biol Chem* **278**, 43628-43635, doi:10.1074/jbc.M308947200 (2003).
- 155 Itier, J. M., Ibanez, P., Mena, M. A., Abbas, N., Cohen-Salmon, C., Bohme, G. A., Laville, M., Pratt, J., Corti, O., Pradier, L., Ret, G., Joubert, C., Periquet, M., Araujo, F., Negroni, J., Casarejos, M. J., Canals, S., Solano, R., Serrano, A., Gallego, E., Sanchez, M., Deneffe, P., Benavides, J., Tremp, G., Rooney, T. A., Brice, A. & Garcia de Yébenes, J. Parkin gene inactivation alters behaviour and dopamine neurotransmission in the mouse. *Hum Mol Genet* **12**, 2277-2291, doi:10.1093/hmg/ddg239 (2003).
- 156 Perez, F. A. & Palmiter, R. D. Parkin-deficient mice are not a robust model of parkinsonism. *Proc Natl Acad Sci U S A* **102**, 2174-2179, doi:10.1073/pnas.0409598102 (2005).
- 157 Palacino, J. J., Sagi, D., Goldberg, M. S., Krauss, S., Motz, C., Wacker, M., Klose, J. & Shen, J. Mitochondrial dysfunction and oxidative damage in parkin-deficient mice. *J Biol Chem* **279**, 18614-18622, doi:10.1074/jbc.M401135200 (2004).
- 158 Shim, J. H., Yoon, S. H., Kim, K. H., Han, J. Y., Ha, J. Y., Hyun, D. H., Paek, S. H., Kang, U. J., Zhuang, X. & Son, J. H. The antioxidant Trolox helps recovery from the familial Parkinson's disease-specific mitochondrial deficits caused by PINK1- and DJ-1-deficiency in dopaminergic neuronal cells. *Mitochondrion* **11**, 707-715, doi:10.1016/j.mito.2011.05.013 (2011).

- 159 Michiorri, S., Gelmetti, V., Giarda, E., Lombardi, F., Romano, F., Marongiu, R., Nerini-Molteni, S., Sale, P., Vago, R., Arena, G., Torosantucci, L., Cassina, L., Russo, M. A., Dallapiccola, B., Valente, E. M. & Casari, G. The Parkinson-associated protein PINK1 interacts with Beclin1 and promotes autophagy. *Cell Death Differ* **17**, 962-974, doi:10.1038/cdd.2009.200 (2010).
- 160 Arena, G., Gelmetti, V., Torosantucci, L., Vignone, D., Lamorte, G., De Rosa, P., Cilia, E., Jonas, E. A. & Valente, E. M. PINK1 protects against cell death induced by mitochondrial depolarization, by phosphorylating Bcl-xL and impairing its pro-apoptotic cleavage. *Cell Death Differ* **20**, 920-930, doi:10.1038/cdd.2013.19 (2013).
- 161 Ramirez, A., Heimbach, A., Grundemann, J., Stiller, B., Hampshire, D., Cid, L. P., Goebel, I., Mubaidin, A. F., Wriekat, A. L., Roeper, J., Al-Din, A., Hillmer, A. M., Karsak, M., Liss, B., Woods, C. G., Behrens, M. I. & Kubisch, C. Hereditary parkinsonism with dementia is caused by mutations in ATP13A2, encoding a lysosomal type 5 P-type ATPase. *Nat Genet* **38**, 1184-1191, doi:10.1038/ng1884 (2006).
- 162 Dehay, B., Ramirez, A., Martinez-Vicente, M., Perier, C., Canron, M. H., Doudnikoff, E., Vital, A., Vila, M., Klein, C. & Bezdard, E. Loss of P-type ATPase ATP13A2/PARK9 function induces general lysosomal deficiency and leads to Parkinson disease neurodegeneration. *Proc Natl Acad Sci U S A* **109**, 9611-9616, doi:10.1073/pnas.1112368109 (2012).
- 163 Bento, C. F., Ashkenazi, A., Jimenez-Sanchez, M. & Rubinsztein, D. C. The Parkinson's disease-associated genes ATP13A2 and SYT11 regulate autophagy via a common pathway. *Nat Commun* **7**, 11803, doi:10.1038/ncomms11803 (2016).
- 164 Cabreira, V. & Massano, J. [Parkinson's Disease: Clinical Review and Update]. *Acta Med Port* **32**, 661-670, doi:10.20344/amp.11978 (2019).
- 165 Kim, C. Y. & Alcalay, R. N. Genetic Forms of Parkinson's Disease. *Semin Neurol* **37**, 135-146, doi:10.1055/s-0037-1601567 (2017).
- 166 Choubey, V., Safiulina, D., Vaarmann, A., Cagalinec, M., Wareski, P., Kuun, M., Zharkovsky, A. & Kaasik, A. Mutant A53T alpha-synuclein induces neuronal death by increasing mitochondrial autophagy. *J Biol Chem* **286**, 10814-10824, doi:10.1074/jbc.M110.132514 (2011).
- 167 van Es, M. A., Hardiman, O., Chio, A., Al-Chalabi, A., Pasterkamp, R. J., Veldink, J. H. & van den Berg, L. H. Amyotrophic lateral sclerosis. *Lancet* **390**, 2084-2098, doi:10.1016/S0140-6736(17)31287-4 (2017).
- 168 Hulisz, D. Amyotrophic lateral sclerosis: disease state overview. *Am J Manag Care* **24**, S320-S326 (2018).
- 169 Hardiman, O., Al-Chalabi, A., Chio, A., Corr, E. M., Logroscino, G., Robberecht, W., Shaw, P. J., Simmons, Z. & van den Berg, L. H. Amyotrophic lateral sclerosis. *Nat Rev Dis Primers* **3**, 17071, doi:10.1038/nrdp.2017.71 (2017).
- 170 Brown, R. H. & Al-Chalabi, A. Amyotrophic Lateral Sclerosis. *N Engl J Med* **377**, 162-172, doi:10.1056/NEJMra1603471 (2017).
- 171 Ralli, M., Lambiase, A., Artico, M., de Vincentiis, M. & Greco, A. Amyotrophic Lateral Sclerosis: Autoimmune Pathogenic Mechanisms, Clinical Features, and Therapeutic Perspectives. *Isr Med Assoc J* **21**, 438-443 (2019).
- 172 Nguyen, D. K. H., Thombre, R. & Wang, J. Autophagy as a common pathway in amyotrophic lateral sclerosis. *Neurosci Lett* **697**, 34-48, doi:10.1016/j.neulet.2018.04.006 (2019).
- 173 Blokhuis, A. M., Groen, E. J., Koppers, M., van den Berg, L. H. & Pasterkamp, R. J. Protein aggregation in amyotrophic lateral sclerosis. *Acta Neuropathol* **125**, 777-794, doi:10.1007/s00401-013-1125-6 (2013).

- 174 Morimoto, N., Nagai, M., Ohta, Y., Miyazaki, K., Kurata, T., Morimoto, M., Murakami, T., Takehisa, Y., Ikeda, Y., Kamiya, T. & Abe, K. Increased autophagy in transgenic mice with a G93A mutant SOD1 gene. *Brain Res* **1167**, 112-117, doi:10.1016/j.brainres.2007.06.045 (2007).
- 175 Zhang, X., Li, L., Chen, S., Yang, D., Wang, Y., Zhang, X., Wang, Z. & Le, W. Rapamycin treatment augments motor neuron degeneration in SOD1(G93A) mouse model of amyotrophic lateral sclerosis. *Autophagy* **7**, 412-425, doi:10.4161/auto.7.4.14541 (2011).
- 176 Nassif, M., Valenzuela, V., Rojas-Rivera, D., Vidal, R., Matus, S., Castillo, K., Fuentealba, Y., Kroemer, G., Levine, B. & Hetz, C. Pathogenic role of BECN1/Beclin 1 in the development of amyotrophic lateral sclerosis. *Autophagy* **10**, 1256-1271, doi:10.4161/auto.28784 (2014).
- 177 Chen, Y., Liu, H., Guan, Y., Wang, Q., Zhou, F., Jie, L., Ju, J., Pu, L., Du, H. & Wang, X. The altered autophagy mediated by TFEB in animal and cell models of amyotrophic lateral sclerosis. *Am J Transl Res* **7**, 1574-1587 (2015).
- 178 Zhang, X., Chen, S., Song, L., Tang, Y., Shen, Y., Jia, L. & Le, W. MTOR-independent, autophagic enhancer trehalose prolongs motor neuron survival and ameliorates the autophagic flux defect in a mouse model of amyotrophic lateral sclerosis. *Autophagy* **10**, 588-602, doi:10.4161/auto.27710 (2014).
- 179 Castillo, K., Nassif, M., Valenzuela, V., Rojas, F., Matus, S., Mercado, G., Court, F. A., van Zundert, B. & Hetz, C. Trehalose delays the progression of amyotrophic lateral sclerosis by enhancing autophagy in motoneurons. *Autophagy* **9**, 1308-1320, doi:10.4161/auto.25188 (2013).
- 180 Wang, I. F., Guo, B. S., Liu, Y. C., Wu, C. C., Yang, C. H., Tsai, K. J. & Shen, C. K. Autophagy activators rescue and alleviate pathogenesis of a mouse model with proteinopathies of the TAR DNA-binding protein 43. *Proc Natl Acad Sci U S A* **109**, 15024-15029, doi:10.1073/pnas.1206362109 (2012).
- 181 Farg, M. A., Sundaramoorthy, V., Sultana, J. M., Yang, S., Atkinson, R. A. K., Levina, V., Halloran, M. A., Gleeson, P. A., Blair, I. P., Soo, K. Y., King, A. E. & Atkin, J. D. C9ORF72, implicated in amyotrophic lateral sclerosis and frontotemporal dementia, regulates endosomal trafficking. *Hum Mol Genet* **26**, 4093-4094, doi:10.1093/hmg/ddx309 (2017).
- 182 Teuling, E., van Dis, V., Wulf, P. S., Haasdijk, E. D., Akhmanova, A., Hoogenraad, C. C. & Jaarsma, D. A novel mouse model with impaired dynein/dynactin function develops amyotrophic lateral sclerosis (ALS)-like features in motor neurons and improves lifespan in SOD1-ALS mice. *Hum Mol Genet* **17**, 2849-2862, doi:10.1093/hmg/ddn182 (2008).
- 183 Ikenaka, K., Kawai, K., Katsuno, M., Huang, Z., Jiang, Y. M., Iguchi, Y., Kobayashi, K., Kimata, T., Waza, M., Tanaka, F., Mori, I. & Sobue, G. dnc-1/dynactin 1 knockdown disrupts transport of autophagosomes and induces motor neuron degeneration. *PLoS One* **8**, e54511, doi:10.1371/journal.pone.0054511 (2013).
- 184 Rumpfolt, J. A., Lepock, J. R. & Meiering, E. M. Unfolding and folding kinetics of amyotrophic lateral sclerosis-associated mutant Cu,Zn superoxide dismutases. *J Mol Biol* **385**, 278-298, doi:10.1016/j.jmb.2008.10.003 (2009).
- 185 Fecto, F., Yan, J., Vemula, S. P., Liu, E., Yang, Y., Chen, W., Zheng, J. G., Shi, Y., Siddique, N., Arrat, H., Donkervoort, S., Ajroud-Driss, S., Sufit, R. L., Heller, S. L., Deng, H. X. & Siddique, T. SQSTM1 mutations in familial and sporadic amyotrophic lateral sclerosis. *Arch Neurol* **68**, 1440-1446, doi:10.1001/archneurol.2011.250 (2011).
- 186 Puls, I., Jonnakuty, C., LaMonte, B. H., Holzbaur, E. L., Tokito, M., Mann, E., Floeter, M. K., Bidus, K., Drayna, D., Oh, S. J., Brown, R. H., Jr., Ludlow, C. L. & Fischbeck, K. H. Mutations in the ubiquitin-proteasome pathway in amyotrophic lateral sclerosis. *Hum Mol Genet* **11**, 103-111, doi:10.1093/hmg/ddi001 (2002).

- K. H. Mutant dynactin in motor neuron disease. *Nat Genet* **33**, 455-456, doi:10.1038/ng1123 (2003).
- 187 Weedon, M. N., Hastings, R., Caswell, R., Xie, W., Paszkiewicz, K., Antoniadis, T., Williams, M., King, C., Greenhalgh, L., Newbury-Ecob, R. & Ellard, S. Exome sequencing identifies a DYNC1H1 mutation in a large pedigree with dominant axonal Charcot-Marie-Tooth disease. *Am J Hum Genet* **89**, 308-312, doi:10.1016/j.ajhg.2011.07.002 (2011).
- 188 Meissner, F., Molawi, K. & Zychlinsky, A. Mutant superoxide dismutase 1-induced IL-1beta accelerates ALS pathogenesis. *Proc Natl Acad Sci U S A* **107**, 13046-13050, doi:10.1073/pnas.1002396107 (2010).
- 189 Crippa, V., Sau, D., Rusmini, P., Boncoraglio, A., Onesto, E., Bolzoni, E., Galbiati, M., Fontana, E., Marino, M., Carra, S., Bendotti, C., De Biasi, S. & Poletti, A. The small heat shock protein B8 (HspB8) promotes autophagic removal of misfolded proteins involved in amyotrophic lateral sclerosis (ALS). *Hum Mol Genet* **19**, 3440-3456, doi:10.1093/hmg/ddq257 (2010).
- 190 Diaz-Hernandez, M., Valera, A. G., Moran, M. A., Gomez-Ramos, P., Alvarez-Castelao, B., Castano, J. G., Hernandez, F. & Lucas, J. J. Inhibition of 26S proteasome activity by huntingtin filaments but not inclusion bodies isolated from mouse and human brain. *J Neurochem* **98**, 1585-1596, doi:10.1111/j.1471-4159.2006.03968.x (2006).
- 191 Martinez-Vicente, M., Tallozy, Z., Wong, E., Tang, G., Koga, H., Kaushik, S., de Vries, R., Arias, E., Harris, S., Sulzer, D. & Cuervo, A. M. Cargo recognition failure is responsible for inefficient autophagy in Huntington's disease. *Nat Neurosci* **13**, 567-576, doi:10.1038/nn.2528 (2010).
- 192 Heng, M. Y., Duong, D. K., Albin, R. L., Tallaksen-Greene, S. J., Hunter, J. M., Lesort, M. J., Osmand, A., Paulson, H. L. & Detloff, P. J. Early autophagic response in a novel knock-in model of Huntington disease. *Hum Mol Genet* **19**, 3702-3720, doi:10.1093/hmg/ddq285 (2010).
- 193 Koga, H., Martinez-Vicente, M., Arias, E., Kaushik, S., Sulzer, D. & Cuervo, A. M. Constitutive upregulation of chaperone-mediated autophagy in Huntington's disease. *J Neurosci* **31**, 18492-18505, doi:10.1523/JNEUROSCI.3219-11.2011 (2011).
- 194 Croce, K. R. & Yamamoto, A. A role for autophagy in Huntington's disease. *Neurobiol Dis* **122**, 16-22, doi:10.1016/j.nbd.2018.08.010 (2019).
- 195 Jeong, H., Then, F., Melia, T. J., Jr., Mazzulli, J. R., Cui, L., Savas, J. N., Voisine, C., Paganetti, P., Tanese, N., Hart, A. C., Yamamoto, A. & Krainc, D. Acetylation targets mutant huntingtin to autophagosomes for degradation. *Cell* **137**, 60-72, doi:10.1016/j.cell.2009.03.018 (2009).
- 196 Ravikumar, B., Vacher, C., Berger, Z., Davies, J. E., Luo, S., Oroz, L. G., Scaravilli, F., Easton, D. F., Duden, R., O'Kane, C. J. & Rubinsztein, D. C. Inhibition of mTOR induces autophagy and reduces toxicity of polyglutamine expansions in fly and mouse models of Huntington disease. *Nat Genet* **36**, 585-595, doi:10.1038/ng1362 (2004).
- 197 Bauer, P. O., Goswami, A., Wong, H. K., Okuno, M., Kurosawa, M., Yamada, M., Miyazaki, H., Matsumoto, G., Kino, Y., Nagai, Y. & Nukina, N. Harnessing chaperone-mediated autophagy for the selective degradation of mutant huntingtin protein. *Nat Biotechnol* **28**, 256-263, doi:10.1038/nbt.1608 (2010).
- 198 Jimenez-Sanchez, M., Licitra, F., Underwood, B. R. & Rubinsztein, D. C. Huntington's Disease: Mechanisms of Pathogenesis and Therapeutic Strategies. *Cold Spring Harb Perspect Med* **7**, doi:10.1101/cshperspect.a024240 (2017).
- 199 Lee, J. H., Tecedor, L., Chen, Y. H., Monteys, A. M., Sowada, M. J., Thompson, L. M. & Davidson, B. L. Reinstating aberrant mTORC1 activity in Huntington's disease mice

- improves disease phenotypes. *Neuron* **85**, 303-315, doi:10.1016/j.neuron.2014.12.019 (2015).
- 200 Roscic, A., Baldo, B., Crochemore, C., Marcellin, D. & Paganetti, P. Induction of autophagy with catalytic mTOR inhibitors reduces huntingtin aggregates in a neuronal cell model. *J Neurochem* **119**, 398-407, doi:10.1111/j.1471-4159.2011.07435.x (2011).
- 201 Cuervo, A. M. & Dice, J. F. Age-related decline in chaperone-mediated autophagy. *J Biol Chem* **275**, 31505-31513, doi:10.1074/jbc.M002102200 (2000).
- 202 Wu, J. C., Qi, L., Wang, Y., Kegel, K. B., Yoder, J., Difulgia, M., Qin, Z. H. & Lin, F. The regulation of N-terminal Huntingtin (Htt552) accumulation by Beclin1. *Acta Pharmacol Sin* **33**, 743-751, doi:10.1038/aps.2012.14 (2012).
- 203 Nagaoka, U., Kim, K., Jana, N. R., Doi, H., Maruyama, M., Mitsui, K., Oyama, F. & Nukina, N. Increased expression of p62 in expanded polyglutamine-expressing cells and its association with polyglutamine inclusions. *J Neurochem* **91**, 57-68, doi:10.1111/j.1471-4159.2004.02692.x (2004).
- 204 Cortes, C. J. & La Spada, A. R. The many faces of autophagy dysfunction in Huntington's disease: from mechanism to therapy. *Drug Discov Today* **19**, 963-971, doi:10.1016/j.drudis.2014.02.014 (2014).
- 205 Sarkar, S. & Rubinsztein, D. C. Huntington's disease: degradation of mutant huntingtin by autophagy. *FEBS J* **275**, 4263-4270, doi:10.1111/j.1742-4658.2008.06562.x (2008).
- 206 Shibata, M., Lu, T., Furuya, T., Degterev, A., Mizushima, N., Yoshimori, T., MacDonald, M., Yankner, B. & Yuan, J. Regulation of intracellular accumulation of mutant Huntingtin by Beclin 1. *J Biol Chem* **281**, 14474-14485, doi:10.1074/jbc.M600364200 (2006).
- 207 Thompson, L. M., Aiken, C. T., Kaltenbach, L. S., Agrawal, N., Illes, K., Khoshnan, A., Martinez-Vincente, M., Arrasate, M., O'Rourke, J. G., Khashwji, H., Lukacsovich, T., Zhu, Y. Z., Lau, A. L., Massey, A., Hayden, M. R., Zeitlin, S. O., Finkbeiner, S., Green, K. N., LaFerla, F. M., Bates, G., Huang, L., Patterson, P. H., Lo, D. C., Cuervo, A. M., Marsh, J. L. & Steffan, J. S. IKK phosphorylates Huntingtin and targets it for degradation by the proteasome and lysosome. *J Cell Biol* **187**, 1083-1099, doi:10.1083/jcb.200909067 (2009).
- 208 Ravikumar, B., Duden, R. & Rubinsztein, D. C. Aggregate-prone proteins with polyglutamine and polyalanine expansions are degraded by autophagy. *Hum Mol Genet* **11**, 1107-1117, doi:10.1093/hmg/11.9.1107 (2002).
- 209 Sarkar, S., Davies, J. E., Huang, Z., Tunnacliffe, A. & Rubinsztein, D. C. Trehalose, a novel mTOR-independent autophagy enhancer, accelerates the clearance of mutant huntingtin and alpha-synuclein. *J Biol Chem* **282**, 5641-5652, doi:10.1074/jbc.M609532200 (2007).
- 210 Martin, D. D., Ladha, S., Ehrnhoefer, D. E. & Hayden, M. R. Autophagy in Huntington disease and huntingtin in autophagy. *Trends Neurosci* **38**, 26-35, doi:10.1016/j.tins.2014.09.003 (2015).
- 211 Saudou, F. & Humbert, S. The Biology of Huntingtin. *Neuron* **89**, 910-926, doi:10.1016/j.neuron.2016.02.003 (2016).
- 212 Hodges, A., Strand, A. D., Aragaki, A. K., Kuhn, A., Sengstag, T., Hughes, G., Elliston, L. A., Hartog, C., Goldstein, D. R., Thu, D., Hollingsworth, Z. R., Collin, F., Synek, B., Holmans, P. A., Young, A. B., Wexler, N. S., Delorenzi, M., Kooperberg, C., Augood, S. J., Faull, R. L., Olson, J. M., Jones, L. & Luthi-Carter, R. Regional and cellular gene expression changes in human Huntington's disease brain. *Hum Mol Genet* **15**, 965-977, doi:10.1093/hmg/ddl013 (2006).
- 213 Ravikumar, B., Imarisio, S., Sarkar, S., O'Kane, C. J. & Rubinsztein, D. C. Rab5 modulates aggregation and toxicity of mutant huntingtin through macroautophagy in

- cell and fly models of Huntington disease. *J Cell Sci* **121**, 1649-1660, doi:10.1242/jcs.025726 (2008).
- 214 Ochaba, J., Lukacsovich, T., Csikos, G., Zheng, S., Margulis, J., Salazar, L., Mao, K., Lau, A. L., Yeung, S. Y., Humbert, S., Saudou, F., Klionsky, D. J., Finkbeiner, S., Zeitlin, S. O., Marsh, J. L., Housman, D. E., Thompson, L. M. & Steffan, J. S. Potential function for the Huntingtin protein as a scaffold for selective autophagy. *Proc Natl Acad Sci U S A* **111**, 16889-16894, doi:10.1073/pnas.1420103111 (2014).
- 215 Caviston, J. P., Ross, J. L., Antony, S. M., Tokito, M. & Holzbaur, E. L. Huntingtin facilitates dynein/dynactin-mediated vesicle transport. *Proc Natl Acad Sci U S A* **104**, 10045-10050, doi:10.1073/pnas.0610628104 (2007).
- 216 Caviston, J. P. & Holzbaur, E. L. Huntingtin as an essential integrator of intracellular vesicular trafficking. *Trends Cell Biol* **19**, 147-155, doi:10.1016/j.tcb.2009.01.005 (2009).
- 217 Caviston, J. P., Zajac, A. L., Tokito, M. & Holzbaur, E. L. Huntingtin coordinates the dynein-mediated dynamic positioning of endosomes and lysosomes. *Mol Biol Cell* **22**, 478-492, doi:10.1091/mbc.E10-03-0233 (2011).
- 218 Wong, Y. C. & Holzbaur, E. L. The regulation of autophagosome dynamics by huntingtin and HAP1 is disrupted by expression of mutant huntingtin, leading to defective cargo degradation. *J Neurosci* **34**, 1293-1305, doi:10.1523/JNEUROSCI.1870-13.2014 (2014).
- 219 MacDonald, M. E., Barnes, G., Srinidhi, J., Duyao, M. P., Ambrose, C. M., Myers, R. H., Gray, J., Conneally, P. M., Young, A., Penney, J. & et al. Gametic but not somatic instability of CAG repeat length in Huntington's disease. *J Med Genet* **30**, 982-986 (1993).
- 220 Reiner, A., Albin, R. L., Anderson, K. D., D'Amato, C. J., Penney, J. B. & Young, A. B. Differential loss of striatal projection neurons in Huntington disease. *Proc Natl Acad Sci U S A* **85**, 5733-5737 (1988).
- 221 Rowe, K. C., Paulsen, J. S., Langbehn, D. R., Duff, K., Beglinger, L. J., Wang, C., O'Rourke, J. J., Stout, J. C. & Moser, D. J. Self-paced timing detects and tracks change in prodromal Huntington disease. *Neuropsychology* **24**, 435-442, doi:10.1037/a0018905 (2010).
- 222 Kiernan, M. C., Vucic, S., Cheah, B. C., Turner, M. R., Eisen, A., Hardiman, O., Burrell, J. R. & Zoing, M. C. Amyotrophic lateral sclerosis. *Lancet* **377**, 942-955, doi:10.1016/S0140-6736(10)61156-7 (2011).
- 223 Rosenblatt, A. Neuropsychiatry of Huntington's disease. *Dialogues Clin Neurosci* **9**, 191-197 (2007).
- 224 Nance, M. A. Huntington disease: clinical, genetic, and social aspects. *J Geriatr Psychiatry Neurol* **11**, 61-70, doi:10.1177/089198879801100204 (1998).
- 225 McColgan, P. & Tabrizi, S. J. Huntington's disease: a clinical review. *Eur J Neurol* **25**, 24-34, doi:10.1111/ene.13413 (2018).
- 226 Finkbeiner, S. Huntington's Disease. *Cold Spring Harb Perspect Biol* **3**, doi:10.1101/cshperspect.a007476 (2011).
- 227 Goh, A. M., Wibawa, P., Loi, S. M., Walterfang, M., Velakoulis, D. & Looi, J. C. Huntington's disease: Neuropsychiatric manifestations of Huntington's disease. *Australas Psychiatry* **26**, 366-375, doi:10.1177/1039856218791036 (2018).
- 228 Huntington, G. On chorea. George Huntington, M.D. *J Neuropsychiatry Clin Neurosci* **15**, 109-112, doi:10.1176/jnp.15.1.109 (2003).
- 229 Albin, R. L., Young, A. B. & Penney, J. B. The functional anatomy of basal ganglia disorders. *Trends Neurosci* **12**, 366-375, doi:10.1016/0166-2236(89)90074-x (1989).

- 230 Hallett, M. Physiology of basal ganglia disorders: an overview. *Can J Neurol Sci* **20**, 177-183, doi:10.1017/s0317167100047909 (1993).
- 231 Herrero, M. T., Barcia, C. & Navarro, J. M. Functional anatomy of thalamus and basal ganglia. *Childs Nerv Syst* **18**, 386-404, doi:10.1007/s00381-002-0604-1 (2002).
- 232 Haber, S. N. The place of dopamine in the cortico-basal ganglia circuit. *Neuroscience* **282**, 248-257, doi:10.1016/j.neuroscience.2014.10.008 (2014).
- 233 Gerfen, C. R. & Surmeier, D. J. Modulation of striatal projection systems by dopamine. *Annu Rev Neurosci* **34**, 441-466, doi:10.1146/annurev-neuro-061010-113641 (2011).
- 234 Albin, R. L., Young, A. B. & Penney, J. B. The functional anatomy of disorders of the basal ganglia. *Trends Neurosci* **18**, 63-64 (1995).
- 235 Vonsattel, J. P., Myers, R. H., Stevens, T. J., Ferrante, R. J., Bird, E. D. & Richardson, E. P., Jr. Neuropathological classification of Huntington's disease. *J Neuropathol Exp Neurol* **44**, 559-577, doi:10.1097/00005072-198511000-00003 (1985).
- 236 Vonsattel, J. P. & DiFiglia, M. Huntington disease. *J Neuropathol Exp Neurol* **57**, 369-384 (1998).
- 237 Mielcarek, M. Huntington's disease is a multi-system disorder. *Rare Dis* **3**, e1058464, doi:10.1080/21675511.2015.1058464 (2015).
- 238 Marques Sousa, C. & Humbert, S. Huntingtin: here, there, everywhere! *J Huntingtons Dis* **2**, 395-403, doi:10.3233/JHD-130082 (2013).
- 239 Jeong, S. J., Kim, M., Chang, K. A., Kim, H. S., Park, C. H. & Suh, Y. H. Huntingtin is localized in the nucleus during preimplantation embryo development in mice. *Int J Dev Neurosci* **24**, 81-85, doi:10.1016/j.ijdevneu.2005.10.001 (2006).
- 240 Duyao, M. P., Auerbach, A. B., Ryan, A., Persichetti, F., Barnes, G. T., McNeil, S. M., Ge, P., Vonsattel, J. P., Gusella, J. F., Joyner, A. L. & et al. Inactivation of the mouse Huntington's disease gene homolog Hdh. *Science* **269**, 407-410 (1995).
- 241 Nasir, J., Floresco, S. B., O'Kusky, J. R., Diewert, V. M., Richman, J. M., Zeisler, J., Borowski, A., Marth, J. D., Phillips, A. G. & Hayden, M. R. Targeted disruption of the Huntington's disease gene results in embryonic lethality and behavioral and morphological changes in heterozygotes. *Cell* **81**, 811-823 (1995).
- 242 Zeitlin, S., Liu, J. P., Chapman, D. L., Papaioannou, V. E. & Efstratiadis, A. Increased apoptosis and early embryonic lethality in mice nullizygous for the Huntington's disease gene homologue. *Nat Genet* **11**, 155-163, doi:10.1038/ng1095-155 (1995).
- 243 Xia, J., Lee, D. H., Taylor, J., Vandelft, M. & Truant, R. Huntingtin contains a highly conserved nuclear export signal. *Hum Mol Genet* **12**, 1393-1403 (2003).
- 244 Li, S. H. & Li, X. J. Huntingtin-protein interactions and the pathogenesis of Huntington's disease. *Trends Genet* **20**, 146-154, doi:10.1016/j.tig.2004.01.008 (2004).
- 245 Sun, Y., Savanenin, A., Reddy, P. H. & Liu, Y. F. Polyglutamine-expanded huntingtin promotes sensitization of N-methyl-D-aspartate receptors via post-synaptic density 95. *J Biol Chem* **276**, 24713-24718, doi:10.1074/jbc.M103501200 (2001).
- 246 Liu, Y. F., Deth, R. C. & Devys, D. SH3 domain-dependent association of huntingtin with epidermal growth factor receptor signaling complexes. *J Biol Chem* **272**, 8121-8124, doi:10.1074/jbc.272.13.8121 (1997).
- 247 Colomer, V., Engelender, S., Sharp, A. H., Duan, K., Cooper, J. K., Lanahan, A., Lyford, G., Worley, P. & Ross, C. A. Huntingtin-associated protein 1 (HAP1) binds to a Trio-like polypeptide, with a rac1 guanine nucleotide exchange factor domain. *Hum Mol Genet* **6**, 1519-1525, doi:10.1093/hmg/6.9.1519 (1997).
- 248 Harjes, P. & Wanker, E. E. The hunt for huntingtin function: interaction partners tell many different stories. *Trends Biochem Sci* **28**, 425-433, doi:10.1016/S0968-0004(03)00168-3 (2003).

- 249 Podvin, S., Reardon, H. T., Yin, K., Mosier, C. & Hook, V. Multiple clinical features of Huntington's disease correlate with mutant HTT gene CAG repeat lengths and neurodegeneration. *J Neurol* **266**, 551-564, doi:10.1007/s00415-018-8940-6 (2019).
- 250 Waelter, S., Scherzinger, E., Hasenbank, R., Nordhoff, E., Lurz, R., Goehler, H., Gauss, C., Sathasivam, K., Bates, G. P., Lehrach, H. & Wanker, E. E. The huntingtin interacting protein HIP1 is a clathrin and alpha-adaptin-binding protein involved in receptor-mediated endocytosis. *Hum Mol Genet* **10**, 1807-1817 (2001).
- 251 Zuccato, C. & Cattaneo, E. Role of brain-derived neurotrophic factor in Huntington's disease. *Prog Neurobiol* **81**, 294-330, doi:10.1016/j.pneurobio.2007.01.003 (2007).
- 252 Baquet, Z. C., Gorski, J. A. & Jones, K. R. Early striatal dendrite deficits followed by neuron loss with advanced age in the absence of anterograde cortical brain-derived neurotrophic factor. *J Neurosci* **24**, 4250-4258, doi:10.1523/JNEUROSCI.3920-03.2004 (2004).
- 253 Zuccato, C., Ciammola, A., Rigamonti, D., Leavitt, B. R., Goffredo, D., Conti, L., MacDonald, M. E., Friedlander, R. M., Silani, V., Hayden, M. R., Timmusk, T., Sipione, S. & Cattaneo, E. Loss of huntingtin-mediated BDNF gene transcription in Huntington's disease. *Science* **293**, 493-498, doi:10.1126/science.1059581 (2001).
- 254 Gauthier, L. R., Charrin, B. C., Borrell-Pages, M., Dompierre, J. P., Rangone, H., Cordelieres, F. P., De Mey, J., MacDonald, M. E., Lessmann, V., Humbert, S. & Saudou, F. Huntingtin controls neurotrophic support and survival of neurons by enhancing BDNF vesicular transport along microtubules. *Cell* **118**, 127-138, doi:10.1016/j.cell.2004.06.018 (2004).
- 255 Ho, L. W., Brown, R., Maxwell, M., Wyttenbach, A. & Rubinsztein, D. C. Wild type Huntingtin reduces the cellular toxicity of mutant Huntingtin in mammalian cell models of Huntington's disease. *J Med Genet* **38**, 450-452 (2001).
- 256 Luo, S., Vacher, C., Davies, J. E. & Rubinsztein, D. C. Cdk5 phosphorylation of huntingtin reduces its cleavage by caspases: implications for mutant huntingtin toxicity. *J Cell Biol* **169**, 647-656, doi:10.1083/jcb.200412071 (2005).
- 257 Roze, E., Saudou, F. & Caboche, J. Pathophysiology of Huntington's disease: from huntingtin functions to potential treatments. *Curr Opin Neurol* **21**, 497-503, doi:10.1097/WCO.0b013e328304b692 (2008).
- 258 Trushina, E., Dyer, R. B., Badger, J. D., 2nd, Ure, D., Eide, L., Tran, D. D., Vrieze, B. T., Legendre-Guillemain, V., McPherson, P. S., Mandavilli, B. S., Van Houten, B., Zeitlin, S., McNiven, M., Aebersold, R., Hayden, M., Parisi, J. E., Seeberg, E., Dragatsis, I., Doyle, K., Bender, A., Chacko, C. & McMurray, C. T. Mutant huntingtin impairs axonal trafficking in mammalian neurons in vivo and in vitro. *Mol Cell Biol* **24**, 8195-8209, doi:10.1128/MCB.24.18.8195-8209.2004 (2004).
- 259 Gunawardena, S. & Goldstein, L. S. Polyglutamine diseases and transport problems: deadly traffic jams on neuronal highways. *Arch Neurol* **62**, 46-51, doi:10.1001/archneur.62.1.46 (2005).
- 260 Smith, R., Brundin, P. & Li, J. Y. Synaptic dysfunction in Huntington's disease: a new perspective. *Cell Mol Life Sci* **62**, 1901-1912, doi:10.1007/s00018-005-5084-5 (2005).
- 261 Suresh, S. N., Verma, V., Sateesh, S., Clement, J. P. & Manjithaya, R. Neurodegenerative diseases: model organisms, pathology and autophagy. *J Genet* **97**, 679-701 (2018).
- 262 van der Staay, F. J., Arndt, S. S. & Nordquist, R. E. Evaluation of animal models of neurobehavioral disorders. *Behav Brain Funct* **5**, 11, doi:10.1186/1744-9081-5-11 (2009).
- 263 Jucker, M. The benefits and limitations of animal models for translational research in neurodegenerative diseases. *Nat Med* **16**, 1210-1214, doi:10.1038/nm.2224 (2010).

- 264 Gray, M., Shirasaki, D. I., Cepeda, C., Andre, V. M., Wilburn, B., Lu, X. H., Tao, J., Yamazaki, I., Li, S. H., Sun, Y. E., Li, X. J., Levine, M. S. & Yang, X. W. Full-length human mutant huntingtin with a stable polyglutamine repeat can elicit progressive and selective neuropathogenesis in BACHD mice. *J Neurosci* **28**, 6182-6195, doi:10.1523/JNEUROSCI.0857-08.2008 (2008).
- 265 Menalled, L. B., Sison, J. D., Dragatsis, I., Zeitlin, S. & Chesselet, M. F. Time course of early motor and neuropathological anomalies in a knock-in mouse model of Huntington's disease with 140 CAG repeats. *J Comp Neurol* **465**, 11-26, doi:10.1002/cne.10776 (2003).
- 266 Reddy, P. H., Williams, M., Charles, V., Garrett, L., Pike-Buchanan, L., Whetsell, W. O., Jr., Miller, G. & Tagle, D. A. Behavioural abnormalities and selective neuronal loss in HD transgenic mice expressing mutated full-length HD cDNA. *Nat Genet* **20**, 198-202, doi:10.1038/2510 (1998).
- 267 Farshim, P. P. & Bates, G. P. Mouse Models of Huntington's Disease. *Methods Mol Biol* **1780**, 97-120, doi:10.1007/978-1-4939-7825-0_6 (2018).
- 268 Mangiarini, L., Sathasivam, K., Seller, M., Cozens, B., Harper, A., Hetherington, C., Lawton, M., Trotter, Y., Leach, H., Davies, S. W. & Bates, G. P. Exon 1 of the HD gene with an expanded CAG repeat is sufficient to cause a progressive neurological phenotype in transgenic mice. *Cell* **87**, 493-506, doi:10.1016/s0092-8674(00)81369-0 (1996).
- 269 Stack, E. C., Kubilus, J. K., Smith, K., Cormier, K., Del Signore, S. J., Guelin, E., Ryu, H., Hersch, S. M. & Ferrante, R. J. Chronology of behavioral symptoms and neuropathological sequela in R6/2 Huntington's disease transgenic mice. *J Comp Neurol* **490**, 354-370, doi:10.1002/cne.20680 (2005).
- 270 Luesse, H. G., Schiefer, J., Spruenken, A., Puls, C., Block, F. & Kosinski, C. M. Evaluation of R6/2 HD transgenic mice for therapeutic studies in Huntington's disease: behavioral testing and impact of diabetes mellitus. *Behav Brain Res* **126**, 185-195, doi:10.1016/s0166-4328(01)00261-3 (2001).
- 271 Lione, L. A., Carter, R. J., Hunt, M. J., Bates, G. P., Morton, A. J. & Dunnett, S. B. Selective discrimination learning impairments in mice expressing the human Huntington's disease mutation. *J Neurosci* **19**, 10428-10437 (1999).
- 272 Bylsma, F. W., Brandt, J. & Strauss, M. E. Aspects of procedural memory are differentially impaired in Huntington's disease. *Arch Clin Neuropsychol* **5**, 287-297 (1990).
- 273 Heindel, W. C., Butters, N. & Salmon, D. P. Impaired learning of a motor skill in patients with Huntington's disease. *Behav Neurosci* **102**, 141-147, doi:10.1037//0735-7044.102.1.141 (1988).
- 274 Lange, K. W., Sahakian, B. J., Quinn, N. P., Marsden, C. D. & Robbins, T. W. Comparison of executive and visuospatial memory function in Huntington's disease and dementia of Alzheimer type matched for degree of dementia. *J Neurol Neurosurg Psychiatry* **58**, 598-606, doi:10.1136/jnnp.58.5.598 (1995).
- 275 Carter, R. J., Lione, L. A., Humby, T., Mangiarini, L., Mahal, A., Bates, G. P., Dunnett, S. B. & Morton, A. J. Characterization of progressive motor deficits in mice transgenic for the human Huntington's disease mutation. *J Neurosci* **19**, 3248-3257 (1999).
- 276 Sun, Z., Xie, J. & Reiner, A. The differential vulnerability of striatal projection neurons in 3-nitropropionic acid-treated rats does not match that typical of adult-onset Huntington's disease. *Exp Neurol* **176**, 55-65, doi:10.1006/exnr.2002.7947 (2002).
- 277 Dodds, L., Chen, J., Berggren, K. & Fox, J. Characterization of Striatal Neuronal Loss and Atrophy in the R6/2 Mouse Model of Huntington's Disease. *PLoS Curr* **6**, doi:10.1371/currents.hd.48727b68b39b82d5fe350f753984bcf9 (2014).

- 278 Turmaine, M., Raza, A., Mahal, A., Mangiarini, L., Bates, G. P. & Davies, S. W. Nonapoptotic neurodegeneration in a transgenic mouse model of Huntington's disease. *Proc Natl Acad Sci U S A* **97**, 8093-8097, doi:10.1073/pnas.110078997 (2000).
- 279 Menalled, L. B. & Chesselet, M. F. Mouse models of Huntington's disease. *Trends Pharmacol Sci* **23**, 32-39, doi:10.1016/s0165-6147(00)01884-8 (2002).
- 280 Bjorkqvist, M., Fex, M., Renstrom, E., Wierup, N., Petersen, A., Gil, J., Bacos, K., Popovic, N., Li, J. Y., Sundler, F., Brundin, P. & Mulder, H. The R6/2 transgenic mouse model of Huntington's disease develops diabetes due to deficient beta-cell mass and exocytosis. *Hum Mol Genet* **14**, 565-574, doi:10.1093/hmg/ddi053 (2005).
- 281 Shelbourne, P. F., Killeen, N., Hevner, R. F., Johnston, H. M., Tecott, L., Lewandoski, M., Ennis, M., Ramirez, L., Li, Z., Iannicola, C., Littman, D. R. & Myers, R. M. A Huntington's disease CAG expansion at the murine Hdh locus is unstable and associated with behavioural abnormalities in mice. *Hum Mol Genet* **8**, 763-774, doi:10.1093/hmg/8.5.763 (1999).
- 282 Wheeler, V. C., Auerbach, W., White, J. K., Srinidhi, J., Auerbach, A., Ryan, A., Duyao, M. P., Vrbanc, V., Weaver, M., Gusella, J. F., Joyner, A. L. & MacDonald, M. E. Length-dependent gametic CAG repeat instability in the Huntington's disease knock-in mouse. *Hum Mol Genet* **8**, 115-122, doi:10.1093/hmg/8.1.115 (1999).
- 283 Heng, M. Y., Tallaksen-Greene, S. J., Detloff, P. J. & Albin, R. L. Longitudinal evaluation of the Hdh(CAG)150 knock-in murine model of Huntington's disease. *J Neurosci* **27**, 8989-8998, doi:10.1523/JNEUROSCI.1830-07.2007 (2007).
- 284 Slow, E. J., van Raamsdonk, J., Rogers, D., Coleman, S. H., Graham, R. K., Deng, Y., Oh, R., Bissada, N., Hossain, S. M., Yang, Y. Z., Li, X. J., Simpson, E. M., Gutekunst, C. A., Leavitt, B. R. & Hayden, M. R. Selective striatal neuronal loss in a YAC128 mouse model of Huntington disease. *Hum Mol Genet* **12**, 1555-1567, doi:10.1093/hmg/ddg169 (2003).
- 285 Pouladi, M. A., Graham, R. K., Karasinska, J. M., Xie, Y., Santos, R. D., Petersen, A. & Hayden, M. R. Prevention of depressive behaviour in the YAC128 mouse model of Huntington disease by mutation at residue 586 of huntingtin. *Brain* **132**, 919-932, doi:10.1093/brain/awp006 (2009).
- 286 Pouladi, M. A., Stanek, L. M., Xie, Y., Franciosi, S., Southwell, A. L., Deng, Y., Butland, S., Zhang, W., Cheng, S. H., Shihabuddin, L. S. & Hayden, M. R. Marked differences in neurochemistry and aggregates despite similar behavioural and neuropathological features of Huntington disease in the full-length BACHD and YAC128 mice. *Hum Mol Genet* **21**, 2219-2232, doi:10.1093/hmg/dds037 (2012).
- 287 Cha, J. H., Kosinski, C. M., Kerner, J. A., Alsdorf, S. A., Mangiarini, L., Davies, S. W., Penney, J. B., Bates, G. P. & Young, A. B. Altered brain neurotransmitter receptors in transgenic mice expressing a portion of an abnormal human huntington disease gene. *Proc Natl Acad Sci U S A* **95**, 6480-6485, doi:10.1073/pnas.95.11.6480 (1998).
- 288 Reynolds, G. P., Dalton, C. F., Tillery, C. L., Mangiarini, L., Davies, S. W. & Bates, G. P. Brain neurotransmitter deficits in mice transgenic for the Huntington's disease mutation. *J Neurochem* **72**, 1773-1776, doi:10.1046/j.1471-4159.1999.721773.x (1999).
- 289 Ariano, M. A., Aronin, N., Difiglia, M., Tagle, D. A., Sibley, D. R., Leavitt, B. R., Hayden, M. R. & Levine, M. S. Striatal neurochemical changes in transgenic models of Huntington's disease. *J Neurosci Res* **68**, 716-729, doi:10.1002/jnr.10272 (2002).
- 290 Yohrling, I. G., Jiang, G. C., DeJohn, M. M., Robertson, D. J., Vrana, K. E. & Cha, J. H. Inhibition of tryptophan hydroxylase activity and decreased 5-HT1A receptor binding in a mouse model of Huntington's disease. *J Neurochem* **82**, 1416-1423, doi:10.1046/j.1471-4159.2002.01084.x (2002).

- 291 Levine, M. S., Klapstein, G. J., Koppel, A., Gruen, E., Cepeda, C., Vargas, M. E., Jokel, E. S., Carpenter, E. M., Zanjani, H., Hurst, R. S., Efstratiadis, A., Zeitlin, S. & Chesselet, M. F. Enhanced sensitivity to N-methyl-D-aspartate receptor activation in transgenic and knockin mouse models of Huntington's disease. *J Neurosci Res* **58**, 515-532 (1999).
- 292 Cepeda, C., Hurst, R. S., Calvert, C. R., Hernandez-Echeagaray, E., Nguyen, O. K., Jocoy, E., Christian, L. J., Ariano, M. A. & Levine, M. S. Transient and progressive electrophysiological alterations in the corticostriatal pathway in a mouse model of Huntington's disease. *J Neurosci* **23**, 961-969 (2003).
- 293 Hansson, O., Guatteo, E., Mercuri, N. B., Bernardi, G., Li, X. J., Castilho, R. F. & Brundin, P. Resistance to NMDA toxicity correlates with appearance of nuclear inclusions, behavioural deficits and changes in calcium homeostasis in mice transgenic for exon 1 of the huntington gene. *Eur J Neurosci* **14**, 1492-1504, doi:10.1046/j.0953-816x.2001.01767.x (2001).
- 294 Behrens, P. F., Franz, P., Woodman, B., Lindenberg, K. S. & Landwehrmeyer, G. B. Impaired glutamate transport and glutamate-glutamine cycling: downstream effects of the Huntington mutation. *Brain* **125**, 1908-1922, doi:10.1093/brain/awf180 (2002).
- 295 Hickey, M. A., Reynolds, G. P. & Morton, A. J. The role of dopamine in motor symptoms in the R6/2 transgenic mouse model of Huntington's disease. *J Neurochem* **81**, 46-59, doi:10.1046/j.1471-4159.2002.00804.x (2002).
- 296 Hurlbert, M. S., Zhou, W., Wasmeier, C., Kaddis, F. G., Hutton, J. C. & Freed, C. R. Mice transgenic for an expanded CAG repeat in the Huntington's disease gene develop diabetes. *Diabetes* **48**, 649-651, doi:10.2337/diabetes.48.3.649 (1999).
- 297 Papalexli, E., Persson, A., Bjorkqvist, M., Petersen, A., Woodman, B., Bates, G. P., Sundler, F., Mulder, H., Brundin, P. & Popovic, N. Reduction of GnRH and infertility in the R6/2 mouse model of Huntington's disease. *Eur J Neurosci* **22**, 1541-1546, doi:10.1111/j.1460-9568.2005.04324.x (2005).
- 298 Hansson, O., Petersen, A., Leist, M., Nicotera, P., Castilho, R. F. & Brundin, P. Transgenic mice expressing a Huntington's disease mutation are resistant to quinolinic acid-induced striatal excitotoxicity. *Proc Natl Acad Sci U S A* **96**, 8727-8732, doi:10.1073/pnas.96.15.8727 (1999).
- 299 Klapstein, G. J., Fisher, R. S., Zanjani, H., Cepeda, C., Jokel, E. S., Chesselet, M. F. & Levine, M. S. Electrophysiological and morphological changes in striatal spiny neurons in R6/2 Huntington's disease transgenic mice. *J Neurophysiol* **86**, 2667-2677, doi:10.1152/jn.2001.86.6.2667 (2001).
- 300 Petersen, A., Puschban, Z., Lotharius, J., NicNiocaill, B., Wiekop, P., O'Connor, W. T. & Brundin, P. Evidence for dysfunction of the nigrostriatal pathway in the R6/1 line of transgenic Huntington's disease mice. *Neurobiol Dis* **11**, 134-146, doi:10.1006/nbdi.2002.0534 (2002).
- 301 Luthi-Carter, R., Strand, A., Peters, N. L., Solano, S. M., Hollingsworth, Z. R., Menon, A. S., Frey, A. S., Spektor, B. S., Penney, E. B., Schilling, G., Ross, C. A., Borchelt, D. R., Tapscott, S. J., Young, A. B., Cha, J. H. & Olson, J. M. Decreased expression of striatal signaling genes in a mouse model of Huntington's disease. *Hum Mol Genet* **9**, 1259-1271, doi:10.1093/hmg/9.9.1259 (2000).
- 302 Luthi-Carter, R., Hanson, S. A., Strand, A. D., Bergstrom, D. A., Chun, W., Peters, N. L., Woods, A. M., Chan, E. Y., Kooperberg, C., Krainc, D., Young, A. B., Tapscott, S. J. & Olson, J. M. Dysregulation of gene expression in the R6/2 model of polyglutamine disease: parallel changes in muscle and brain. *Hum Mol Genet* **11**, 1911-1926, doi:10.1093/hmg/11.17.1911 (2002).

- 303 Bogdanov, M. B., Andreassen, O. A., Dedeoglu, A., Ferrante, R. J. & Beal, M. F. Increased oxidative damage to DNA in a transgenic mouse model of Huntington's disease. *J Neurochem* **79**, 1246-1249, doi:10.1046/j.1471-4159.2001.00689.x (2001).
- 304 Santamaria, A., Perez-Severiano, F., Rodriguez-Martinez, E., Maldonado, P. D., Pedraza-Chaverri, J., Rios, C. & Segovia, J. Comparative analysis of superoxide dismutase activity between acute pharmacological models and a transgenic mouse model of Huntington's disease. *Neurochem Res* **26**, 419-424, doi:10.1023/a:1010911417383 (2001).
- 305 Tabrizi, S. J., Workman, J., Hart, P. E., Mangiarini, L., Mahal, A., Bates, G., Cooper, J. M. & Schapira, A. H. Mitochondrial dysfunction and free radical damage in the Huntington R6/2 transgenic mouse. *Ann Neurol* **47**, 80-86, doi:10.1002/1531-8249(200001)47:1<80::aid-ana13>3.3.co;2-b (2000).
- 306 Petersen, A., Larsen, K. E., Behr, G. G., Romero, N., Przedborski, S., Brundin, P. & Sulzer, D. Expanded CAG repeats in exon 1 of the Huntington's disease gene stimulate dopamine-mediated striatal neuron autophagy and degeneration. *Hum Mol Genet* **10**, 1243-1254, doi:10.1093/hmg/10.12.1243 (2001).
- 307 Barker, R. A., Fujimaki, M., Rogers, P. & Rubinsztein, D. C. Huntingtin-lowering strategies for Huntington's disease. *Expert Opin Investig Drugs* **29**, 1125-1132, doi:10.1080/13543784.2020.1804552 (2020).
- 308 He, S., Li, Q., Jiang, X., Lu, X., Feng, F., Qu, W., Chen, Y. & Sun, H. Design of small molecule autophagy modulators: a promising druggable strategy. *Journal of medicinal chemistry* **61**, 4656-4687 (2017).
- 309 Rubinsztein, D. C., Codogno, P. & Levine, B. Autophagy modulation as a potential therapeutic target for diverse diseases. *Nat Rev Drug Discov* **11**, 709-730, doi:10.1038/nrd3802 (2012).
- 310 Tan, C. C., Yu, J. T., Tan, M. S., Jiang, T., Zhu, X. C. & Tan, L. Autophagy in aging and neurodegenerative diseases: implications for pathogenesis and therapy. *Neurobiol Aging* **35**, 941-957, doi:10.1016/j.neurobiolaging.2013.11.019 (2014).
- 311 Blommaert, E. F., Luiken, J. J., Blommaert, P. J., van Woerkom, G. M. & Meijer, A. J. Phosphorylation of ribosomal protein S6 is inhibitory for autophagy in isolated rat hepatocytes. *J Biol Chem* **270**, 2320-2326, doi:10.1074/jbc.270.5.2320 (1995).
- 312 Noda, T. & Ohsumi, Y. Tor, a phosphatidylinositol kinase homologue, controls autophagy in yeast. *J Biol Chem* **273**, 3963-3966, doi:10.1074/jbc.273.7.3963 (1998).
- 313 Cardenas, M. E. & Heitman, J. FKBP12-rapamycin target TOR2 is a vacuolar protein with an associated phosphatidylinositol-4 kinase activity. *EMBO J* **14**, 5892-5907 (1995).
- 314 Ganley, I. G., Lam du, H., Wang, J., Ding, X., Chen, S. & Jiang, X. ULK1.ATG13.FIP200 complex mediates mTOR signaling and is essential for autophagy. *J Biol Chem* **284**, 12297-12305, doi:10.1074/jbc.M900573200 (2009).
- 315 Jung, C. H., Jun, C. B., Ro, S. H., Kim, Y. M., Otto, N. M., Cao, J., Kundu, M. & Kim, D. H. ULK-Atg13-FIP200 complexes mediate mTOR signaling to the autophagy machinery. *Mol Biol Cell* **20**, 1992-2003, doi:10.1091/mbc.E08-12-1249 (2009).
- 316 Berger, Z., Ravikumar, B., Menzies, F. M., Oroz, L. G., Underwood, B. R., Pangalos, M. N., Schmitt, I., Wullner, U., Evert, B. O., O'Kane, C. J. & Rubinsztein, D. C. Rapamycin alleviates toxicity of different aggregate-prone proteins. *Hum Mol Genet* **15**, 433-442, doi:10.1093/hmg/ddi458 (2006).
- 317 Wang, T., Lao, U. & Edgar, B. A. TOR-mediated autophagy regulates cell death in Drosophila neurodegenerative disease. *J Cell Biol* **186**, 703-711, doi:10.1083/jcb.200904090 (2009).

- 318 Benjamin, D., Colombi, M., Moroni, C. & Hall, M. N. Rapamycin passes the torch: a new generation of mTOR inhibitors. *Nat Rev Drug Discov* **10**, 868-880, doi:10.1038/nrd3531 (2011).
- 319 Raynaud, F. I., Eccles, S., Clarke, P. A., Hayes, A., Nutley, B., Alix, S., Henley, A., Di-Stefano, F., Ahmad, Z., Guillard, S., Bjerke, L. M., Kelland, L., Valenti, M., Patterson, L., Gowan, S., de Haven Brandon, A., Hayakawa, M., Kaizawa, H., Koizumi, T., Ohishi, T., Patel, S., Saghir, N., Parker, P., Waterfield, M. & Workman, P. Pharmacologic characterization of a potent inhibitor of class I phosphatidylinositide 3-kinases. *Cancer Res* **67**, 5840-5850, doi:10.1158/0008-5472.CAN-06-4615 (2007).
- 320 Buzzai, M., Jones, R. G., Amaravadi, R. K., Lum, J. J., DeBerardinis, R. J., Zhao, F., Viollet, B. & Thompson, C. B. Systemic treatment with the antidiabetic drug metformin selectively impairs p53-deficient tumor cell growth. *Cancer Res* **67**, 6745-6752, doi:10.1158/0008-5472.CAN-06-4447 (2007).
- 321 Lonskaya, I., Hebron, M. L., Desforges, N. M., Schachter, J. B. & Moussa, C. E. Nilotinib-induced autophagic changes increase endogenous parkin level and ubiquitination, leading to amyloid clearance. *J Mol Med (Berl)* **92**, 373-386, doi:10.1007/s00109-013-1112-3 (2014).
- 322 Hebron, M. L., Lonskaya, I. & Moussa, C. E. Nilotinib reverses loss of dopamine neurons and improves motor behavior via autophagic degradation of alpha-synuclein in Parkinson's disease models. *Hum Mol Genet* **22**, 3315-3328, doi:10.1093/hmg/ddt192 (2013).
- 323 Williams, A., Sarkar, S., Cuddon, P., Ttofi, E. K., Saiki, S., Siddiqi, F. H., Jahreiss, L., Fleming, A., Pask, D., Goldsmith, P., O'Kane, C. J., Floto, R. A. & Rubinsztein, D. C. Novel targets for Huntington's disease in an mTOR-independent autophagy pathway. *Nat Chem Biol* **4**, 295-305, doi:10.1038/nchembio.79 (2008).
- 324 Rose, C., Menzies, F. M., Renna, M., Acevedo-Arozena, A., Corrochano, S., Sadiq, O., Brown, S. D. & Rubinsztein, D. C. Rilmenidine attenuates toxicity of polyglutamine expansions in a mouse model of Huntington's disease. *Hum Mol Genet* **19**, 2144-2153, doi:10.1093/hmg/ddq093 (2010).
- 325 Sarkar, S., Floto, R. A., Berger, Z., Imarisio, S., Cordenier, A., Pasco, M., Cook, L. J. & Rubinsztein, D. C. Lithium induces autophagy by inhibiting inositol monophosphatase. *J Cell Biol* **170**, 1101-1111, doi:10.1083/jcb.200504035 (2005).
- 326 Tanaka, M., Machida, Y., Niu, S., Ikeda, T., Jana, N. R., Doi, H., Kurosawa, M., Nekooki, M. & Nukina, N. Trehalose alleviates polyglutamine-mediated pathology in a mouse model of Huntington disease. *Nat Med* **10**, 148-154, doi:10.1038/nm985 (2004).
- 327 Sanchez, I., Mahlke, C. & Yuan, J. Pivotal role of oligomerization in expanded polyglutamine neurodegenerative disorders. *Nature* **421**, 373-379, doi:10.1038/nature01301 (2003).
- 328 Wang, N., Lu, X. H., Sandoval, S. V. & Yang, X. W. An independent study of the preclinical efficacy of C2-8 in the R6/2 transgenic mouse model of Huntington's disease. *J Huntingtons Dis* **2**, 443-451, doi:10.3233/JHD-130074 (2013).
- 329 Chopra, V., Fox, J. H., Lieberman, G., Dorsey, K., Matson, W., Waldmeier, P., Housman, D. E., Kazantsev, A., Young, A. B. & Hersch, S. A small-molecule therapeutic lead for Huntington's disease: preclinical pharmacology and efficacy of C2-8 in the R6/2 transgenic mouse. *Proc Natl Acad Sci U S A* **104**, 16685-16689, doi:10.1073/pnas.0707842104 (2007).
- 330 Qi, L., Zhang, X. D., Wu, J. C., Lin, F., Wang, J., DiFiglia, M. & Qin, Z. H. The role of chaperone-mediated autophagy in huntingtin degradation. *PLoS One* **7**, e46834, doi:10.1371/journal.pone.0046834 (2012).

- 331 Jabbour, E., Cortes, J., Giles, F., O'Brien, S. & Kantarijan, H. Drug evaluation: Nilotinib - a novel Bcr-Abl tyrosine kinase inhibitor for the treatment of chronic myelocytic leukemia and beyond. *IDrugs* **10**, 468-479 (2007).
- 332 Karuppagounder, S. S., Brahmachari, S., Lee, Y., Dawson, V. L., Dawson, T. M. & Ko, H. S. The c-Abl inhibitor, nilotinib, protects dopaminergic neurons in a preclinical animal model of Parkinson's disease. *Sci Rep* **4**, 4874, doi:10.1038/srep04874 (2014).
- 333 Imam, S. Z., Zhou, Q., Yamamoto, A., Valente, A. J., Ali, S. F., Bains, M., Roberts, J. L., Kahle, P. J., Clark, R. A. & Li, S. Novel regulation of parkin function through c-Abl-mediated tyrosine phosphorylation: implications for Parkinson's disease. *J Neurosci* **31**, 157-163, doi:10.1523/JNEUROSCI.1833-10.2011 (2011).
- 334 Bantscheff, M., Eberhard, D., Abraham, Y., Bastuck, S., Boesche, M., Hobson, S., Mathieson, T., Perrin, J., Raida, M., Rau, C., Reader, V., Sweetman, G., Bauer, A., Bouwmeester, T., Hopf, C., Kruse, U., Neubauer, G., Ramsden, N., Rick, J., Kuster, B. & Drewes, G. Quantitative chemical proteomics reveals mechanisms of action of clinical ABL kinase inhibitors. *Nat Biotechnol* **25**, 1035-1044, doi:10.1038/nbt1328 (2007).
- 335 Rix, U., Hantschel, O., Durnberger, G., Rensing Rix, L. L., Planyavsky, M., Fernbach, N. V., Kaupe, I., Bennett, K. L., Valent, P., Colinge, J., Kocher, T. & Superti-Furga, G. Chemical proteomic profiles of the BCR-ABL inhibitors imatinib, nilotinib, and dasatinib reveal novel kinase and nonkinase targets. *Blood* **110**, 4055-4063, doi:10.1182/blood-2007-07-102061 (2007).
- 336 Hebron, M., Peyton, M., Liu, X., Gao, X., Wang, R., Lonskaya, I. & Moussa, C. E. Discoidin domain receptor inhibition reduces neuropathology and attenuates inflammation in neurodegeneration models. *J Neuroimmunol* **311**, 1-9, doi:10.1016/j.jneuroim.2017.07.009 (2017).
- 337 Fowler, A. J., Hebron, M., Balaraman, K., Shi, W., Missner, A. A., Greenzaid, J. D., Chiu, T. L., Ullman, C., Weatherdon, E., Duka, V., Torres-Yaghi, Y., Pagan, F. L., Liu, X., Resson, H., Ahn, J., Wolf, C. & Moussa, C. Discoidin Domain Receptor 1 is a therapeutic target for neurodegenerative diseases. *Hum Mol Genet* **29**, 2882-2898, doi:10.1093/hmg/ddaa177 (2020).
- 338 Turner, R. S., Hebron, M. L., Lawler, A., Mundel, E. E., Yusuf, N., Starr, J. N., Anjum, M., Pagan, F., Torres-Yaghi, Y., Shi, W., Mulki, S., Ferrante, D., Matar, S., Liu, X., Esposito, G., Berkowitz, F., Jiang, X., Ahn, J. & Moussa, C. Nilotinib Effects on Safety, Tolerability, and Biomarkers in Alzheimer's Disease. *Ann Neurol* **88**, 183-194, doi:10.1002/ana.25775 (2020).
- 339 Pagan, F. L., Hebron, M. L., Wilmarth, B., Torres-Yaghi, Y., Lawler, A., Mundel, E. E., Yusuf, N., Starr, N. J., Anjum, M., Arellano, J., Howard, H. H., Shi, W., Mulki, S., Kurd-Misto, T., Matar, S., Liu, X., Ahn, J. & Moussa, C. Nilotinib Effects on Safety, Tolerability, and Potential Biomarkers in Parkinson Disease: A Phase 2 Randomized Clinical Trial. *JAMA Neurol* **77**, 309-317, doi:10.1001/jamaneurol.2019.4200 (2020).
- 340 Pagan, F. L., Hebron, M. L., Wilmarth, B., Torres-Yaghi, Y., Lawler, A., Mundel, E. E., Yusuf, N., Starr, N. J., Arellano, J., Howard, H. H., Peyton, M., Matar, S., Liu, X., Fowler, A. J., Schwartz, S. L., Ahn, J. & Moussa, C. Pharmacokinetics and pharmacodynamics of a single dose Nilotinib in individuals with Parkinson's disease. *Pharmacol Res Perspect* **7**, e00470, doi:10.1002/prp2.470 (2019).
- 341 Pagan, F., Hebron, M., Valadez, E. H., Torres-Yaghi, Y., Huang, X., Mills, R. R., Wilmarth, B. M., Howard, H., Dunn, C., Carlson, A., Lawler, A., Rogers, S. L., Falconer, R. A., Ahn, J., Li, Z. & Moussa, C. Nilotinib Effects in Parkinson's disease and Dementia with Lewy bodies. *J Parkinsons Dis* **6**, 503-517, doi:10.3233/JPD-160867 (2016).

- 342 La Barbera, L., Vedele, F., Nobili, A., Krashia, P., Spoleti, E., Latagliata, E. C., Cutuli, D., Cauzzi, E., Marino, R., Viscomi, M. T., Petrosini, L., Puglisi-Allegra, S., Melone, M., Keller, F., Mercuri, N. B., Conti, F. & D'Amelio, M. Nilotinib restores memory function by preventing dopaminergic neuron degeneration in a mouse model of Alzheimer's Disease. *Prog Neurobiol*, 102031, doi:10.1016/j.pneurobio.2021.102031 (2021).
- 343 Pagan, F., Hebron, M., Valadez, E. H., Torres-Yaghi, Y., Huang, X., Mills, R. R., Wilmarth, B. M., Howard, H., Dunn, C. & Carlson, A. Nilotinib effects in Parkinson's disease and dementia with Lewy bodies. *Journal of Parkinson's disease* **6**, 503-517 (2016).
- 344 Jankovic, J. & Aguilar, L. G. Current approaches to the treatment of Parkinson's disease. *Neuropsychiatric disease and treatment* **4**, 743 (2008).
- 345 Rodrigues, F. B., Quinn, L. & Wild, E. J. Huntington's disease clinical trials corner: January 2019. *Journal of Huntington's disease* **8**, 115-125 (2019).
- 346 Rodrigues, F. B., Ferreira, J. J. & Wild, E. J. Huntington's disease clinical trials corner: June 2019. *Journal of Huntington's disease* **8**, 363-371 (2019).
- 347 Klionsky, D. J., Abdel-Aziz, A. K., Abdelfatah, S., Abdellatif, M., Abdoli, A., Abel, S., Abeliovich, H., Abildgaard, M. H., Abudu, Y. P., Acevedo-Arozena, A., Adamopoulos, I. E., Adeli, K., Adolph, T. E., Adornetto, A., Aflaki, E., Agam, G., Agarwal, A., Aggarwal, B. B., Agnello, M., Agostinis, P., Agrewala, J. N., Agrotis, A., Aguilar, P. V., Ahmad, S. T., Ahmed, Z. M., Ahumada-Castro, U., Aits, S., Aizawa, S., Akkoc, Y., Akoumianaki, T., Akpinar, H. A., Al-Abd, A. M., Al-Akra, L., Al-Gharaibeh, A., Alaoui-Jamali, M. A., Alberti, S., Alcocer-Gomez, E., Alessandri, C., Ali, M., Alim Al-Bari, M. A., Aliwaini, S., Alizadeh, J., Almacellas, E., Almasan, A., Alonso, A., Alonso, G. D., Altan-Bonnet, N., Altieri, D. C., Alvarez, E. M. C., Alves, S., Alves da Costa, C., Alzaharna, M. M., Amadio, M., Amantini, C., Amaral, C., Ambrosio, S., Amer, A. O., Ammanathan, V., An, Z., Andersen, S. U., Andrabi, S. A., Andrade-Silva, M., Andres, A. M., Angelini, S., Ann, D., Anozie, U. C., Ansari, M. Y., Antas, P., Antebi, A., Anton, Z., Anwar, T., Apetoh, L., Apostolova, N., Araki, T., Araki, Y., Arasaki, K., Araujo, W. L., Araya, J., Arden, C., Arevalo, M. A., Arguelles, S., Arias, E., Arikath, J., Arimoto, H., Ariosa, A. R., Armstrong-James, D., Arnaune-Pelloquin, L., Aroca, A., Arroyo, D. S., Arsov, I., Artero, R., Asaro, D. M. L., Aschner, M., Ashrafzadeh, M., Ashur-Fabian, O., Atanasov, A. G., Au, A. K., Auberger, P., Auner, H. W., Aurelian, L., Autelli, R., Avagliano, L., Avalos, Y., Aveic, S., Aveleira, C. A., Avin-Wittenberg, T., Aydin, Y., Ayton, S., Ayyadevara, S., Azzopardi, M., Baba, M., Backer, J. M., Backues, S. K., Bae, D. H., Bae, O. N., Bae, S. H., Baehrecke, E. H., Baek, A., Baek, S. H., Baek, S. H., Bagetta, G., Bagniewska-Zadworna, A., Bai, H., Bai, J., Bai, X., Bai, Y., Bairagi, N., Baksi, S., Balbi, T., Baldari, C. T., Balduini, W., Ballabio, A., Ballester, M., Balazadeh, S., Balzan, R., Bandopadhyay, R., Banerjee, S., Banerjee, S., Banreti, A., Bao, Y., Baptista, M. S., Baracca, A., Barbati, C., Bargiela, A., Barila, D., Barlow, P. G., Barmada, S. J., Barreiro, E., Barreto, G. E., Bartek, J., Bartel, B., Bartolome, A., Barve, G. R., Basagoudanavar, S. H., Bassham, D. C., Bast, R. C., Jr., Basu, A., Batoko, H., Batten, I., Baulieu, E. E., Baumgarner, B. L., Bayry, J., Beale, R., Beau, I., Beaumatin, F., Bechara, L. R. G., Beck, G. R., Jr., Beers, M. F., Begun, J., Behrends, C., Behrens, G. M. N., Bei, R., Bejarano, E., Bel, S., Behl, C., Belaid, A., Belgareh-Touze, N., Bellarosa, C., Belleudi, F., Bello Perez, M., Bello-Morales, R., Beltran, J. S. O., Beltran, S., Benbrook, D. M., Bendorius, M., Benitez, B. A., Benito-Cuesta, I., Bensalem, J., Berchtold, M. W., Berezowska, S., Bergamaschi, D., Bergami, M., Bergmann, A., Berliocchi, L., Berlioz-Torrent, C., Bernard, A., Berthoux, L., Besirli, C. G., Besteiro, S., Betin, V. M., Beyaert, R., Bezbradica, J. S.,

Bhaskar, K., Bhatia-Kissova, I., Bhattacharya, R., Bhattacharya, S., Bhattacharyya, S., Bhuiyan, M. S., Bhutia, S. K., Bi, L., Bi, X., Biden, T. J., Bijian, K., Billes, V. A., Binart, N., Bincoletto, C., Birgisdottir, A. B., Bjorkoy, G., Blanco, G., Blas-Garcia, A., Blasiak, J., Blomgran, R., Blomgren, K., Blum, J. S., Boada-Romero, E., Boban, M., Boesze-Battaglia, K., Boeuf, P., Boland, B., Bomont, P., Bonaldo, P., Bonam, S. R., Bonfili, L., Bonifacino, J. S., Boone, B. A., Bootman, M. D., Bordi, M., Borner, C., Bornhauser, B. C., Borthakur, G., Bosch, J., Bose, S., Botana, L. M., Botas, J., Boulanger, C. M., Boulton, M. E., Bourdenx, M., Bourgeois, B., Bourke, N. M., Bousquet, G., Boya, P., Bozhkov, P. V., Bozi, L. H. M., Bozkurt, T. O., Brackney, D. E., Brandts, C. H., Braun, R. J., Braus, G. H., Bravo-Sagua, R., Bravo-San Pedro, J. M., Brest, P., Bringer, M. A., Briones-Herrera, A., Broaddus, V. C., Brodersen, P., Brodsky, J. L., Brody, S. L., Bronson, P. G., Bronstein, J. M., Brown, C. N., Brown, R. E., Brum, P. C., Brumell, J. H., Brunetti-Pierri, N., Bruno, D., Bryson-Richardson, R. J., Bucci, C., Buchrieser, C., Bueno, M., Buitrago-Molina, L. E., Buraschi, S., Buch, S., Buchan, J. R., Buckingham, E. M., Budak, H., Budini, M., Bultynck, G., Burada, F., Burgoyne, J. R., Buron, M. I., Bustos, V., Buttner, S., Butturini, E., Byrd, A., Cabas, I., Cabrera-Benitez, S., Cadwell, K., Cai, J., Cai, L., Cai, Q., Cairo, M., Calbet, J. A., Caldwell, G. A., Caldwell, K. A., Call, J. A., Calvani, R., Calvo, A. C., Calvo-Rubio Barrera, M., Camara, N. O., Camonis, J. H., Camougrand, N., Campanella, M., Campbell, E. M., Campbell-Valois, F. X., Campello, S., Campesi, I., Campos, J. C., Camuzard, O., Cancino, J., Candido de Almeida, D., Canesi, L., Caniggia, I., Canonico, B., Canti, C., Cao, B., Caraglia, M., Carames, B., Carchman, E. H., Cardenal-Munoz, E., Cardenas, C., Cardenas, L., Cardoso, S. M., Carew, J. S., Carle, G. F., Carleton, G., Carloni, S., Carmona-Gutierrez, D., Carneiro, L. A., Carnevali, O., Carosi, J. M., Carra, S., Carrier, A., Carrier, L., Carroll, B., Carter, A. B., Carvalho, A. N., Casanova, M., Casas, C., Casas, J., Cassioli, C., Castillo, E. F., Castillo, K., Castillo-Lluva, S., Castoldi, F., Castori, M., Castro, A. F., Castro-Caldas, M., Castro-Hernandez, J., Castro-Obregon, S., Catz, S. D., Cavadas, C., Cavaliere, F., Cavallini, G., Cavinato, M., Cayuela, M. L., Cebollada Rica, P., Cecarini, V., Cecconi, F., Cechowska-Pasko, M., Cenci, S., Ceperuelo-Mallafre, V., Cerqueira, J. J., Cerutti, J. M., Cervia, D., Cetintas, V. B., Cetrullo, S., Chae, H. J., Chagin, A. S., Chai, C. Y., Chakrabarti, G., Chakrabarti, O., Chakraborty, T., Chakraborty, T., Chami, M., Chamilos, G., Chan, D. W., Chan, E. Y. W., Chan, E. D., Chan, H. Y. E., Chan, H. H., Chan, H., Chan, M. T. V., Chan, Y. S., Chandra, P. K., Chang, C. P., Chang, C., Chang, H. C., Chang, K., Chao, J., Chapman, T., Charlet-Berguerand, N., Chatterjee, S., Chaube, S. K., Chaudhary, A., Chauhan, S., Chaum, E., Checler, F., Cheetham, M. E., Chen, C. S., Chen, G. C., Chen, J. F., Chen, L. L., Chen, L., Chen, L., Chen, M., Chen, M. K., Chen, N., Chen, Q., Chen, R. H., Chen, S., Chen, W., Chen, W., Chen, X. M., Chen, X. W., Chen, X., Chen, Y., Chen, Y. G., Chen, Y., Chen, Y., Chen, Y. J., Chen, Y. Q., Chen, Z. S., Chen, Z., Chen, Z. H., Chen, Z. J., Chen, Z., Cheng, H., Cheng, J., Cheng, S. Y., Cheng, W., Cheng, X., Cheng, X. T., Cheng, Y., Cheng, Z., Chen, Z., Cheong, H., Cheong, J. K., Chernyak, B. V., Cherry, S., Cheung, C. F. R., Cheung, C. H. A., Cheung, K. H., Chevet, E., Chi, R. J., Chiang, A. K. S., Chiaradonna, F., Chiarelli, R., Chiariello, M., Chica, N., Chiocca, S., Chiong, M., Chiou, S. H., Chiramel, A. I., Chiurchiu, V., Cho, D. H., Choe, S. K., Choi, A. M. K., Choi, M. E., Choudhury, K. R., Chow, N. S., Chu, C. T., Chua, J. P., Chua, J. J. E., Chung, H., Chung, K. P., Chung, S., Chung, S. H., Chung, Y. L., Cianfanelli, V., Ciechomska, I. A., Cifuentes, M., Cinque, L., Cirak, S., Cirone, M., Clague, M. J., Clarke, R., Clementi, E., Coccia, E. M., Codogno, P., Cohen, E., Cohen, M. M., Colasanti, T., Colasuonno, F., Colbert, R. A., Colell, A., Colic, M., Coll, N. S., Collins, M. O., Colombo, M. I., Colon-Ramos, D. A., Combaret, L., Comincini, S., Cominetti,

M. R., Consiglio, A., Conte, A., Conti, F., Contu, V. R., Cookson, M. R., Coombs, K. M., Coppens, I., Corasaniti, M. T., Corkery, D. P., Cordes, N., Cortese, K., Costa, M. D. C., Costantino, S., Costelli, P., Coto-Montes, A., Crack, P. J., Crespo, J. L., Criollo, A., Crippa, V., Cristofani, R., Csizmadia, T., Cuadrado, A., Cui, B., Cui, J., Cui, Y., Cui, Y., Culetto, E., Cumino, A. C., Cybulsky, A. V., Czaja, M. J., Czuczwar, S. J., D'Adamo, S., D'Amelio, M., D'Arcangelo, D., D'Lugos, A. C., D'Orazi, G., da Silva, J. A., Dafsari, H. S., Dagda, R. K., Dagdas, Y., Daglia, M., Dai, X., Dai, Y., Dai, Y., Dal Col, J., Dalhaimer, P., Dalla Valle, L., Dallenga, T., Dalmasso, G., Damme, M., Dando, I., Dantuma, N. P., Darling, A. L., Das, H., Dasarathy, S., Dasari, S. K., Dash, S., Daumke, O., Dauphinee, A. N., Davies, J. S., Davila, V. A., Davis, R. J., Davis, T., Dayalan Naidu, S., De Amicis, F., De Bosscher, K., De Felice, F., De Franceschi, L., De Leonibus, C., de Mattos Barbosa, M. G., De Meyer, G. R. Y., De Milito, A., De Nunzio, C., De Palma, C., De Santi, M., De Virgilio, C., De Zio, D., Debnath, J., DeBosch, B. J., Decuypere, J. P., Deehan, M. A., Deflorian, G., DeGregori, J., Dehay, B., Del Rio, G., Delaney, J. R., Delbridge, L. M. D., Delorme-Axford, E., Delpino, M. V., Demarchi, F., Dembitz, V., Demers, N. D., Deng, H., Deng, Z., Dengjel, J., Dent, P., Denton, D., DePamphilis, M. L., Der, C. J., Deretic, V., Descoteaux, A., Devis, L., Devkota, S., Devuyt, O., Dewson, G., Dharmasivam, M., Dhiman, R., di Bernardo, D., Di Cristina, M., Di Domenico, F., Di Fazio, P., Di Fonzo, A., Di Guardo, G., Di Guglielmo, G. M., Di Leo, L., Di Malta, C., Di Nardo, A., Di Rienzo, M., Di Sano, F., Diallinas, G., Diao, J., Diaz-Araya, G., Diaz-Laviada, I., Dickinson, J. M., Diederich, M., Dieude, M., Dikic, I., Ding, S., Ding, W. X., Dini, L., Dinic, J., Dinic, M., Dinkova-Kostova, A. T., Dionne, M. S., Distler, J. H. W., Diwan, A., Dixon, I. M. C., Djavaheri-Mergny, M., Dobrinski, I., Dobrovinskaya, O., Dobrowolski, R., Dobson, R. C. J., Dokic, J., Dokmeci Emre, S., Donadelli, M., Dong, B., Dong, X., Dong, Z., Dorn Li, G. W., Dotsch, V., Dou, H., Dou, J., Dowaidar, M., Dridi, S., Drucker, L., Du, A., Du, C., Du, G., Du, H. N., Du, L. L., du Toit, A., Duan, S. B., Duan, X., Duarte, S. P., Dubrovskaja, A., Dunlop, E. A., Dupont, N., Duran, R. V., Dwarakanath, B. S., Dyshlovoy, S. A., Ebrahimi-Fakhari, D., Eckhart, L., Edelstein, C. L., Efferth, T., Eftekharpour, E., Eichinger, L., Eid, N., Eisenberg, T., Eissa, N. T., Eissa, S., Ejarque, M., El Andaloussi, A., El-Hage, N., El-Naggar, S., Eleuteri, A. M., El-Shafey, E. S., Elgendy, M., Eliopoulos, A. G., Elizalde, M. M., Elks, P. M., Elsasser, H. P., Elsherbiny, E. S., Emerling, B. M., Emre, N. C. T., Eng, C. H., Engedal, N., Engelbrecht, A. M., Engelsen, A. S. T., Enserink, J. M., Escalante, R., Esclatine, A., Escobar-Henriques, M., Eskelinen, E. L., Espert, L., Eusebio, M. O., Fabrias, G., Fabrizi, C., Facchiano, A., Facchiano, F., Fadeel, B., Fader, C., Faesen, A. C., Fairlie, W. D., Falco, A., Falkenburger, B. H., Fan, D., Fan, J., Fan, Y., Fang, E. F., Fang, Y., Fang, Y., Fanto, M., Farfel-Becker, T., Faure, M., Fazeli, G., Fedele, A. O., Feldman, A. M., Feng, D., Feng, J., Feng, L., Feng, Y., Feng, Y., Feng, W., Fenz Araujo, T., Ferguson, T. A., Fernandez, A. F., Fernandez-Checa, J. C., Fernandez-Veledo, S., Fernie, A. R., Ferrante, A. W., Jr., Ferraresi, A., Ferrari, M. F., Ferreira, J. C. B., Ferro-Novick, S., Figueras, A., Filadi, R., Filigheddu, N., Filippi-Chiela, E., Filomeni, G., Fimia, G. M., Fineschi, V., Finetti, F., Finkbeiner, S., Fisher, E. A., Fisher, P. B., Flamigni, F., Fliesler, S. J., Flo, T. H., Florance, I., Florey, O., Florio, T., Fodor, E., Follo, C., Fon, E. A., Forlino, A., Fornai, F., Fortini, P., Fracassi, A., Fraldi, A., Franco, B., Franco, R., Franconi, F., Frankel, L. B., Friedman, S. L., Frohlich, L. F., Fruhbeck, G., Fuentes, J. M., Fujiki, Y., Fujita, N., Fujiwara, Y., Fukuda, M., Fulda, S., Furic, L., Furuya, N., Fusco, C., Gack, M. U., Gaffke, L., Galadari, S., Galasso, A., Galindo, M. F., Gallolu Kankanamalage, S., Galluzzi, L., Galy, V., Gammoh, N., Gan, B., Ganley, I. G., Gao, F., Gao, H., Gao, M., Gao, P., Gao, S. J., Gao, W., Gao, X., Garcera, A.,

Garcia, M. N., Garcia, V. E., Garcia-Del Portillo, F., Garcia-Escudero, V., Garcia-Garcia, A., Garcia-Macia, M., Garcia-Moreno, D., Garcia-Ruiz, C., Garcia-Sanz, P., Garg, A. D., Gargini, R., Garofalo, T., Garry, R. F., Gassen, N. C., Gatica, D., Ge, L., Ge, W., Geiss-Friedlander, R., Gelfi, C., Genschik, P., Gentle, I. E., Gerbino, V., Gerhardt, C., Germain, K., Germain, M., Gewirtz, D. A., Ghasemipour Afshar, E., Ghavami, S., Ghigo, A., Ghosh, M., Giamas, G., Giampietri, C., Giatromanolaki, A., Gibson, G. E., Gibson, S. B., Ginet, V., Giniger, E., Giorgi, C., Girao, H., Girardin, S. E., Giridharan, M., Giuliano, S., Giulivi, C., Giuriato, S., Giustiniani, J., Gluschko, A., Goder, V., Goginashvili, A., Golab, J., Goldstone, D. C., Golebiewska, A., Gomes, L. R., Gomez, R., Gomez-Sanchez, R., Gomez-Puerto, M. C., Gomez-Sintes, R., Gong, Q., Goni, F. M., Gonzalez-Gallego, J., Gonzalez-Hernandez, T., Gonzalez-Polo, R. A., Gonzalez-Reyes, J. A., Gonzalez-Rodriguez, P., Goping, I. S., Gorbatyuk, M. S., Gorbunov, N. V., Gorgulu, K., Gorojod, R. M., Gorski, S. M., Goruppi, S., Gotor, C., Gottlieb, R. A., Gozes, I., Gozuacik, D., Graef, M., Graler, M. H., Granatiero, V., Grasso, D., Gray, J. P., Green, D. R., Greenhough, A., Gregory, S. L., Griffin, E. F., Grinstaff, M. W., Gros, F., Grose, C., Gross, A. S., Gruber, F., Grumati, P., Grune, T., Gu, X., Guan, J. L., Guardia, C. M., Guda, K., Guerra, F., Guerri, C., Guha, P., Guillen, C., Gujar, S., Gukovskaya, A., Gukovsky, I., Gunst, J., Gunther, A., Guntur, A. R., Guo, C., Guo, C., Guo, H., Guo, L. W., Guo, M., Gupta, P., Gupta, S. K., Gupta, S., Gupta, V. B., Gupta, V., Gustafsson, A. B., Gutterman, D. D., H, B. R., Haapasalo, A., Haber, J. E., Hac, A., Hadano, S., Hafren, A. J., Haidar, M., Hall, B. S., Hallden, G., Hamacher-Brady, A., Hamann, A., Hamasaki, M., Han, W., Hansen, M., Hanson, P. I., Hao, Z., Harada, M., Harhaji-Trajkovic, L., Hariharan, N., Haroon, N., Harris, J., Hasegawa, T., Hasima Nagoor, N., Haspel, J. A., Haucke, V., Hawkins, W. D., Hay, B. A., Haynes, C. M., Hayrabyan, S. B., Hays, T. S., He, C., He, Q., He, R. R., He, Y. W., He, Y. Y., Heakal, Y., Heberle, A. M., Hejtmancik, J. F., Helgason, G. V., Henkel, V., Herb, M., Hergovich, A., Herman-Antosiewicz, A., Hernandez, A., Hernandez, C., Hernandez-Diaz, S., Hernandez-Gea, V., Herpin, A., Herreros, J., Hervas, J. H., Hesselson, D., Hetz, C., Heussler, V. T., Higuchi, Y., Hilfiker, S., Hill, J. A., Hlavacek, W. S., Ho, E. A., Ho, I. H. T., Ho, P. W., Ho, S. L., Ho, W. Y., Hobbs, G. A., Hochstrasser, M., Hoet, P. H. M., Hofius, D., Hofman, P., Hohn, A., Holmberg, C. I., Hombrebueno, J. R., Yi-Ren Hong, C. H., Hooper, L. V., Hoppe, T., Horos, R., Hoshida, Y., Hsin, I. L., Hsu, H. Y., Hu, B., Hu, D., Hu, L. F., Hu, M. C., Hu, R., Hu, W., Hu, Y. C., Hu, Z. W., Hua, F., Hua, J., Hua, Y., Huan, C., Huang, C., Huang, C., Huang, C., Huang, C., Huang, H., Huang, K., Huang, M. L. H., Huang, R., Huang, S., Huang, T., Huang, X., Huang, Y. J., Huber, T. B., Hubert, V., Hubner, C. A., Hughes, S. M., Hughes, W. E., Humbert, M., Hummer, G., Hurley, J. H., Hussain, S., Hussain, S., Hussey, P. J., Hutabarat, M., Hwang, H. Y., Hwang, S., Ieni, A., Ikeda, F., Imagawa, Y., Imai, Y., Imbriano, C., Imoto, M., Inman, D. M., Inoki, K., Iovanna, J., Iozzo, R. V., Ippolito, G., Irazoqui, J. E., Iribarren, P., Ishaq, M., Ishikawa, M., Ishimwe, N., Isidoro, C., Ismail, N., Issazadeh-Navikas, S., Itakura, E., Ito, D., Ivankovic, D., Ivanova, S., Iyer, A. K. V., Izquierdo, J. M., Izumi, M., Jaattela, M., Jabir, M. S., Jackson, W. T., Jacobo-Herrera, N., Jacomin, A. C., Jacquin, E., Jadiya, P., Jaeschke, H., Jagannath, C., Jakobi, A. J., Jakobsson, J., Janji, B., Jansen-Durr, P., Jansson, P. J., Jantsch, J., Januszewski, S., Jasse, A., Jean, S., Jeltsch-David, H., Jendelova, P., Jenny, A., Jensen, T. E., Jessen, N., Jewell, J. L., Ji, J., Jia, L., Jia, R., Jiang, L., Jiang, Q., Jiang, R., Jiang, T., Jiang, X., Jiang, Y., Jimenez-Sanchez, M., Jin, E. J., Jin, F., Jin, H., Jin, L., Jin, L., Jin, M., Jin, S., Jo, E. K., Joffre, C., Johansen, T., Johnson, G. V. W., Johnston, S. A., Jokitalo, E., Jolly, M. K., Joosten, L. A. B., Jordan, J., Joseph, B., Ju, D., Ju, J. S., Ju, J., Juarez, E., Judith, D., Juhasz, G., Jun, Y., Jung, C. H., Jung, S. C.,

Jung, Y. K., Jungbluth, H., Jungverdorben, J., Just, S., Kaarniranta, K., Kaasik, A., Kabuta, T., Kaganovich, D., Kahana, A., Kain, R., Kajimura, S., Kalamvoki, M., Kalia, M., Kalinowski, D. S., Kaludercic, N., Kalvari, I., Kaminska, J., Kaminsky, V. O., Kanamori, H., Kanasaki, K., Kang, C., Kang, R., Kang, S. S., Kaniyappan, S., Kanki, T., Kanneganti, T. D., Kanthasamy, A. G., Kanthasamy, A., Kantorow, M., Kapuy, O., Karamouzis, M. V., Karim, M. R., Karmakar, P., Katare, R. G., Kato, M., Kaufmann, S. H. E., Kauppinen, A., Kaushal, G. P., Kaushik, S., Kawasaki, K., Kazan, K., Ke, P. Y., Keating, D. J., Keber, U., Kehrl, J. H., Keller, K. E., Keller, C. W., Kemper, J. K., Kenific, C. M., Kepp, O., Kermorgant, S., Kern, A., Ketteler, R., Keulers, T. G., Khalfin, B., Khalil, H., Khambu, B., Khan, S. Y., Khandelwal, V. K. M., Khandia, R., Kho, W., Khobreakar, N. V., Khuansuwan, S., Khundadze, M., Killackey, S. A., Kim, D., Kim, D. R., Kim, D. H., Kim, D. E., Kim, E. Y., Kim, E. K., Kim, H. R., Kim, H. S., Hyung-Ryong, K., Kim, J. H., Kim, J. K., Kim, J. H., Kim, J., Kim, J. H., Kim, K. I., Kim, P. K., Kim, S. J., Kimball, S. R., Kimchi, A., Kimmelman, A. C., Kimura, T., King, M. A., Kinghorn, K. J., Kinsey, C. G., Kirkin, V., Kirshenbaum, L. A., Kiselev, S. L., Kishi, S., Kitamoto, K., Kitaoka, Y., Kitazato, K., Kitsis, R. N., Kittler, J. T., Kjaerulff, O., Klein, P. S., Klopstock, T., Klucken, J., Knaevelsrud, H., Knorr, R. L., Ko, B. C. B., Ko, F., Ko, J. L., Kobayashi, H., Kobayashi, S., Koch, I., Koch, J. C., Koenig, U., Kogel, D., Koh, Y. H., Koike, M., Kohlwein, S. D., Kocaturk, N. M., Komatsu, M., Konig, J., Kono, T., Kopp, B. T., Korcsmaros, T., Korkmaz, G., Korolchuk, V. I., Korsnes, M. S., Koskela, A., Kota, J., Kotake, Y., Kotler, M. L., Kou, Y., Koukourakis, M. I., Koustas, E., Kovacs, A. L., Kovacs, T., Koya, D., Kozako, T., Kraft, C., Krainc, D., Kramer, H., Krasnodembskaya, A. D., Kretz-Remy, C., Kroemer, G., Ktistakis, N. T., Kuchitsu, K., Kuenen, S., Kuerschner, L., Kukar, T., Kumar, A., Kumar, A., Kumar, D., Kumar, D., Kumar, S., Kume, S., Kumsta, C., Kundu, C. N., Kundu, M., Kunnumakkara, A. B., Kurgan, L., Kutateladze, T. G., Kutlu, O., Kwak, S., Kwon, H. J., Kwon, T. K., Kwon, Y. T., Kyrmizi, I., La Spada, A., Labonte, P., Ladoire, S., Laface, I., Lafont, F., Lagace, D. C., Lahiri, V., Lai, Z., Laird, A. S., Lakkaraju, A., Lamark, T., Lan, S. H., Landajuela, A., Lane, D. J. R., Lane, J. D., Lang, C. H., Lange, C., Langel, U., Langer, R., Lapaquette, P., Laporte, J., LaRusso, N. F., Lastres-Becker, I., Lau, W. C. Y., Laurie, G. W., Lavandero, S., Law, B. Y. K., Law, H. K., Layfield, R., Le, W., Le Stunff, H., Leary, A. Y., Lebrun, J. J., Leck, L. Y. W., Leduc-Gaudet, J. P., Lee, C., Lee, C. P., Lee, D. H., Lee, E. B., Lee, E. F., Lee, G. M., Lee, H. J., Lee, H. K., Lee, J. M., Lee, J. S., Lee, J. A., Lee, J. Y., Lee, J. H., Lee, M., Lee, M. G., Lee, M. J., Lee, M. S., Lee, S. Y., Lee, S. J., Lee, S. Y., Lee, S. B., Lee, W. H., Lee, Y. R., Lee, Y. H., Lee, Y., Lefebvre, C., Legouis, R., Lei, Y. L., Lei, Y., Leikin, S., Leitinger, G., Lemus, L., Leng, S., Lenoir, O., Lenz, G., Lenz, H. J., Lenzi, P., Leon, Y., Leopoldino, A. M., Leschczyk, C., Leskela, S., Letellier, E., Leung, C. T., Leung, P. S., Leventhal, J. S., Levine, B., Lewis, P. A., Ley, K., Li, B., Li, D. Q., Li, J., Li, J., Li, J., Li, K., Li, L., Li, M., Li, M., Li, M., Li, M., Li, M., Li, P. L., Li, M. Q., Li, Q., Li, S., Li, T., Li, W., Li, W., Li, X., Li, Y. P., Li, Y., Li, Z., Li, Z., Li, Z., Lian, J., Liang, C., Liang, Q., Liang, W., Liang, Y., Liang, Y., Liao, G., Liao, L., Liao, M., Liao, Y. F., Librizzi, M., Lie, P. P. Y., Lilly, M. A., Lim, H. J., Lima, T. R. R., Limana, F., Lin, C., Lin, C. W., Lin, D. S., Lin, F. C., Lin, J. D., Lin, K. M., Lin, K. H., Lin, L. T., Lin, P. H., Lin, Q., Lin, S., Lin, S. J., Lin, W., Lin, X., Lin, Y. X., Lin, Y. S., Linden, R., Lindner, P., Ling, S. C., Lingor, P., Linnemann, A. K., Liou, Y. C., Lipinski, M. M., Lipovsek, S., Lira, V. A., Lisiak, N., Liton, P. B., Liu, C., Liu, C. H., Liu, C. F., Liu, C. H., Liu, F., Liu, H., Liu, H. S., Liu, H. F., Liu, H., Liu, J., Liu, J., Liu, J., Liu, L., Liu, L., Liu, M., Liu, Q., Liu, W., Liu, W., Liu, X. H., Liu, X., Liu, X., Liu, X., Liu, X., Liu, Y., Liu, Y., Liu, Y., Liu, Y., Livingston, J. A., Lizard, G., Lizcano, J. M.,

Ljubojevic-Holzer, S., ME, L. L., Llobet-Navas, D., Llorente, A., Lo, C. H., Lobato-Marquez, D., Long, Q., Long, Y. C., Loos, B., Loos, J. A., Lopez, M. G., Lopez-Domenech, G., Lopez-Guerrero, J. A., Lopez-Jimenez, A. T., Lopez-Perez, O., Lopez-Valero, I., Lorenowicz, M. J., Lorente, M., Lorincz, P., Lossi, L., Lotersztajn, S., Lovat, P. E., Lovell, J. F., Lovy, A., Low, P., Lu, G., Lu, H., Lu, J. H., Lu, J. J., Lu, M., Lu, S., Luciani, A., Lucocq, J. M., Ludovico, P., Luftig, M. A., Luhr, M., Luis-Ravelo, D., Lum, J. J., Luna-Dulcey, L., Lund, A. H., Lund, V. K., Lunemann, J. D., Luningschor, P., Luo, H., Luo, R., Luo, S., Luo, Z., Luparello, C., Luscher, B., Luu, L., Lyakhovich, A., Lyamzaev, K. G., Lystad, A. H., Lytvynchuk, L., Ma, A. C., Ma, C., Ma, M., Ma, N. F., Ma, Q. H., Ma, X., Ma, Y., Ma, Z., MacDougald, O. A., Macian, F., MacIntosh, G. C., MacKeigan, J. P., Macleod, K. F., Maday, S., Madeo, F., Madesh, M., Madl, T., Madrigal-Matute, J., Maeda, A., Maejima, Y., Magarinos, M., Mahavadi, P., Maiani, E., Maiese, K., Maiti, P., Maiuri, M. C., Majello, B., Major, M. B., Makareeva, E., Malik, F., Mallilankaraman, K., Malorni, W., Maloyan, A., Mammadova, N., Man, G. C. W., Manai, F., Mancias, J. D., Mandelkow, E. M., Mandell, M. A., Manfredi, A. A., Manjili, M. H., Manjithaya, R., Manque, P., Manshian, B. B., Manzano, R., Manzoni, C., Mao, K., Marchese, C., Marchetti, S., Marconi, A. M., Marcucci, F., Mardente, S., Mareninova, O. A., Margeta, M., Mari, M., Marinelli, S., Marinelli, O., Marino, G., Mariotto, S., Marshall, R. S., Marten, M. R., Martens, S., Martin, A. P. J., Martin, K. R., Martin, S., Martin, S., Martin-Segura, A., Martin-Acebes, M. A., Martin-Burriel, I., Martin-Rincon, M., Martin-Sanz, P., Martina, J. A., Martinet, W., Martinez, A., Martinez, A., Martinez, J., Martinez Velazquez, M., Martinez-Lopez, N., Martinez-Vicente, M., Martins, D. O., Martins, J. O., Martins, W. K., Martins-Marques, T., Marzetti, E., Masaldan, S., Masclaux-Daubresse, C., Mashek, D. G., Massa, V., Massieu, L., Masson, G. R., Masuelli, L., Masyuk, A. I., Masyuk, T. V., Matarrese, P., Matheu, A., Matoba, S., Matsuzaki, S., Mattar, P., Matte, A., Mattoscio, D., Mauriz, J. L., Mauthe, M., Mauvezin, C., Maverakis, E., Maycotte, P., Mayer, J., Mazzocchi, G., Mazzoni, C., Mazzulli, J. R., McCarty, N., McDonald, C., McGill, M. R., McKenna, S. L., McLaughlin, B., McLoughlin, F., McNiven, M. A., McWilliams, T. G., Mehta-Grigoriou, F., Medeiros, T. C., Medina, D. L., Megeney, L. A., Megyeri, K., Mehrpour, M., Mehta, J. L., Meijer, A. J., Meijer, A. H., Mejlvang, J., Melendez, A., Melk, A., Memisoglu, G., Mendes, A. F., Meng, D., Meng, F., Meng, T., Menna-Barreto, R., Menon, M. B., Mercer, C., Mercier, A. E., Mergny, J. L., Merighi, A., Merkle, S. D., Merla, G., Meske, V., Mestre, A. C., Metur, S. P., Meyer, C., Meyer, H., Mi, W., Miale-Perez, J., Miao, J., Micale, L., Miki, Y., Milan, E., Milczarek, M., Miller, D. L., Miller, S. I., Miller, S., Millward, S. W., Milosevic, I., Minina, E. A., Mirzaei, H., Mirzaei, H. R., Mirzaei, M., Mishra, A., Mishra, N., Mishra, P. K., Misirkic Marjanovic, M., Misasi, R., Misra, A., Misso, G., Mitchell, C., Mitou, G., Miura, T., Miyamoto, S., Miyazaki, M., Miyazaki, M., Miyazaki, T., Miyazawa, K., Mizushima, N., Mogensen, T. H., Mograbi, B., Mohammadinejad, R., Mohamud, Y., Mohanty, A., Mohapatra, S., Mohlmann, T., Mohammed, A., Moles, A., Moley, K. H., Molinari, M., Mollace, V., Moller, A. B., Mollereau, B., Mollinedo, F., Montagna, C., Monteiro, M. J., Montella, A., Montes, L. R., Montico, B., Mony, V. K., Monzio Compagnoni, G., Moore, M. N., Moosavi, M. A., Mora, A. L., Mora, M., Morales-Alamo, D., Moratalla, R., Moreira, P. I., Morelli, E., Moreno, S., Moreno-Blas, D., Moresi, V., Morga, B., Morgan, A. H., Morin, F., Morishita, H., Moritz, O. L., Moriyama, M., Moriyasu, Y., Morleo, M., Morselli, E., Moruno-Manchon, J. F., Moscat, J., Mostowy, S., Motori, E., Moura, A. F., Moustaid-Moussa, N., Mrakovcic, M., Mucino-Hernandez, G., Mukherjee, A., Mukhopadhyay, S., Mulcahy Levy, J. M., Mulero, V., Muller, S., Munch, C., Munjal, A., Munoz-Canoves, P., Munoz-Galdeano, T., Munz, C.,

Murakawa, T., Muratori, C., Murphy, B. M., Murphy, J. P., Murthy, A., Myohanen, T. T., Mysorekar, I. U., Mytych, J., Nabavi, S. M., Nabissi, M., Nagy, P., Nah, J., Nahimana, A., Nakagawa, I., Nakamura, K., Nakatogawa, H., Nandi, S. S., Nanjundan, M., Nanni, M., Napolitano, G., Nardacci, R., Narita, M., Nassif, M., Nathan, I., Natsumeda, M., Naude, R. J., Naumann, C., Naveiras, O., Navid, F., Nawrocki, S. T., Nazarko, T. Y., Nazio, F., Negoita, F., Neill, T., Neisch, A. L., Neri, L. M., Netea, M. G., Neubert, P., Neufeld, T. P., Neumann, D., Neutzner, A., Newton, P. T., Ney, P. A., Nezis, I. P., Ng, C. C. W., Ng, T. B., Nguyen, H. T. T., Nguyen, L. T., Ni, H. M., Ni Cheallaigh, C., Ni, Z., Nicolao, M. C., Nicoli, F., Nieto-Diaz, M., Nilsson, P., Ning, S., Niranjan, R., Nishimune, H., Niso-Santano, M., Nixon, R. A., Nobili, A., Nobrega, C., Noda, T., Nogueira-Recalde, U., Nolan, T. M., Nombela, I., Novak, I., Novoa, B., Nozawa, T., Nukina, N., Nussbaum-Krammer, C., Nylandsted, J., O'Donovan, T. R., O'Leary, S. M., O'Rourke, E. J., O'Sullivan, M. P., O'Sullivan, T. E., Oddo, S., Oehme, I., Ogawa, M., Ogier-Denis, E., Ogmundsdottir, M. H., Ogretmen, B., Oh, G. T., Oh, S. H., Oh, Y. J., Ohama, T., Ohashi, Y., Ohmuraya, M., Oikonomou, V., Ojha, R., Okamoto, K., Okazawa, H., Oku, M., Oliven, S., Oliveira, J. M. A., Ollmann, M., Olzmann, J. A., Omari, S., Omary, M. B., Onal, G., Ondrej, M., Ong, S. B., Ong, S. G., Onnis, A., Orellana, J. A., Orellana-Munoz, S., Ortega-Villaizan, M. D. M., Ortiz-Gonzalez, X. R., Ortona, E., Osiewacz, H. D., Osman, A. K., Osta, R., Otegui, M. S., Otsu, K., Ott, C., Ottobriani, L., Ou, J. J., Outeiro, T. F., Oynebraten, I., Ozturk, M., Pages, G., Pahari, S., Pajares, M., Pajvani, U. B., Pal, R., Paladino, S., Pallet, N., Palmieri, M., Palmisano, G., Palumbo, C., Pampaloni, F., Pan, L., Pan, Q., Pan, W., Pan, X., Panasyuk, G., Pandey, R., Pandey, U. B., Pandya, V., Paneni, F., Pang, S. Y., Panzarini, E., Papademetrio, D. L., Papaleo, E., Papinski, D., Papp, D., Park, E. C., Park, H. T., Park, J. M., Park, J. I., Park, J. T., Park, J., Park, S. C., Park, S. Y., Parola, A. H., Parys, J. B., Pasquier, A., Pasquier, B., Passos, J. F., Pastore, N., Patel, H. H., Patschan, D., Pattingre, S., Pedraza-Alva, G., Pedraza-Chaverri, J., Pedrozo, Z., Pei, G., Pei, J., Peled-Zehavi, H., Pellegrini, J. M., Pelletier, J., Penalva, M. A., Peng, D., Peng, Y., Penna, F., Pennuto, M., Pentimalli, F., Pereira, C. M., Pereira, G. J. S., Pereira, L. C., Pereira de Almeida, L., Perera, N. D., Perez-Lara, A., Perez-Oliva, A. B., Perez-Perez, M. E., Periyasamy, P., Perl, A., Perrotta, C., Perrotta, I., Pestell, R. G., Petersen, M., Petrache, I., Petrovski, G., Pfirrmann, T., Pfister, A. S., Philips, J. A., Pi, H., Picca, A., Pickrell, A. M., Picot, S., Pierantoni, G. M., Pierdominici, M., Pierre, P., Pierrefite-Carle, V., Pierzynowska, K., Pietrocola, F., Pietruczuk, M., Pignata, C., Pimentel-Muinos, F. X., Pinar, M., Pinheiro, R. O., Pinkas-Kramarski, R., Pinton, P., Pircs, K., Piya, S., Pizzo, P., Plantinga, T. S., Platta, H. W., Plaza-Zabala, A., Plomann, M., Plotnikov, E. Y., Plun-Favreau, H., Pluta, R., Pocock, R., Poggeler, S., Pohl, C., Poirot, M., Poletti, A., Ponpuak, M., Popelka, H., Popova, B., Porta, H., Porte Alcon, S., Portilla-Fernandez, E., Post, M., Potts, M. B., Poulton, J., Powers, T., Prahlad, V., Prajsnar, T. K., Pratico, D., Prencipe, R., Priault, M., Proikas-Cezanne, T., Promponas, V. J., Proud, C. G., Puertollano, R., Puglielli, L., Pulinilkunnil, T., Puri, D., Puri, R., Puyal, J., Qi, X., Qi, Y., Qian, W., Qiang, L., Qiu, Y., Quadrilatero, J., Quarleri, J., Raben, N., Rabinowich, H., Ragona, D., Ragusa, M. J., Rahimi, N., Rahmati, M., Raia, V., Raimundo, N., Rajasekaran, N. S., Ramachandra Rao, S., Rami, A., Ramirez-Pardo, I., Ramsden, D. B., Randow, F., Rangarajan, P. N., Ranieri, D., Rao, H., Rao, L., Rao, R., Rathore, S., Ratnayaka, J. A., Ratovitski, E. A., Ravanan, P., Ravegnini, G., Ray, S. K., Razani, B., Rebecca, V., Reggiori, F., Regnier-Vigouroux, A., Reichert, A. S., Reigada, D., Reiling, J. H., Rein, T., Reipert, S., Rekha, R. S., Ren, H., Ren, J., Ren, W., Renault, T., Renga, G., Reue, K., Rewitz, K., Ribeiro de Andrade Ramos, B., Riazuddin, S. A., Ribeiro-Rodrigues, T. M., Ricci, J. E., Ricci, R., Riccio, V.,

Richardson, D. R., Rikihisa, Y., Risbud, M. V., Risueno, R. M., Ritis, K., Rizza, S., Rizzuto, R., Roberts, H. C., Roberts, L. D., Robinson, K. J., Roccheri, M. C., Rocchi, S., Rodney, G. G., Rodrigues, T., Rodrigues Silva, V. R., Rodriguez, A., Rodriguez-Barrueco, R., Rodriguez-Henche, N., Rodriguez-Rocha, H., Roelofs, J., Rogers, R. S., Rogov, V. V., Rojo, A. I., Rolka, K., Romanello, V., Romani, L., Romano, A., Romano, P. S., Romeo-Guitart, D., Romero, L. C., Romero, M., Roney, J. C., Rongo, C., Roperto, S., Rosenfeldt, M. T., Rosenstiel, P., Rosenwald, A. G., Roth, K. A., Roth, L., Roth, S., Rouschop, K. M. A., Roussel, B. D., Roux, S., Rovere-Querini, P., Roy, A., Rozieres, A., Ruano, D., Rubinsztein, D. C., Rubtsova, M. P., Ruckdeschel, K., Ruckenstuhl, C., Rudolf, E., Rudolf, R., Ruggieri, A., Ruparelia, A. A., Rusmini, P., Russell, R. R., Russo, G. L., Russo, M., Russo, R., Ryabaya, O. O., Ryan, K. M., Ryu, K. Y., Sabater-Arcis, M., Sachdev, U., Sacher, M., Sachse, C., Sadhu, A., Sadoshima, J., Safren, N., Saftig, P., Sagona, A. P., Sahay, G., Sahebkar, A., Sahin, M., Sahin, O., Sahni, S., Saito, N., Saito, S., Saito, T., Sakai, R., Sakai, Y., Sakamaki, J. I., Saksela, K., Salazar, G., Salazar-Degracia, A., Salekdeh, G. H., Saluja, A. K., Sampaio-Marques, B., Sanchez, M. C., Sanchez-Alcazar, J. A., Sanchez-Vera, V., Sancho-Shimizu, V., Sanderson, J. T., Sandri, M., Santaguida, S., Santambrogio, L., Santana, M. M., Santoni, G., Sanz, A., Sanz, P., Saran, S., Sardiello, M., Sargeant, T. J., Sarin, A., Sarkar, C., Sarkar, S., Sarrias, M. R., Sarkar, S., Sarmah, D. T., Sarparanta, J., Sathyanarayan, A., Sathyanarayanan, R., Scaglione, K. M., Scatozza, F., Schaefer, L., Schafer, Z. T., Schaible, U. E., Schapira, A. H. V., Scharl, M., Schatzl, H. M., Schein, C. H., Scheper, W., Scheuring, D., Schiaffino, M. V., Schiappacassi, M., Schindl, R., Schlattner, U., Schmidt, O., Schmitt, R., Schmidt, S. D., Schmitz, I., Schmukler, E., Schneider, A., Schneider, B. E., Schober, R., Schoijet, A. C., Schott, M. B., Schramm, M., Schroder, B., Schuh, K., Schuller, C., Schulze, R. J., Schurmanns, L., Schwamborn, J. C., Schwarten, M., Scialo, F., Sciarretta, S., Scott, M. J., Scotto, K. W., Scovassi, A. I., Scrima, A., Scrivo, A., Sebastian, D., Sebti, S., Sedej, S., Segatori, L., Segev, N., Seglen, P. O., Seiliez, I., Seki, E., Selleck, S. B., Sellke, F. W., Selsby, J. T., Sendtner, M., Senturk, S., Seranova, E., Sergi, C., Serra-Moreno, R., Sesaki, H., Settembre, C., Setty, S. R. G., Sgarbi, G., Sha, O., Shacka, J. J., Shah, J. A., Shang, D., Shao, C., Shao, F., Sharbati, S., Sharkey, L. M., Sharma, D., Sharma, G., Sharma, K., Sharma, P., Sharma, S., Shen, H. M., Shen, H., Shen, J., Shen, M., Shen, W., Shen, Z., Sheng, R., Sheng, Z., Sheng, Z. H., Shi, J., Shi, X., Shi, Y. H., Shiba-Fukushima, K., Shieh, J. J., Shimada, Y., Shimizu, S., Shimosawa, M., Shintani, T., Shoemaker, C. J., Shojaei, S., Shoji, I., Shrivage, B. V., Shridhar, V., Shu, C. W., Shu, H. B., Shui, K., Shukla, A. K., Shutt, T. E., Sica, V., Siddiqui, A., Sierra, A., Sierra-Torre, V., Signorelli, S., Sil, P., Silva, B. J. A., Silva, J. D., Silva-Pavez, E., Silvente-Poirot, S., Simmonds, R. E., Simon, A. K., Simon, H. U., Simons, M., Singh, A., Singh, L. P., Singh, R., Singh, S. V., Singh, S. K., Singh, S. B., Singh, S., Singh, S. P., Sinha, D., Sinha, R. A., Sinha, S., Sirko, A., Sirohi, K., Sivridis, E. L., Skendros, P., Skiryecz, A., Slaninova, I., Smaili, S. S., Smertenko, A., Smith, M. D., Soenen, S. J., Sohn, E. J., Sok, S. P. M., Solaini, G., Soldati, T., Soleimanpour, S. A., Soler, R. M., Solovchenko, A., Somarelli, J. A., Sonawane, A., Song, F., Song, H. K., Song, J. X., Song, K., Song, Z., Soria, L. R., Sorice, M., Soukas, A. A., Soukup, S. F., Sousa, D., Sousa, N., Spagnuolo, P. A., Spector, S. A., Srinivas Bharath, M. M., St Clair, D., Stagni, V., Staiano, L., Stalneck, C. A., Stankov, M. V., Stathopoulos, P. B., Stefan, K., Stefan, S. M., Stefanis, L., Steffan, J. S., Steinkasserer, A., Stenmark, H., Sternecker, J., Stevens, C., Stoka, V., Storch, S., Stork, B., Strappazzon, F., Strohecker, A. M., Stupack, D. G., Su, H., Su, L. Y., Su, L., Suarez-Fontes, A. M., Subauste, C. S., Subbian, S., Subirada, P. V., Sudhandiran, G., Sue, C. M., Sui, X., Summers, C., Sun, G., Sun, J., Sun, K., Sun, M. X., Sun, Q., Sun,

Y., Sun, Z., Sunahara, K. K. S., Sundberg, E., Susztak, K., Sutovsky, P., Suzuki, H., Sweeney, G., Symons, J. D., Sze, S. C. W., Szewczyk, N. J., Tabecka-Lonczynska, A., Tabolacci, C., Tacke, F., Taegtmeier, H., Tafani, M., Tagaya, M., Tai, H., Tait, S. W. G., Takahashi, Y., Takats, S., Talwar, P., Tam, C., Tam, S. Y., Tampellini, D., Tamura, A., Tan, C. T., Tan, E. K., Tan, Y. Q., Tanaka, M., Tanaka, M., Tang, D., Tang, J., Tang, T. S., Tanida, I., Tao, Z., Taouis, M., Tatenhorst, L., Tavernarakis, N., Taylor, A., Taylor, G. A., Taylor, J. M., Tchetina, E., Tee, A. R., Tegeder, I., Teis, D., Teixeira, N., Teixeira-Clerc, F., Tekirdag, K. A., Tencomnao, T., Tenreiro, S., Tepikin, A. V., Testillano, P. S., Tettamanti, G., Tharoux, P. L., Thedieck, K., Thekkinghat, A. A., Thellung, S., Thinwa, J. W., Thirumalaikumar, V. P., Thomas, S. M., Thomes, P. G., Thorburn, A., Thukral, L., Thum, T., Thumm, M., Tian, L., Tichy, A., Till, A., Timmerman, V., Titorenko, V. I., Todi, S. V., Todorova, K., Toivonen, J. M., Tomaipitnca, L., Tomar, D., Tomas-Zapico, C., Tomic, S., Tong, B. C., Tong, C., Tong, X., Tooze, S. A., Torgersen, M. L., Torii, S., Torres-Lopez, L., Torriglia, A., Towers, C. G., Towns, R., Toyokuni, S., Trajkovic, V., Tramontano, D., Tran, Q. G., Travassos, L. H., Trelford, C. B., Tremel, S., Trougakos, I. P., Tsao, B. P., Tschan, M. P., Tse, H. F., Tse, T. F., Tsugawa, H., Tsvetkov, A. S., Tumbarello, D. A., Tumtas, Y., Tunon, M. J., Turcotte, S., Turk, B., Turk, V., Turner, B. J., Tuxworth, R. I., Tyler, J. K., Tyutereva, E. V., Uchiyama, Y., Ugun-Klusek, A., Uhlig, H. H., Ulamek-Koziol, M., Ulasov, I. V., Umekawa, M., Ungermann, C., Unno, R., Urbe, S., Uribe-Carretero, E., Ustun, S., Uversky, V. N., Vaccari, T., Vaccaro, M. I., Vahsen, B. F., Vakifahmetoglu-Norberg, H., Valdor, R., Valente, M. J., Valko, A., Vallee, R. B., Valverde, A. M., Van den Berghe, G., van der Veen, S., Van Kaer, L., van Loosdregt, J., van Wijk, S. J. L., Vandenberghe, W., Vanhorebeek, I., Vannier-Santos, M. A., Vannini, N., Vanrell, M. C., Vantaggiato, C., Varano, G., Varela-Nieto, I., Varga, M., Vasconcelos, M. H., Vats, S., Vavvas, D. G., Vega-Naredo, I., Vega-Rubin-de-Celis, S., Velasco, G., Velazquez, A. P., Vellai, T., Vellenga, E., Velotti, F., Verdier, M., Verginis, P., Vergne, I., Verkade, P., Verma, M., Verstreken, P., Vervliet, T., Vervoorts, J., Vessoni, A. T., Victor, V. M., Vidal, M., Vidoni, C., Vieira, O. V., Vierstra, R. D., Viganò, S., Vihinen, H., Vijayan, V., Vila, M., Vilar, M., Villalba, J. M., Villalobo, A., Villarejo-Zori, B., Villarroya, F., Villarroya, J., Vincent, O., Vindis, C., Viret, C., Viscomi, M. T., Visnjic, D., Vitale, I., Vocadlo, D. J., Voitsekhevskaja, O. V., Volonte, C., Volta, M., Vomero, M., Von Haefen, C., Vooijs, M. A., Voos, W., Vucicevic, L., Wade-Martins, R., Waguri, S., Waite, K. A., Wakatsuki, S., Walker, D. W., Walker, M. J., Walker, S. A., Walter, J., Wandosell, F. G., Wang, B., Wang, C. Y., Wang, C., Wang, C., Wang, C., Wang, C. Y., Wang, D., Wang, F., Wang, F., Wang, F., Wang, G., Wang, H., Wang, H., Wang, H., Wang, H. G., Wang, J., Wang, J., Wang, J., Wang, J., Wang, K., Wang, L., Wang, L., Wang, M. H., Wang, M., Wang, N., Wang, P., Wang, P., Wang, P., Wang, P., Wang, Q. J., Wang, Q., Wang, Q. K., Wang, Q. A., Wang, W. T., Wang, W., Wang, X., Wang, X., Wang, Y., Wang, Y., Wang, Y., Wang, Y. Y., Wang, Y., Wang, Y., Wang, Y., Wang, Y., Wang, Z., Wang, Z., Wang, Z., Warnes, G., Warnsmann, V., Watada, H., Watanabe, E., Watchon, M., Wawrzynska, A., Weaver, T. E., Wegrzyn, G., Wehman, A. M., Wei, H., Wei, L., Wei, T., Wei, Y., Weiergraber, O. H., Weihl, C. C., Weindl, G., Weiskirchen, R., Wells, A., Wen, R. H., Wen, X., Werner, A., Weykopf, B., Wheatley, S. P., Whitton, J. L., Whitworth, A. J., Wiktorska, K., Wildenberg, M. E., Wileman, T., Wilkinson, S., Willbold, D., Williams, B., Williams, R. S. B., Williams, R. L., Williamson, P. R., Wilson, R. A., Winner, B., Winsor, N. J., Witkin, S. S., Wodrich, H., Woehlbier, U., Wollert, T., Wong, E., Wong, J. H., Wong, R. W., Wong, V. K. W., Wong, W. W., Wu, A. G., Wu, C., Wu, J., Wu, J., Wu, K. K., Wu, M., Wu, S. Y., Wu, S., Wu, S. Y., Wu, S., Wu, W. K. K., Wu, X.,

- Wu, X., Wu, Y. W., Wu, Y., Xavier, R. J., Xia, H., Xia, L., Xia, Z., Xiang, G., Xiang, J., Xiang, M., Xiang, W., Xiao, B., Xiao, G., Xiao, H., Xiao, H. T., Xiao, J., Xiao, L., Xiao, S., Xiao, Y., Xie, B., Xie, C. M., Xie, M., Xie, Y., Xie, Z., Xie, Z., Xilouri, M., Xu, C., Xu, E., Xu, H., Xu, J., Xu, J., Xu, L., Xu, W. W., Xu, X., Xue, Y., Yakhine-Diop, S. M. S., Yamaguchi, M., Yamaguchi, O., Yamamoto, A., Yamashina, S., Yan, S., Yan, S. J., Yan, Z., Yanagi, Y., Yang, C., Yang, D. S., Yang, H., Yang, H. T., Yang, H., Yang, J. M., Yang, J., Yang, J., Yang, L., Yang, L., Yang, M., Yang, P. M., Yang, Q., Yang, S., Yang, S., Yang, S. F., Yang, W., Yang, W. Y., Yang, X., Yang, X., Yang, Y., Yang, Y., Yao, H., Yao, S., Yao, X., Yao, Y. G., Yao, Y. M., Yasui, T., Yazdankhah, M., Yen, P. M., Yi, C., Yin, X. M., Yin, Y., Yin, Z., Yin, Z., Ying, M., Ying, Z., Yip, C. K., Yiu, S. P. T., Yoo, Y. H., Yoshida, K., Yoshii, S. R., Yoshimori, T., Yousefi, B., Yu, B., Yu, H., Yu, J., Yu, J., Yu, L., Yu, M. L., Yu, S. W., Yu, V. C., Yu, W. H., Yu, Z., Yu, Z., Yuan, J., Yuan, L. Q., Yuan, S., Yuan, S. F., Yuan, Y., Yuan, Z., Yue, J., Yue, Z., Yun, J., Yung, R. L., Zacks, D. N., Zaffagnini, G., Zambelli, V. O., Zanella, I., Zang, Q. S., Zanivan, S., Zappavigna, S., Zaragoza, P., Zarbalis, K. S., Zarebkohan, A., Zarrouk, A., Zeitlin, S. O., Zeng, J., Zeng, J. D., Zerovnik, E., Zhan, L., Zhang, B., Zhang, D. D., Zhang, H., Zhang, H., Zhang, H., Zhang, H., Zhang, H., Zhang, H., Zhang, H., Zhang, H. L., Zhang, J., Zhang, J., Zhang, J. P., Zhang, K. Y. B., Zhang, L. W., Zhang, L., Zhang, L., Zhang, L., Zhang, L., Zhang, M., Zhang, P., Zhang, S., Zhang, W., Zhang, X., Zhang, X. W., Zhang, X., Zhang, X., Zhang, X., Zhang, X., Zhang, X. D., Zhang, Y., Zhang, Y., Zhang, Y., Zhang, Y. D., Zhang, Y., Zhang, Y. Y., Zhang, Y., Zhang, Z., Zhang, Z., Zhang, Z., Zhang, Z., Zhang, Z., Zhang, Z., Zhang, Z., Zhao, H., Zhao, L., Zhao, S., Zhao, T., Zhao, X. F., Zhao, Y., Zhao, Y., Zhao, Y., Zhao, Y., Zheng, G., Zheng, K., Zheng, L., Zheng, S., Zheng, X. L., Zheng, Y., Zheng, Z. G., Zhivotovsky, B., Zhong, Q., Zhou, A., Zhou, B., Zhou, C., Zhou, G., Zhou, H., Zhou, H., Zhou, H., Zhou, J., Zhou, J., Zhou, J., Zhou, J., Zhou, K., Zhou, R., Zhou, X. J., Zhou, Y., Zhou, Y., Zhou, Y., Zhou, Z. Y., Zhou, Z., Zhu, B., Zhu, C., Zhu, G. Q., Zhu, H., Zhu, H., Zhu, H., Zhu, W. G., Zhu, Y., Zhu, Y., Zhuang, H., Zhuang, X., Zientara-Rytter, K., Zimmermann, C. M., Ziviani, E., Zoladek, T., Zong, W. X., Zorov, D. B., Zorzano, A., Zou, W., Zou, Z., Zou, Z., Zuryin, S., Zwerschke, W., Brand-Saberi, B., Dong, X. C., Kenchappa, C. S., Li, Z., Lin, Y., Oshima, S., Rong, Y., Sluimer, J. C., Stallings, C. L. & Tong, C. K. Guidelines for the use and interpretation of assays for monitoring autophagy (4th edition)(1). *Autophagy* **17**, 1-382, doi:10.1080/15548627.2020.1797280 (2021).
- 348 Landles, C. & Bates, G. P. Huntingtin and the molecular pathogenesis of Huntington's disease. Fourth in molecular medicine review series. *EMBO Rep* **5**, 958-963, doi:10.1038/sj.embor.7400250 (2004).
- 349 Bates, G. Huntingtin aggregation and toxicity in Huntington's disease. *Lancet* **361**, 1642-1644, doi:10.1016/S0140-6736(03)13304-1 (2003).
- 350 DiFiglia, M., Sapp, E., Chase, K. O., Davies, S. W., Bates, G. P., Vonsattel, J. P. & Aronin, N. Aggregation of huntingtin in neuronal intranuclear inclusions and dystrophic neurites in brain. *Science* **277**, 1990-1993, doi:10.1126/science.277.5334.1990 (1997).
- 351 Cattaneo, E., Zuccato, C. & Tartari, M. Normal huntingtin function: an alternative approach to Huntington's disease. *Nat Rev Neurosci* **6**, 919-930, doi:10.1038/nrn1806 (2005).
- 352 Gutekunst, C. A., Li, S. H., Yi, H., Mulroy, J. S., Kuemmerle, S., Jones, R., Rye, D., Ferrante, R. J., Hersch, S. M. & Li, X. J. Nuclear and neuropil aggregates in Huntington's disease: relationship to neuropathology. *J Neurosci* **19**, 2522-2534 (1999).

- 353 Lunkes, A., Lindenberg, K. S., Ben-Haiem, L., Weber, C., Devys, D., Landwehrmeyer, G. B., Mandel, J. L. & Trotter, Y. Proteases acting on mutant huntingtin generate cleaved products that differentially build up cytoplasmic and nuclear inclusions. *Mol Cell* **10**, 259-269 (2002).
- 354 Schilling, G., Klevytska, A., Tebbenkamp, A. T., Juenemann, K., Cooper, J., Gonzales, V., Slunt, H., Poirer, M., Ross, C. A. & Borchelt, D. R. Characterization of huntingtin pathologic fragments in human Huntington disease, transgenic mice, and cell models. *J Neuropathol Exp Neurol* **66**, 313-320, doi:10.1097/nen.0b013e318040b2c8 (2007).
- 355 Juenemann, K., Wiemhoefer, A. & Reits, E. A. Detection of ubiquitinated huntingtin species in intracellular aggregates. *Front Mol Neurosci* **8**, 1, doi:10.3389/fnmol.2015.00001 (2015).
- 356 Wang, C. E., Tydlacka, S., Orr, A. L., Yang, S. H., Graham, R. K., Hayden, M. R., Li, S., Chan, A. W. & Li, X. J. Accumulation of N-terminal mutant huntingtin in mouse and monkey models implicated as a pathogenic mechanism in Huntington's disease. *Hum Mol Genet* **17**, 2738-2751, doi:10.1093/hmg/ddn175 (2008).
- 357 Ratovitski, T., Gucek, M., Jiang, H., Chighladze, E., Waldron, E., D'Ambola, J., Hou, Z., Liang, Y., Poirier, M. A., Hirschhorn, R. R., Graham, R., Hayden, M. R., Cole, R. N. & Ross, C. A. Mutant huntingtin N-terminal fragments of specific size mediate aggregation and toxicity in neuronal cells. *J Biol Chem* **284**, 10855-10867, doi:10.1074/jbc.M804813200 (2009).
- 358 DiFiglia, M. Huntingtin fragments that aggregate go their separate ways. *Mol Cell* **10**, 224-225 (2002).
- 359 Juenemann, K., Schipper-Krom, S., Wiemhoefer, A., Kloss, A., Sanz Sanz, A. & Reits, E. A. Expanded polyglutamine-containing N-terminal huntingtin fragments are entirely degraded by mammalian proteasomes. *J Biol Chem* **288**, 27068-27084, doi:10.1074/jbc.M113.486076 (2013).
- 360 Ferrante, R. J. Mouse models of Huntington's disease and methodological considerations for therapeutic trials. *Biochim Biophys Acta* **1792**, 506-520, doi:10.1016/j.bbadis.2009.04.001 (2009).
- 361 Li, J. Y., Popovic, N. & Brundin, P. The use of the R6 transgenic mouse models of Huntington's disease in attempts to develop novel therapeutic strategies. *NeuroRx* **2**, 447-464, doi:10.1602/neurorx.2.3.447 (2005).
- 362 Pouladi, M. A., Morton, A. J. & Hayden, M. R. Choosing an animal model for the study of Huntington's disease. *Nat Rev Neurosci* **14**, 708-721, doi:10.1038/nrn3570 (2013).
- 363 Menalled, L. B. Knock-in mouse models of Huntington's disease. *NeuroRx* **2**, 465-470, doi:10.1602/neurorx.2.3.465 (2005).
- 364 Gestwicki, J. E. & Garza, D. Protein quality control in neurodegenerative disease. *Prog Mol Biol Transl Sci* **107**, 327-353, doi:10.1016/B978-0-12-385883-2.00003-5 (2012).
- 365 Arrasate, M. & Finkbeiner, S. Protein aggregates in Huntington's disease. *Exp Neurol* **238**, 1-11, doi:10.1016/j.expneurol.2011.12.013 (2012).
- 366 Sieradzan, K. A., Mechan, A. O., Jones, L., Wanker, E. E., Nukina, N. & Mann, D. M. Huntington's disease intranuclear inclusions contain truncated, ubiquitinated huntingtin protein. *Exp Neurol* **156**, 92-99, doi:10.1006/exnr.1998.7005 (1999).
- 367 Wyttenbach, A., Carmichael, J., Swartz, J., Furlong, R. A., Narain, Y., Rankin, J. & Rubinsztein, D. C. Effects of heat shock, heat shock protein 40 (HDJ-2), and proteasome inhibition on protein aggregation in cellular models of Huntington's disease. *Proc Natl Acad Sci U S A* **97**, 2898-2903, doi:10.1073/pnas.97.6.2898 (2000).
- 368 Waelter, S., Boeddrich, A., Lurz, R., Scherzinger, E., Lueder, G., Lehrach, H. & Wanker, E. E. Accumulation of mutant huntingtin fragments in aggresome-like

- inclusion bodies as a result of insufficient protein degradation. *Mol Biol Cell* **12**, 1393-1407, doi:10.1091/mbc.12.5.1393 (2001).
- 369 Qin, Z. H., Wang, Y., Kegel, K. B., Kazantsev, A., Apostol, B. L., Thompson, L. M., Yoder, J., Aronin, N. & DiFiglia, M. Autophagy regulates the processing of amino terminal huntingtin fragments. *Hum Mol Genet* **12**, 3231-3244, doi:10.1093/hmg/ddg346 (2003).
- 370 Li, X., Wang, C. E., Huang, S., Xu, X., Li, X. J., Li, H. & Li, S. Inhibiting the ubiquitin-proteasome system leads to preferential accumulation of toxic N-terminal mutant huntingtin fragments. *Hum Mol Genet* **19**, 2445-2455, doi:10.1093/hmg/ddq127 (2010).
- 371 Davies, S. W., Turmaine, M., Cozens, B. A., DiFiglia, M., Sharp, A. H., Ross, C. A., Scherzinger, E., Wanker, E. E., Mangiarini, L. & Bates, G. P. Formation of neuronal intranuclear inclusions underlies the neurological dysfunction in mice transgenic for the HD mutation. *Cell* **90**, 537-548, doi:10.1016/s0092-8674(00)80513-9 (1997).
- 372 Veldman, M. B. & Yang, X. W. Molecular insights into cortico-striatal miscommunications in Huntington's disease. *Curr Opin Neurobiol* **48**, 79-89, doi:10.1016/j.conb.2017.10.019 (2018).
- 373 Hershko, A. & Ciechanover, A. The ubiquitin system. *Annu Rev Biochem* **67**, 425-479, doi:10.1146/annurev.biochem.67.1.425 (1998).
- 374 Jana, N. R., Dikshit, P., Goswami, A., Kotliarova, S., Murata, S., Tanaka, K. & Nukina, N. Co-chaperone CHIP associates with expanded polyglutamine protein and promotes their degradation by proteasomes. *J Biol Chem* **280**, 11635-11640, doi:10.1074/jbc.M412042200 (2005).
- 375 Donaldson, K. M., Li, W., Ching, K. A., Batalov, S., Tsai, C. C. & Joazeiro, C. A. Ubiquitin-mediated sequestration of normal cellular proteins into polyglutamine aggregates. *Proc Natl Acad Sci U S A* **100**, 8892-8897, doi:10.1073/pnas.1530212100 (2003).
- 376 Juenemann, K., Jansen, A. H. P., van Riel, L., Merckx, R., Mulder, M. P. C., An, H., Statsyuk, A., Kirstein, J., Ovaa, H. & Reits, E. A. Dynamic recruitment of ubiquitin to mutant huntingtin inclusion bodies. *Sci Rep* **8**, 1405, doi:10.1038/s41598-018-19538-0 (2018).
- 377 Gong, B., Kielar, C. & Morton, A. J. Temporal separation of aggregation and ubiquitination during early inclusion formation in transgenic mice carrying the Huntington's disease mutation. *PLoS One* **7**, e41450, doi:10.1371/journal.pone.0041450 (2012).
- 378 Kim, Y. E., Hosp, F., Frottin, F., Ge, H., Mann, M., Hayer-Hartl, M. & Hartl, F. U. Soluble oligomers of PolyQ-expanded huntingtin target a multiplicity of key cellular factors. *Molecular cell* **63**, 951-964 (2016).
- 379 Xi, W., Wang, X., Laue, T. M. & Denis, C. L. Multiple discrete soluble aggregates influence polyglutamine toxicity in a Huntington's disease model system. *Scientific reports* **6**, 1-14 (2016).
- 380 Leitman, J., Hartl, F. U. & Lederkremer, G. Z. Soluble forms of polyQ-expanded huntingtin rather than large aggregates cause endoplasmic reticulum stress. *Nature communications* **4**, 1-10 (2013).
- 381 Lajoie, P. & Snapp, E. L. Formation and toxicity of soluble polyglutamine oligomers in living cells. *PLoS one* **5**, e15245 (2010).
- 382 Takahashi, T., Kikuchi, S., Katada, S., Nagai, Y., Nishizawa, M. & Onodera, O. Soluble polyglutamine oligomers formed prior to inclusion body formation are cytotoxic. *Human molecular genetics* **17**, 345-356 (2008).

- 383 Nagai, Y., Inui, T., Popiel, H. A., Fujikake, N., Hasegawa, K., Urade, Y., Goto, Y., Naiki, H. & Toda, T. A toxic monomeric conformer of the polyglutamine protein. *Nature structural & molecular biology* **14**, 332-340 (2007).
- 384 Menzies, F. M., Fleming, A. & Rubinsztein, D. C. Compromised autophagy and neurodegenerative diseases. *Nat Rev Neurosci* **16**, 345-357, doi:10.1038/nrn3961 (2015).
- 385 Rubinsztein, D. C., Gestwicki, J. E., Murphy, L. O. & Klionsky, D. J. Potential therapeutic applications of autophagy. *Nat Rev Drug Discov* **6**, 304-312, doi:10.1038/nrd2272 (2007).
- 386 Hansen, M., Rubinsztein, D. C. & Walker, D. W. Autophagy as a promoter of longevity: insights from model organisms. *Nat Rev Mol Cell Biol* **19**, 579-593, doi:10.1038/s41580-018-0033-y (2018).
- 387 Li, X., Standley, C., Sapp, E., Valencia, A., Qin, Z. H., Kegel, K. B., Yoder, J., Comer-Tierney, L. A., Esteves, M., Chase, K., Alexander, J., Masso, N., Sobin, L., Bellve, K., Tuft, R., Lifshitz, L., Fogarty, K., Aronin, N. & DiFiglia, M. Mutant huntingtin impairs vesicle formation from recycling endosomes by interfering with Rab11 activity. *Mol Cell Biol* **29**, 6106-6116, doi:10.1128/MCB.00420-09 (2009).
- 388 Smith, R., Bacos, K., Fedele, V., Soulet, D., Walz, H. A., Obermuller, S., Lindqvist, A., Bjorkqvist, M., Klein, P., Onnerfjord, P., Brundin, P., Mulder, H. & Li, J. Y. Mutant huntingtin interacts with β -tubulin and disrupts vesicular transport and insulin secretion. *Hum Mol Genet* **18**, 3942-3954, doi:10.1093/hmg/ddp336 (2009).
- 389 Erie, C., Sacino, M., Houle, L., Lu, M. L. & Wei, J. Altered lysosomal positioning affects lysosomal functions in a cellular model of Huntington's disease. *Eur J Neurosci* **42**, 1941-1951, doi:10.1111/ejn.12957 (2015).
- 390 Benito-Cuesta, I., Diez, H., Ordonez, L. & Wandosell, F. Assessment of Autophagy in Neurons and Brain Tissue. *Cells* **6**, doi:10.3390/cells6030025 (2017).
- 391 Kulkarni, A., Chen, J. & Maday, S. Neuronal autophagy and intercellular regulation of homeostasis in the brain. *Curr Opin Neurobiol* **51**, 29-36, doi:10.1016/j.conb.2018.02.008 (2018).
- 392 Baldo, B., Soyly, R. & Petersen, A. Maintenance of basal levels of autophagy in Huntington's disease mouse models displaying metabolic dysfunction. *PLoS One* **8**, e83050, doi:10.1371/journal.pone.0083050 (2013).
- 393 Engelender, S., Sharp, A. H., Colomer, V., Tokito, M. K., Lanahan, A., Worley, P., Holzbaur, E. L. & Ross, C. A. Huntingtin-associated protein 1 (HAP1) interacts with the p150Glued subunit of dynactin. *Hum Mol Genet* **6**, 2205-2212 (1997).
- 394 Hodges, A., Strand, A. D., Aragaki, A. K., Kuhn, A., Sengstag, T., Hughes, G., Elliston, L. A., Hartog, C., Goldstein, D. R. & Thu, D. Regional and cellular gene expression changes in human Huntington's disease brain. *Human molecular genetics* **15**, 965-977 (2006).
- 395 Baldo, B., Soyly, R. & Petersén, Å. Maintenance of basal levels of autophagy in Huntington's disease mouse models displaying metabolic dysfunction. *PLoS One* **8**, e83050 (2013).
- 396 Nagata, E., Sawa, A., Ross, C. A. & Snyder, S. H. Autophagosome-like vacuole formation in Huntington's disease lymphoblasts. *Neuroreport* **15**, 1325-1328, doi:10.1097/01.wnr.0000127073.66692.8f (2004).
- 397 Rudnicki, D. D., Pletnikova, O., Vonsattel, J. P., Ross, C. A. & Margolis, R. L. A comparison of huntington disease and huntington disease-like 2 neuropathology. *J Neuropathol Exp Neurol* **67**, 366-374, doi:10.1097/NEN.0b013e31816b4aee (2008).
- 398 Frake, R. A., Ricketts, T., Menzies, F. M. & Rubinsztein, D. C. Autophagy and neurodegeneration. *J Clin Invest* **125**, 65-74, doi:10.1172/JCI73944 (2015).

- 399 Tsvetkov, A. S., Miller, J., Arrasate, M., Wong, J. S., Pleiss, M. A. & Finkbeiner, S. A small-molecule scaffold induces autophagy in primary neurons and protects against toxicity in a Huntington disease model. *Proc Natl Acad Sci U S A* **107**, 16982-16987, doi:10.1073/pnas.1004498107 (2010).
- 400 Suresh, S. N., Chavalmane, A. K., Dj, V., Yarreiphang, H., Rai, S., Paul, A., Clement, J. P., Alladi, P. A. & Manjithaya, R. A novel autophagy modulator 6-Bio ameliorates SNCA/alpha-synuclein toxicity. *Autophagy* **13**, 1221-1234, doi:10.1080/15548627.2017.1302045 (2017).
- 401 Suresh, S. N., Chavalmane, A. K., Pillai, M., Ammanathan, V., Vidyadhara, D. J., Yarreiphang, H., Rai, S., Paul, A., Clement, J. P., Alladi, P. A. & Manjithaya, R. Modulation of Autophagy by a Small Molecule Inverse Agonist of ERRalpha Is Neuroprotective. *Front Mol Neurosci* **11**, 109, doi:10.3389/fnmol.2018.00109 (2018).
- 402 Hebron, M. L., Lonskaya, I. & Moussa, C. E.-H. Nilotinib reverses loss of dopamine neurons and improves motor behavior via autophagic degradation of α -synuclein in Parkinson's disease models. *Human molecular genetics* **22**, 3315-3328 (2013).
- 403 Nasir, J., Goldberg, Y. P. & Hayden, M. R. Huntington disease: new insights into the relationship between CAG expansion and disease. *Human molecular genetics* **5**, 1431-1435 (1996).
- 404 MacDonald, M. E., Ambrose, C. M., Duyao, M. P., Myers, R. H., Lin, C., Srinidhi, L., Barnes, G., Taylor, S. A., James, M. & Groot, N. A novel gene containing a trinucleotide repeat that is expanded and unstable on Huntington's disease chromosomes. *Cell* **72**, 971-983 (1993).
- 405 Andrew, S. E., Goldberg, Y. P., Kremer, B., Telenius, H., Theilmann, J., Adam, S., Starr, E., Squitieri, F., Lin, B. & Kalchman, M. A. The relationship between trinucleotide (CAG) repeat length and clinical features of Huntington's disease. *Nature genetics* **4**, 398-403 (1993).
- 406 Ehrnhoefer, D. E., Butland, S. L., Pouladi, M. A. & Hayden, M. R. Mouse models of Huntington disease: variations on a theme. *Dis Model Mech* **2**, 123-129, doi:10.1242/dmm.002451 (2009).
- 407 Hartl, F. U., Bracher, A. & Hayer-Hartl, M. Molecular chaperones in protein folding and proteostasis. *Nature* **475**, 324-332, doi:10.1038/nature10317 (2011).
- 408 Yue, Z., Friedman, L., Komatsu, M. & Tanaka, K. The cellular pathways of neuronal autophagy and their implication in neurodegenerative diseases. *Biochim Biophys Acta* **1793**, 1496-1507, doi:10.1016/j.bbamcr.2009.01.016 (2009).
- 409 Li, H., Li, S. H., Johnston, H., Shelbourne, P. F. & Li, X. J. Amino-terminal fragments of mutant huntingtin show selective accumulation in striatal neurons and synaptic toxicity. *Nat Genet* **25**, 385-389, doi:10.1038/78054 (2000).
- 410 Wellington, C. L., Singaraja, R., Ellerby, L., Savill, J., Roy, S., Leavitt, B., Cattaneo, E., Hackam, A., Sharp, A., Thornberry, N., Nicholson, D. W., Bredesen, D. E. & Hayden, M. R. Inhibiting caspase cleavage of huntingtin reduces toxicity and aggregate formation in neuronal and nonneuronal cells. *J Biol Chem* **275**, 19831-19838, doi:10.1074/jbc.M001475200 (2000).
- 411 Osmand, A. P., Bichell, T. J., Bowman, A. B. & Bates, G. P. Embryonic Mutant Huntingtin Aggregate Formation in Mouse Models of Huntington's Disease. *J Huntingtons Dis* **5**, 343-346, doi:10.3233/JHD-160217 (2016).
- 412 Li, H., Li, S. H., Cheng, A. L., Mangiarini, L., Bates, G. P. & Li, X. J. Ultrastructural localization and progressive formation of neuropil aggregates in Huntington's disease transgenic mice. *Hum Mol Genet* **8**, 1227-1236, doi:10.1093/hmg/8.7.1227 (1999).
- 413 Thoreen, C. C. & Sabatini, D. M. Huntingtin aggregates ask to be eaten. *Nat Genet* **36**, 553-554, doi:10.1038/ng0604-553 (2004).

- 414 Yang, H. & Hu, H. Y. Sequestration of cellular interacting partners by protein aggregates: implication in a loss-of-function pathology. *FEBS J* **283**, 3705-3717, doi:10.1111/febs.13722 (2016).
- 415 Qin, Z. H., Wang, Y., Sapp, E., Cuiffo, B., Wanker, E., Hayden, M. R., Kegel, K. B., Aronin, N. & DiFiglia, M. Huntingtin bodies sequester vesicle-associated proteins by a polyproline-dependent interaction. *J Neurosci* **24**, 269-281, doi:10.1523/JNEUROSCI.1409-03.2004 (2004).
- 416 Hakim-Eshed, V., Boulos, A., Cohen-Rosenzweig, C., Yu-Taeger, L., Ziv, T., Kwon, Y. T., Riess, O., Phuc Nguyen, H. H., Ziv, N. E. & Ciechanover, A. Site-specific ubiquitination of pathogenic huntingtin attenuates its deleterious effects. *Proc Natl Acad Sci U S A* **117**, 18661-18669, doi:10.1073/pnas.2007667117 (2020).
- 417 Trottier, Y., Devys, D., Imbert, G., Saudou, F., An, I., Lutz, Y., Weber, C., Agid, Y., Hirsch, E. C. & Mandel, J. L. Cellular localization of the Huntington's disease protein and discrimination of the normal and mutated form. *Nat Genet* **10**, 104-110, doi:10.1038/ng0595-104 (1995).
- 418 Arrasate, M., Mitra, S., Schweitzer, E. S., Segal, M. R. & Finkbeiner, S. Inclusion body formation reduces levels of mutant huntingtin and the risk of neuronal death. *nature* **431**, 805-810 (2004).
- 419 Sun, C.-S., Lee, C.-C., Li, Y.-N., Yang, S. Y.-C., Lin, C.-H., Chang, Y.-C., Liu, P.-F., He, R.-Y., Wang, C.-H. & Chen, W. Conformational switch of polyglutamine-expanded huntingtin into benign aggregates leads to neuroprotective effect. *Scientific reports* **5**, 1-13 (2015).
- 420 Burton, A. Inclusion bodies may be neuroprotective in Huntington's disease. *The Lancet Neurology* **3**, 699 (2004).
- 421 Albin, R. L. Polyglutamine inclusion body toxicity. (2017).
- 422 Takahashi, T., Katada, S. & Onodera, O. Polyglutamine diseases: where does toxicity come from? what is toxicity? where are we going? *Journal of molecular cell biology* **2**, 180-191 (2010).
- 423 Cisbani, G. & Cicchetti, F. An in vitro perspective on the molecular mechanisms underlying mutant huntingtin protein toxicity. *Cell death & disease* **3**, e382-e382 (2012).
- 424 Sahl, S. J., Weiss, L. E., Duim, W. C., Frydman, J. & Moerner, W. Cellular inclusion bodies of mutant huntingtin exon 1 obscure small fibrillar aggregate species. *Scientific reports* **2**, 895 (2012).
- 425 Safren, N., El Ayadi, A., Chang, L., Terrillion, C. E., Gould, T. D., Boehning, D. F. & Monteiro, M. J. Ubiquilin-1 overexpression increases the lifespan and delays accumulation of Huntingtin aggregates in the R6/2 mouse model of Huntington's disease. *PLoS One* **9**, e87513, doi:10.1371/journal.pone.0087513 (2014).
- 426 Yu, H. C., Lin, C. S., Tai, W. T., Liu, C. Y., Shiau, C. W. & Chen, K. F. Nilotinib induces autophagy in hepatocellular carcinoma through AMPK activation. *J Biol Chem* **288**, 18249-18259, doi:10.1074/jbc.M112.446385 (2013).
- 427 Simuni, T., Fiske, B., Merchant, K., Coffey, C. S., Klingner, E., Caspell-Garcia, C., Lafontant, D. E., Matthews, H., Wyse, R. K., Brundin, P., Simon, D. K., Schwarzschild, M., Weiner, D., Adams, J., Venuto, C., Dawson, T. M., Baker, L., Kostrzebski, M., Ward, T., Rafaloff, G., Parkinson Study Group, N.-P. D. I. & Collaborators. Efficacy of Nilotinib in Patients With Moderately Advanced Parkinson Disease: A Randomized Clinical Trial. *JAMA Neurol* **78**, 312-320, doi:10.1001/jamaneurol.2020.4725 (2021).